THE UNIVERSITY
of EDINBURGH

The valve and the ventricle: advances in the assessment and management of aortic stenosis

Dr Rong Bing

MBBS, BMedSci, FRACP

A thesis for the degree of Doctor of Philosophy

2021

Contents

DECLARATION **1**

LAY SUMMARY **2**

ACKNOWLEDGEMENTS **4**

ABBREVIATIONS **5**

ABSTRACT **6**

CHAPTER 1 – AORTIC STENOSIS: THE CURRENT PARADIGM AND TURNING TIDES **12**

1.1 Simple, simplicated or complicated? 13

1.2 Back to basics 15

Figure 1.1 *A booming field* *15*

Figure 1.2 *The most famous plot in cardiology?* *16*

1.3 Diagnostic dilemmas 22

Figure 1.3 *Categories of aortic stenosis* *24*

Figure 1.4 *Algorithmic approach to aortic stenosis assessment* *25*

1.4 Time is muscle 27

Figure 1.5 *Left ventricular remodelling in aortic stenosis* *28*

Figure 1.6 *Not the most famous plot in cardiology* *30*

1.5 A pill a day keeps the surgeon away 32

1.6 A new valve - ‘til death do us part 34

1.7 Hypotheses 37

CHAPTER 2 - METHODS **38**

2.1 Patient cohorts 39

2.2 Image acquisition.....41

2.2.1 Echocardiography.....41

2.2.2 Cardiac magnetic resonance.....42

2.2.3 Computed tomography.....44

2.2.4 Positron emission tomography.....46

2.3 Image analysis.....48

2.3.1 Echocardiography.....48

2.3.2 Cardiac magnetic resonance.....48

2.3.3 Computed tomography.....49

2.3.4 Positron emission tomography-computed tomography.....50

2.4 Statistical analysis.....52

CHAPTER 3 – CONTRAST-ENHANCED COMPUTED TOMOGRAPHY ASSESSMENT OF AORTIC STENOSIS.....53

3.1 Abstract.....54

3.2 Introduction.....56

3.3 Methods.....58

3.4 Results.....63

Table 3.1 *Baseline demographics*.....*63*

Table 3.2 *Imaging parameters*.....*65*

Figure 3.1 *Indexed contrast CT leaflet volumes and aortic stenosis severity*.....*66*

Table 3.3 *Correlations between CT and echocardiography*.....*67*

Figure 3.2 *Fibro-calcific volume and standard measures of aortic stenosis severity*.....*69*

Figure 3.3 *Indexed contrast CT leaflet volumes and sex*.....*70*

Table 3.4 *Multivariable linear regression models for prediction of peak aortic jet velocity* *71*

Figure 3.4 *Correlations with valve weight* *73*

Figure 3.5 *Contrast CT and histology* *75*

3.5 Discussion 76

Figure 3.6 *Autoplaque software* ..... ***Error! Bookmark not defined.***

3.6 Conclusion 85

CHAPTER 4 – ECHOCARDIOGRAPHIC FIRST-PHASE EJECTION FRACTION IN AORTIC STENOSIS 86

4.1 Abstract 87

4.2 Introduction 89

4.3 Methods 91

4.4 Results 94

Figure 4.1 *Study flow chart* *95*

Table 4.1 *Baseline characteristics* *96*

Figure 4.2 *Distribution of EF1 and ejection fraction by aortic stenosis severity* *97*

Table 4.2 *Multivariable linear regression models for EF1* *98*

Table 4.3 *Outcomes stratified by EF1* *100*

Figure 4.3 *Association between EF1 and outcomes* *101*

Figure 4.4 *Discriminators of aortic valve replacement or death* *102*

Figure 4.5 *Multivariable predictors of aortic valve replacement or death* *103*

4.5 Discussion 105

4.6 Conclusion 109

CHAPTER 5 – EFFECT OF DENOSUMAB OR ALENDRONIC ACID ON THE PROGRESSION OF AORTIC STENOSIS 110

5.1 Abstract 111

5.2 Introduction 113

5.3 Methods 116

5.4 Results 121

Figure 5.1 *CONSORT diagram 122*

Table 5.1 *Baseline characteristics 122*

Figure 5.2 *C-terminal telopeptide concentrations 125*

Figure 5.3 *Primary and key secondary endpoints 126*

Table 5.2 *Aortic valve calcium score measurements and calculations 127*

Table 5.3 *Sensitivity analyses for the primary endpoint 129*

5.5 Discussion 132

5.6 Conclusion 138

CHAPTER 6 – 18F-GP1 POSITRON EMISSION TOMOGRAPHY-COMPUTED TOMOGRAPHY IN BIOPROSTHETIC AORTIC VALVES 139

6.1 Abstract 140

6.2 Introduction 142

6.3 Methods 144

6.4 Results 153

Figure 6.1 *In vitro 18F-GP1 activity 154*

Figure 6.2 *Ex vivo 18F-GP1 validation on prosthetic aortic valves - 1 ..... 155*

Figure 6.3 *Ex vivo 18F-GP1 validation on prosthetic aortic valves - 2 ..... 159*

Table 6.1 *Baseline characteristics 161*

Figure 6.4 *In vivo assessment of aortic valve leaflets* *166*

Figure 6.5 *18F-GP1 uptake in native and bioprosthetic aortic valves* *167*

Figure 6.6 *Subclinical valve thrombosis* *168*

Figure 6.7 *Obstructive valve thrombosis* *171*

Table 6.2 *Correlations between echocardiography, 18F-GP1 and duration of valve implantation* *172*

Table 6.3 *Linear regression models for aortic valve maximum 18F-GP1 target-to-background ratio* *172*

Figure 6.8 *Incidental cardiac 18F-GP1 uptake in patients with prosthetic material* *175*

6.5 Discussion 177

6.6 Conclusion 182

CHAPTER 7 – SUMMARY AND THE FUTURE 183

7.1. Axial imaging in cardiology is here to stay 184

7.2 Subtle changes in left ventricular contractility - the devil is in the detail 187

7.3 Medical therapy for aortic stenosis – a Celtic unicorn 189

7.4 18F-GP1 and pluripotentiality 191

Figure 7.1 *18F-GP1 in recovered COVID-19 patients with pulmonary embolism* *193*

Figure 7.2 *18F-GP1 in myocardial infarction due to coronary thromboembolism* *195*

7.5 Precise timing in precision medicine – the EVOLVED trial and its compatriots . 196

Figure 7.3 *EVOLVED trial flow chart* *200*

Table 7.1 *Ongoing randomised controlled trials of early intervention in asymptomatic severe aortic stenosis* *200*

7.6 Conclusion 201

PUBLICATIONS DURING PHD 203

REFERENCES 213

Declaration

This body of work represents research undertaken at the Centre for Cardiovascular Science, University of Edinburgh and the Edinburgh Heart Centre, Royal Infirmary of Edinburgh. Data are from works that are published in the public domain or under submission, as cited throughout the thesis, for which I was the principal investigator or first author, with contributions including but not limited to study conception, design and conduct, data acquisition and analysis, and manuscript drafting and editing.

This thesis is of my own composition and has not been submitted for any other degree or professional qualification.

Funding was provided by the British Heart Foundation (PG/19/40/34422) and the Sir Jules Thorn Charitable Trust (15/JTA). Life Molecular Imaging GmbH provided reagents for the production of 18F-GP1.

I have no personal disclosures.

Dr Rong Bing

8th June 2021

Lay summary

The aortic valve allows blood to leave the heart and supply the body, opening and closing with every heartbeat. Aortic stenosis is a stiffening of the aortic valve that stops it from opening properly. It is the most common valve disease in the Western world, always gets worse, and has no effective medicine to treat it. Left untreated, aortic stenosis leads to symptoms such as breathlessness and chest pain, followed by cardiac failure and death. Valve replacement is the only treatment, for which open heart surgery has been the main method for decades. “Keyhole” techniques, which are much less invasive, mean that more people can now have aortic valve replacement treatment.

Several controversies and questions exist. These include: 1) What is the best way to determine how severely narrowed the aortic valve is? 2) Are there bad effects on heart muscle health from aortic stenosis that cannot be found by standard tests? 3) Are there drug treatments that could stop the valve stiffening? 4) After valve replacement, can small amounts of clot, which might affect how long the valve lasts, be detected on valve leaflets with new technology?

The following body of work explores these key questions. First, we developed a new unique method of assessing the valve using a heart scan called contrast-enhanced computed tomography. This method was accurate at measuring how severely the valve was narrowed, as is better than standard scans in some important ways. Second, we applied a new measurement of how well the heart pumps based on routine heart ultrasound images. We showed that this measurement, EF1, can be impaired even when the overall pump function of

the heart is good, and that an impaired EF1 might help us pick people who might do poorly in future. Third, we undertook a randomised controlled clinical trial of two drugs to determine whether they could slow down the valve stiffening process. We conclusively demonstrated that they did not work – a disappointing but important finding for the field. Finally, we undertook the first ever cardiac study of 18F-GP1. This is a novel heart scan that can pick up small amounts of clot. We found that there was 18F-GP1 binding on the leaflets of valve replacements in all the valves that we studied, even normal appearing ones. The binding that we saw was reduced with blood-thinning medication. Although this study was new and small, it highlights the potential role for this tracer in detecting small amounts of clot in the body, which, on valve replacements, may affect how long the valve lasts.

The studies presented here have uncovered useful findings and are the result of great teamwork.

Acknowledgements

A big team effort. Briefly:

Dave: A top bloke in all regards, unwaveringly generous and totally inimitable. Marc: fantastic support, above and beyond. Two office doors across the corridor that are always open, literally and metaphorically - hard to beat.

Various fellow barn dwellers, past and present – particularly Snoop and PDA. Various NHS colleagues - particularly Nick Cruden for his support on multiple fronts.

Ki and family, mates old and new – because balance in life is important.

Abbreviations

18F-NaF	18F-sodium fluoride
AVC	aortic valve calcium scoring
AVR	aortic valve replacement
CMR	cardiac magnetic resonance
CT	computed tomography
DIAMOND	Dual Antiplatelet Therapy to Reduce Myocardial Injury
EF1	first-phase ejection fraction
EVOLVED	Early Valve Replacement Guided by Biomarkers of Left Ventricular Decompensation in Asymptomatic Patients with Severe Aortic Stenosis
HALT	hypoattenuated leaflet thickening
PET	positron emission tomography
SALTIRE2	Study Investigating the Effect of Drugs Used to Treat Osteoporosis on the Progression of Calcific Aortic Stenosis
TAVI	transcatheter aortic valve implantation

Abstract

Background

Aortic stenosis is the commonest valve disease in the Western world, progresses inexorably over years and has no effective lifestyle or drug treatments. Left untreated, aortic stenosis leads to symptoms such as breathlessness and chest pain, followed by cardiac failure and death. Aortic valve replacement (AVR) is the only treatment, for which surgery has been the default technique for decades. Transcatheter aortic valve implantation (TAVI), a much less invasive strategy, has substantially expanded the population in whom we now consider AVR. Importantly, the implantation of a prosthetic valve should be considered a means of converting a patient with severe native valve disease to a patient with a well-functioning prosthesis, rather than a cure for valve disease per se. There are potential complications that can arise following successful valve replacement, including valve thrombosis and structural valve degeneration.

Given the above, several controversies and questions exist. These include: 1) What is the optimal method of assessing aortic stenosis severity in low-flow states and in valves where fibrosis contributes significantly to valve obstruction? 2) Are there deleterious effects on myocardial health from aortic stenosis that occur prior to symptom onset or a fall in ejection fraction, and that provide prognostic information? 3) Are there drug therapies that can retard the progression of aortic stenosis? 4) Are there novel methods of detecting bioprosthetic valve thrombus that may provide insight into mechanisms governing valve durability?

Methods

In study one, we developed a unique method of assessing the anatomy of the aortic valve and the severity of aortic stenosis using contrast-enhanced computed tomography (CT). This method has several advantages over non-contrast CT aortic valve calcium scoring (CT-AVC) – the current standard flow-independent measure of aortic stenosis severity – which include spatial resolution, anatomical definition and the ability to quantify non-calcific leaflet thickening in addition to calcific volume. This technique was applied in a post-hoc analysis of a prospectively recruited population of patients with aortic stenosis enrolled in a randomised controlled trial. Patients had undergone standardised echocardiography, non-contrast CT and contrast-enhanced CT.

In study two, we investigated a novel echocardiographic measurement, first-phase ejection fraction (EF1), in aortic stenosis. This parameter is the ejection fraction measured at the time of peak aortic velocity, rather than across the entire cardiac cycle, and is a measure of early left ventricular contractility which can be impaired in aortic stenosis. This technique was applied in a post-hoc analysis of a prospectively recruited population of patients with aortic stenosis enrolled in an observational study. Patients had undergone standardised echocardiography and cardiac magnetic resonance (CMR). Subsequent AVR and death were captured from medical records.

In study three, we undertook a double-blind randomised controlled clinical trial of the anti-osteoporotic drugs denosumab and alendronic acid to determine whether they could slow disease progression in aortic stenosis. This hypothesis arose from a body of pre-clinical and observational data suggesting that bone turnover and osteoblastic differentiation of valvular interstitial cells are important contributory mechanisms to aortic valve calcification, and that

modification of the receptor activator of nuclear kappa B (RANK) ligand/RANK/osteoprotegerin axis might ameliorate valvular calcification. Patients were randomised in a 2:1:2:1 ratio to denosumab (60 mg every 6 months), placebo injection, alendronic acid (70 mg once weekly) or placebo capsule. Participants underwent serial assessments with Doppler echocardiography, CT-AVC and 18F-sodium fluoride (18F-NaF) positron emission tomography and computed tomography (PET-CT). The primary endpoint was the calculated 24-month change in CT-AVC.

In study four, we undertook the first ever cardiac study of 18F-GP1. This is a novel radiotracer that binds to the glycoprotein IIb/IIIa receptor, which are upregulated on activated platelets. We investigated whether 18F-GP1 PET-CT could detect thrombus formation on bioprosthetic aortic valves. First, *ex vivo* validation of 18F-GP1 binding was conducted in explanted bioprosthetic valves leaflets using histology (Movat's pentachrome), immunohistochemistry (CD41) and autoradiography (18F-GP1). Second, patients with bioprosthetic aortic valve prostheses who were not on anticoagulation were enrolled and underwent standardised echocardiography and 18F-GP1 PET-CT. Patients with normal native aortic valves who had undergone 18F-GP1 PET-CT as part of a contemporaneous study formed a control cohort. Two patients with clinically confirmed obstructive bioprosthetic valve thrombosis, recruited as part of a proof-of-concept case series by collaborators in Germany, were also included in the analysis.

Results

In study one, 164 patients with aortic stenosis were included for analysis (78% male; 41 mild, 89 moderate, 34 severe). We demonstrated that non-calcific and calcific aortic valve leaflet

volumes on contrast-enhanced CT correlated well with echocardiographic peak aortic jet velocity ($r=0.67$, $p<0.001$). In particular, quantification of the total non-calcific and calcific leaflet volume demonstrated better correlation with echocardiographic peak aortic velocity than non-contrast CT-AVC in women ($r=0.72$ and $r=0.38$ respectively).

In study two, 149 patients with aortic stenosis were included for analysis (70% male; 34 mild, 40 moderate, 75 severe). We demonstrated that EF1 can be impaired despite a normal overall ejection fraction, that a low EF1 is associated with increased global left ventricular afterload and more myocardial fibrosis, and that there is a potential for EF1 to improve following AVR. Importantly, a low EF1 was associated with future AVR or death, independent of mean aortic valve gradient (hazard ratio 5.6, 95% confidence interval 3.4-9.1).

In study three, we enrolled and randomised 150 patients (mean age 72±8 years, 21% female, peak aortic jet velocity 3.36 [interquartile range 2.93 to 3.82] m/s) to denosumab (n=49), alendronic acid (n=51) or placebo tablet or injection (total n=50). Despite an unequivocal pharmacodynamic effect of the active drugs, as confirmed by a halving of the serum C-terminal telopeptide concentration at 6 months in the denosumab and alendronic acid arms, we found no differences in 24-month change in CT-AVC between denosumab and placebo (343 [198 to 804] Agatston Units (AU) *versus* 354 [76 to 675] AU, p=0.41), or alendronic acid and placebo (326 [138 to 813] AU *versus* 354 [76 to 675] AU, p=0.49). Similarly, there were no differences in change in peak aortic jet velocity or 18F-NaF aortic valve uptake.

In study four, we undertook 18F-GP1 PET-CT in 75 participants (53 with bioprosthetic valves, median time from implantation 37 [12 to 80] months; 22 with normal native valves).

All bioprosthetic valves, but no native aortic valves, demonstrated focal 18F-GP1 uptake in the valve leaflets. On multivariable analysis, higher 18F-GP1 uptake was independently associated with duration of valve implantation (p=0.002) and hypoattenuated leaflet thickening (p=0.004) but not with valve type. One patient had suspected clinical valve thrombosis, confirmed on 18F-GP1 PET-CT, in addition to the two patients with known obstructive valve thrombosis. All 3 were anticoagulated for 3 months, leading to resolution of symptoms, improvement in mean valve gradients and a reduction in 18F-GP1 uptake. Extra-valvular 18F-GP1 uptake was evident across a range of extra-valvular prosthetic material such as aortic interposition grafts and pacemaker leads.

Conclusions

We have demonstrated that contrast-enhanced CT assessments of non-calcific and calcific aortic valve leaflet volumes correlated well with echocardiographic assessments of aortic stenosis severity. This technique has clear benefits over non-contrast CT-AVC. We envisage the potential for standard integration of contrast-enhanced leaflet volume assessments into routine TAVI workflows, where a large proportion of patients have discordant echocardiographic findings, and in patients where the contribution of fibrosis, rather than purely calcium, may lead to underestimation of stenosis severity as assessed by CT-AVC. We went on to show that EF1 is a potentially useful echocardiographic measure of early left ventricular systolic dysfunction that may help risk stratification in patients with asymptomatic severe aortic stenosis. This is pertinent in the current era where early AVR is being tested in several randomised controlled trials. Additionally, we conclusively demonstrate in a randomised controlled trial that neither denosumab nor alendronic acid substantially affect the progression of aortic stenosis. This was a disappointing result but an

important finding that also highlights the importance of randomised controlled trials when investigating causal relationships. Finally, 18F-GP1 PET-CT may have utility in identifying focal areas of thrombus and distinguishing them from other causes of hypoattenuation on CT as well as providing a novel approach to explore factors that may influence valve thrombogenicity and durability. Taken together, these four studies have provided incremental advances in the diagnosis, assessment and follow-up of patients with aortic stenosis as well as generated major impetus for future clinical studies in this important and topical field.

Chapter 1 – Aortic stenosis: the current paradigm and turning tides

Adapted from:

Bing R, Dweck M. Management of asymptomatic severe aortic stenosis: check or all in? Heart. 2020 Nov 4:heartjnl-2020-317160. doi: 10.1136/heartjnl-2020-317160.

Bing R, Dweck MR. The quest for an aortic stenosis cure. Heart. 2020 Sep 11:heartjnl-2020-317421.

Bing R, Dweck M. Myocardial fibrosis – why image, how to image and clinical implications. Heart. 2019. doi: 10.1136/heartjnl-2019-315560.

Bing R, Cavalcante JL, Everett RJ, Clavel MA, Newby DE, Dweck MD. Imaging and impact of myocardial fibrosis in aortic stenosis. J Am Coll Cardiol Img. Feb 2019, 12 (2) 283-296; doi: 0.1016/j.jcmg.2018.11.026.

1.1 Simple, simplicated or complicated?

What is aortic stenosis? A simple question, posed to me on numerous occasions by a senior cardiologist as a stimulus and provocation to think. At face value, aortic stenosis is the archetypal valvular heart disease, elegant and easily grasped in its perceived simplicity. Progressive valve calcification leading to ventricular outflow obstruction and symptoms of exertional cardiac insufficiency is a most comprehensible pathway that requires no great expertise to understand. Frequently encountered on the ward and in clinic, aortic stenosis greets us early in our exposure to cardiology as medical students and is probably the valve disease with which many clinicians, cardiologists or otherwise, retain the most familiarity. A harsh ejection systolic murmur with radiation to the carotids and an anacrotic pulse? The diagnosis is secure.

The simplistic view of aortic stenosis as a mechanical problem that requires an optimally timed mechanical solution – aortic valve replacement (AVR) – forms the basis of safe management of clinically stable patients. Routine follow-up, regular valve surveillance and referral for AVR upon the onset of symptoms or reduction in left ventricular ejection fraction is a straightforward algorithm. When patients oblige by adhering to textbook definitions of disease progression, symptom onset and haemodynamic thresholds for stenosis severity, aortic stenosis is altogether one of the more easily managed chronic cardiac conditions. In fact, on occasion one may even question the need for the extensive range of measures that are now involved in disease severity assessment. Velocity or gradient? Derived or planimetered and indexed or non-indexed valve area? Dimensionless index? Calcium score? Ejection fraction? Flow state? Contractile reserve? Stage of cardiac damage? (Tastet et al., 2019;

Vollema et al., 2019). After all, the more artificial cut points there are for a naturally continuous spectrum of disease, the more grey zones are created. Frequently, a patient with borderline “severe” aortic stenosis is simply that, and applications of multiple arbiters of disease severity, in the absence of a major limitation of the original test, will similarly yield borderline results. Are we complicating a simple condition, or attempting to simplicate a complex disease process?

The truth is, of course, that aortic stenosis is more complex than we – or at least, I - may appreciate in our day-to-day practice. In a privileged era of cardiology where there are few easy therapeutic advances to be made and incrementalism is the name of the game, a detailed understanding of the mechanisms and mechanics governing aortic stenosis is essential if we wish to improve patient outcomes. This philosophy underpins the following thesis, which explores the assessment of valvular stenosis severity, interactions between aortic stenosis and the left ventricle, targeted drug therapies to ameliorate the progression of valve calcification and prosthetic valve imaging – as we must consider that AVR is a stop along the line, and not the destination.

What is aortic stenosis? My responses have become somewhat longer over the last three years.

1.2 Back to basics

We should concisely revisit the seminal science which forms the foundation for current and ongoing research. As we proceed, it is important to appreciate the small details of past and present studies which may influence their interpretation and generalisability. With the exponential increase in publication volume (Figure 1.1) and bite-sized snippets of information promulgated on #medtwitter, relevant points can be increasingly harder to unearth.

Figure 1.1 A booming field

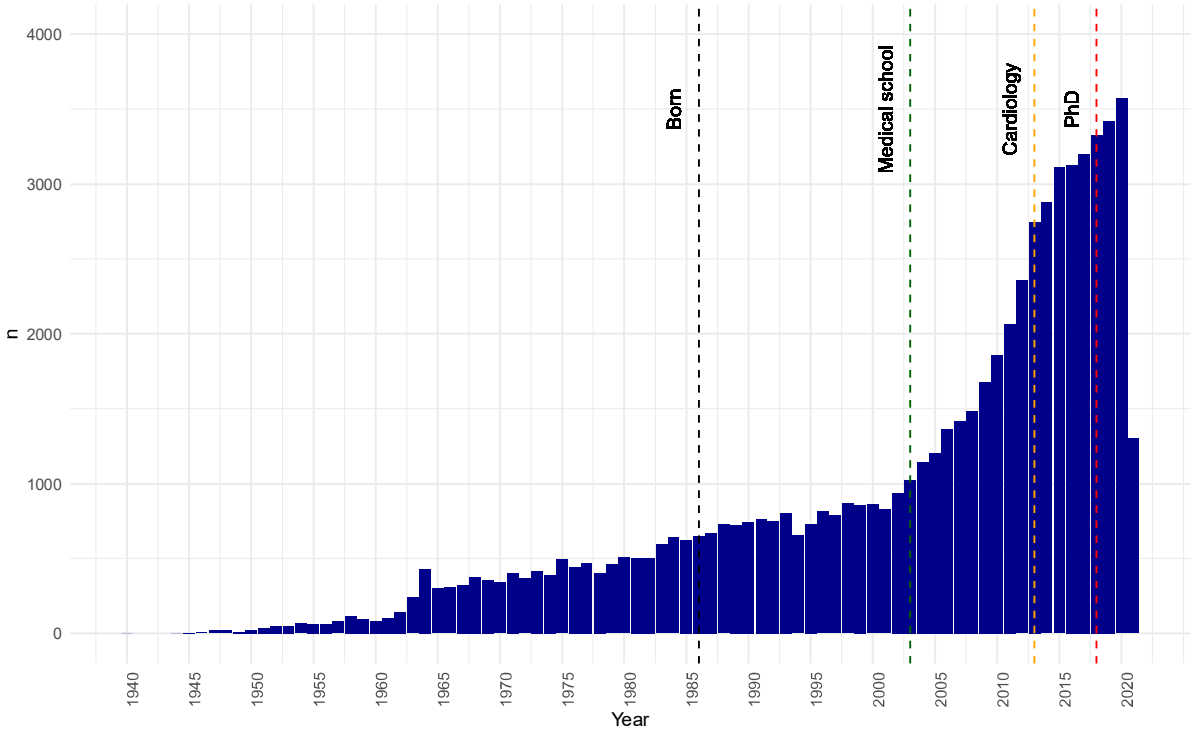

A PubMed search for "aortic stenosis" on 18th May 2021 showing publications by year, with some personal timepoints for context.

For instance, if the adjective "legendary" can be ascribed to a graph in the field of cardiology –a questionable proposition – Ross and Braunwald's plot of survival in aortic stenosis surely

qualifies (Figure 1.2) (Ross & Braunwald, 1968). The accompanying title and caption that delineate the nature of the data, which were assembled in their review paper from several small post-mortem studies and thereby constitute a weak form of evidence by contemporary standards, are less well known and often missing from various reproductions.

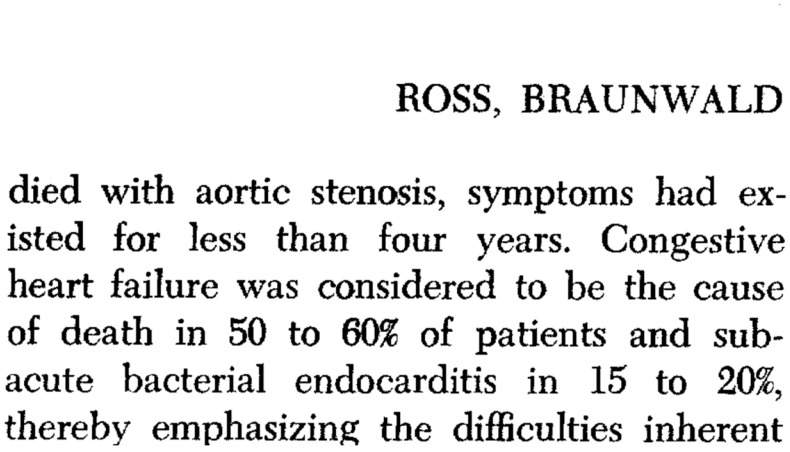

ROSS, BRAUNWALD

died with aortic stenosis, symptoms had existed for less than four years. Congestive heart failure was considered to be the cause of death in 50 to 60% of patients and subacute bacterial endocarditis in 15 to 20%, thereby emphasizing the difficulties inherent

Figure 1.2 The most famous plot in cardiology?

"Average course of valvular aortic stenosis in adults. Data assembled from post-mortem studies" (Ross & Braunwald, 1968).

With this in mind, the epidemiology and natural history of aortic stenosis is relatively well understood. The primary causes of aortic stenosis in our population here are calcific disease and congenital abnormalities, with other aetiologies rarely encountered. Aortic stenosis is the most common valvular heart disease in those with known disease and those referred for valve intervention, with a prevalence that increases with age (Eveborn et al., 2013; Iung et al., 2003; lung & Vahanian, 2011; Nkomo et al., 2006). Increasing patient longevity and iterative improvements in device technologies have led to a rapid expansion of the pool of potential transcatheter aortic valve implantation (TAVI) candidates and procedures performed (Carroll et al., 2020; Durko et al., 2018). The state of play with regards to the natural history of aortic stenosis in 1990 was summarised brilliantly by Braunwald in a succinct editorial (Braunwald, 1990), where he emphasised the generally favourable prognosis of patients with asymptomatic aortic stenosis, and opined that "operative treatment is the most common cause of sudden death in asymptomatic patients with aortic stenosis" – an accurate contention for the era that is up for debate 31 years later (Chapter 7.2). Multiple cohorts have shown that a majority of patient with asymptomatic severe aortic stenosis will develop symptoms within 5 years, and that the annual risk of sudden death prior to the onset of symptoms is ~1% (Lancellotti et al., 2018; Otto et al., 1997; Pellikka et al., 1990; Pellikka et al., 2005; Rosenhek et al., 2000; Rosenhek et al., 2010; Zilberszac et al., 2017). This is a small but real risk, and of course the outcome for a given patient is binary. Even mild and moderate aortic stenosis have been independently associated with increased all-cause and cardiovascular mortality, although one cannot infer a causal relationship between valve disease and death from these observational data (Rosenhek et al., 2004; Strange et al., 2019). For instance, in a post-hoc analysis of the randomised Scottish Computed Tomography of the Heart trial, the presence of aortic or mitral valve calcification was associated with the composite endpoint of

cardiovascular mortality, non-fatal myocardial infarction, or non-fatal stroke, but not after adjusting for coronary artery calcification (Williams et al., 2020). The rate of aortic stenosis progression has been studied invasively and non-invasively in observational studies, largely depends on baseline stenosis severity as well as valve calcification, and is thought to be approximately 0.3 m/s/year (peak velocity), 3-7 mmHg/year (mean gradient) or -0.1 cm^2/year (aortic valve area), although there is substantial variation between patients and cohorts (Brener et al., 1995; Davies et al., 1991; Eveborn et al., 2013; Otto et al., 1997; Otto et al., 1989; Palta et al., 2000).

The pathophysiology of aortic stenosis is less clear. There has been a clear shift away from the paradigm of passive "wear and tear" to a metabolically active process, although mechanical stress with early injury is thought to be an important early trigger. Inflammation is increasingly recognised to be crucial in initiating and propagating disease progression across a range of cardiovascular diseases, and aortic stenosis is no exception. In brief, a model is proposed that comprises an initiation and propagation phase (Pawade et al., 2015). Valve leaflet endothelial injury commences a cycle of inflammatory cell infiltration and lipid deposition, regions of which co-localise with microcalcification and areas of mineralisation (Otto et al., 1994). These changes induce osteoblastic differentiation of valve interstitial cells which then promulgate collagen matrix deposition, leading to leaflet thickening, before subsequent calcium deposition. This disruption to leaflet pliability and motion leads to increased mechanical stress and cellular injury, forming a self-perpetuating cycle of valve injury, inflammation and calcium deposition (Pawade et al., 2015) – the inexorable progression of aortic stenosis. Similarities with skeletal bone formation have been noted, with the receptor activator of nuclear kappa B (RANK) ligand (RANKL)/RANK/osteoprotegerin

(OPG) axis in particularly being implicated in valve calcium deposition and bone turnover (Chapter 5.2). Although other large scale observational data have demonstrated associations between aortic stenosis/valve calcification and hypertension, hypercholesterolaemia and other risk factors for atherosclerotic disease (Brener et al., 1995; Katz et al., 2006; Nazarzadeh et al., 2019; Rahimi et al., 2018; Stewart et al., 1997; Stritzke et al., 2009), causality has not been demonstrated.

We must next consider the effect of the valve disease on the myocardium, which has not been linked to a disease process specific to aortic stenosis per se, but rather is a result of the chronic and progressively increasing afterload on the heart. In addition, the importance of arterial stiffness and systemic pulsatile arterial load, which contribute to afterload, should be recognised (Lindman et al., 2017; Yotti et al., 2015). Ultimately, one cannot separate the ventricle and the arterial system, a concept which is encompassed by the study of cardiac mechanics and ventriculoarterial coupling - a complex field beyond the remit of this thesis. The interplay between afterload, pressure, wall stress and chamber geometry is nevertheless fascinating, and our clinical understanding of these relationships is grounded in core research from a previous era of cardiac catheterisation (rather than coronary angiography, to which the label of "cath" is now applied) and early echocardiography. A fine example is Dr Otto's study of invasive pressure-flow relationships in aortic stenosis (Bermejo et al., 2002), which she brought to my attention in the course of correspondence regarding one of our studies (Chapter 4). The progressive pressure overload on the left ventricle induces a compensatory remodelling and hypertrophic response to limit increases in wall stress and preserve contractility (Chambers, 2006), broadly in accordance with the law of Laplace:

$$\sigma \propto \frac{P \times r}{h}$$

where σ is wall stress, P is pressure, r is radius and h is wall thickness. The relationships are inexact as the left ventricle is, of course, not a sphere or cylinder, nor is its geometry static. Ventricular pressure continues to rise with progressive valvular obstruction, accompanied by a compensatory increase in wall thickness. This mechanism is naturally finite and also unpredictable, correlating poorly with outflow obstruction (Griffith et al., 1991; Krayenbuehl et al., 1988). Eventually, systolic function is compromised and heart failure ensues. Alternatively, the left ventricular response may be predominantly dilatation rather than concentric remodelling and hypertrophy, with a consequently high wall stress and reduction in systolic function (Chambers, 2006; DePace et al., 1983). Another means of describing this relationship is afterload mismatch, whereby ejection as modulated by preload is compromised as a consequence of decreased contractility due to increased afterload (progressive aortic stenosis) (Ross, 1976). The distinction between afterload mismatch-induced systolic dysfunction and intrinsic systolic dysfunction due to a concomitant cardiomyopathy is posited to be a reason why some patients may recover systolic function after AVR and others do not – although this latter group may still benefit from AVR due to ventricular unloading (Otto et al., 2021; Ross, 1985). This evolution of myocardial disease is complex but closely related to the development of myocardial fibrosis, myocyte injury and cell death. Furthermore, there is adverse remodelling of the extracellular matrix, with degradation and disruption of the matrix structure (Kandalam et al., 2011). These changes are regulated by several factors, including the renin-angiotensin-aldosterone system,

transforming growth factor beta, apoptosis signal-regulating kinase 1 and tissue inhibitor of metalloproteinase (Heymans et al., 2005; Weber & Brilla, 1991; Yang et al., 2017). Two distinct myocardial fibrosis patterns have been described. Reactive interstitial fibrosis is diffuse and follows increased myofibroblast activity and collagen deposition that begins even in the early stages of aortic stenosis. Importantly, this diffuse fibrosis is reversible and has been demonstrated to regress following AVR (Krayenbuehl et al., 1989). In contrast, replacement fibrosis appears to occur later and is irreversible (Treibel, Kozor, et al., 2018). Treibel et al recently demonstrated that patients with advanced disease undergoing AVR manifest a complex combined pattern of both replacement and diffuse fibrosis (Treibel, Lopez, et al., 2018). They also observed a fibrosis gradient from the subendocardium to the mid-myocardium, perhaps suggesting supply-demand ischaemia as a contributing factor. The degree of myocardial remodelling and fibrosis is closely related to haemodynamic markers of myocardial performance such as left ventricular end-diastolic pressure and ejection fraction (Dweck, Boon, et al., 2012). Multiple histological studies have now demonstrated an association between myocardial fibrosis at the time of AVR and both impaired recovery of left ventricular systolic function and poor long-term outcomes after AVR (Azevedo et al., 2010; Hein et al., 2003; Herrmann et al., 2011; Weidemann et al., 2009).

1.3 Diagnostic dilemmas

The clinical diagnosis of aortic stenosis as an entity – a reduction in aortic valve leaflet excursion due to fibrosis and calcification that eventually leads to left ventricular outflow obstruction – is not typically difficult to make. The dilemma most often arises at the artificial but clinically important juncture when moderate aortic stenosis becomes severe aortic stenosis. This threshold, as with most in medicine, is required in order to provide some guidance for ongoing management, whether that be more frequent follow-up or referral for valve intervention. When the full hand of haemodynamic measures is met (Baumgartner et al., 2017; Otto et al., 2021) and accompanied by typical symptoms and signs of severe aortic stenosis, the diagnosis is again straightforward. However, the picture is often clouded by uncertainty regarding parameters of stenosis severity, as well as their correlation with, or contribution to, symptoms. After all, the classical symptoms of aortic stenosis – exertional dyspnoea, exertional pre-syncope or syncope and exertional angina - are non-specific, while the examination findings of a low volume, slow-rising carotid pulse, late-peaking ejection systolic murmur and an absent A2 are difficult to study and are generally sensitive or specific but not both (Etchells et al., 1997; Munt et al., 1999). Nor does contemporary classification of aortic stenosis simply comprise mild, moderate or severe disease. The latest American College of Cardiology/American Heart Association guidelines suggest no less than seven categories of aortic stenosis (Figure 1.3).

Echocardiographic measures of aortic stenosis – velocities, gradients and derived valve areas – have both technical and intrinsic limitations. They require meticulous interrogation of the valve from several views to acquire maximal representative values, which is dependent upon

multiple factors such as operator expertise and patient body habitus. They are also, crucially, dynamic and dependent on haemodynamic conditions and transaortic flow. Discordant measurements are seen in around one-third of patients, and are governed by complex interactions between the ventricle, the valve and systemic arterial compliance (Clavel et al., 2013). Contemporary classifications include severe high-gradient aortic stenosis, severe low-flow low-gradient aortic stenosis with reduced ejection fraction and severe paradoxical low-flow low-gradient aortic stenosis with preserved ejection fraction (as well as a more nebulous entity of severe normal-flow low-gradient aortic stenosis) (Clavel et al., 2016). These categories require the accurate assessment of flow (indexed stroke volume) as well as the ability to augment flow with dobutamine in those with low ejection fraction (Figure 1.4), which in daily practice may be more difficult to achieve. The lack of contractile reserve in

some patients adds further complexity – is the diagnosis severe low-flow low-gradient aortic stenosis with reduced ejection fraction, or pseudo-severe aortic stenosis?

Stage	Definition	Valve Anatomy	Valve Hemodynamics	Hemodynamic Consequences	Symptoms
A	At risk of AS	BAV (or other congenital valve anomaly) Aortic valve sclerosis	Aortic V_{max} <2 m/s with normal leaflet motion	None	None
B	Progressive AS	Mild to moderate leaflet calcification/fibrosis of a bicuspid or trileaflet valve with some reduction in systolic motion or Rheumatic valve changes with commissural fusion	Mild AS: aortic V_{max} 2.0–2.9 m/s or mean ΔP <20 mm Hg Moderate AS: aortic V_{max} 3.0–3.9 m/s or mean ΔP 20–39 mm Hg	Early LV diastolic dysfunction may be present Normal LVEF	None
C: Asymptomatic severe AS					
C1	Asymptomatic severe AS	Severe leaflet calcification/fibrosis or congenital stenosis with severely reduced leaflet opening	Aortic V_{max} ≥4 m/s or mean ΔP ≥40 mm Hg AVA typically is ≤1.0 cm^2 (or AVAi 0.6 cm^2/m^2) but not required to define severe AS Very severe AS is an aortic V_{max} ≥5 m/s or mean P ≥60 mm Hg	LV diastolic dysfunction Mild LV hypertrophy Normal LVEF	None Exercise testing is reasonable to confirm symptom status
C2	Asymptomatic severe AS with LV systolic dysfunction	Severe leaflet calcification/fibrosis or congenital stenosis with severely reduced leaflet opening	Aortic V_{max} ≥4 m/s or mean ΔP ≥40 mm Hg AVA typically ≤1.0 cm^2 (or AVAi 0.6 cm^2/m^2) but not required to define severe AS	LVEF <50%	None
D: Symptomatic severe AS					
D1	Symptomatic severe high-gradient AS	Severe leaflet calcification/fibrosis or congenital stenosis with severely reduced leaflet opening	Aortic V_{max} ≥4 m/s or mean ΔP ≥40 mm Hg AVA typically ≤1.0 cm^2 (or AVAi ≤0.6 cm^2/m^2) but may be larger with mixed AS/AR	LV diastolic dysfunction LV hypertrophy Pulmonary hypertension may be present	Exertional dyspnea, decreased exercise tolerance, or HF Exertional angina Exertional syncope or presyncope
D2	Symptomatic severe low-flow, low-gradient AS with reduced LVEF	Severe leaflet calcification/fibrosis with severely reduced leaflet motion	AVA ≤1.0 cm^2 with resting aortic V_{max} <4 m/s or mean ΔP <40 mm Hg Dobutamine stress echocardiography shows AVA <1.0 cm^2 with V_{max} ≥4 m/s at any flow rate	LV diastolic dysfunction LV hypertrophy LVEF <50%	HF Angina Syncope or presyncope
D3	Symptomatic severe low-gradient AS with normal LVEF or paradoxical low-flow severe AS	Severe leaflet calcification/fibrosis with severely reduced leaflet motion	AVA ≤1.0 cm^2 (indexed AVA ≤0.6 cm^2/m^2) with an aortic V_{max} <4 m/s or mean ΔP <40 mm Hg AND Stroke volume index <35 mL/m^2 Measured when patient is normotensive (systolic blood pressure <140 mm Hg)	Increased LV relative wall thickness Small LV chamber with low stroke volume Restrictive diastolic filling LVEF ≥50%	HF Angina Syncope or presyncope

AR indicates aortic regurgitation; AS, aortic stenosis; AVA, aortic valve area circulation; AVAi, AVA indexed to body surface area; BAV, bicuspid aortic valve; ΔP, pressure gradient between the LV and aorta HF, heart failure; LV, left ventricular; LVEF, left ventricular ejection fraction; and V_{max}, maximum velocity.

Figure 1.3 Categories of aortic stenosis

From the 2020 ACC/AHA guideline for the management of patients with valvular heart disease (Otto et al., 2021).

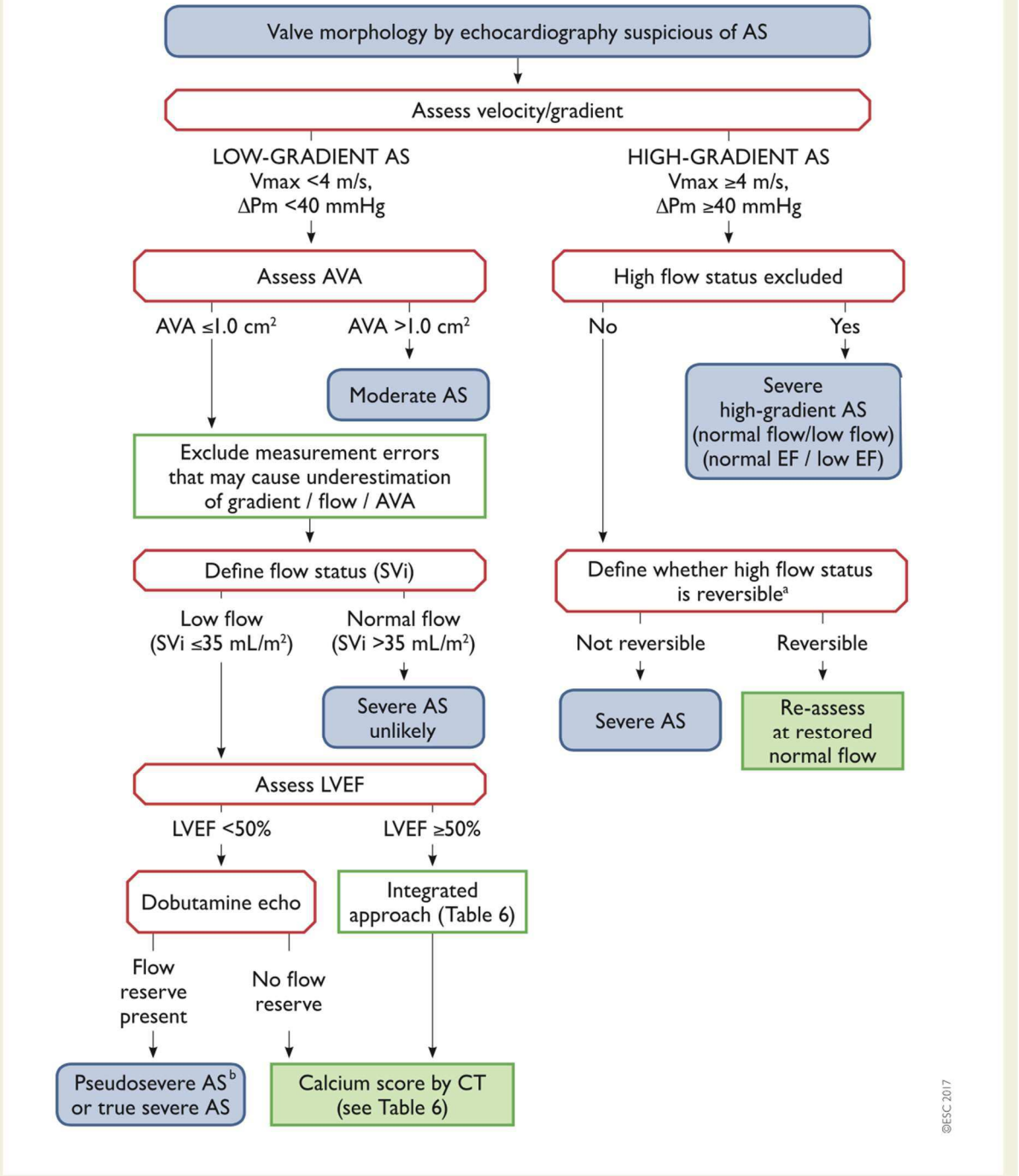

ΔPm = mean transvalvular pressure gradient; AS = aortic stenosis; AVA = aortic valve area; CT = computed tomography; EF = ejection fraction; LVEF = left ventricular ejection fraction; SVi = stroke volume index; Vmax = peak transvalvular velocity.

Figure 1.4 Algorithmic approach to aortic stenosis assessment

From the 2017 European Society of Cardiology/European Association for Cardiothoracic Surgery guidelines for the management of valvular heart disease (Baumgartner et al., 2017).

Non-contrast computed tomography calcium scoring (CT-AVC) was developed to provide a flow-independent assessment of stenosis severity. As an anatomical measure of valvular calcium density and volume, its associated with subsequent AVR and sex-specific thresholds for severe aortic stenosis are now recommended in certain situations to help clarify stenosis severity (Baumgartner et al., 2017; Clavel et al., 2014; Otto et al., 2021; Pawade et al., 2018). However, CT-AVC has several important limitations, principally to do with poor anatomical definition, inability to characterise non-calcific tissue and limited spatial resolution. Conveniently, these are factors that can be addressed with modern contrast-enhanced cardiac CT, which is now a routine modality for assessing coronary artery disease as well as procedural planning for transcatheter aortic valve implantation (TAVI). The use of contrast-enhanced CT to assess native aortic valve disease is therefore appealing, relevant and easily translatable to clinical practice. We examined this in study one.

1.4 Time is muscle

When associating time with cell death, stroke and myocardial infarction spring to mind as the prototypical models of acute ischaemia - minutes matter. Although certainly not analogous, with a far less direct causal pathway, we might consider the more indolent and protracted effect of aortic stenosis on the myocardium as central to overall disease progression – not simply progression of valve calcification – and prognosis.

Although we have briefly discussed the underlying pathology of aortic stenosis and the different stages of disease above, they have been studied over many years and are covered in detailed elsewhere (Otto & Prendergast, 2014; Pawade et al., 2015). For our current purposes, it is important to appreciate that symptom development and adverse events relate not only to the degree of valvular obstruction, but also the deleterious effects of a chronic and progressive pressure load on the heart. The adaptive hypertrophic response to limit increases in wall stress is, as previously mentioned, a temporising and limited response. Fibroblast proliferation is followed by ventricular remodelling, extracellular matrix expansion, myocyte cell death and reparative scar formation – with fibrosis representing the pathological correlate of heart failure (Figure 1.5).

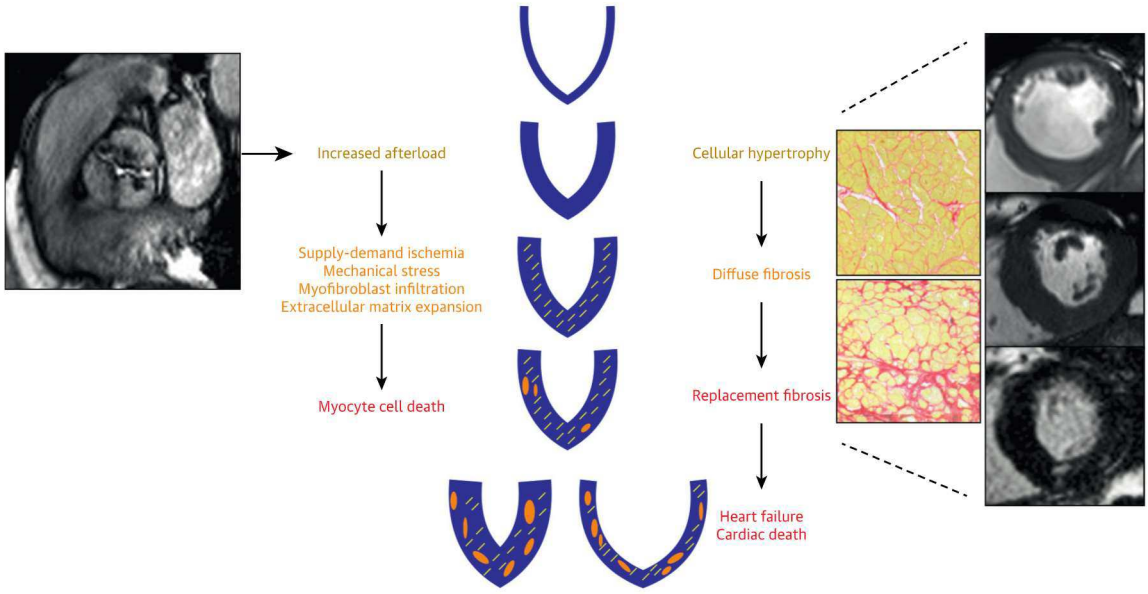

Figure 1.5 Left ventricular remodelling in aortic stenosis

Schematic of the left ventricular remodelling response in aortic stenosis (Bing, Cavalcante, et al., 2019).

Symptoms may manifest only late in this process, and as such are a crude surrogate of disease progression and myocardial health. We have all encountered the previously stable asymptomatic patient with severe aortic stenosis and preserved left ventricular ejection fraction who presents in decompensated heart failure with a struggling ventricle in between routine follow-up appointments. Inevitably, these cases raise a pertinent question – have we missed a trick?

The role of structural myocardial abnormalities in aortic stenosis and the potential for regression is well established. Data from more than 30 years ago demonstrated both the impact of pressure overload on the left ventricle and the potential for reverse remodelling following aortic valve replacement, with a differential reduction in the cellular and extracellular compartments of the myocardium. Reduction in mass is predominantly cellular

regression, whereas there is incomplete resolution of fibrosis (Krayenbuehl et al., 1989). These findings have been consistently demonstrated with histological, and more recently, cardiac magnetic resonance (CMR) data (Everett et al., 2018; Treibel, Kozor, et al., 2018; Weidemann et al., 2009). The rise of the latter modality has permitted non-invasive quantitative and qualitative assessments of myocardial composition and differentiation of diffuse interstitial fibrosis, which is at least partially reversible, from replacement fibrosis, which represents irreversible scar following myocyte necrosis (Bing, Cavalcante, et al., 2019; Puntmann et al., 2016). Most recently, combining histology and CMR has provided a deeper understanding of the pathological myocardial changes seen in aortic stenosis, with, unsurprisingly, a more complex pattern of disease than appreciated with imaging alone (Treibel, Lopez, et al., 2018).

Why is this important? There is now a large body of prospective observational data from multiple independent cohorts demonstrating that CMR measures of myocardial fibrosis and extracellular matrix expansion, which develop in a latent phase prior to valve intervention, are independently associated with mortality in aortic stenosis – even after AVR (Azevedo et al., 2010; Barone-Rochette et al., 2014; Chin et al., 2017; Dweck et al., 2011; Everett et al., 2020; Musa et al., 2018). Lending further credence to these observations are similar associations between fibrosis and outcomes across a breadth of other cardiovascular diseases, including ischaemic, non-ischaemic and infiltrative cardiomyopathies. Thus, the question naturally arises: if myocardial disease in aortic stenosis is due to pressure overload, accrues subclinically, may be irreversible and is prognostically relevant in a “dose-dependent” fashion, can assessments of myocardial health be used to better risk stratify patients with asymptomatic severe aortic stenosis and refine the timing of valve intervention (Figure 1.6)?

Different strategies have been proposed for risk stratification. At the far end of this spectrum is the current practice of using echocardiography to monitor for a fall in ejection fraction. Although echocardiography is unequivocally the first-line imaging modality in aortic stenosis, a reduction in ejection fraction is a late marker of end-stage disease that

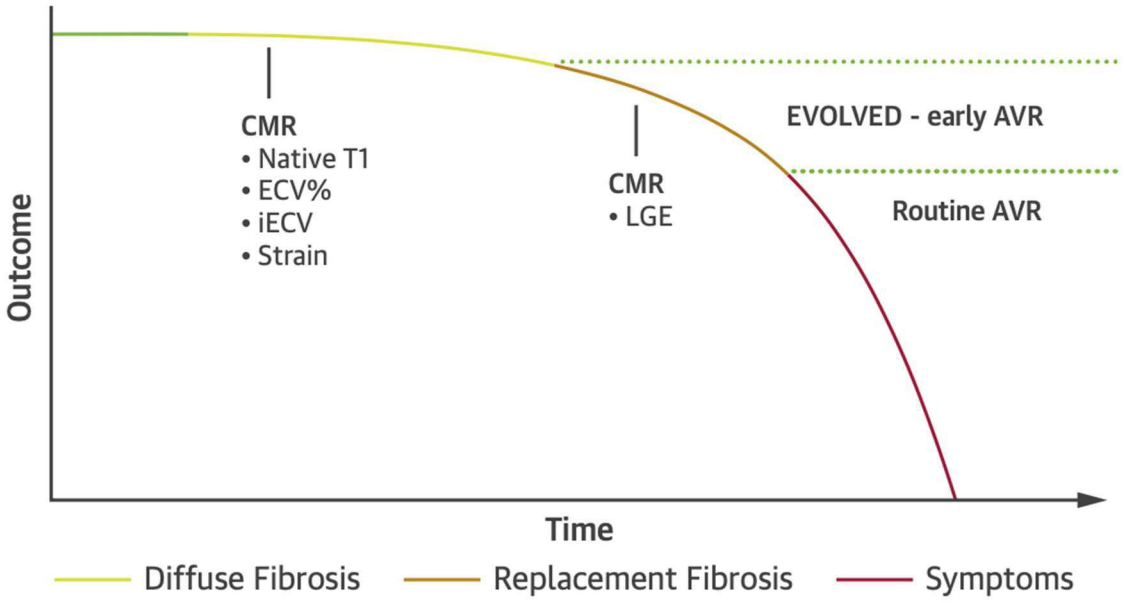

Figure 1.6 Not the most famous plot in cardiology

A schematic inspired by Braunwald's plot, proposing an integration of myocardial imaging to risk stratify patients and guide valve intervention prior to the onset of symptoms (Bing, Cavalcante, et al., 2019).

can be irreversible. Other methods include exercise testing, advanced imaging and blood biomarkers, each with their own advantages and disadvantages. In study two, we examined a novel echocardiographic measure of early left ventricular systolic function, first-phase

ejection fraction, to determine whether it might be of use in early prognostication as a more sensitive assessment of myocardial function than overall ejection fraction.

In reviewing the merits of any risk stratification tool, we must remember that assigning a label of “high risk” does not necessarily imply that the risk is modifiable with a particular intervention. It is unknown whether the adverse prognosis associated with the various advanced imaging and biomarker parameters can be mitigated if these markers are used to trigger AVR. Only randomised controlled trial data can confirm or refute such hypotheses.

1.5 A pill a day keeps the surgeon away

Or so we wish.

There is an unmet need here. Prevention (which we lack for aortic stenosis) is, as the saying goes, better than a cure (which we also lack, in some regard).

Although TAVI has revolutionised the interventional paradigm in aortic stenosis and is an unequivocal success, we recognise that a prosthesis is not a cure for aortic valve disease, and that complications – both short- and long-term – are not abolished. Even in the context of randomised controlled trials of low surgical risk patients, the rate of death or disabling stroke at 1 year after TAVI or surgical AVR was 2.9% and 4.6% respectively in the Evolut low risk trial (Popma et al., 2019), while death, stroke or re-hospitalisation at 2 years after TAVI or surgical AVR was 11.5% and 17.4% respectively in PARTNER 3 (Leon et al., 2021). Consequently, although recent clinical research has largely focused on iterative improvements in devices, procedural techniques and risk assessment with a view to optimising the delivery and timing of valve replacement, the search for an effective medical therapy to retard the inexorable progression of aortic stenosis continues.

The only drugs to be tested prospectively in randomised controlled trials as disease modifiers in aortic stenosis are statins, with conclusively negative results from three seminal trials (Chan et al., 2010; Cowell et al., 2005; Rossebo et al., 2008). Other data have hinted at possible roles for other therapies such as renin-angiotensin-aldosterone system blockade and anti-osteoporosis medications, with a handful of small, randomised trials with surrogate

safety and efficacy endpoints for the former (Marquis-Gravel et al., 2016), but it is not possible to confirm causal relationships and draw actionable conclusions from these data. Meanwhile, a deeper understanding of the complex processes governing aortic stenosis has shifted the field away from a purely degenerative disease model, with more emphasis on valve mineralisation, lipoprotein infiltration, active inflammation and tissue remodelling (Pawade et al., 2015).

There are clear similarities between the actively regulated valvular inflammation and calcification of aortic stenosis and skeletal bone formation, with osteoblastic differentiation of valvular interstitial cells and osteoclast activity in the bone playing important roles (Dayanand et al., 2018; Goody et al., 2020; Otto et al., 1994; Pawade et al., 2015; Rajamannan et al., 2011; Rajamannan et al., 2003). Based upon pre-clinical animal models and observational clinical data, we undertook a randomised controlled trial in study three, testing whether the anti-osteoporotic drugs denosumab and alendronic acid could retard the progression of aortic valve calcification.

1.6 A new valve - 'til death do us part

We now arrive at the culmination of diagnosis, risk stratification, valve surveillance, symptom correlation and the decision to intervene – valve replacement. In one comprehensive procedure, the majority of left ventricular outflow obstruction is resolved with the implantation of a new prosthesis – most commonly a bioprosthesis - whether by surgical or transcatheter means. One of the more satisfying interventions in cardiology is measuring a left ventricular systolic pressure >200 mmHg that is accompanied by a high transvalvular pressure gradient, implanting a bioprosthetic valve percutaneously and immediately abolishing most of this gradient. Surely this is curative?

Although AVR may be, in the most striking cases, transformative with regards to symptoms or left ventricular ejection fraction, we must remember that the patient is converted from one with severe native aortic valve disease to one with a well-functioning prosthesis – one which has a limited lifespan (Bloomfield et al., 1991; Oxenham et al., 2003). Accompanying the implantation of a bioprosthesis is a predilection for several recognised sequelae, recently encapsulated by Valve Academic Research Consortium 3 definitions of bioprosthetic valve dysfunction – structural valve deterioration, non-structural valve dysfunction, valve thrombosis and endocarditis (Genereux et al., 2021). These sequelae are becoming increasingly relevant, as TAVI has expanded the population of patients being considered for AVR, whilst being implanted in increasingly younger patients, where valve durability is of paramount importance (Durko et al., 2018). Recently published data from the Society of Thoracic Surgeons–American College of Cardiology Transcatheter Valve Therapy Registry have demonstrated a clear temporal trend from 2011 to 2019, with a broadening spectrum of

patients and an annually increasing TAVI volume that, in 2019, exceeded surgical AVR (Carroll et al., 2020). Although medium term data from randomised trials and registry data suggest that contemporary transcatheter prostheses have similar rates of bioprosthetic valve failure to surgical prostheses (Blackman et al., 2019; Pibarot et al., 2020; Sondergaard et al., 2019), more long-term data are required.

The question of subclinical valve thrombosis in particular is of current interest. Valve thrombus is often a subclinical finding on imaging, with a variable prevalence of 12-40% reported in registries (Chakravarty et al., 2017; Makkar et al., 2015) and sub-studies of randomized controlled trials (De Backer et al., 2020; Makkar et al., 2020). Valve obstruction is one potential clinical sequelae, which is treatable with anticoagulation. There is also a suggestion that leaflet thrombosis may be associated with premature structural valve deterioration (Cartlidge et al., 2019) and that anticoagulation after transcatheter aortic valve replacement (TAVI) may be associated with less valvular haemodynamic deterioration (Del Trigo et al., 2018; Del Trigo et al., 2016). The usual caveats regarding observational data apply, but there is certainly biological plausibility and a clinical question to be explored.

Contrast-enhanced cardiac CT, ideally with retrospective electrocardiogram gating, is the current diagnostic modality of choice for the detection of subclinical leaflet abnormalities, given its high spatial resolution, but provides only an appearance of hypoattenuation as a surrogate for thrombus, which must then be contextualised with the pattern and distribution of the imaging findings to determine whether thrombus is likely. In contrast, 18F-GP1 is a new radiotracer that binds to the glycoprotein IIb/IIIa receptor on activated platelets (Lohrke et al., 2017), and molecular imaging with this radiotracer has demonstrating promising early

results for the detection of *in vivo* venous and arterial thrombus (Chae et al., 2019; Kim et al., 2018). In study four, we performed the first cardiac study of 18F-GP1 positron emission tomography (PET)-CT to determine whether this modality could be used to detect bioprosthetic aortic valve thrombus.

1.7 Hypotheses

This thesis examines novel approaches to the diagnosis, risk stratification, treatment and follow-up of patients with aortic stenosis. The following hypotheses are tested:

1. Contrast-enhanced CT can be used to assess aortic stenosis severity and characterise valve tissue.

2. EF1 can offer prognostic information in patients with aortic stenosis, even in patients with normal ejection fraction.

3. Denosumab and alendronic acid can slow the progression of aortic valve calcification in aortic stenosis.

4. 18F-GP1 PET-CT can detect bioprosthetic aortic valve thrombus beyond the resolution of CT.

Chapter 2 - Methods

2.1 Patient cohorts

The cohorts presented are primarily comprised of patients recruited in the following studies:

Study Investigating the Effect of Drugs Used to Treat Osteoporosis on the Progression of Calcific Aortic Stenosis (SALTIRE2) (NCT02132026; Chapters 3 and 5). This was a randomised controlled trial testing whether denosumab or alendronate could reduce the progression of aortic stenosis. Patients were recruited from clinic across South-East Scotland between August 2015 and November 2017, and underwent study visits at the Edinburgh Heart Centre (n=199). Chapter 3 was a post-hoc study using imaging studies from the trial cohort. For this chapter, I undertook statistical analysis, data interpretation, drafting and revision of the manuscript, and was subsequently involved in the conception and development of the next iteration of the imaging technique which is ongoing. Chapter 5 is the primary trial manuscript. For this chapter (and for the main trial), I was the final principal investigator, undertaking study visits, image analysis, data entry, data interpretation, all requisite study close-out administration, data analysis and drafting and revision of the manuscript.

Role of Myocardial Fibrosis in Patients with Aortic Stenosis study (NCT01755936; Chapter 4). This was an existing cohort of patients from an observational study investigating the role of CMR and fibrosis imaging in patients with aortic stenosis. The primary results of this study have been published and cited in the corresponding chapter. Patients were recruited from the Edinburgh Heart Centre between March 2012 and August 2014 (n=203). Chapter 4 was a post-hoc study involving echocardiographic image analysis of this cohort. For this

chapter, I was involved in the post-hoc study conception and design and undertook statistical analysis, data interpretation and drafting and revision of the manuscript.

Biothrombus study (NCT04073875; Chapter 5). This was an observational study using 18F-GP1 to investigate bioprosthetic aortic valve thrombus. Chapter 5 is the primary manuscript for this study and is currently under submission. Patients were recruited from the Edinburgh Heart Centre between October 2019 and March 2021 (n=83). I was involved in the study conception, design, funding acquisition, all aspects of study set-up, all patient recruitment and visits, all image analysis, all statistical analysis and data interpretation and drafting and revision of the manuscript.

All patients provided written informed consent at the time of recruitment. All studies were conducted in accordance with the Declaration of Helsinki, were approved by regional Scotland Research Ethics Committees and were sponsored by the Academic and Clinical Central Office for Research and Development (ACCORD), which is a partnership between the University of Edinburgh and the NHS Lothian Health Board.

2.2 Image acquisition

2.2.1 Echocardiography

Echocardiography is the first-line imaging investigation for many cardiac conditions, including valvular heart disease. In brief, transthoracic echocardiography is a safe, non-invasive technique that uses does not require the use of iodinated contrast or ionising radiation. Using ultrasound, standard transthoracic echocardiography acquires two-dimensional images at a high temporal resolution to provide structural and functional information. Doppler echocardiography provides assessments of blood or tissue velocities across selected structures or along a chosen tissue plane. The limitations of echocardiography largely revolve around the central issue of accurate and reproducible imaging. Two-dimensional image quality is subject to various factors such as tissue characteristics, anatomy, patient position and respiration, while Doppler signals can be markedly affected by the orientation and angle of the transducer in relation to the direction of blood flow or tissue movement. Imaging is also dependent on operator skill and expertise: instantly recognisable scenarios include the apparent regression of aortic stenosis (due to underestimation of transvalvular velocities) and the mysterious disappearing pericardial effusion (a more elusive phenomenon, perhaps encountered emergently in the early morning hours after an initial scan by another party).

The Edinburgh Clinical Research Facility has a dedicated echocardiogram machine (Affiniti 70, Philips, Amsterdam, Netherlands) and British Society of Echocardiography-accredited cardiac sonographer. Research transthoracic echocardiograms conducted were undertaken by this sonographer or study investigators (cardiology fellows) according to contemporaneous

major society guidelines. Routine dataset acquisition included standard two-dimensional views and pulsed and continuous wave Doppler measurements, the latter averaged over three cardiac cycles or five if the patient was in atrial fibrillation (Baumgartner et al., 2009). Despite the limitations mentioned above, we have demonstrated good scan-rescan reproducibility for key parameters of aortic stenosis in the setting of a dedicated research trial (Doris et al., 2020) which is in keeping with other data (Bunting et al., 2019; Otto et al., 1989). Adjuncts such as contrast agents have been shown to provide modest improvements in the interobserver reproducibility of several measurements, being summations of scan-rescan reproducibility as well as the measurements themselves (Smith et al., 2004), but are uncommonly used in clinical practice and were not used in these studies.

2.2.2 Cardiac magnetic resonance

Cardiac magnetic resonance (CMR) provides unparalleled soft tissue characterization and quantification of cardiac volumes and flow, utilising a directional magnetic field and radiofrequency pulses to generate magnetic moments and induce measurable radiofrequency signals from hydrogen nuclei. Tissues demonstrate different voxel intensities based on proton density and tissue-specific relaxation times. As with echocardiography, the lack of iodinated contrast and ionising radiation is a distinct advantage. Some of the more prominent limitations of CMR include the existence of relative or absolute contraindications to entering the magnetic field, claustrophobia, and cost and access to a facility with the requisite scanner, software and staff. CMR techniques offer the best available non-invasive method of capturing the spectrum of fibrotic changes within the left ventricular myocardium, which is of particular interest in aortic stenosis.

The detection and quantification of replacement fibrosis using CMR is an established technique and has a larger evidence base than techniques which assess diffuse interstitial fibrosis. It requires the use of gadolinium-based contrast agents (GBCAs) which shorten the T1 time – broadly, the tissue-specific recovery time following magnetization – and provide a high intensity signal on T1-weighted imaging. These large molecule agents distribute at different rates into healthy and diseased myocardium, partitioning into extracellular space and washing out of regions of focal replacement fibrosis at a slower rate than healthy tissue. The contrast in signal provides a visual difference between areas of replacement fibrosis (white) and healthy myocardium (black), although it is insensitive for detecting diffuse interstitial fibrosis. Late gadolinium enhancement (>7 min after injection, LGE) is the standard parameter and is usually presented as either a dichotomous finding or a percentage of myocardial volume.

T1 mapping is the cornerstone of interstitial fibrosis imaging with CMR. There are several different approaches, including native T1, extracellular volume fraction (ECV%) and indexed extracellular volume (iECV) (Messroghli et al., 2017; Puntmann et al., 2016). There are various T1 mapping protocols. Images are acquired at several timepoints during tissue recovery, with T1 times encoded as signal intensities within each voxel. Clinical interpretation is facilitated by applying colour look-up tables for visual assessment. Native T1 values (milliseconds) are measured without GBCAs and reflect the combined intracellular and extracellular compartments. Values increase with a greater burden of fibrosis and are usually measured on a per-segment basis. In contrast, ECV% and iECV (mL or mL/m2) use GBCAs to target the extracellular space. ECV% represents the extracellular matrix as a proportion of total left ventricular myocardial volume, whereas iECV adjusts for left

ventricular myocardial volume (ECV% x left ventricular myocardial volume) and offers a measure of absolute matrix volume (Chin et al., 2017; Treibel, Kozor, et al., 2018). A barrier to the widespread adoption of T1 mapping has been standardization between vendors and sequences and unclear thresholds for normal values. Recently, extensive research has been conducted as part of the International T1 Multicentre Outcome CMR Study (NCT02407197, NCT03749343) to develop and validate cross-vendor sequences that are transferable, reproducible and easy to acquire. Consequently, T1 mapping is now at the forefront of myocardial imaging research. Given the distinct differences between reactive interstitial fibrosis and replacement fibrosis, the combination of CMR T1 mapping and LGE offers a comprehensive assessment of myocardial disease that is currently unmatched by any other imaging modality.

All CMR scans were performed on a 3 Tesla scanner (MAGNETOM Verio, Siemens) with ECG gating. A standardised protocol included localiser sequences, left ventricular imaging (long-axis cines and short-axis stacks [8mm slice thickness, no gap]), and phase contrast imaging. Late-gadolinium enhancement imaging was acquired 15 minutes after administration of 0.1 mmol/kg gadobutrol with two-dimensional gradient echo recall sequences and phase swaps. T1 mapping was performed using the modified Look-Locker inversion recovery sequence (Messroghli et al., 2007) with two left ventricular short-axis slices (basal and mid-ventricular). T1 mapping techniques with various protocols have been shown to have good inter-, intra- and scan-rescan reproducibility, particularly ECV% (Chin et al., 2014; Fontana et al., 2012; Singh et al., 2015).

2.2.3 Computed tomography

Computed tomography (CT) is based on the fundamental principles that the density of an object through which an x-ray beam passes can be calculated by measuring the attenuation coefficient of the beam, and that multiple projections allow reconstruction of the object. For the purposes of cardiac imaging, the high spatial resolution of CT is offset by cardiac motion which must be accounted for during image acquisition. Although the intravenous administration of iodinated contrast provides enhanced anatomical definition, this has predominantly been to facilitate visualisation of the epicardial coronary arteries for the investigation of coronary artery disease, or for delineation of the aortic valve annulus, aorta and peripheral vasculature for transcatheter aortic valve implantation (TAVI) pre-procedural planning. Aortic valve assessment to determine disease severity has remained the purview of non-contrast CT calcium scoring (CT-AVC). A substantial body of observational derivation and validation data have provided clinically applicable thresholds of calcium scores for defining severe aortic stenosis – 1300 Agatston units for women and 2000 for men - that are incorporated into international guidelines (Baumgartner et al., 2017; Clavel et al., 2013; Clavel et al., 2014; Otto et al., 2021; Pawade et al., 2018). Despite the limitations of the technique as previously discussed, we have demonstrated excellent scan-rescan reproducibility (Doris et al., 2020).

Unless contraindicated, intravenous or oral metoprolol was administered to patients with a heart rate >65 /min. Imaging was performed on a 128-multislice scanner (Biograph mCT, Siemens, Germany) in a dedicated research imaging centre (Edinburgh Imaging Facility, Queen's Medical Research Institute, University of Edinburgh). All CT imaging was performed with ECG gating and a standardised protocol. Non-contrast CT for CT-AVC was performed using automated dose modulation (120kV CARE Dose4D, Siemens) with 3-mm

slice thickness, spiral acquisition at 70% R-R interval and on inspiratory breath-hold. Contrast-enhanced CT was undertaken following PET acquisition (see below). Intravenous iodinated contrast (80 mL Iomeron-400, Bracco Imaging, Italy) was given, followed by CT image acquisition. This was undertaken in diastole with prospective ECG gating (50-75% R-R interval, expiratory breath-hold) or across the entire cardiac cycle with retrospective ECG gating (0-90% R-R interval, expiratory breath-hold). The latter was used in the Biothrombus study to facilitate assessment of bioprosthetic aortic valve leaflet motion (Genereux et al., 2021; Jilaihawi et al., 2017).

2.2.4 Positron emission tomography

Molecular cardiac imaging with positron emission tomography (PET) is a technique that remains largely investigational for cardiovascular applications but has a broad range of potential applications. Hybrid scanners permit combined assessments of disease activity and anatomy with PET-CT or PET-CMR. Radiotracers are injected intravenously and localise to areas where the disease process of interest is active. The photons ejected following collision of the emitted positron with a free electron can then be detected and localised by the PET scanner. This data can then be fused with the anatomical datasets. In principle, this approach can be used to investigate the activity of any pathological process, subject to the availability of a relevant radiotracer. The radiotracer must have a clear biological pathway to target, which then governs the specificity of the radiotracer for a given disease process, and must have favourable pharmacokinetics and pharmacodynamics. Consequently, the clinical use of this technique, cardiac or otherwise, has been largely limited to 18F-fluorodeoxyglucose, which is an analogue of glucose and therefore provides information about non-specific metabolic activity in a region of interest. Our institution has helped pioneer research into the

use of 18F-sodium fluoride (NaF) to detect active microcalcification in the cardiovascular system. We have shown minimal bias and good concordance on scan-rescan analysis of the coronary arteries (Moss et al., 2019) – a challenging structure to image due to their small volume, cardiac motion and the limited spatial resolution of PET. With collaborators, we have demonstrated similar findings in 18F-NaF PET of the aortic valve (Massera et al., 2020). When interpreting scan-rescan reproducibility for PET, it is particularly important to adjust for blood pool activity, which will vary due to radiotracer handling on a given day, as well as be cognizant of the very recent iterative improvements in image reconstruction and analysis that have added further precision to the technique (Chapter 2.3.4).

18F-NaF or 18F-GP1 cardiac PET-CT was performed on a 128-multislice scanner (Biograph mCT, Siemens, Germany). Image acquisition was performed approximately 60 min after intravenous injection of 125 MBq 18F-NaF or 250 MBq 18F-GP1 with a single bed position centred on the aortic valve, preceded by an attenuation correction CT scan. Images were reconstructed using an ordered subset expectation maximisation algorithm with time-of-flight capability enabled, undergoing 4 iterations of 21 subsets and split into 4 equal gates, each representing 25% of the cardiac cycle. Reconstructions were scaled to a 256 x 256-pixel matrix and used a zoom factor of 2. Gaussian smoothing was applied with a 3-mm full-width at half-maximum kernel.

2.3 Image analysis

2.3.1 Echocardiography

Image analysis was performed using EchoPAC (GE Healthcare, Chicago, Illinois). Aortic valve pressure gradient was calculated using the modified Bernoulli equation (change in pressure = 4(velocity^2)), with inclusion of the proximal (left ventricular outflow tract) velocity if >1.5 m/s (change in pressure = 4($V2^2 – V1^2$) (Baumgartner et al., 2009). Aortic valve area or effective orifice area of prosthetic valves was estimated using the continuity equation (estimated circular left ventricular outflow tract area multiplied by left ventricular outflow tract velocity-time integral, divided by aortic velocity-time integral and indexed to body surface area according to the Du Bois method (Du Bois & Du Bois, 1989)). Aortic stenosis was categorised using standard definitions for peak velocity (mild: 2.6-2.9, moderate: 3.0-4.0, severe: >4.0 m/s) – which is generally the most reproducible measure of aortic stenosis severity (Moura et al., 2011; Sacchi et al., 2018) - and mean gradient (mild: <20, moderate: 20-40, severe: >40 mmHg) (Baumgartner et al., 2009). Ejection fraction was visually estimated and categorised as normal (≥55%), mildly impaired (45-54%), moderately impaired (36-44%) or severely impaired (≤35%) (Harkness et al., 2020). For studies where ejection fraction was quantified, the Simpson's bi-plane method was used to estimate left ventricular volumes. Valvuloarterial impedance (Zva), a validated and prognostic measure of global left ventricular afterload in aortic stenosis, was calculated where relevant as follows: (systolic blood pressure + mean aortic valve gradient)/stroke volume indexed to body surface area (Briand et al., 2005). Dedicated EF1 measurements were performed (Chapter 4.2).

2.3.2 Cardiac magnetic resonance

Existing image analysis had been performed using OsiriX v4.1.1 (Pixmeo SARL, Geneva, Switzerland). Standard measurements of left ventricular mass and volumes were acquired from short-axis cine stacks. Late-gadolinium enhancement was assessed qualitatively. Native T1, extracellular volume fraction (ECV%) and indexed extracellular volume (iECV = ECV% x left ventricular diastolic myocardial volume indexed to body surface area) were also measured. The latter measurement provides an absolute estimate of the extracellular compartment, in contrast to ECV% which estimates this volume relative to cellular volume (Chin et al., 2017; Treibel, Kozor, et al., 2018). Both ECV% and iECV included non-infarct and excluded infarct LGE (Treibel, Kozor, et al., 2018). Global longitudinal strain (GLS) was measured using CVI4.2 (Circle Cardiovascular Imaging, Canada) (Spath et al., 2019). A fully automated strain analysis was carried out and two-dimensional GLS was used as the primary strain assessment. Echocardiographic GLS software was not available for this cohort, but measurements acquired on echocardiography and CMR have been shown to correlate well (Obokata et al., 2016).

2.3.3 Computed tomography

Image analysis was performed using Vitrea v6.9.68.1 (Vitrea Advanced, Vital Images, Minnetonka, USA) or OsiriX v8.0.3 / v12.0.1. Aortic valve calcium scores were measured using a standardised and reproducible technique from non-contrast CT imaging (Pawade et al., 2019), with regions of interest drawn around areas of valvular calcification on sequential axial slices. Care was taken to exclude calcification in adjacent structures such as the left ventricular outflow tract or sinuses of Valsalva. A standard threshold of 130 Hounsfield units was used to define calcification. The Agatston score was semi-automatically calculated in Vitrea using standard weightings (Agatston et al., 1990). A dedicated technique of measuring

calcific and non-calcific leaflet volumes on contrast-enhanced CT was developed (Chapter 3.2). For patients with bioprosthetic aortic valves who underwent retrospectively-gated CT, the presence or absence of hypoattenuated leaflet thickening (HALT) was established in diastole. If HALT was present, the percentage of leaflet involvement was semi-qualitatively assessed along a curvilinear orientation of the affected leaflet on a long axis view (Blanke et al., 2019) and maximal leaflet opening examined in systole to determine if there was reduced leaflet motion. The percentage of reduced leaflet motion was quantified as the distance from the frame to the affected leaflet tip at maximal excursion divided by the valve radius at that level (Jilaihawi et al., 2017).

2.3.4 Positron emission tomography-computed tomography

Image analysis was performed using bespoke software developed for hybrid PET imaging (FusionQuant v1.20.05.14 (Cedars-Sinai, CA, USA) which allows more rapid analysis than other commercially available software (Massera et al., 2020). 18F-NaF and 18F-GP1 native and bioprosthetic aortic valve uptake was measured using a standardised technique, with accurate co-registration of PET and contrast CT based on blood pool uptake in the cardiac chambers followed by *en face* orientation of the valve (Massera et al., 2020; Pawade et al., 2016). The valve region of interest was defined by a three-dimensional polyhedron 6-mm in height, centred on the valvular region of highest visual uptake in the *z* plane and contoured manually around the valve perimeter at the widest point. In patients with bioprosthetic aortic valves, the polyhedron was contoured to the valve frame at the leaflet coaptation point. Blood pool activity was calculated from a region drawn at the centre of the right atrium. In the case of 18F-GP1, care was taken to avoid the inclusion of pacemaker leads in the blood pool region of interest, since these leads demonstrated discrete elevated 18F-GP1 uptake. The

mean and maximum target to background ratios (TBR_{mean} and TBR_{max}) were calculated by dividing the mean and maximum standardised uptake values in the valve region of interest by the mean blood pool standardised uptake value. These measures have excellent inter- and intra-observer reproducibility (Doris et al., 2020; Pawade et al., 2018; Pawade et al., 2016).

2.4 Statistical analysis

Categorical variables are presented as number (percent). Continuous variables were assessed with quantile-quantile plots and the Shapiro-Wilk test and presented as mean ± standard deviation or median [interquartile range]. Between group comparisons were predominantly undertaken with the Wilcoxon rank sum test (non-parametric continuous variables); the Chi-square test (categorical variables), Student's t-test (parametric continuous variables) and Kruskal-Wallis test (>2 non-parametric continuous variables) were applied where appropriate. Correlations between independent non-parametric variables were assessed with Spearman's rank correlation coefficient. Univariable and multivariable regression models were constructed to assess associations between dependent variables of interests and selected independent co-variates. Time-to-event analyses were undertaken with Kaplan-Meier curves and Cox proportional hazards regression models. Throughout, covariate selection and model construction were based upon prior data or proposed plausible mechanistic relationships rather than stepwise selection, and model fits were examined by plotting model residuals against fitted values and checking residual distributions with quantile-quantile plots. Two-sided p-values <0.05 were considered statistically significant. All analyses were performed using R (R Foundation for Statistical Computing, Vienna, Austria).

Chapter 3 – Contrast-enhanced computed tomography assessment of aortic stenosis

Adapted from:

Cartlidge TR*, Bing R*, Kwiecinski J, Guzzetti E, Pawade TA, Doris MK, Adamson PD, Massera D, Lembo M, Peeters FECM, Couture C, Berman DS, Dey D, Slomka P, Pibarot P, Newby DE, Clavel MA, Dweck MR. Contrast-enhanced computed tomography assessment of aortic stenosis. Heart. 2021 Jan 29:heartjnl-2020-318556. doi: 10.1136/heartjnl-2020-318556.

* Authors contributed equally.

3.1 Abstract

Objectives

Non-contrast computed tomography (CT) aortic valve calcium scoring ignores the contribution of valvular fibrosis in aortic stenosis. We assessed aortic valve calcific and non-calcific disease using contrast-enhanced CT.

Methods

This was a post-hoc analysis of 164 patients (median age 71 [interquartile range 66-77] years, 78% male) with aortic stenosis (41 mild, 89 moderate, 34 severe; 7% bicuspid) who underwent echocardiography and contrast-enhanced CT as part of imaging studies. Calcific and non-calcific (fibrosis) valve tissue volumes were quantified and indexed to annulus area, using Hounsfield unit thresholds calibrated against blood-pool radiodensity. The fibro-calcific ratio assessed the relative contributions of valve fibrosis and calcification. The fibro-calcific volume (sum of indexed non-calcific and calcific volumes) was compared to aortic valve peak velocity and, in a subgroup, histology and valve weight.

Results

Contrast-enhanced CT calcium volumes correlated with CT calcium score ($r=0.80$, $p<0.001$) and peak aortic jet velocity ($r=0.55$, $p<0.001$). The fibro-calcific ratio decreased with increasing aortic stenosis severity (mild: 1.29 [0.98-2.38], moderate: 0.87 [1.48-1.72], severe: 0.47 [0.33-0.78], $p<0.001$), while the fibro-calcific volume increased (mild: 109 [75-150], moderate: 191 [117-253], severe: 274 [213-344] mm^3/cm^2). Fibro-calcific volume correlated with *ex vivo* valve weight ($r=0.72$, $p<0.001$). Compared with the Agatston score,

fibro-calcific volume demonstrated a better correlation with peak aortic jet velocity (r=0.59 and r=0.67 respectively), particularly in females (r=0.38 and r=0.72 respectively).

Conclusions

Contrast-enhanced CT assessment of aortic valve calcific and non-calcific volumes correlates with aortic stenosis severity and may be preferable to non-contrast CT when fibrosis is a significant contributor to valve obstruction.

3.2 Introduction

The pathogenesis of aortic stenosis involves an initiation phase characterized by mechanical injury, lipid deposition and a localized inflammatory response, followed by a propagation phase wherein progressive valve fibrosis and calcification promote worsening valvular stenosis (Pawade et al., 2015). Recent guidelines recommend non-contrast CT calcium scoring of the aortic valve (CT-AVC) as an arbiter of aortic stenosis severity when echocardiographic measurements are discordant (Baumgartner et al., 2017). This recommendation is based upon data demonstrating the diagnostic accuracy of CT-AVC as a flow-independent measure and its correlation with disease progression and clinical events (Clavel et al., 2013; Clavel et al., 2014; Pawade et al., 2018). However, CT-AVC has several important limitations. First, it offers little detail about valve morphology and is unable to localize the anatomical distribution of calcium in the valve and surrounding structures. Second, CT-AVC cannot quantify fibrosis, an important contributor to valve stenosis, and may therefore misclassify disease severity, particularly in young females and those with bicuspid valves (Shen et al., 2017; Simard et al., 2017). Third, it demonstrates only moderate associations with haemodynamic severity on echocardiography. Fourth, different thresholds for severe aortic stenosis have been proposed for males and females, with females consistently demonstrating lower calcium burden for a given degree of valvular stenosis, even after correction for body size (Clavel et al., 2013; Clavel et al., 2014; Pawade et al., 2018).

Contrast CT angiography is widely used to assess and to quantify calcific and non-calcific plaques in the coronary vasculature (Dweck et al., 2016). It is the gold standard method of

anatomical assessment before transcatheter aortic valve intervention (TAVI) and is routinely incorporated into clinical workflows (Achenbach et al., 2012; Blanke et al., 2019). In the present study, we used contrast-enhanced cardiac CT to evaluate aortic valve calcium volumes and also non-calcific leaflet thickening as a marker of valve fibrosis. We hypothesized that this technique would provide insights into the pathogenesis of aortic stenosis whilst accurately quantifying disease severity.

3.3 Methods

Study populations

This was a post-hoc analysis of patients with aortic stenosis (peak aortic jet velocity >2.5 m/s) from two study cohorts. The first cohort was the Study Investigating the Effect of Drugs Used to Treat Osteoporosis on the Progression of Calcific Aortic Stenosis (SALTIRE2) randomized controlled trial of novel drug treatments in aortic stenosis (NCT 02132026) which recruited individuals >50 years of age with aortic stenosis from the Edinburgh Heart Centre, as described previously. The second cohort comprised patients >18 years of age from the AVCa study (Quebec Heart and Lung Institute) in whom contrast-enhanced CT was performed <3 months prior to surgical aortic valve replacement (AVR). Exclusion criteria were non-calcific aortic stenosis (i.e. rheumatic aortic stenosis, history of infective endocarditis, cervical or thoracic radiotherapy-induced valve lesions), left ventricular ejection fraction (<50%), moderate-to-severe or severe aortic regurgitation, or previous aortic valve procedure. A control group was selected from patients without aortic stenosis in the Dual Antiplatelet Therapy to Reduce Myocardial Injury (DIAMOND) trial (NCT02110303), based on the lack of visual aortic valve calcification on CT. These studies were approved by the South East Scotland Research Ethics Committee, the Medicine and Healthcare products Regulatory Agency of the United Kingdom, the research ethics committee of the Quebec Heart and Lung Institute and conducted in accordance with the Declaration of Helsinki. Written informed consent was obtained from all participants.

Study assessments and data collection

Clinical evaluation and echocardiography were undertaken as study-based procedures. CT-AVC and contrast-enhanced CT were performed in SALTIRE2 and DIAMOND, while contrast-enhanced CT scans, explanted aortic valve weights and histology were available in patients from AVCa.

Image analysis

Standard echocardiography and CT image acquisition and image analysis were performed as previously described.

Contrast CT analysis was performed blinded to echocardiographic assessments and vice versa. A multi-planar reconstruction was oriented in the short-axis plane of the aortic valve and, using the annulus as the reference slice, resliced in 3-mm increments through the valve (Pawade et al., 2019; Pawade et al., 2016). Slice thickness was selected to be consistent with CT-AVC. Blood pool contrast attenuation (Hounsfield Units, HU) was sampled within a 2-cm^2 circular region of interest in the centre of the aortic root lumen at the level of the sinotubular junction. Quantification of aortic valve leaflet calcific and non-calcific leaflet volume was then performed using SliceOmatic (Tomovision, Magog, Canada). Using the *en face* multi-planar reconstructions, the region-growing tool was employed to select voxels within a defined range of attenuation. The lower threshold for detection of calcium was set at 3 standard deviations above the mean attenuation measured within the blood pool region of interest. For non-calcific leaflet tissue, a fixed lower threshold of 30 HU was employed to exclude artifact (e.g. photon starvation adjacent to dense calcification). The upper threshold for non-calcific tissue was calibrated to blood pool attenuation according to analysis of a derivation cohort (DIAMOND) comprising 100 scans of patients with non-calcified aortic

valves. Two independent observers titrated the upper threshold for non-calcific leaflet thickening starting at 200 HU and adjusting by increments of 25 HU in either direction until the margins of the 3 aortic valve cusps were delineated without any highlighting of the blood pool. When this visually determined threshold (x) was plotted against mean blood pool attenuation (y), a strong linear relationship was identified (r^2=0.90, p<0.001) with the equation x = 41.46 + 0.42(y). Using these thresholds, areas of calcific and non-calcific leaflet thickening were assessed and quantified. Each adjacent 3-mm slice was assessed so that the whole volume of the valve was covered, with care to avoid regions of calcification in the aorta and coronary arteries. Leaflet volumes were indexed to the annulus area measured on contrast-enhanced CT. This method is widely used and repeatable (Achenbach et al., 2012; Gurvitch et al., 2011). Valve weights were also indexed to the annulus area.

Inter-observer reproducibility

Measurements of non-calcific and calcific leaflet volumes were performed independently in 20 patients by two experienced operators (TC, JK) in order to assess inter-observer reproducibility. For this purpose, non-calcific and calcific volumes were not indexed to aortic valve area as the reproducibility of annular dimensions measured by CT angiography has been well described.

Fibro-calcific ratio and fibro-calcific volume

The fibro-calcific ratio was derived by dividing the non-calcific by the calcific indexed leaflet volumes. A ratio >1.0 indicated a predominance of non-calcific (fibrotic) volume in the valve, whilst a ratio ≤1.0 indicated that ≥50% of the measured volume was comprised of

calcification. The fibro-calcific volume was calculated by adding the indexed calcific and non-calcific leaflet volumes.

Valve histology

In the AVCa cohort, aortic valves were excised at surgery, placed in a container filled with HEPES solution and examined by a single pathologist who was blinded to the CT and echocardiographic assessments. One of the cusps was decalcified in Cal-Ex (Fisher, Nepean, Ontario, Canada) for 24 hours and fixed in formaldehyde 10% for histological processing. Aortic valve leaflets were embedded in optimal cutting temperature compound and 6-µm sections were obtained from a skilled operator using a cryotome. At least 5 histological sections per leaflet were analysed with Masson's trichrome or Verhoeff-Van Giesson staining to assess regions of fibrosis, calcification, thrombus or lipid. Semi-quantitative assessment of valve fibrosis (1: mild, 2: moderate, 3: severe) and calcification (Warren-Yong score - 1: absent, 2: mild valve thickening and early nodular calcification, 3: moderate thickening with many calcified nodules, 4: severe thickening with many calcified nodules) was performed according to previously published techniques (Cote et al., 2014; Simard et al., 2017; Warren & Yong, 1997). Valve cusps and any accompanying fragments were removed from 4-(2-hydroxyethyl)-1-piperazineethanesulfonic acid solution, placed on absorbing paper, and then weighed on laboratory scales with a tolerance of 0.01 g. Areas of non-calcific leaflet thickening observed on the CT were targeted for histological analysis.

Statistical analysis

Analyses specific to this study are as follows. Spearman's rank correlation coefficient was performed to assess the relationship between non-contrast and contrast CT and

echocardiographic measures. Linear regression models were constructed with peak aortic jet velocity as the dependent variable and age, female sex and either Agatston score or indexed fibro-calcific volume (both log 2-transformed) as the dependent variables, with female sex and each of the latter as interaction terms. Inter-observer reproducibility was tested using the intraclass correlation coefficient (ICC; two-way random effects, agreement).

3.4 Results

A total of 164 participants with aortic stenosis (41 mild, 89 moderate, 34 severe) were included in the main analysis (Table 3.1). The median age was 71 (66-77) years and the majority were male (78%). All patients had a left ventricular ejection fraction ≥50%. Peak aortic jet velocity was slightly higher in men (Table 3.2), although this was not statistically significant. Four of 36 females were classified as severe aortic stenosis (11%) compared with 30 of 128 males (23%). Other baseline characteristics were similar between females and males. The time from echocardiography to CT was 0 (0-9) days. Thirty-eight participants (50% female, 67 [60-73] years) without evidence of aortic stenosis comprised the control group.

Aortic valve calcification

In the control group, no aortic valve calcification was observed on either non-contrast or contrast-enhanced CT. In the aortic stenosis cohort, the indexed contrast CT calcium volume increased with stenosis severity (mild: 39 [19-64], moderate: 85 [46-187], severe: 190 [113-254] mm^3/cm^2; Figure 3.1-A) and correlated moderately well with peak aortic jet velocity ($r=0.62$, $p<0.001$; Table 3.3). There was excellent inter-observer reproducibility (ICC 0.95 [95% confidence interval (CI) 0.88 to 0.98], $p<0.001$). Females had lower Agatston scores as well as indexed contrast CT calcium volumes compared with males (Table 3.2).

Table 3.1 Baseline demographics

	Overall N=164	**Female N=36**	**Male N=128**	**p**

Age	71 (66-77)	71 (66-77)	71 (66-77)	0.82
Hypertension	116 (70.7)	25 (69.4)	91 (71.1)	0.99
Hypercholesterolaemia	95 (57.9)	22 (61.1)	73 (57.0)	0.75
Diabetes mellitus	43 (26.2)	8 (22.2)	35 (27.3)	0.71
Coronary artery disease	62 (37.8)	15 (41.7)	47 (36.7)	0.70
Current/ex-smoker	65 (39.6)	12 (33.3)	53 (41.4)	0.51
Medications				
Antiplatelets	92 (56.1)	16 (44.4)	76 (59.4)	0.15
Oral anticoagulation	17 (10.4)	3 (8.3)	14 (10.9)	0.15
ACE inhibitor / ARB	82 (50.0)	17 (47.2)	65 (50.8)	0.85
Beta-blocker	61 (37.2)	11 (30.6)	50 (39.1)	0.46
Statin	107 (65.2)	19 (52.8)	88 (68.8)	0.09
Abbreviations: ACE, angiotensin converting enzyme; ARB, angiotensin 2 receptor blocker				

Table 3.2 Imaging parameters

	Overall N=164	**Female N=36**	**Male N=128**	**p**
Echocardiography				
Peak aortic jet velocity (m/s)	3.44 (3.00-3.87)	3.26 (2.96-3.61)	3.53 (3.00-3.94)	0.11
Mean aortic valve gradient (mmHg)	27 (18-34)	24 (18-32)	28 (19-34)	0.40
Aortic valve area (cm^2)	1.01 (0.82-1.24)	1.03 (0.84-1.18)	1.01 (0.81-1.27)	0.74
Computed tomography				
Bicuspid aortic valve	11 (7)	0 (0)	11(9)	0.12
Agatston score	1163 (670-2169)	460 (206-1010)	1474 (823-2362)	<0.001
Indexed contrast CT calcific volume (mm^3/cm^2)	82 (42-181)	33 (17-75)	103 (55-194)	<0.001
Indexed contrast non-calcific volume (mm^3/cm^2)	79 (49-104)	57 (39-98)	82 (56-104)	0.09
Indexed fibro-calcific volume (mm^3/cm^2)	187 (115-265)	115 (72-184)	203 (130-279)	<0.001
Fibro-calcific ratio	0.86 (0.47-1.54)	1.27 (0.78-4.23)	0.76 (0.41-1.45)	0.002
Blood pool radiodensity (HU)	401 (326-511)	550 (453-600)	366 (319-467)	<0.001

Abbreviations: CT, computed tomography; HU, Hounsfield units

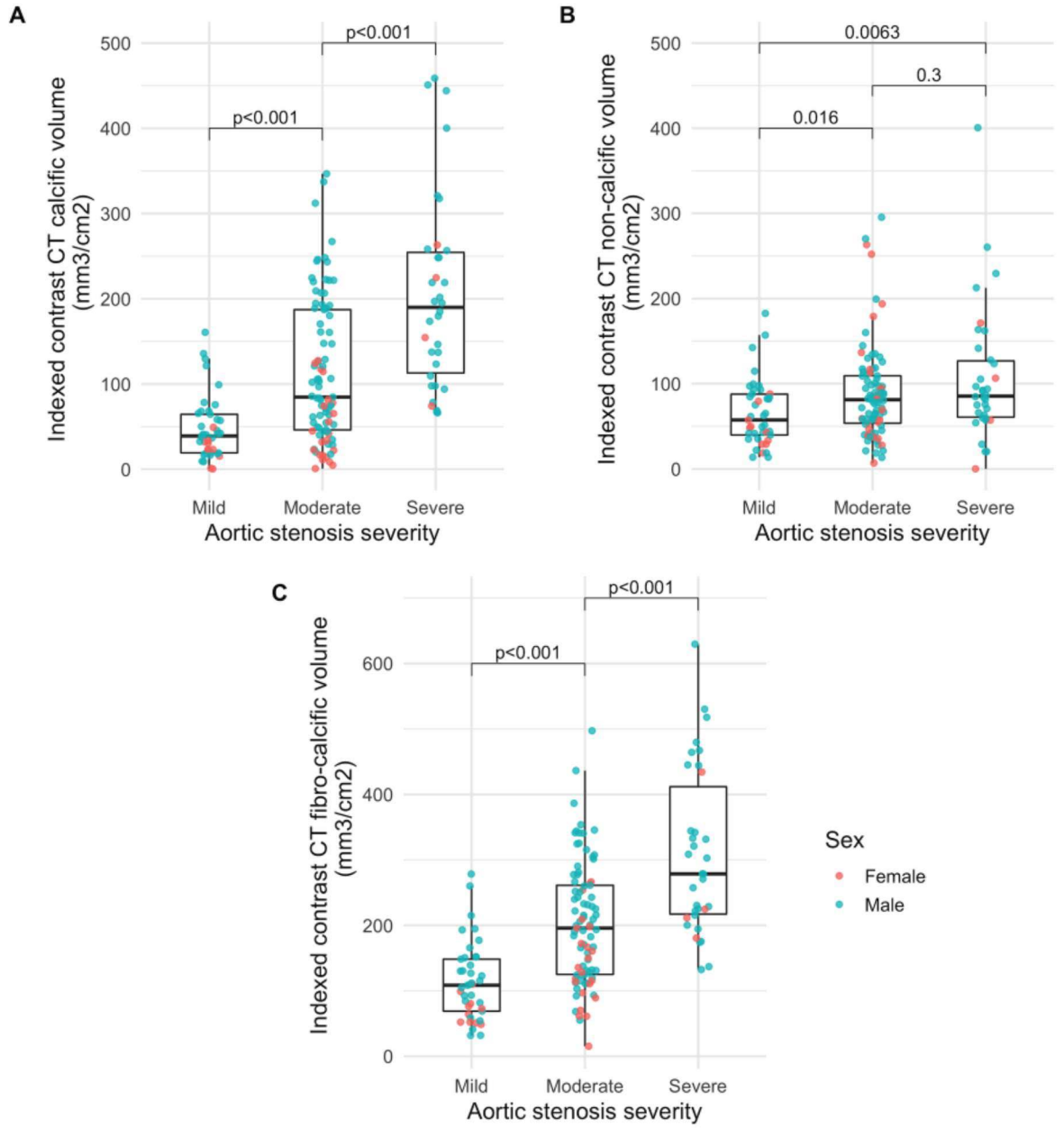

Figure 3.1 Indexed contrast CT leaflet volumes and aortic stenosis severity

Box plots of indexed contrast CT calcific (A), non-calcific (B) and fibro-calcific (C) volumes stratified by aortic stenosis severity. P values for Wilcoxon rank sum test.

Abbreviations: CT, computed tomography.

Table 3.3 Correlations between CT and echocardiography			
		Peak aortic jet velocity*	**p***
Indexed contrast CT calcific volume	**All**	0.62	<0.001
	Male	0.61	<0.001
	Female	0.52	0.001
Indexed contrast CT non-calcific volume	**All**	0.27	<0.001
	Male	0.26	0.003
	Female	0.32	0.053
Indexed contrast CT fibro-calcific volume	**All**	0.67	<0.001
	Male	0.66	<0.001
	Female	0.72	<0.001
Agatston score^	**All**	0.59	<0.001
	Male	0.57	<0.001
	Female	0.38	0.054
* Spearman's rank correlation coefficients ^n = 135 / 164 Abbreviations: CT, computed tomography			

Non-calcific leaflet volume

In the control cohort, the indexed non-calcific leaflet volume was 30 (20-43) mm^3/cm^2 with no sex differences (females: 33 [19-43] versus males: 27 [21-39] mm^3/cm^2, p=0.18). In patients with aortic stenosis, indexed non-calcific leaflet volumes were higher than in the control cohort but only trended towards an increase with more severe stenosis (mild: 57 [40-

88], moderate: 81 [54-109], severe: 85 [61-127] mm^3/cm^2; Figure 3.1-B). There was a weak correlation with peak velocity (r=0.27, p<0.001, Table 3.3). Inter-observer reproducibility was excellent (ICC: 1.00 (95% CI 0.99 to 1.00), p<0.001). In contrast to the indexed calcific volume, the indexed non-calcific volume was only slightly lower in females than males (Table 3.2).

Fibro-calcific volume and fibro-calcific ratio

The indexed fibro-calcific volume increased across aortic stenosis severity categories (mild: 109 [69-148], moderate: 196 [125-261], severe: 279 [217-412] mm^3/cm^2; Figure 3.1-C). Compared with the Agatston score, fibro-calcific volume demonstrated a better correlation with peak aortic jet velocity (r=0.59 and r=0.67 respectively), particularly in females (r=0.38 and r=0.72 respectively) (Table 3.3, Figure 3.2). The fibro-calcific ratio decreased with increasing stenosis severity (mild: 1.29 [0.90-2.30], moderate: 0.83 [0.47-1.57], severe: (0.52 [0.34-0.94]) and was higher in females than in males (Figure 3.3).

On multivariable linear regression modelling with peak aortic jet velocity as the dependent variable and adjusting for age, sex and Agatston score, the latter two covariates were independently associated with peak velocity (p=0.001 and p<0.001, model adjusted r^2=0.31), with an interaction between female sex and Agatston score (p=0.002; Table 3.4). When constructing the same model but replacing Agatston score with indexed fibro-calcific volume, the only independent predictor of peak aortic jet velocity was the indexed fibro-calcific volume (p<0.001, model adjusted r^2=0.36). There was no interaction with female sex or difference in model fit on one-way analysis of variance (p=0.27).

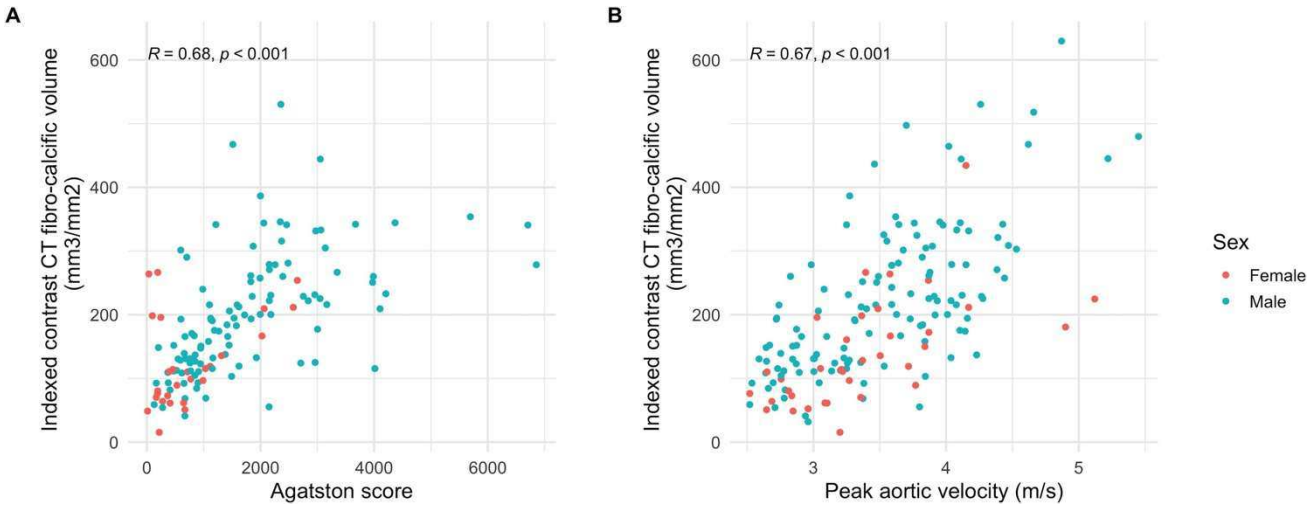

Figure 3.2 Fibro-calcific volume and standard measures of aortic stenosis severity

Scatter plots of indexed fibro-calcific volume, Agatston score (A) and peak aortic jet velocity (B). R and p values for Spearman rank correlation coefficient.

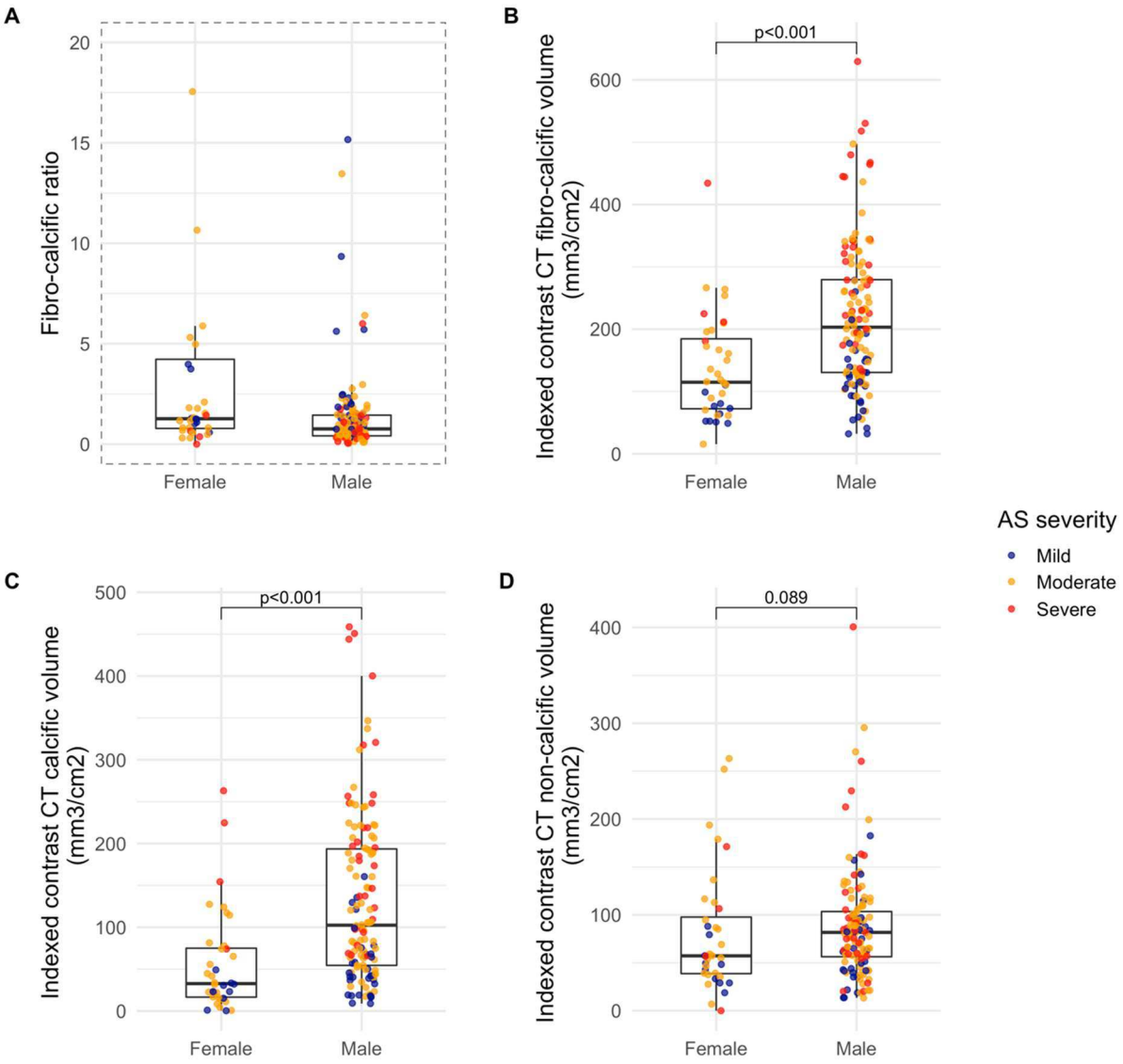

Figure 3.3 Indexed contrast CT leaflet volumes and sex

A: Box plots of fibro-calcific ratio according to sex. For visualization purposes only, 4 patients with high fibro-calcific ratios (356, 127, 74 and 42) have not been included in the plot. All 4 were female. Wilcoxon rank sum p<0.001. B-D: Box plots of indexed contrast CT fibro-calcific (B), calcific (C) and non-calcific (D) volumes according to sex. P values for Wilcoxon rank sum test.

Table 3.4 Multivariable linear regression models for prediction of peak aortic jet velocity			
	Coefficient	**p value**	**Adjusted R^2**
Model 1			0.31
Intercept	0.47		
Age (per year)	0.00	0.97	
Sex (female)	0.86	0.001	
log2(Agatston score)	0.12	<0.001	
Sex*log2(Agatston score)	-0.09	0.002	
Model 2*			0.36
Intercept	0.29		
Age (per year)	0.00	0.65	
Sex (female)	0.20	0.59	
log2(indexed contrast CT fibro-calcific volume)	0.19	<0.001	
Sex*log2(indexed contrast CT fibro-calcific volume)	-0.03	0.64	
*Restricted to same patients in Model 1, i.e. those with Agatston score available. Abbreviations: CT, computed tomography			

Histology

Valve weight was available in 26 patients. There was a strong correlation between indexed fibro-calcific volume and indexed valve weight (Figure 3.4-A), in contrast to a probable weak correlation between peak aortic jet velocity and indexed valve weight ($r=0.37$, $p=0.06$). Histological examination confirmed the presence of valve fibrosis that spatially correlated with areas of non-calcific leaflet thickening on CT (Figure 3.5). There was no thrombus or gross lipid deposition observed in these areas. The indexed fibro-calcific volume was higher in patients with higher Warren-Yong and fibrosis scores (Figures 3.4-B,C).

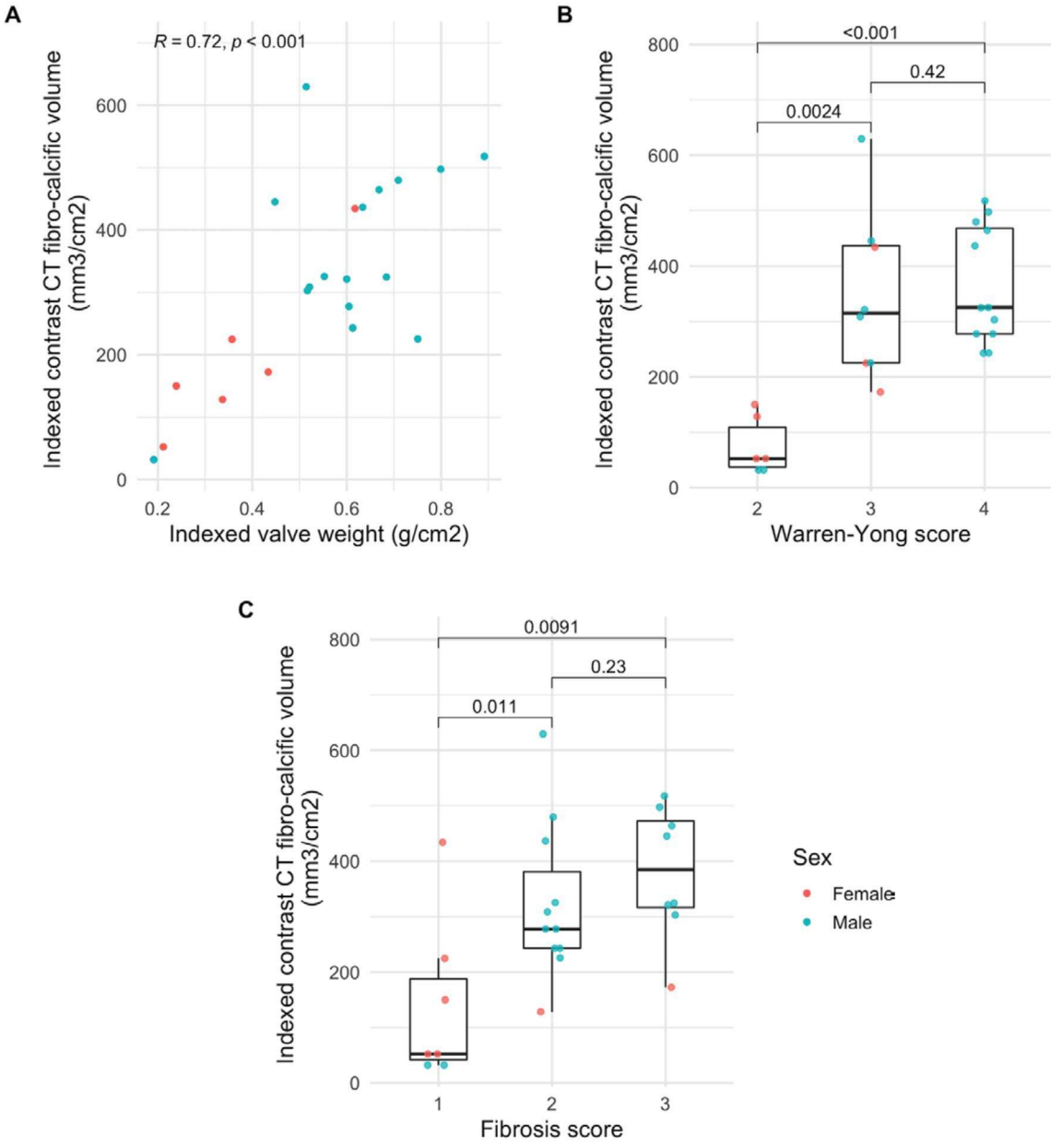

Figure 3.4 Correlations with valve weight

A: Scatter plots of indexed valve weight and indexed fibro-calcific volume. B: Box plots of indexed fibro-calcific volume and Warren-Yong score. C: Box plots of indexed fibro-calcific volume and fibrosis score. R and p values for Spearman rank correlation coefficient.

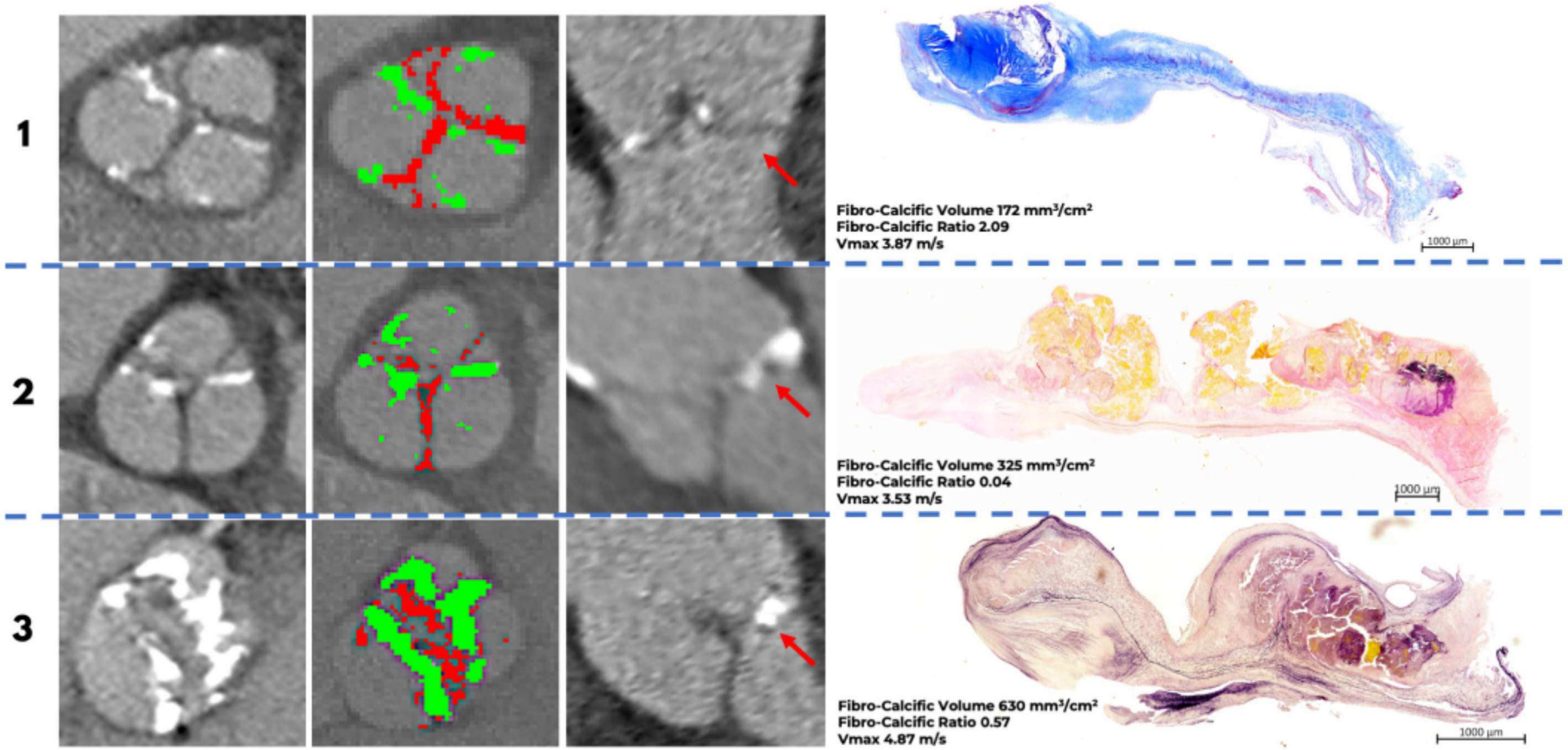
1
2
3
Fibro-Calcific Volume 172 mm³/cm²
Fibro-Calcific Ratio 2.09
Vmax 3.87 m/s
1000 µm
Fibro-Calcific Volume 325 mm³/cm²
Fibro-Calcific Ratio 0.04
Vmax 3.53 m/s
1000 µm
Fibro-Calcific Volume 630 mm³/cm²
Fibro-Calcific Ratio 0.57
Vmax 4.87 m/s
1000 µm

Figure 3.5 Contrast CT and histology

Case 1. A tricuspid aortic valve from a female with a large amount of fibrosis (red) compared to calcification (green) on CT. Histology confirms a preponderance of fibrosis in the valve consistent with the CT findings. There was no clear evidence of valve thrombosis or lipid infiltration. Red arrow denotes the leaflet corresponding to histology. Time from CT to surgery: 15 days. Trichrome Masson staining: blue sections represent collagen; red/purple represents calcium.

Case 2. A tricuspid aortic valve from a male with a small amount of fibrosis compared to calcification (from the 3 CT slices containing the aortic valve this one was the only one with significant fibrosis). This was again confirmed on histological analysis of the valve leaflet. Red arrow denotes the leaflet corresponding to histology. Time from CT to surgery: 15 days. Verhoeff-Van Giesson staining: Black represents elastic fibres, pink collagen fibres, and yellow calcium.

Case 3. A bicuspid aortic valve from a male with extensive fibrosis and calcification in the valve. Findings were again confirmed on histology with the spatial distribution of calcium and fibrosis on histology appearing similar to the calcific and non-calcific leaflet thickening on CT (Verhoeff-Van Giesson staining). Red arrow denotes the leaflet corresponding to histology. Time from CT to surgery: 21 days.

Abbreviations: CT, computed tomography.

3.5 Discussion

We describe a novel method of contrast-enhanced CT analysis that allows assessment of both aortic valve calcification and non-calcific leaflet thickening (fibrosis) in patients with aortic stenosis. We demonstrate the feasibility of contrast-enhanced CT assessment of aortic stenosis severity, with the indexed fibro-calcific volume correlating better with peak aortic jet velocity than CT-AVC in this cohort, particularly in females. Quantifying valve fibrosis, a facet of valvular disease that cannot be assessed with non-contrast CT, may therefore be important in some patients. Given the routine use of contrast-enhanced CT in clinical workflows for TAVI, fibro-calcific volumes could be readily integrated into clinical practice, providing an alternative assessment for patients with uncertain disease severity.

Discordant echocardiographic measures of aortic stenosis severity are observed in around one-third of patients (Clavel et al., 2013; Minners et al., 2010). CT-AVC has emerged as a useful tool in these patients, providing an anatomical, flow-independent assessment of disease severity that is well-validated in concordant disease and supported by international guidelines. We found that assessments of valve calcification on contrast-enhanced CT correlated well with CT-AVC. However, progressive valve stiffening and narrowing in aortic stenosis occurs due to both fibrosis and calcification (Hinton et al., 2006; Yetkin & Waltenberger, 2009), and CT-AVC, which quantifies only the latter, may underestimate aortic stenosis severity in cases where valve obstruction is predominantly due to the former. Sex-specific CT-AVC thresholds for severe aortic stenosis may indirectly adjust for the increased valve fibrosis observed in females and generally offer good diagnostic accuracy compared to echocardiography (Pawade et al., 2018). However, patients with severe aortic

stenosis and concordant haemodynamic assessments of valve disease severity can have low Agatston scores (Shen et al., 2017). In addition, it can be challenging to differentiate valvular calcification from calcification of the aorta, left ventricular outflow tract, mitral valve or coronary arteries on axial non-contrast CT images. As such, there is a clear rationale for exploring alternative anatomical assessments of aortic stenosis that can overcome these issues.

We found the fibro-calcific volume to be a good measure of aortic stenosis severity that correlated well with echocardiographic measurements of valve haemodynamics and compared favourably with CT-AVC. Contrast-enhanced CT leaflet volumes also correlated with valve weight and semi-quantitative histological assessments of calcification and fibrosis, although these findings are limited by our small sample size. Given the superior anatomical detail afforded by contrast-enhanced CT, calcific and non-calcific volumes also had excellent reproducibility.

The fibro-calcific ratio, a reflection of the relative contributions of non-calcific and calcific tissue to leaflet thickening, is highly variable. As an isolated measure, it is not necessarily useful in mildly or non-diseased aortic valves, where the ratio is infinite when calcium is absent. However, in our study, it is notable that although females – who comprised a minority of the cohort - had only slightly lower peak aortic jet velocities, their Agatston scores and indexed contrast CT calcific volumes were much lower than in males. Consequently, the fibro-calcific ratio was higher in females. It would therefore be congruent that the Agatston score correlated less well with peak aortic jet velocity in females. This finding is out of keeping with the larger evidence base, where the validation of CT-AVC was undertaken in

populations with more severe disease (Pawade et al., 2018). This is further emphasised by multivariable regression models in our cohort, which demonstrated that although Agatston score was independently associated with peak aortic jet velocity after adjusting for age and sex, there was an interaction between sex and Agatston score. Overall, we would suggest our findings do concur with existing data that demonstrate similar degrees of valve obstruction in females with lower valve calcium load, even indexed for body size. The poor performance of the Agatston score likely reflects the small sample size of females enrolled in this study, most of whom had non-severe aortic stenosis.

Our study has several strengths. It is comprised of patients prospectively recruited into studies across the spectrum of aortic stenosis severity, with systematic multi-modality imaging assessments undertaken. The novel image analysis protocol proposes the use of flexible thresholds for defining calcific and non-calcific valve thickening based upon contrast attenuation in the blood pool, and defines the aortic valve plane and annulus sizing in a uniform fashion that is well-established. As a consequence, our technique is very reproducible. However, there are also some important limitations. The formula to set Hounsfield unit thresholds is derived, and as such will inevitably under- or overestimate non-calcific or calcific volumes in tissues that approach these thresholds, or where there is substantial variation in blood pool opacification. Accurate image analysis also requires adequate image quality and contrast opacification, and is challenging at the upper and lower extremes of blood-pool contrast load. The majority of the cohort was comprised of patients with non-severe aortic stenosis, which differs from the derivation and validation cohorts for CT-AVC. A minority of the cohort were female and as such the sex differences observed must be interpreted with caution. Similarly, the number of patients with bicuspid valves – an

important subgroup that differs from “degenerative” aortic stenosis – was too limited to examine. We did not study patients with a low-flow state, which is a particular cohort where there is often diagnostic uncertainty. Consequently, the generalizability of this initial report is limited, and requires further validation in a larger cohort that is comprised of more females and more patients with severe aortic stenosis. Finally, our image analysis method is relatively time consuming, involving multiple steps and transfer of data between different software packages (~45 min per case). An integrated software solution to facilitate more rapid image analysis whilst maintaining accuracy and reproducibility is currently being investigated, with promising pilot validation data (Figure 3.6). A step-by-step image analysis protocol is presented below to provide a gestalt of the software implementation.

Key points where operator care is required are:

- selecting scans of sufficient image quality with no motion artefact and good contrast opacification of the lumen
- accurate orientation of the multi-planar reconstruction in the en face valve view (annular plane)

1. Load a diastolic phase (usually 70% R-R interval).
2. Orient the CT in the annular plane. This is a standardized method used for TAVI assessment (Blanke et al., 2019).

Step & Description	Multiplanar reformats
Step 1: Start out with multi-planar images in default axial, sagittal, and coronal orientation; center cross-hairs onto the aortic valve	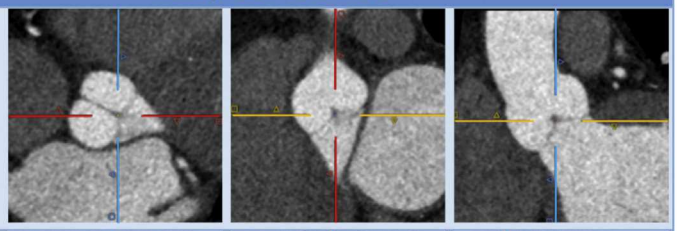
Step 2: Align the cross-hairs in the sagittal and coronal views with the long axis of the aortic root; the resulting double oblique transverse view will depict the aortic valve en face.	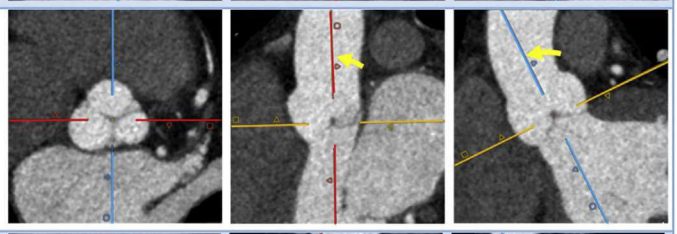
Step 3: Move the double oblique transverse plane up and down to identify the lowest insertion point of the right coronary cusp which is usually located at about 1 o´clock. Position the center of the cross-hairs exactly at the most basal insertion point of the right coronary cusp (white arrow head).	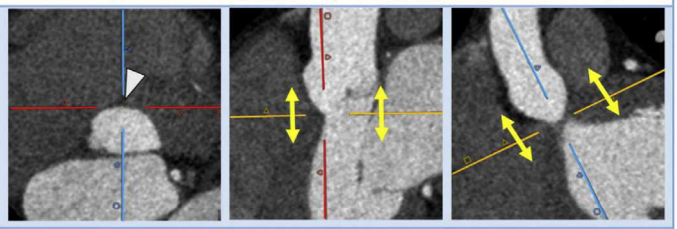
Step 4: Rotate the cross-hairs counter-clock-wise without moving up and down while maintaining its center position so that the formerly coronal view (here red cross-hair) transects the lowest insertion point of the non-coronary cusp, which is located at approximately 8 o´clock (white arrow head).	
Step 5: The formerly coronal, now double-oblique view will show the lowest insertion point both of the right coronary cusp and the non-coronary cusp (white arrow heads). In this view, rotate the (here orange) cross-hair indicating the double-oblique transverse view to transect exactly through the most basal insertion point of the non-coronary cusps. Once this is achieved, the transverse double oblique plane will contain two of the three lowest cusp insertion points.	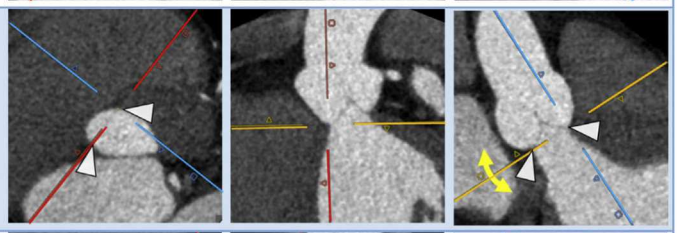
Step 6: In the formerly sagittal view, rotate (without moving it) the cross-hair of the transverse double oblique plane (here orange) until the lowest insertion point of the left coronary cusp just barely appears in the double oblique transverse view (white arrow head). Now, the formerly axial plane is exactly aligned with the lowest cusp insertion points of all three aortic cusps and represents both the orientation as well as the level of the annular plane.	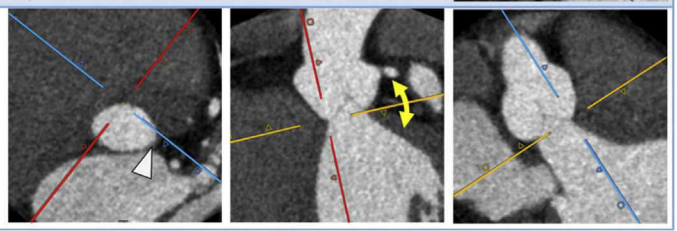

3. Set the ROI. At this stage, it is better to include more tissue than less.

- Centre the cylinder on the valve in the short axis view at the widest point.

- Select the appropriate radius, ensuring that perimeter is just large enough to encompass the whole valve.

- Move to the longitudinal views and set change the valve height until all the valve leaflet tissue is within the ROI. The lower border of the cylinder should ideally be just below the annular plane. The upper border of the cylinder should ideally by just below the origin of the right coronary artery.

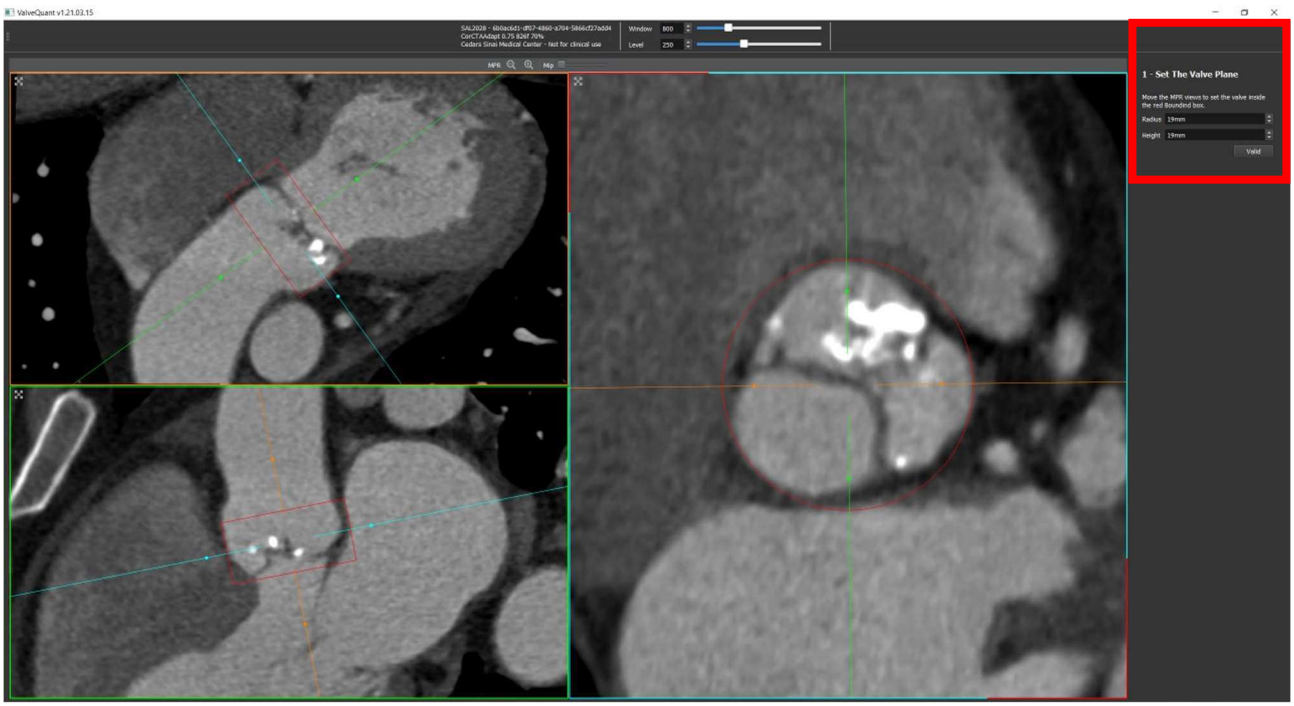

4. Fine-tune the ROI contours. It is now better to be precise about the contours. Be careful not to include tissue from adjacent structures.

- The ROI is automatically segmented into 5 slices in the short axis view.

- The ROI at each slice can be manually adjusted to follow the contours of the valve and sinuses, adding or removing individual points along the contour line as per the software instructions.

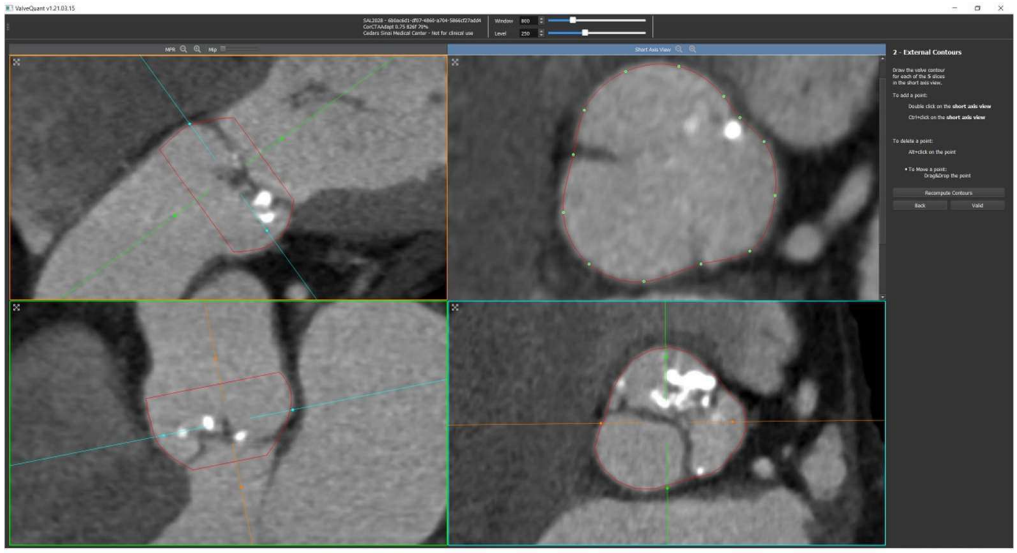

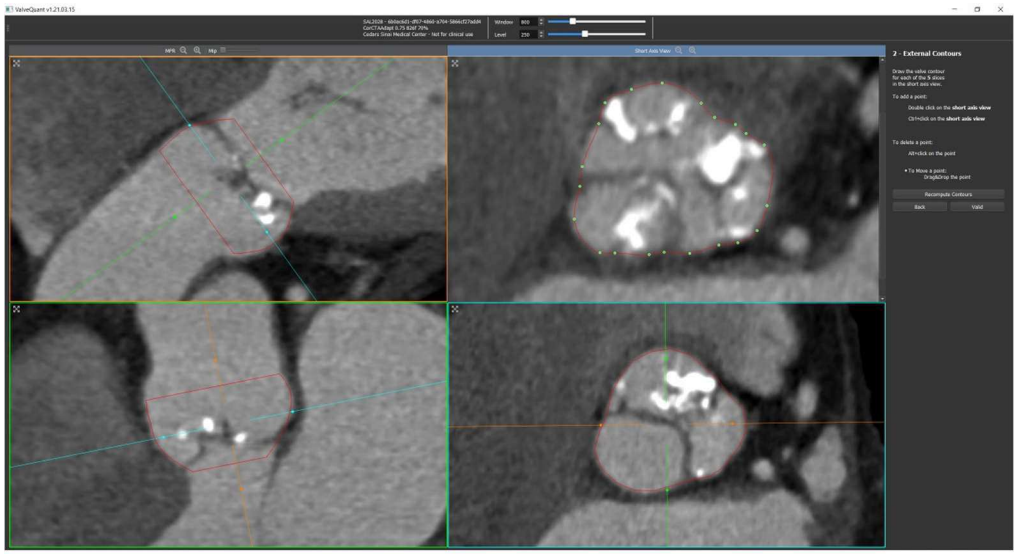

5. Setting HU thresholds for different tissues.

- Keep the low attenuation at 45 HU.

- In filters select “none” and check “remove calcium spot”.

- Select an appropriate shrinking radius (e.g. 2 mm). This uniformly brings the contours in to exclude adjacent structures such as the aortic wall.

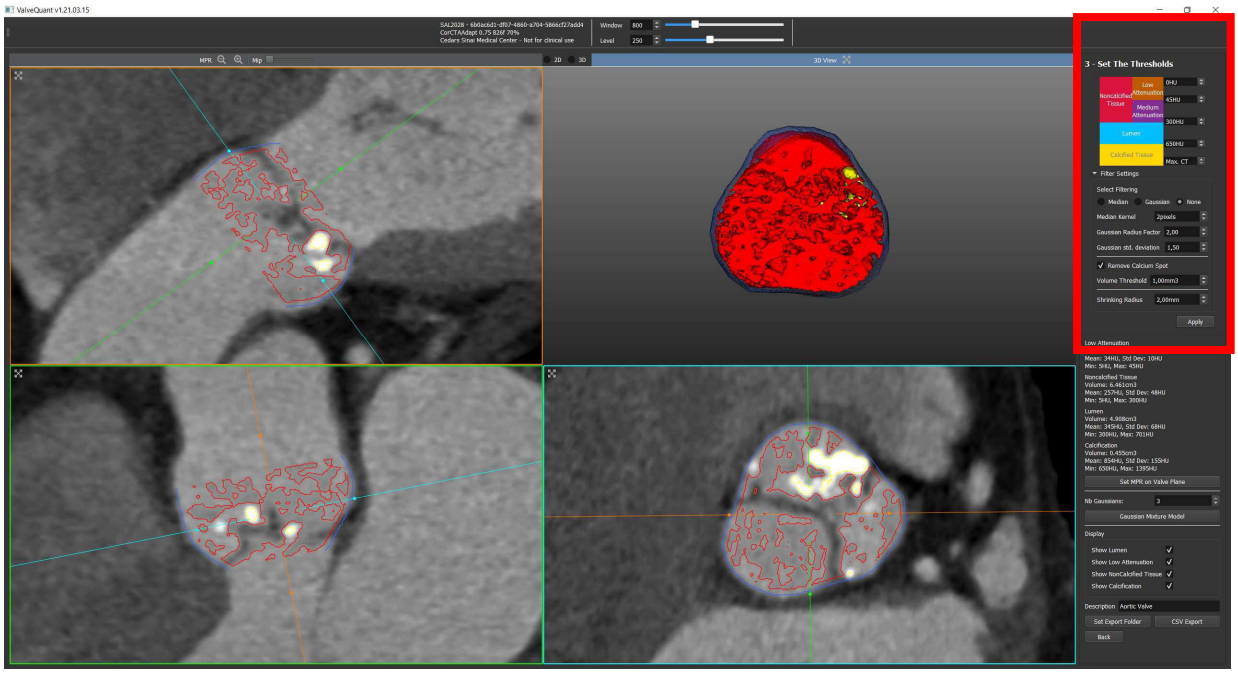

- Select the button “Gaussian Mixture Model”

    - the software estimates the HU distribution of n populations (set as “No. Gaussians, default 3 for blood pool, non-calcific and calcific tissue).

    - thresholds for non-calcific (lower 99.7 percentile of blood pool HU) and calcific tissue (upper 99.7 percentile blood pool HU) are automatically generated.

    - if there is no calcium (e.g. control patient), set “No. Gaussians” to n=2 (blood pool and non-calcific tissue).

    - a density plot of the HU for each of the n Gaussian populations is also shown.

6. Apply HU thresholds and export data

- the automated HU thresholds are applied and the different tissue populations are now differentiated in the 2D and 3D images.

- check contours throughout the valve.

- data including tissue volumes are presented and can be exported to a .csv file.

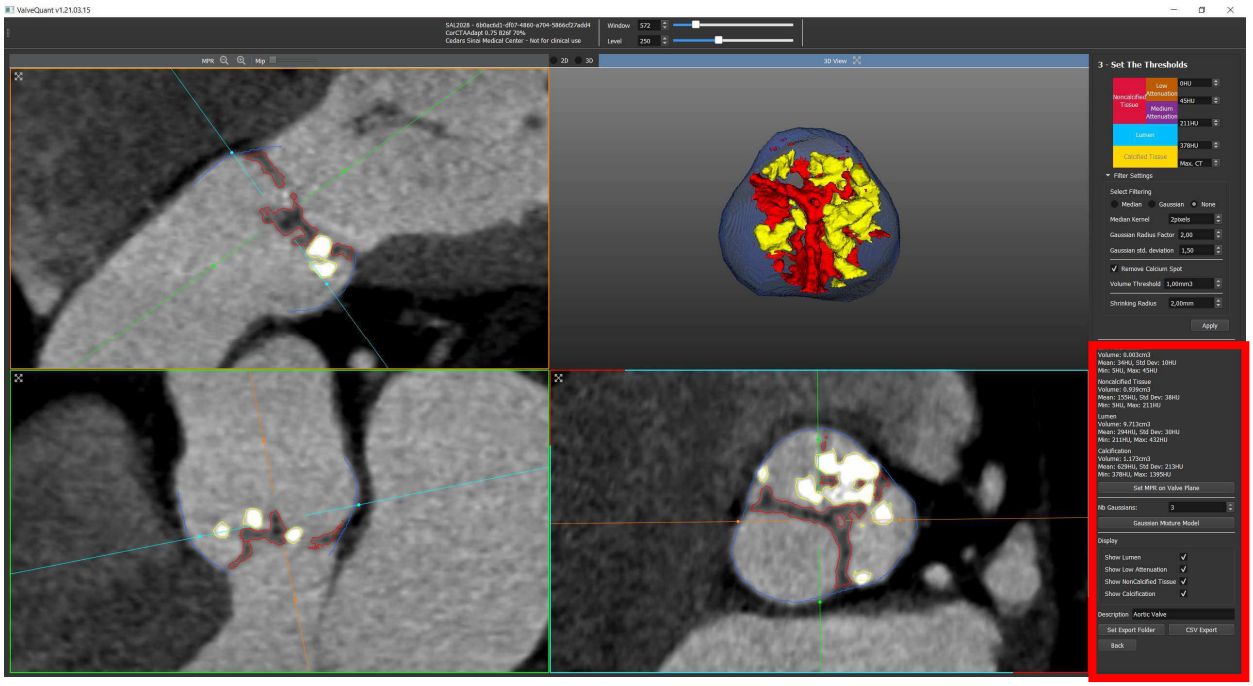

3.6 Conclusion

The aortic valve fibro-calcific volume as assessed by contrast-enhanced CT is an accurate and reproducible measure of aortic stenosis severity that quantifies both calcific and non-calcific leaflet volume. As a promising tool for the assessment of aortic stenosis, the next steps are to improve efficiencies in image analysis, followed by larger-scale validation to determine clinically useful thresholds.

Chapter 4 – Echocardiographic first-phase ejection fraction in aortic stenosis

Adapted from:

Bing R*, Gu H*, Chin C, Fang L, White A, Everett R, Spath N, Park E, Jenkins W, Shah A, Mills N, Flapan A, Chamber J, Newby D, Chowienczyk P*, Dweck M*. Determinants and prognostic value of echocardiographic first-phase ejection fraction in aortic stenosis. Heart. 2020. 10.1136/heartjnl-2020-316684.

* Authors contributed equally.

4.1 Abstract

Objective

First-phase ejection fraction (EF1) is a novel measure of early left ventricular systolic dysfunction. We investigated determinants of EF1 and its prognostic value in aortic stenosis.

Methods

EF1 was measured retrospectively in participants of an echocardiography/cardiovascular magnetic resonance (CMR) cohort study which recruited patients with aortic stenosis (peak aortic velocity ≥2 m/s) between 2012 and 2014. Linear regression models were constructed to examine variables associated with EF1. Cox proportional hazards were used to determine the prognostic power of EF1 for aortic valve replacement (AVR, performed as part of clinical care in accordance with international guidelines) or death.

Results

Total follow-up of the 149 participants (69.8% male, 70 [65-76] years, mean gradient 33 [21-42] mmHg) was 238,029 person-days. Sixty-seven participants (45%) had a low baseline EF1 (<25%) despite normal ejection fraction (67 [62-71]%). Patients with low EF1 had more severe aortic stenosis (mean gradient 39 [34-45] *versus* 24 [16-35] mmHg, p<0.001) and more myocardial fibrosis (indexed extracellular volume [iECV] (24.2 [19.6-28.7] *versus* 20.6 [16.8-24.3] mL/m^2, p=0.002; late gadolinium enhancement [LGE] prevalence 52 *versus* 20%, p<0.001). Valvuloarterial impedance, iECV and infarct LGE were independent predictors of EF1. EF1 improved post-AVR (n=57 with post-AVR EF1 available, baseline 16 [12-24]

versus follow-up 27 [22-31]%, p<0.001). Low baseline EF1 was an independent predictor of AVR/death (hazard ratio 5.6, 95% confidence interval 3.4-9.4), driven by AVR.

Conclusions

EF1 quantifies early potentially reversible systolic dysfunction in aortic stenosis, is associated with global afterload and myocardial fibrosis, and is an independent predictor of AVR.

4.2 Introduction

Aortic stenosis is the commonest indication for valve intervention in the Western world, with a rising incidence due to an aging population and increasing numbers of potential candidates for intervention (Durko et al., 2018; Nkomo et al., 2006). The current treatment paradigm is based on clinical surveillance for symptom development in patients with severe stenosis. However, there is now growing interest in the development of earlier markers of left ventricular decompensation that might facilitate more sophisticated risk stratification and thus optimize the timing of aortic valve replacement (AVR).

First-phase ejection fraction (EF1) is a novel measure of myocardial function that is easily measured on routine clinical echocardiography (Gu et al., 2017). It represents left ventricular ejection fraction from the time of aortic valve opening to the time of peak aortic velocity, in contrast to overall ejection fraction. The rationale for EF1 is based upon the biophysics of myocyte contraction. As a consequence of early myocardial dysfunction, the first period of ventricular contraction is delayed, even though overall ejection fraction may still be preserved. This altered physiology is quantified by EF1 and is of particular relevance in aortic stenosis, where time to peak aortic valve velocity prolongs with increasing stenosis severity. Preliminary data have demonstrated the feasibility of EF1 measurement in aortic stenosis, proposing a cut-off of <25% that is associated with an increased risk of future AVR, heart failure or death (Gu et al., 2019).

In aortic stenosis, impaired ventricular function can reflect afterload mismatch, where ventricular hypertrophy is insufficient to normalise wall stress and preload reserve is

exhausted, or alternatively myocardial fibrosis, which can be related to the chronic effects of aortic stenosis or concomitant coronary artery disease. Echocardiography is the standard imaging modality for assessment of haemodynamics, while cardiovascular magnetic resonance (CMR) is used for volumetric and structural analysis and tissue characterisation, and can identify myocardial fibrosis before ejection fraction falls (Bing, Cavalcante, et al., 2019). In this study we investigate the associations between haemodynamics, myocardial fibrosis and EF1 in aortic stenosis. We also examine the associations between EF1 and clinical outcomes.

4.3 Methods

Study population

This was an existing cohort of patients from the prospective, observational Role of Myocardial Fibrosis in Patients with Aortic Stenosis study (NCT01755936) imaging study. The primary results have been published (Chin et al., 2017). Briefly, patients with at least mild aortic stenosis (peak aortic velocity ≥2 m/s) undergoing follow-up at the Edinburgh Heart Centre were prospectively recruited. Major exclusion criteria included other moderate or severe valvular heart disease, significant comorbidities with limited life expectancy, contraindications to gadolinium-enhanced cardiac magnetic resonance (CMR), and acquired or inherited non-ischaemic cardiomyopathies as assessed by history or CMR. Patients underwent clinical evaluation, venous blood sampling for plasma high-sensitivity cardiac troponin I (ARCHITECT STAT assay (Abbott Laboratories, Abbott Park, Illinois)) and brain natriuretic peptide (Triage assay (Biosite Inc., San Diego, California)) concentrations, electrocardiography (ECG), transthoracic echocardiography and CMR. Patients were referred for aortic valve replacement (AVR) by the treating cardiologist in accordance with routine practice and contemporary guidelines, with heart team discussion where appropriate. The study was conducted in accordance with the Declaration of Helsinki and approved by the regional ethics committee (10/S1102/24). Informed consent was obtained from all subjects.

Echocardiography and CMR acquisition and image analysis are as previously described. EF1 was calculated as follows: (left ventricular end-diastolic volume – left ventricular volume at time of peak aortic velocity [V1])/left ventricular end-diastolic volume x 100 (Briand et al., 2005). Time to V1 is measured on continuous wave Doppler through the aortic valve. This

time is converted to 2D frames based on the echocardiogram frame rate, thus identifying the frame that corresponds to V1. Left ventricular end-diastolic volume and left ventricular volume at V1 are then measured using the Simpson's bi-plane method. Clinical outcomes including AVR were captured from medical records, while deaths were identified through the General Register of Scotland. Post-AVR EF1 was measured as close to 1-year follow-up as possible on research or clinical echocardiograms.

Statistical analysis

Analyses specific to this study are as follows. Non-normally distributed continuous variables were log2-transformed. GLS was log2-transformed after addition of a constant (greatest GLS + 1). EF1 was dichotomized as high (≥25%) and low (<25%) (Gu et al., 2019). Univariable linear regression modelling was performed to identify the associations between EF1 and relevant clinical and CMR variables. Covariables identified for inclusion in multivariable models were age (per decade), male sex, Zva, infarct LGE, iECV, hs-cTnI and BNP. These models were constructed with haemodynamics and CMR parameters followed by the addition of biochemistry and clinical parameters. As this model explored potential mechanistic associations, Zva was included as an integrated measure of function and haemodynamics. Infarct LGE and iECV were chosen due to collinearity between other fibrosis measures. Cumulative event rates were examined using Kaplan-Meier curves for the combined primary endpoint of AVR or all-cause mortality. Assumptions for proportionality were checked and Cox proportional hazard models constructed to assess the prognostic utility of EF1, with the covariables of age (per decade), male sex, New York Heart Association (NYHA) dyspnoea class, mean gradient, EF1, infarct LGE and iECV. Mean gradient, rather than Zva, was chosen as a more commonly utilised parameter for this clinical outcome model.

4.4 Results

Patient characteristics

EF1 was measurable in 149 of 166 (90%) participants. Seventeen were excluded due to suboptimal echocardiographic left ventricular endocardial definition (Figure 4.1); these patients had higher aortic valve gradients than the remaining study cohort (mean gradient 42 [30-54] *versus* 33 [21-42] mmHg, p=0.006). The study cohort comprised patients with mild (n=34), moderate (n=40) and severe (n=75) aortic stenosis, of whom 67 (45%) had a low baseline EF1 (<25%) (Table 4.1). Twenty-eight patients were categorised as severe based on aortic valve area <1.0cm^2 with a discordant mean gradient <40mmHg, of whom 4 had an indexed stroke volume <35ml/m^2. Patients with low EF1 were of similar age and had more severe aortic stenosis than those with an EF1≥25% (Figure 4.2). Markers of left ventricular decompensation were more common in those with a low EF1, including worse NYHA class, higher plasma hs-cTnI concentrations and more non-infarct myocardial fibrosis. The prevalence of infarct LGE and coronary artery disease was also higher in patients with a low EF1. Importantly, there was no difference in ejection fraction between the low and normal EF1 groups (67 [62-71] *versus* 67 [63-70]%, p=0.47). Only 4 patients in the low EF1 group had an ejection fraction <50% (range 42-46%), while 13 patients in the low EF1 group had an ejection fraction <60%.

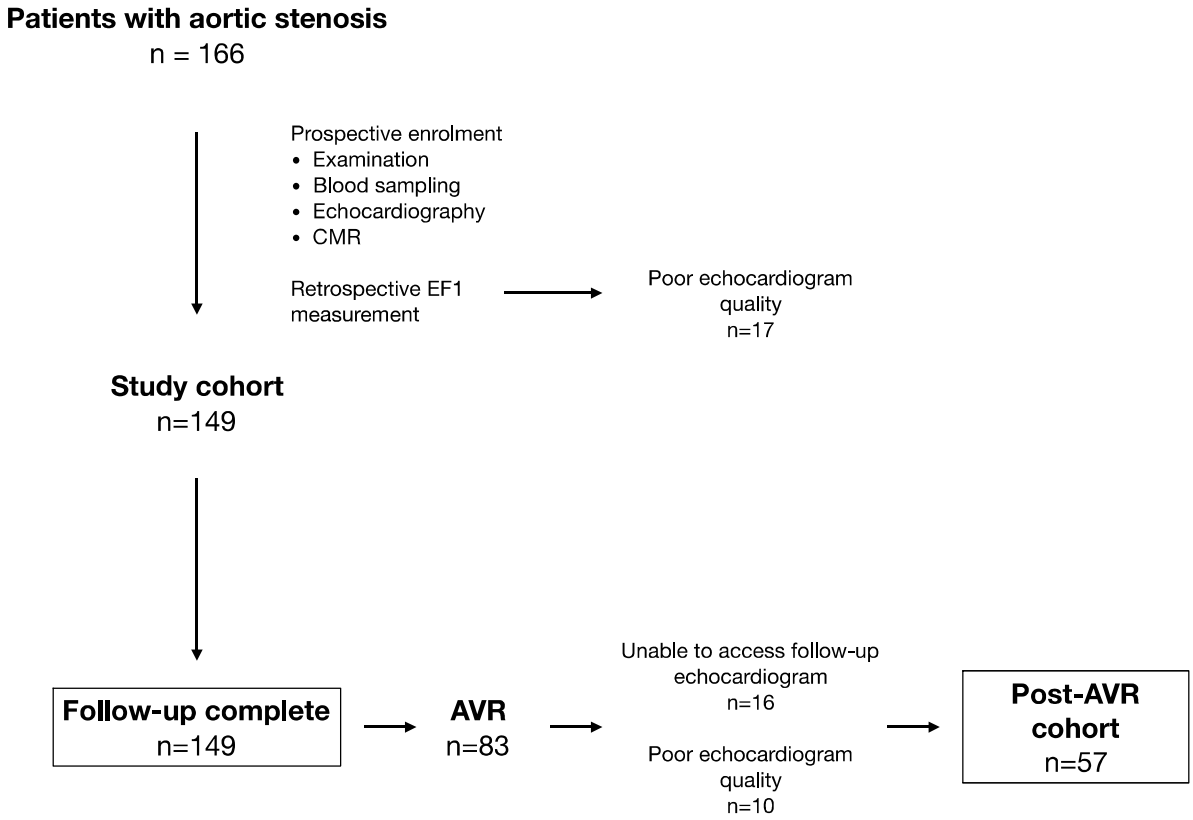

Figure 4.1 Study flow chart

Study design showing patient population and investigations at baseline and follow-up.

Table 4.1 Baseline characteristics

	Overall	**EF1 ≥25%**	**EF1 <25%**	**p value**
n	149	82	67	
Age	70.0 [65.0, 76.0]	70.5 [63.0, 77.0]	69.0 [66.0, 75.0]	0.97
Male sex	104 (69.8)	51 (62.2)	53 (79.1)	**0.04**
Hypertension	102 (68.5)	58 (70.7)	44 (65.7)	0.63
Hyperlipidaemia	67 (45.0)	35 (42.7)	32 (47.8)	0.65
Diabetes	21 (14.1)	14 (17.1)	7 (10.4)	0.36
Coronary artery disease	56 (37.6)	20 (24.4)	36 (53.7)	**<0.001**
Systolic blood pressure (mmHg)	148.5 [137.0, 165.5]	153.0 [140.5, 169.6]	144.0 [134.5, 159.0]	0.10
Diastolic blood pressure (mmHg)	84.0 [77.0, 92.0]	82.0 [76.5, 90.0]	84.5 [79.2, 92.8]	0.21
NYHA				**0.005**
I	71 (47.7)	48 (58.5)	23 (34.3)	
II	49 (32.9)	25 (30.5)	24 (35.8)	
III	26 (17.4)	9 (11.0)	17 (25.4)	
IV	3 (2.0)	0 (0.0)	3 (4.5)	
AV Vmax (m/s)	3.8 [3.2, 4.3]	3.4 [2.8, 3.9]	4.1 [3.8, 4.5]	**<0.001**
AV mean gradient (mmHg)	32.9 [20.7, 41.7]	24.0 [16.3, 35.2]	38.7 [33.8, 45.2]	**<0.001**
AV area (cm2)	0.9 [0.7, 1.1]	1.0 [0.8, 1.2]	0.8 [0.7, 0.9]	**<0.001**
Valvuloarterial compliance (mmHg/ml/m2)	4.0 [3.3, 4.4]	3.9 [3.2, 4.3]	4.1 [3.4, 4.6]	0.18
Indexed LV mass (g/m2)	87.0 [73.0, 99.0]	81.5 [69.2, 93.0]	95.0 [81.5, 101.5]	**0.001**
Indexed stroke volume (ml/m2)	47.0 [41.0, 54.0]	47.0 [41.0, 53.0]	47.0 [41.0, 54.4]	0.83
Ejection fraction (%)	66.7 [63.0, 70.7]	66.7 [63.2, 70.4]	66.7 [62.4, 70.9]	0.47
EF1 (%)	25.6 [17.7, 29.9]	29.6 [27.3, 32.8]	15.7 [12.2, 20.9]	**<0.001**
Global longitudinal strain (%)	-17.9 [-20.1, -15.4]	-18.0 [-20.7, -16.0]	-17.7 [-19.3, -14.7]	**0.047**
Native T1	1179.0 [1157.0, 1207.0]	1174.0 [1149.5, 1201.5]	1188.5 [1165.0, 1209.2]	0.08
ECV fraction (%)	27.6 [25.6, 29.1]	27.3 [25.6, 28.4]	27.9 [25.8, 30.0]	0.16
iECV (ml/m2)	22.3 [18.7, 26.2]	20.6 [16.8, 24.3]	24.2 [19.6, 28.7]	**0.002**
Infarct LGE	21 (14.1)	5 (6.1)	16 (23.9)	**0.004**
Non-infarct LGE	36 (24.2)	13 (15.9)	23 (34.3)	**0.015**
hs-cTnI (ng/L)	6.6 [3.6, 12.4]	4.9 [3.2, 9.1]	9.3 [4.3, 15.3]	**0.009**
BNP (ng/L)	26.8 [12.4, 54.2]	23.9 [10.3, 49.9]	30.0 [14.5, 71.4]	0.07

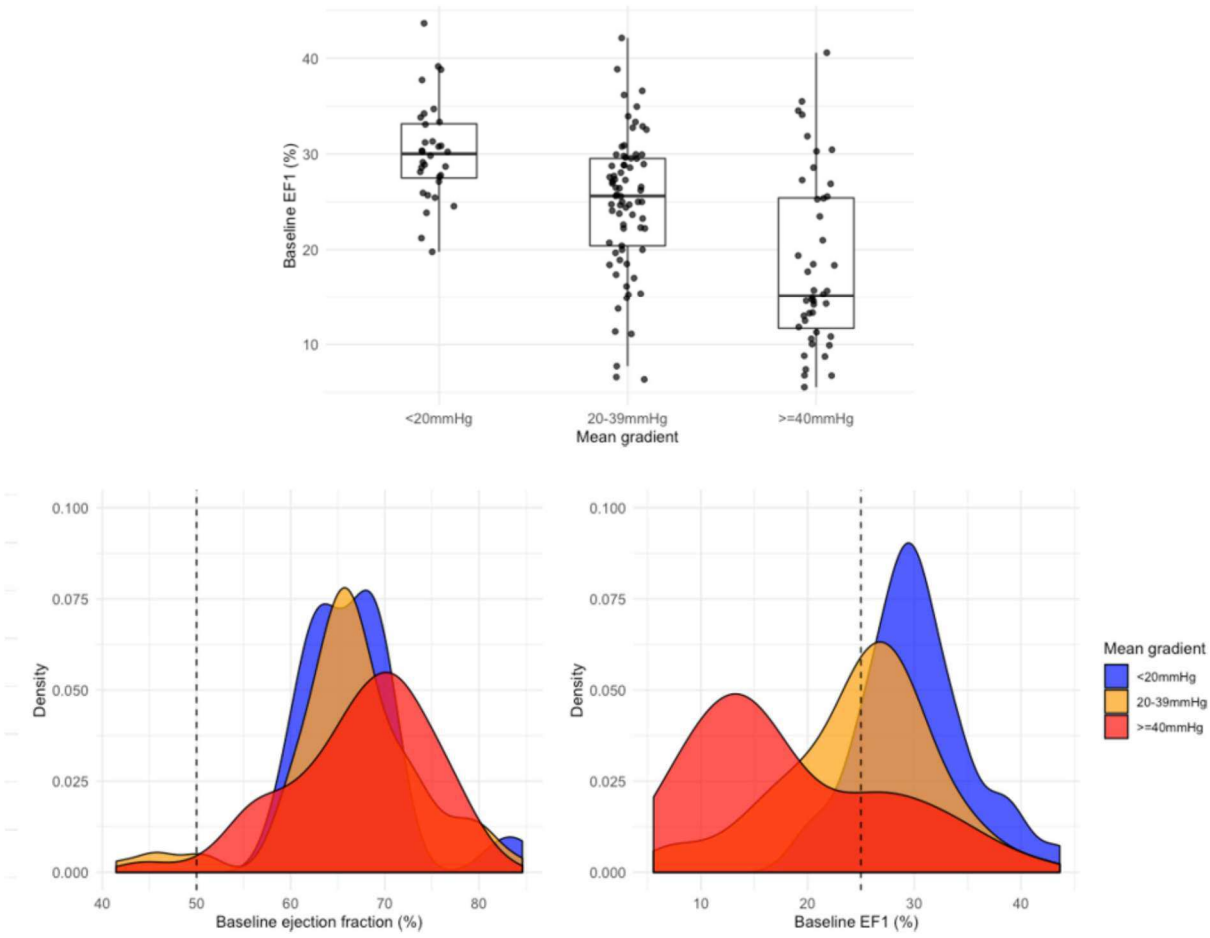

Figure 4.2 Distribution of EF1 and ejection fraction by aortic stenosis severity

Box plot demonstrates EF1 according to mean gradient (<20mmHg: 30 (27-33)%, 20-39mmHg: 26 (20-30)%, ≥40mmHg: 15 (12-25)%). Density plots demonstrate the distribution of EF1 and ejection fraction amongst patients with aortic stenosis stratified by mean gradient. The dashed reference lines denote 25% and 50% for EF1 and ejection fraction respectively.

Clinical characteristics associated with EF1

On univariable linear regression analyses, EF1 was associated with aortic valve mean gradient, Zva, indexed left ventricular mass, native T1, iECV, LGE, GLS and hs-cTnI. Multivariable linear regression models using the pre-specified covariables (Table 4.2) demonstrated Zva, iECV (both p<0.001) and infarct LGE (p=0.047) to be independently associated with EF1, although there remained substantial unexplained variance (r^2=0.25, p<0.001). Of note, there was no correlation between EF1 and ejection fraction (Pearson's r=0.14, p=0.10).

Table 4.2 Multivariable linear regression models for EF1

	Model 1 (r^2 0.19) n=145			**Model 2 (r^2 0.25)** n=126			**Model 3 (r^2 0.25)** n=126		
	Coefficient	**95% CI**	**p value**	**Coefficient**	**95% CI**	**p value**	**Coefficient**	**95% CI**	**p value**
Zva	-0.48	-0.75, -0.20	**<0.001**	-0.64	-0.95, -0.33	**<0.001**	-0.66	-0.99, -0.34	**<0.001**
iECV	-0.49	-0.75, -0.23	**<0.001**	-0.72	-1.06, -0.37	**<0.001**	-0.70	-1.05, -0.34	**<0.001**
Infarct LGE	-0.35	-0.63, -0.07	**0.01**	-0.33	-0.63, -0.02	**0.036**	-0.31	-0.63, 0.00	**0.047**
hs-cTnI				0.025	-0.06, 0.11	0.57	0.02	-0.06, 0.11	0.61
BNP				0.04	-0.04, 0.11	0.32	0.03	-0.06, 0.11	0.55
Age per 10 years							0.03	-0.08, 0.13	0.63
Male							-0.03	-0.26, 0.21	0.81

Zva, iECV, hs-cTnI and BNP were log_2-transformed.

Change in EF1 after AVR

In patients who underwent AVR, we examined the change in EF1 after relief of afterload. Of the 149 patients with baseline EF1 data, 83 (56%) underwent AVR (baseline echocardiogram to AVR 14.9 [2.9-35.5] months). The primary indications for AVR were dyspnoea (n=48), chest pain (n=12), pre-syncope/syncope (n=9), rapid progression or very severe stenosis (n=7), heart failure (n=3), or asymptomatic left ventricular dysfunction (n=2). One patient was referred due to a positive exercise treadmill test and one patient underwent AVR to facilitate hip replacement. Sixteen patients did not have post-AVR echocardiograms available, while 10 had echocardiograms of insufficient quality to measure EF1, leaving 57 patients for analysis (AVR to follow-up echocardiogram 11.2 [6.0-13.1] months).

Overall, EF1 increased after AVR (baseline 16 [12-24] *versus* follow-up 27 [22-31] %, $p<0.001$). A cut-off of ≥3% was then applied as a threshold for improvement based on prior intraobserver variability (Gu et al., 2019). Thirty-nine (68%) patients improved while 18 (32%) did not. Of these 18 patients, 11 had a low EF1 at baseline. Baseline clinical and imaging characteristics in these 11 patients with a fixed low EF1 were similar to the remaining cohort, including aortic stenosis severity, Zva, EF1 and ejection fraction. However, patients with a fixed low EF1 had a much higher prevalence of infarct LGE (64 *versus* 9%, $p<0.001$). On univariable logistic regression analysis, infarct LGE was the only parameter that was associated with a fixed low EF1 (coefficient 2.9, 95% confidence interval [CI] 1.3-4.5, $p<0.001$).

EF1 and outcomes

Patients were followed up for a total of 238,029 person-days. More than double the proportion of patients with a low EF1 reached the primary endpoint of AVR or death,

compared to patients with a normal EF1 (93 *versus* 45%, p<0.001) (Table 4.3, Figure 4.3). This was driven by AVR (81 *versus* 35%, p<0.001). Death was numerically higher in the low EF1 group (21 *versus* 12%, p=0.23), and all 5 patients that died after AVR had a fixed low EF. The optimal threshold in our cohort for prediction of the primary endpoint was 24% (Youden's index 0.55), almost identical to the cut-off of 25% described previously (Gu et al., 2019) and applied here (Figure 4.4). There were no differences in other cardiovascular outcomes, although there were few events. Multivariable Cox proportional hazard modelling demonstrated low EF1 to be an independent predictor of the primary endpoint (hazard ratio [HR] 5.6, 95% CI 3.4-9.1) alongside mean gradient and NYHA class (Figure 4.5-A). CMR assessments of myocardial fibrosis were not independent predictors of the primary outcome. Excluding patients with mild aortic stenosis did not alter these associations. A limited Cox proportional hazards model in patients with a mean gradient ≥40 mmHg (n=44; 36 had AVR, 5 died before AVR) again demonstrated EF1 to be an independent predictor of the primary endpoint. Of note, mean gradient and NYHA class were not predictors in this model after adjusting for EF1 (Figure 4.5-B). In this subgroup, the optimal threshold for the composite endpoint was 25% (Youden's index 0.76).

Table 4.3 Outcomes stratified by EF1

	EF1 ≥25%	**EF1 (<25%)**	**p value**
n	82	67	
Aortic valve replacement or death	37 (45.1)	62 (92.5)	**<0.001**
Aortic valve replacement	29 (35.4)	54 (80.6)	**<0.001**
Death	10 (12.2)	14 (20.9)	0.23
Cardiovascular death	6 (7.3)	5 (7.5)	1.00
Myocardial infarction	3 (3.7)	4 (6.0)	0.78

Cerebrovascular event	6 (7.3)	4 (6.0)	1.00
Heart failure	5 (6.1)	4 (6.0)	1.00

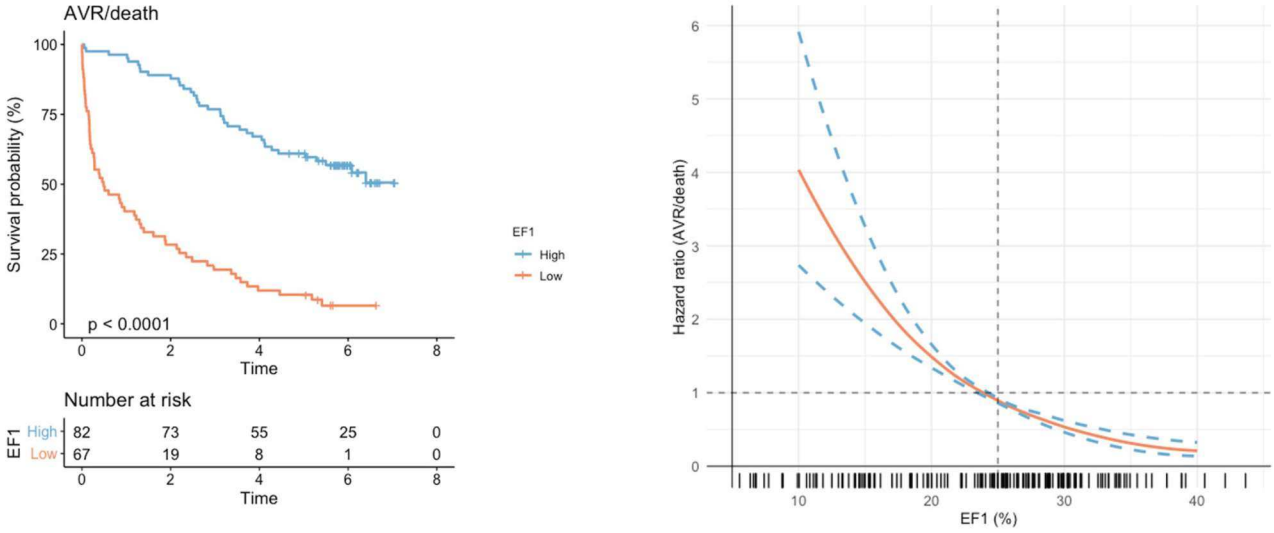

Figure 4.3 Association between EF1 and outcomes

The Kaplan-Meier curve (left) demonstrates unadjusted survival free of AVR or death in the study cohort (n=149), stratified by high (≥25%) or low (<25%) EF1 (p value for log-rank test). The Cox regression curve (bottom right) demonstrates the predicted hazard ratio for AVR or death according to EF1, adjusted for age, mean gradient and indexed extracellular volume. The distribution of EF1 in the study cohort is presented in the rug plot below the regression curve.

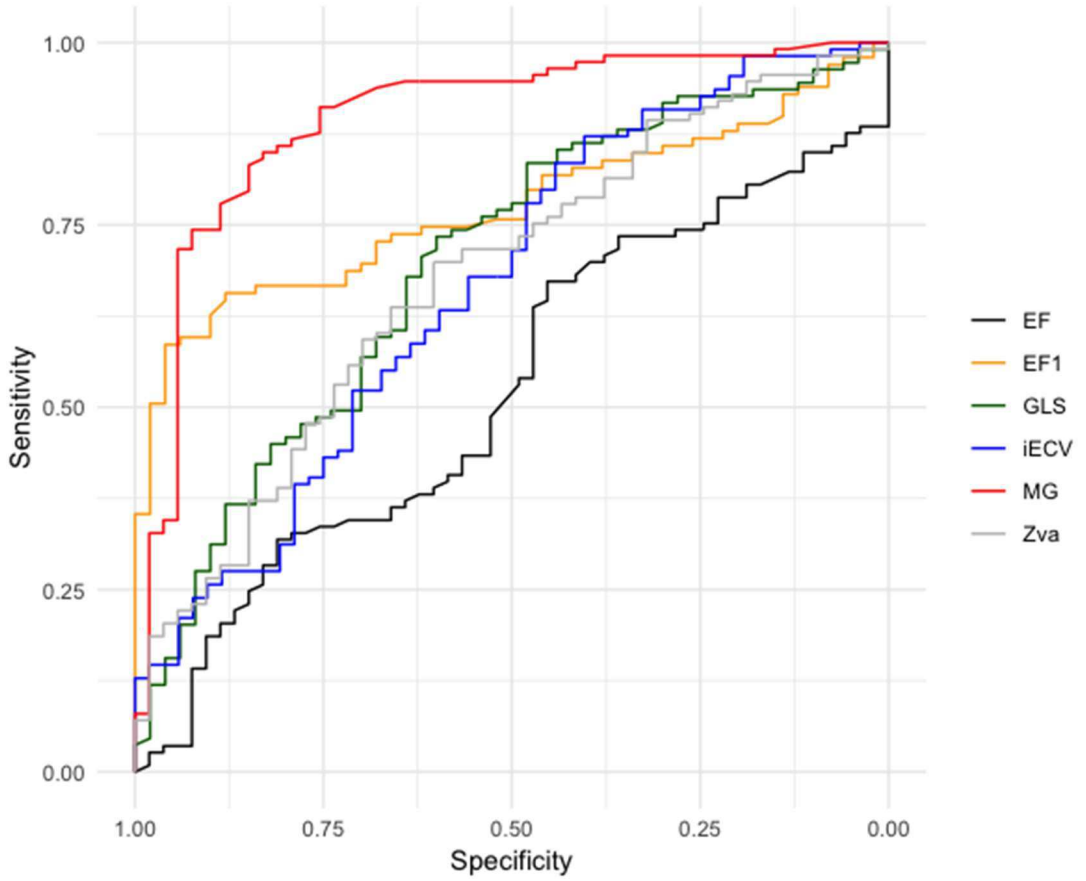

Figure 4.4 Discriminators of aortic valve replacement or death

Receiver operating curves for aortic valve replacement or death. Variables (area under curve) are EF (0.52), EF1 (0.77), GLS (0.70), iECV (0.67), MG (0.90) and Zva (0.68). The optimal cut-off for EF1 was determined using Youden's index (sensitivity + specificity – 1).

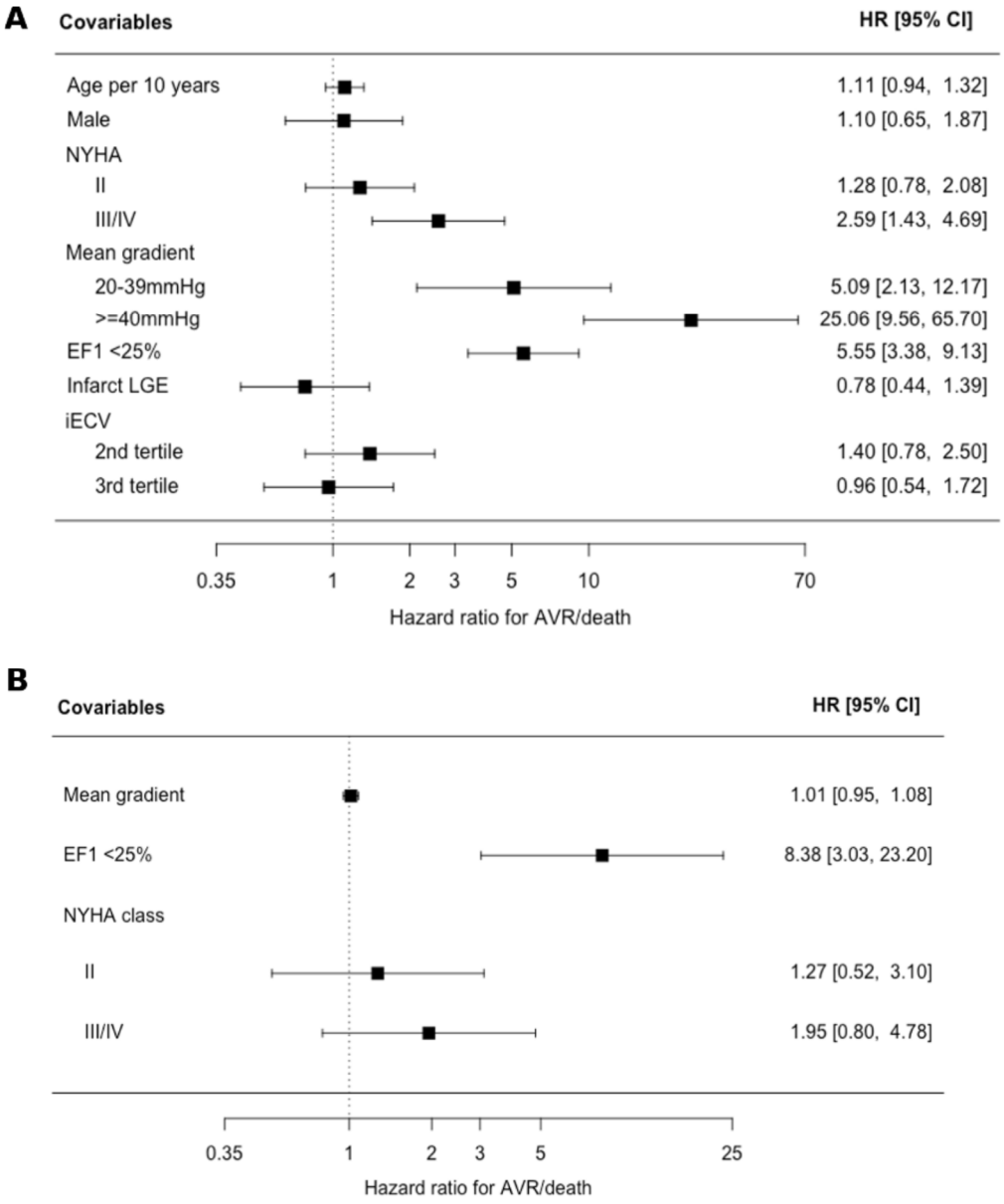

Figure 4.5 Multivariable predictors of aortic valve replacement or death

Forest plots of multivariable Cox proportional hazards models for the composite endpoint of aortic valve replacement or death. Hazard ratio scales are presented as logarithmic scales. NYHA was stratified according to class (reference: class I).

A) Model for the whole cohort. Aortic stenosis severity was stratified by mean gradient (<20mmHg [reference], 20-39mmHg and ≥40mmHg). iECV was stratified by tertiles (1st tertile as reference).

B) Model for patients with a mean gradient ≥40 mmHg (n=44; 36 had AVR, 5 died before AVR). The model was restricted to these three variables to avoid overfitting. Mean gradient was analysed as a continuous variable in keeping with the lack of a clear threshold in clinical practice for these patients.

For comparison, we performed an exploratory analysis of GLS and ejection fraction as alternative markers of impaired ventricular function in the whole cohort. On univariable analysis, a reduced GLS was associated with an increased incidence of AVR or death (HR 2.3, 95% CI 1.5-3.5). However, after constructing the same multivariable Cox proportional hazards model as used for EF1, GLS was no longer a predictor of the primary endpoint (HR 1.54, 95% CI 0.92-2.6). Similarly, ejection fraction was not an independent predictor of the primary endpoint when replacing EF1 in the final model (HR 0.99, 95% CI 0.96-1.00).

4.5 Discussion

We have demonstrated associations between EF1 and myocardial disease in patients with aortic stenosis. In particular, we report that EF1 decreases with increasing aortic stenosis severity despite preserved overall ejection fraction, and that this reduction in EF1 is associated with increased global afterload and myocardial fibrosis burden. Of note, a low EF1 is generally reversible after relief of afterload. Finally, we show that EF1 is a powerful predictor of future AVR - independent of mean gradient – that appears to outperform other markers of impaired left ventricular function.

EF1 – rationale and associations

The development of symptoms and adverse events in aortic stenosis are related not only to progressive valve narrowing but also the remodelling response of the left ventricle (Dweck, Boon, et al., 2012). Current guidelines recommend AVR in patients with severe aortic stenosis and symptoms or evidence of left ventricular decompensation - for example, a reduction in ejection fraction or an elevated BNP (Baumgartner et al., 2017; Nishimura et al., 2017). However, symptoms are often difficult to assess, whilst deterioration in ejection fraction and elevation of BNP may occur relatively late. Consequently, there is a clinical need for a sensitive, dynamic biomarker that identifies the onset of early, reversible left ventricular dysfunction. Although CMR assessments of myocardial fibrosis show promise and have prognostic value (Azevedo et al., 2010; Barone-Rochette et al., 2014; Bing, Cavalcante, et al., 2019; Dweck et al., 2011; Musa et al., 2018; Puntmann et al., 2016), they require an additional, less accessible scan. In contrast, EF1 can be easily performed on

routinely acquired echocardiograms in <10 minutes without the need for dedicated software or imaging techniques.

EF1 differs from overall ejection fraction. We observed no correlation between these two parameters, with marked reductions in EF1 seen in the context of a preserved ejection fraction. Three measures were independently associated with EF1: Zva, a measure of global LV afterload, iECV, reflecting non-infarct fibrosis, and infarct LGE. This is not surprising given that these processes are recognised determinants of left ventricular systolic function in aortic stenosis (Weidemann et al., 2009). Importantly, reductions in EF1 generally improved following AVR, consistent with the reversible nature of afterload mismatch and diffuse fibrosis (Chin et al., 2017; Treibel, Kozor, et al., 2018). The small number of patients with a fixed low EF1 (n=11) had a much higher prevalence of infarct-related, non-reversible replacement fibrosis despite relatively preserved ejection fraction (66 [53-69]%).

EF1 - prognosis

We have shown that EF1 is a powerful and independent predictor of AVR or death when utilizing the previously reported threshold of 25%, a cut-off very similar to the optimal threshold in our cohort. This was driven by AVR and was independent of aortic stenosis severity and myocardial fibrosis. Notably, in our cohort, the same independent associations were not seen with CMR 2D-GLS or ejection fraction. GLS in particular is a recognised marker of early ventricular dysfunction, but there was only a small difference in baseline GLS between the high and low EF1 groups. This could reflect the sensitivity of EF1, with changes occurring earlier in the disease course. We were unable to show an independent association between GLS and the primary endpoint, despite this association being

demonstrated in other larger cohorts. As such, our findings should be interpreted with caution and in the context of the existing body of literature. Further larger studies of EF1 and GLS to explore their comparative associations and prognostic value would be most interesting. Particularly relevant for future clinical application is the predictive power of EF1 in patients with severe aortic stenosis – the group of patients in whom EF1 is most likely to be used. When limited to patients with a mean gradient ≥40 mmHg, a low EF1 was the only predictor of AVR or death after adjusting for mean gradient and NYHA class. Although this is a hypothesis-generating subgroup analysis, this finding is of relevance as there is substantial interest in optimizing the timing of AVR in asymptomatic severe aortic stenosis, with several randomised controlled trials underway (NCT03042104, NCT02436655, NCT03094143) (Banovic et al., 2016; Bing, Everett, et al., 2019). The study of EF1 in patients with low gradient severe aortic stenosis – either low-flow, paradoxical low-flow or normal flow – would be valuable but our numbers were insufficient to investigate this. Finally, all 5 deaths after AVR occurred in the group of 11 patients with a fixed low EF1, a finding that is in keeping with the poor long-term prognosis associated with the presence of LGE - representing irreversible replacement fibrosis - in aortic stenosis (Azevedo et al., 2010; Barone-Rochette et al., 2014; Dweck et al., 2011; Musa et al., 2018).

Strengths and limitations

Our study has several strengths. It is the first to establish the relationship between EF1 and both afterload and myocardial fibrosis, using a cohort enrolled in a multimodality imaging study and meticulously characterized with clinical assessment, echocardiography and CMR. The investigators measuring EF1 were blinded to all patient characteristics, CMR findings and outcomes, thus minimizing bias. There are, however, several important limitations. This

is a post-hoc analysis of an observational cohort. EF1 was measured retrospectively and was unmeasurable in 10% of patients. Whilst this proportion is similar to previously published data (Gu et al., 2019), all baseline echocardiograms in this cohort were performed for research purposes by a dedicated research sonographer or cardiologist. In clinical practice, routine image quality may be inferior. Furthermore, EF1 performed as a single measurement does not account for beat-to-beat variation in atrial fibrillation – a weakness common to most haemodynamic measurements. There was a low prevalence of atrial fibrillation at baseline in this cohort (n=5). Although future study and application of EF1 may be most pertinent in patients with asymptomatic severe aortic stenosis, this was less than half of the present cohort as we aimed to investigate associations with other measures of myocardial disease in addition to prognosis. Additionally, our analyses examining post-AVR change in EF1 and the relationship between a fixed low EF1 and long-term mortality, although of interest and clinically plausible, are limited by a small sample size and modest event rate. Similarly, we had insufficient patients with both iECV and EF1 available pre-and post-AVR (n=18) to conduct a meaningful analysis of how changes in these parameters are related, although previous studies have demonstrated a reduction in iECV following AVR (Everett et al., 2018; Treibel, Kozor, et al., 2018).

4.6 Conclusion

EF1 quantifies early, impaired left ventricular function in patients with aortic stenosis and is associated with global afterload and myocardial fibrosis. Changes in EF1 occur before reduction in overall ejection fraction is seen. EF1 has a robust threshold that strongly predicts future AVR, independent of mean gradient. Further prospective study is required to investigate the incremental utility of this novel measure in aortic stenosis.

Chapter 5 – Effect of denosumab or alendronic acid on the progression of aortic stenosis

Adapted from:

Pawade TA*, Doris MK*, Bing R*, White AC, Forsyth L, Evans E, Graham C, Williams MC, van Beek EJR, Fletcher A, Adamson PD, Andrews JPM, Cartlidge TRG, Jenkins WSA, Syed M, Fujisawa T, Lucatelli C, Fraser W, Ralston SH, Boon N, Prendergast B, Newby DR, Dweck MRD. Effect of Denosumab or Alendronic Acid on the Progression of Aortic Stenosis: A Double-Blind Randomized Controlled Trial. Circulation. 2021 Apr 29. doi: 10.1161/CIRCULATIONAHA.121.053708

* Authors contributed equally.

5.1 Abstract

Background

Valvular calcification is central to the pathogenesis and progression of aortic stenosis, with pre-clinical and observational studies suggesting that bone turnover and osteoblastic differentiation of valvular interstitial cells are important contributory mechanisms. We aimed to establish whether inhibition of these pathways with denosumab or alendronic acid could reduce disease progression in aortic stenosis.

Methods

In a single-centre parallel group double-blind randomized controlled trial, patients over 50 years of age with calcific aortic stenosis (peak aortic jet velocity >2.5 m/s) were randomized 2:1:2:1 to denosumab (60 mg every 6 months), placebo injection, alendronic acid (70 mg once weekly) or placebo capsule. Participants underwent serial assessments with Doppler echocardiography, computed tomography aortic valve calcium scoring and 18F-sodium fluoride positron emission tomography and computed tomography. The primary endpoint was the calculated 24-month change in aortic valve calcium score.

Results

One-hundred and fifty patients (mean age 72±8 years; 21% female) with calcific aortic stenosis (peak aortic jet velocity 3.36 [2.93 to 3.82] m/s; aortic valve calcium score 1152 [655 to 2065] Agatston Units) were randomized and received the allocated trial intervention: denosumab (n=49), alendronic acid (n=51) and placebo (injection n=25, capsule n=25; pooled for analysis). Serum C-terminal telopeptide, a measure of bone turnover, halved from

baseline to 6 months with denosumab (0.23 [0.18 to 0.33] to 0.11 [0.08 to 0.17] μg/L) and alendronic acid (0.20 [0.14 to 0.28] to 0.09 [0.08 to 0.13] μg/L) but was unchanged with placebo (0.23 [0.17 to 0.30] to 0.26 [0.16 to 0.31] μg/L). There were no differences in 24-month change in aortic valve calcium score between denosumab and placebo (343 [198 to 804] AU versus 354 [76 to 675] AU, p=0.41), or alendronic acid and placebo (326 [138 to 813] AU versus 354 [76 to 675] AU, p=0.49). Similarly, there were no differences in change in peak aortic jet velocity or 18F-sodium fluoride aortic valve uptake.

Conclusions

Neither denosumab nor alendronic acid affected progression of aortic valve calcification in patients with calcific aortic stenosis. Alternative pathways and mechanisms need to be explored to identify disease-modifying therapies for the growing population of patients with this potentially fatal condition.

5.2 Introduction

Despite decades of research and several randomized controlled trials (Chan et al., 2010; Cowell et al., 2005; Rossebo et al., 2008), aortic stenosis remains a disease without an effective medical treatment. Prolonged longevity and the subsequent aging of the general population means that the prevalence of aortic stenosis continues to rise. This has led to the increased use of valve replacement interventions which remain the only treatment for end-stage disease, although they carry potentially significant peri-procedural and long-term risks (Durko et al., 2018; Osnabrugge et al., 2013). A medical therapy that slows the progression of aortic stenosis would therefore be a major advance and address an important unmet clinical need.

The pathology of aortic stenosis is driven by actively regulated inflammation and calcification and has clear similarities to skeletal bone formation (Dayanand et al., 2018; Otto et al., 1994; Pawade et al., 2015; Rajamannan et al., 2011; Rajamannan et al., 2003). Activity of both osteoblasts in the valve and osteoclasts in the bone appears to be important, with multiple potential pathways involved in regulating bone turnover and valvular calcification (Goody et al., 2020; Pawade et al., 2015).The receptor activator of nuclear kappa B (RANK) ligand (RANKL)/RANK/osteoprotegerin (OPG) axis is one such pathway. In the valve, RANKL binding stimulates osteogenic differentiation of valvular interstitial cell into osteoblasts, leading to formation of calcific nodules and expression of alkaline phosphatase and osteocalcin. In the bone, RANKL binding stimulates osteoclastic activity, causing release of calcium and phosphate into the cardiovascular system. In murine models, targeted inactivation of OPG, a decoy receptor for RANKL, leads to widespread vascular calcification

and severe osteoporosis which can be rescued by administration of osteoprotegerin (Bucay et al., 1998; Morony et al., 2008). Pre-clinical studies also demonstrate that bisphosphonates can reduce production of pro-inflammatory cytokines, decrease bone osteoclastic activity and inhibit arterial as well as valvular calcification (Sansoni et al., 1995). Mechanistic clinical data have demonstrated a link between aortic stenosis progression, vitamin D and bone re-modelling (Hekimian et al., 2013), while observational clinical studies have demonstrated an association between bisphosphonate use and reduced aortic stenosis progression and coronary calcification (Chen et al., 2020; Price et al., 2001; Skolnick et al., 2009). Further support comes from the Multi-Ethnic Study of Atherosclerosis registry which found that bisphosphonate use was associated with a lower prevalence of cardiovascular calcification (defined as the prevalence of aortic valve, aortic valve ring, mitral annulus, thoracic aorta, and coronary artery calcification on computed tomography) in women over 65 years of age (Elmariah et al., 2010). However, such associations are not a universal finding (Aksoy et al., 2012), and a causal relationship cannot be established without randomized controlled trial data.

We have demonstrated the active nature of aortic valve degeneration with *in vivo* 18F-sodium fluoride (18F-NaF) positron emission tomography and computed tomography (PET-CT) (Dweck et al., 2014). 18F-NaF is a bone tracer that binds to hydroxyapatite, a key crystalline component of valvular calcification which has a greater surface area in regions of developing microscopic calcification. Higher valvular 18F-NaF uptake is independently associated with more rapid disease progression and therefore represents a potentially sensitive biomarker of aortic stenosis disease activity (Jenkins et al., 2015).

On the basis of these data, we conducted a randomized controlled trial to determine whether the administration of the RANKL inhibitor denosumab or the bisphosphonate, alendronic acid, can reduce disease progression in patients with calcific aortic stenosis.

5.3 Methods

Study population and protocol

The Study Investigating the Effect of Drugs Used to Treat Osteoporosis on the Progression of Calcific Aortic Stenosis (SALTIRE2) was a single centre parallel group double blind randomised controlled trial (NCT02132026). The Trial Steering Committee oversaw the conduct and progress of the trial. All patients provided written informed consent. The study was conducted in accordance with the Declaration of Helsinki and approved by the regional ethics committee (Scotland A Research Ethics Committee, 14/SS/0064).

Patients over 50 years of age with a peak aortic jet velocity >2.5 m/s on Doppler echocardiography and grade 2-4 aortic valve calcification on semi-quantitative echocardiographic assessment were identified from cardiology outpatient clinics across the south east of Scotland: Edinburgh Heart Centre, Borders General Hospital, Victoria Hospital, Ninewells Hospital and Forth Valley Royal Hospital. Exclusion criteria were anticipated or planned aortic valve surgery in the next 6 months, life expectancy <2 years, inability to undergo scanning, treatment for osteoporosis with bisphosphonates or denosumab, long-term corticosteroid use, abnormalities of the oesophagus or conditions which delay gastric emptying, inability to sit or stand for at least 30 minutes, known allergy or intolerance to alendronic acid, denosumab or any of their excipients, hypocalcaemia, regular calcium supplementation, dental extraction within 6 months, history of osteonecrosis of the jaw, major or untreated cancers, poor dental hygiene, women of child-bearing potential who had experienced menarche, were pre-menopausal, had not been sterilised or were pregnant, women who were breastfeeding, chronic kidney disease (estimated glomerular filtration rate

of <30 mL/min/1.73 m2), allergy or contraindication to iodinated contrast, inability or unwillingness to give informed consent, or a likelihood of non-compliance to treatment allocation or study protocol.

Participants underwent clinical history and examination, 6-minute walk test, blood sampling, 12-lead ECG, echocardiography, combined 18F-sodium fluoride (18F-NaF) positron emission tomography and computed tomography (PET-CT) and non-contrast computed tomography (CT). Participants were randomized using computer-based randomization (Edinburgh Clinical Trials Unit, University of Edinburgh) to ensure allocation concealment 4 to 8 weeks after the baseline visit. Patients were allocated to one of four groups - subcutaneous denosumab (Prolia, Amgen, CA) 60 mg every 6 months, placebo injection every 6 months, oral alendronic acid (TEVA UK, UK) 70 mg once weekly or matching placebo capsule once weekly - in a 2:1:2:1 ratio using a minimization algorithm that incorporated a random component. Minimization criteria were age (<73 and ≥73 years), sex, presence or absence of a bicuspid valve and baseline non-contrast CT aortic valve calcium scores (CT-AVC; ≤1607 and >1607 Agatston units [AU]). Participants were randomized in advance of their randomization visit in order to ensure that the study drug was available to be dispensed at the visit. The placebo capsule contained lactose monohydrate and was manufactured by the Investigational Supplies Group (University of Edinburgh) to be indistinguishable from the encapsulated alendronic acid used. The placebo injection was 0.9% saline, with drug preparation and administration for the injection undertaken by a nominated group of research nurses who remained unblinded. The injection syringes were covered in foil to ensure patients and the research team remained blinded to treatment allocation.

A telephone visit was undertaken 2 weeks after randomisation to assess for symptoms of hypocalcaemia. Further study follow-up visits were performed at 6, 12, 18 and 24 months, where clinical examination, ECG, echocardiogram and blood sampling were undertaken. Serum C-terminal telopeptide, a marker of bone resorption, was measured at baseline and 6 months. Repeat 18F-NaF PET-CT and non-contrast CT were performed at 12 months and repeat non-contrast CT performed at 24 months. Where possible, participants who were subsequently scheduled for AVR had their pending 12- or 24-month visit brought forward, after which the trial intervention was discontinued, and no further trial imaging was performed.

The trial was classified as a Clinical Trial of an Investigational Medicinal Product.

Trial endpoints

The primary endpoint was the calculated change in aortic valve calcium score at 24 months. Key secondary endpoints included change in peak aortic jet velocity at 24 months and change in aortic valve uptake at 12 months. The primary endpoint was calculated as follows: [(final visit aortic valve calcium score – baseline visit aortic valve calcium score) / days from baseline visit to final visit] * 730. Where the participant did not attend a 24-month visit but did attend a 12-month visit, the 12-month visit was used as the final visit. Other imaging endpoints were calculated in the same way. In the case of endpoints with 12-month change (aortic valve 18F-NaF uptake), the daily rate of change was multiplied by 365 rather than 730.

Statistical analysis

Statistical analyses were conducted in accordance with the pre-specified trial statistical analysis plan. To be clinically meaningful, we posited that a disease-modifying therapy would need to delay the time to surgery by 1-2 years. In the previous Simvastatin and Ezetimibe in Aortic Stenosis (SEAS) trial (Rossebo et al., 2008), ~40% of trial participants either died (11%) or underwent aortic valve replacement (30%) within 4 years with an overall rate of disease progression of 0.61±0.59 m/s. This suggests we would need to see a difference in the rates of disease progression of approximately 40% (from 0.16 to 0.10 m/s/year) to delay the need for surgery by 1-2 years. Based on aortic valve calcium score progression in participants from our prior studies (Cowell et al., 2005; Jenkins et al., 2015) who had an aortic valve calcium score ≥400 (median 2-year change 565 [interquartile range, 190-910] AU), we calculated that a sample size of 47 participants would be required per group to detect a 40% difference in the primary endpoint with a two-sided 5% level of significance and 80% power. To account for missing data, the total study sample size was increased to 150. For the primary endpoint and secondary imaging endpoints, 24- or 12-month change was calculated based upon a daily rate of change from baseline to the relevant follow-up scan, using an intention to treat analysis regardless of compliance. Both placebo groups were combined for analysis. For the primary endpoint, if the baseline non-contrast CT scan was degraded by artefact but 12- and 24-month scans were available, these scans were used to determine the daily rate of change. Sensitivity analyses for the primary endpoint were performed after excluding scans with artefact or incorporating only those participants with at least 50% or 70% compliance.

Categorical variables are presented as number (%) while continuous variables are presented as median [interquartile range] or mean ± standard deviation. Distributions of data were tested for normality with the Shapiro-Wilk test and quantile-quantile plots. Between-group differences were compared with the Wilcoxon rank sum test or Kruskal-Wallis test as appropriate. To take into account repeated measurements, mixed-effects linear regression models were constructed for each treatment arm with aortic valve calcium score as the dependent variable, study arm and timepoint as fixed effects and participant as a random effect. Least square means for each active trial arm model were calculated and compared with placebo separately. Spearman's rank correlation coefficient was performed to assess the relationship between continuous variables. Analysis was performed using SAS Enterprise Guide v 7.15 (SAS Institute Inc., Cary, NC, USA). A two-sided p value of <0.05 was considered statistically significant.

5.4 Results

Trial population

Between 19th August 2015 and 6th November 2017, 199 patients were consented, of whom 152 were randomised to denosumab, alendronic acid or matched placebo. Two participants who were randomized to denosumab and were unaware of their study allocation, did not attend the randomization visit or participate further in the study, leaving 150 participants for inclusion in the final analysis (Figure 5.1).

Baseline characteristics were balanced between study arms (Table 5.1). The mean age was 72±8 years, 21% of the cohort were female, and most were of white Scottish ethnicity. There was a high prevalence of hypertension and hypercholesterolemia. The median aortic valve peak velocity and mean gradient were 3.36 [2.93 to 3.82] m/s and 23 [18 to 32] mmHg respectively. The median aortic valve calcium score was 1152 [655 to 2065] AU (Table 5.1).

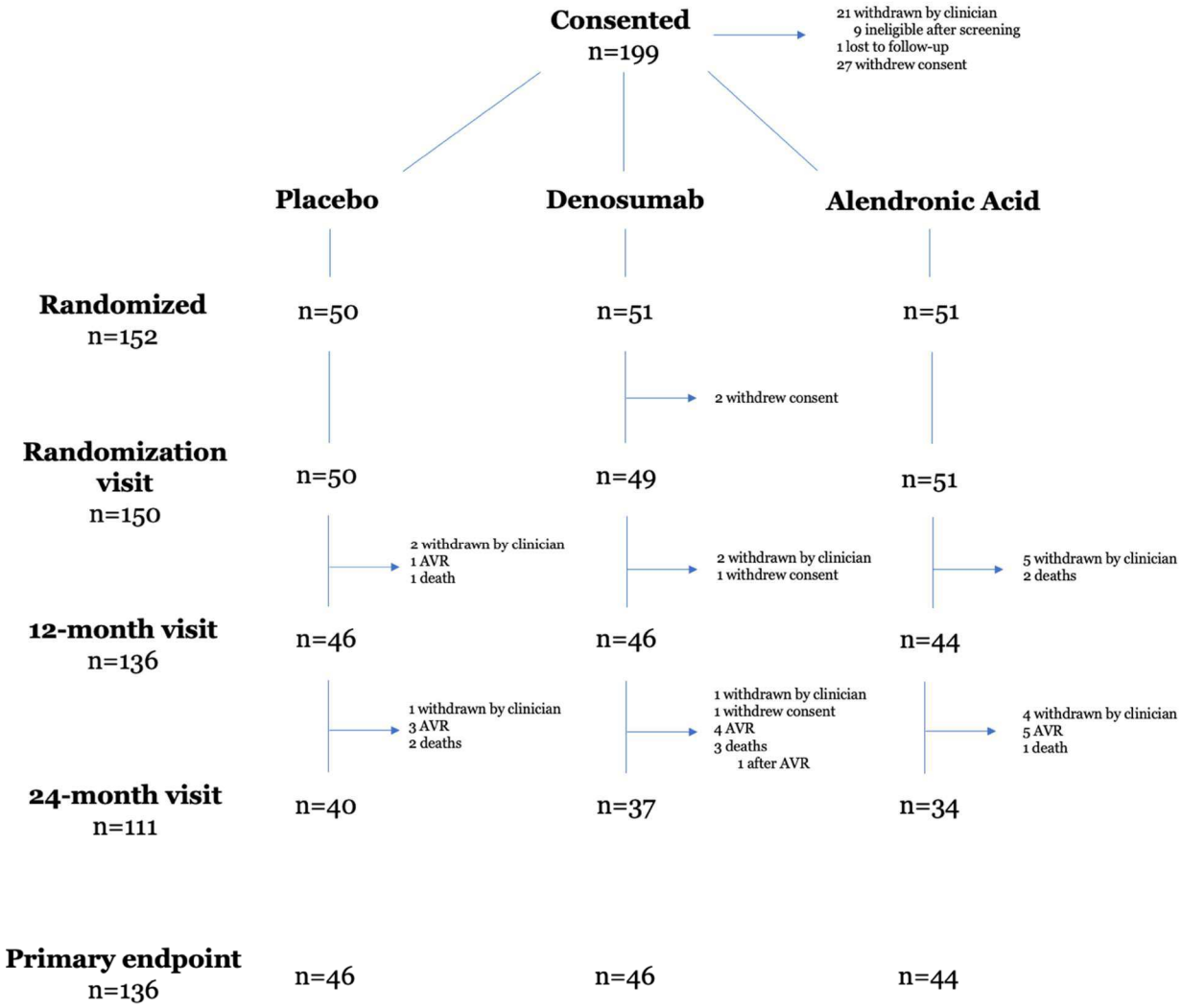

Figure 5.1 CONSORT diagram

CONSORT diagram. The primary endpoint (24-month change in aortic valve calcium score) was calculated from a daily rate of change based on the difference between baseline and final aortic valve calcium score, whether this was at 12 months or 24 months.

Abbreviations: AVR, aortic valve replacement.

Table 5.1 Baseline characteristics

	Overall n = 150	Placebo n = 50	Denosumab n = 49	Alendronate n = 51
Clinical				
Age (years)	73±8	72±7	72±8	73±8
Female	31 (21%)	10 (20%)	11 (22%)	10 (20%)
White Scottish	136 (91%)	46 (92%)	44 (90%)	46 (90%)
Hypertension	114 (76%)	41 (82%)	35 (71%)	38 (75%)
Hypercholesterolemia	91 (61%)	35 (70%)	34 (69%)	22 (43%)
Type 2 diabetes mellitus	35 (23%)	12 (24%)	12 (24%)	11 (22%)
Chronic kidney disease	12 (8.0%)	2 (4.0%)	6 (12%)	4 (7.8%)
Chronic liver disease	1 (0.7%)	1 (2.0%)	0 (0%)	0 (0%)
Osteoporosis	0 (0%)	0 (0%)	0 (0%)	0 (0%)
Prior angina	39 (26%)	13 (26%)	12 (24%)	14 (27%)
Previous myocardial infarction	17 (11%)	4 (8.0%)	8 (16%)	5 (9.8%)
Previous PCI	33 (22%)	11 (22%)	9 (18%)	13 (25%)
Previous CABG	15 (10%)	8 (16%)	3 (6.1%)	4 (7.8%)
Previous TIA/CVA	20 (13%)	6 (12%)	9 (18%)	5 (9.8%)
Malignancy	31 (21%)	10 (20%)	8 (16%)	13 (25%)
Current smoker	13 (8.7%)	3 (6.0%)	2 (4.1%)	8 (16%)
Ex-smoker	77 (51%)	27 (54%)	26 (53%)	24 (47%)
Height (m)	1.71±0.09	1.70±0.08	1.71±0.10	1.71±0.08
Weight (kg)	86 [76 to 93]	85 [79 to 91]	85 [76 to 91]	88 [76 to 100]
Systolic blood pressure (mmHg)	150±19	150±19	149±20	150±20
Diastolic blood pressure (mmHg)	78±11	77±10	79±12	76±11
Heart rate (/min)	67 [59 to 77]	70 [62 to 76]	67 [59 to 80]	66 [56 to 75]
C-terminal telopeptide (μg/L)	0.22 [0.16 to 0.30]	0.22 [0.17 to 0.30]	0.23 [0.18 to 0.32]	0.20 [0.14 to 0.27]
Imaging				
Bicuspid valve	11 (7.3%)	5 (10%)	3 (6.1%)	3 (5.9%)
Peak aortic jet velocity (m/s)	3.36 [2.93 to 3.82]	3.27 [3.03 to 3.73]	3.40 [2.89 to 3.80]	3.38 [2.86 to 3.87]
Mean aortic valve gradient (mmHg)	23 [18 to 32]	22 [18 to 29]	24 [18 to 33]	24 [18 to 32]
Stroke volume index (mL/m^2)	42 [37 to 47]	42 [38 to 47]	41 [35 to 49]	42 [36 to 49]
Aortic valve calcium score (AU)	1,152 [655 to 2,065]	1,127 [617 to 2,059]	1,163 [598 to 2,151]	1,268 [672 to 2,065]
Aortic valve 18F-NaF TBRmax	2.57 [2.21 to 3.07]	2.49 [2.22 to 3.00]	2.79 [2.34 to 3.14]	2.55 [2.10 to 3.17]
Aortic valve 18F-NaF TBRmean	1.67 [1.45 to 1.86]	1.56 [1.43 to 1.80]	1.72 [1.54 to 1.86]	1.66 [1.44 to 1.89]

Median [interquartile range]; mean ± standard deviation; n (%)
Abbreviations: PCI, percutaneous coronary intervention; CABG, coronary artery bypass graft surgery; TIA, transient ischemic attack; CVA, cerebrovascular accident; NaF, sodium fluoride; TBR, tissue to background ratio

Trial intervention

Compliance was similar between placebo and active drug for each method of administration (proportion of participants receiving >70% expected dose: denosumab 94%, placebo injection 92%, alendronic acid 88%, placebo capsule 84%). Baseline serum C-terminal telopeptide concentrations were similar between treatment arms (Table 5.1) and halved from baseline to 6 months with denosumab (0.23 [0.18 to 0.33] to 0.11 [0.08 to 0.17] µg/L) and alendronic acid (0.20 [0.14 to 0.28] to 0.09 [0.08 to 0.13] µg/L) but were unchanged with placebo (0.23 [0.17 to 0.30] to 0.26 [0.16 to 0.31] µg/L; Figure 5.2).

Primary endpoint

The primary endpoint was calculated in 136 participants (46 placebo, 46 denosumab, 44 alendronic acid; Figure 5.1) with a median time to final scan of 784 [770 to 793] days, in whom the overall aortic valve calcium score at baseline was 1110 [622 to 1998] AU. Compared to placebo, there were no differences in the 24-month change in aortic valve calcium score for either denosumab or alendronic acid (denosumab 343 [198 to 804] AU *versus* placebo 354 [76 to 675] AU, p=0.41; alendronic acid 326 [138 to 813] AU *versus* placebo 354 [76 to 675] AU, p=0.49; Figure 5.3-A; Table 5.2).

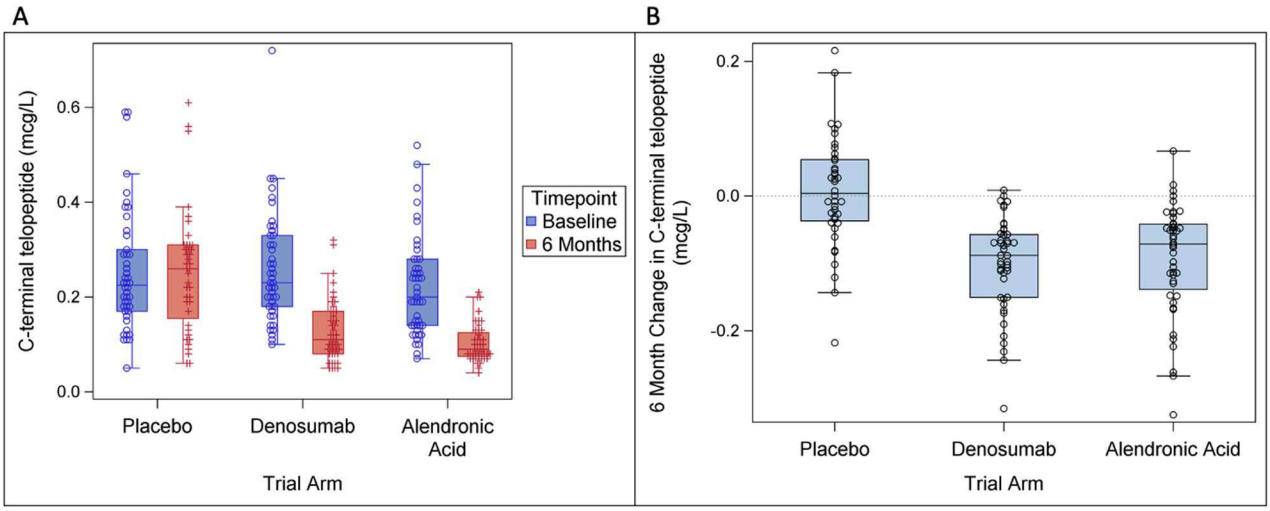

Figure 5.2 C-terminal telopeptide concentrations

A: C-terminal telopeptide concentrations at baseline and 6 months for each trial arm

(p values: placebo >0.5, denosumab <0.001, alendronic acid <0.001; Wilcoxon rank sum test).

B: Six-month change in C-terminal telopeptide for each trial arm

($p<0.001$ for both denosumab and alendronic acid compared to placebo; Wilcoxon rank sum test).

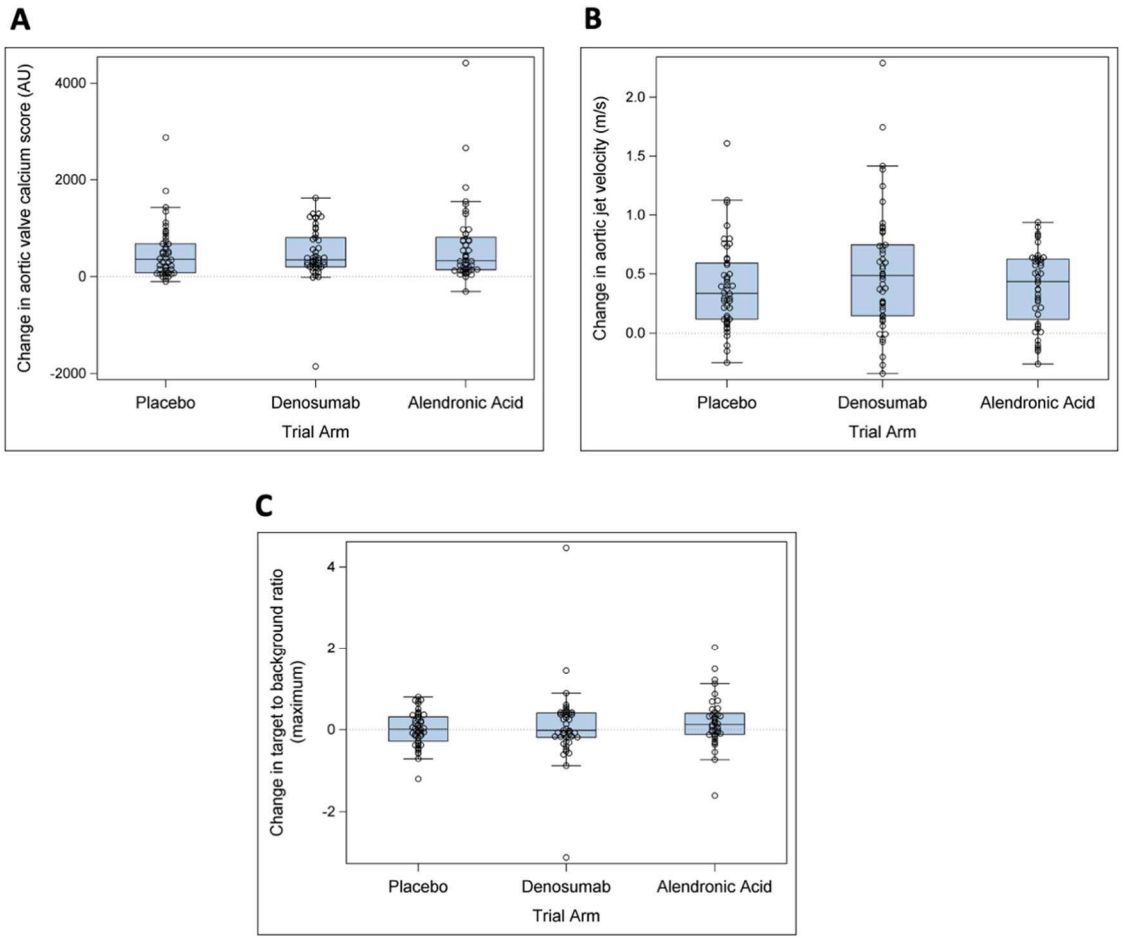

Figure 5.3 Primary and key secondary endpoints

A: Calculated change in 24-month aortic valve calcium score (p=0.41 for denosumab *vs* placebo; p=0.49 for alendronic acid *vs* placebo; Wilcoxon rank sum test).

B: calculated change in 24-month peak aortic jet velocity (p=0.21 for denosumab *vs* placebo; p=0.74 for alendronic acid *vs* placebo; Wilcoxon rank sum test).

C: calculated change in 12-month aortic valve maximum target to background ratio (p=0.61 for denosumab *vs* placebo; p=0.15 for alendronic acid *vs* placebo; Wilcoxon rank sum test).

Table 5.2 Aortic valve calcium score measurements and calculations

Timepoint	Trial allocation	N	Calcium score (AU)
Baseline - whole cohort	Placebo	50	1127 (617 to 2059)
	Denosumab	49	1163 (598 to 2151)
	Alendronate	51	1268 (672 to 2065)
Baseline - those included in primary endpoint analysis	Placebo	46	1053 (539 to 2027)
	Denosumab	46	1176 (598 to 2157)
	Alendronate	44	1076 (671 to 1851)
12-month final visit - those who attended 12-month but not 24-month visit	Placebo	6	1150 (830 to 2438)
	Denosumab	9	1531 (858 to 2455)
	Alendronate	10	1498 (902 to 3446)
24-month final visit	Placebo	40	1902 (683 to 2522)
	Denosumab	37	1502 (973 to 3465)
	Alendronate	34	1381 (848 to 2770)
Final visit - all who attended either 12 or 24-month	Placebo	46	1664 (686 to 2517)
	Denosumab	46	1517 (899 to 3465)
	Alendronate	44	1460 (857 to 2779)
Calculated 24-month change - primary endpoint*	Placebo	46	354 (76 to 675)
	Denosumab	46	343 (198 to 804)
	Alendronate	44	326 (138 to 813)

* The primary endpoint was calculated using the two green shaded rows as follows: [(final visit aortic valve calcium score – baseline visit aortic valve calcium score) / days from baseline visit to final visit] * 730. Where the participant did not attend a 24-month visit but did attend a 12-month visit, the 12-month visit was used as the final visit.
AU, Agatston Units
Median (interquartile range)

Mixed-effects linear regression showed no evidence of a difference between trial arms for either the denosumab-placebo model (least squares mean 1768 (95% CI 1434 to 2101) AU *versus* 1599 (95% CI 1262 to 1936) AU, difference in means 169 (95% CI -304 to 643) AU, p=0.48) or the alendronic acid-placebo model (least squares mean 1792 (95% CI 1452 to 2132) AU *versus* 1596 (95% CI 1253 to 1939) AU, difference in means 196 (95% CI -286 to 679) AU, p=0.42). Pre-specified sensitivity analyses limited to those at least 50% (n=129) or 70% (n=118) compliant demonstrated no differences in the primary outcome (Table 5.3). A further sensitivity analysis of the primary outcome excluding calcium scores affected by artefact in 19 participants also demonstrated no differences in the primary outcome.

Table 5.3 Sensitivity analyses for the primary endpoint		
Excluding scans with artefact		
n=127	**Change in calcium score (AU)**	**P value**
Placebo	292 (74 to 560)	0.16
Denosumab	339 (198 to 748)	
Placebo	292 (74 to 560)	0.36
Capsule	316 (138 to 732)	
At least 50% compliance		
n=129	**Change in calcium score (AU)**	**P value**
Placebo	364 (115 to 740)	0.55
Denosumab	343 (198 to 804)	
Placebo	364 (115 to 740)	0.68
Capsule	316 (138 to 813)	
At least 70% compliance		
n=118	**Change in calcium score (AU)**	**P value**
Placebo	357 (115 to 807)	0.78
Denosumab	329 (197 to 760)	
Placebo	357 (115 to 807)	0.87
Capsule	282 (138 to 754)	
AU, Agatston Units Median (interquartile range) P values - Wilcoxon rank sum test		

Secondary endpoints

Twenty-four month change in peak aortic jet velocity was calculated in 136 patients (46 placebo, 46 denosumab, 44 alendronic acid) with a median time to final echocardiogram of 780 [749 to 798] days, in whom the baseline peak aortic jet velocity was 3.35 [2.91 to 3.77] m/s. There were no differences in the calculated 24-month change in peak aortic jet velocity, either between denosumab and placebo (0.49 [0.15 to 0.75] *versus* 0.33 [0.12 to 0.59] m/s,

p=0.21) or between alendronic acid and placebo (0.44 [0.11 to 0.63] *versus* 0.33 [0.12 to 0.59] m/s, p=0.74; Figure 5.3-B). There were no statistically significant between-group differences in calculated 24-month change in mean gradient or aortic valve area.

Aortic valve 18F-NaF uptake was measured in 130 participants (46 placebo, 44 alendronic acid, 40 denosumab) who underwent baseline and 12-month PET-CT (median time to scan 418 [406 to 429] days). There were no differences in the calculated 12-month change in aortic valve TBR_{mean} either between denosumab and placebo (0.00 [-0.11 to 0.16] *versus* 0.03 [-0.19 to 0.15], p=0.87) or alendronic acid and placebo (0.06 [-0.09 to 0.21] *versus* 0.03 [-0.19 to 0.15], p=0.20; Figure 5.3-C). There were no differences in the 12-month change in aortic valve TBR_{max} either between denosumab and placebo (-0.02 [-0.19 to 0.40] *versus* 0.01 [-0.29 to 0.31], p=0.61) or alendronic acid and placebo (0.12 [-0.12 to 0.40] *versus* 0.01 [-0.29 to 0.31], p=0.15). There were no differences in calculated 12-month change in SUV_{mean} or SUV_{max} between groups (Supplementary Table 1). Baseline aortic valve 18F-NaF TBR_{mean} and TBR_{max} correlated with the calculated 24-month change in aortic valve calcium score (r=0.39 and r=0.40, p<0.001 for both) and peak aortic jet velocity (r=0.26 and r=0.25, p=0.002 and 0.005 respectively).

Clinical and safety outcomes

A total of 41 participants (10 placebo, 14 denosumab, 17 alendronic acid) did not complete the final 24-month visit, 27 of whom attended at least one follow up visit and therefore contributed to the primary endpoint (Figure 5.1). There were 3 deaths in each of the study arms prior to the final study visit. There were no differences in the median number of adverse events (placebo 2 [1 to 3], alendronic acid 2 [1 to 2], denosumab 2 [1 to 3]) or serious adverse

events (0 [0 to 1] for all groups). One serious adverse event was deemed related to a study drug (alendronic acid): oesophagitis leading to dysphagia approximately 10 months after the study baseline visit, diagnosed on endoscopy and treated with proton pump inhibition and cessation of the study drug. No participants were unblinded during the study.

5.5 Discussion

In this single-centre parallel group double blind randomized controlled trial, we demonstrate that treatment with denosumab or alendronic acid had no significant effect on the progression of aortic valve calcification over 24 months in asymptomatic patients with calcific aortic stenosis. We confirmed that both active trial interventions achieved inhibition of bone resorption but were unable to demonstrate an impact on the progression of aortic stenosis. We conclude that these treatments for osteoporosis do not have a major impact on the progression of aortic stenosis.

There remains a major unmet need for an effective disease-modifying non-invasive therapy in aortic stenosis. Following the failure of lipid-lowering therapies (Chan et al., 2010; Cowell et al., 2005; Rossebo et al., 2008), we hypothesised that targeting active valvular calcification might be a feasible therapeutic avenue to slow disease progression. This hypothesis was based on pre-clinical data demonstrating the importance of molecular triggers for calcification in the valve, as well as clinical observational data showing the close association between calcification activity measured with 18F-NaF PET and the subsequent progression of aortic valve calcification and stenosis severity (Bucay et al., 1998; Dweck, Jones, et al., 2012; Jenkins et al., 2015; Morony et al., 2008). Moreover, there have been several reports linking increased bone resorption and osteoporosis with calcification in the aorta and aortic valve (Farhat et al., 2006; Hak et al., 2000), and the role of active aortic valve calcification has been highlighted in previous consensus statements (Yutzey et al., 2014). The close associations between osteoporosis, bone turnover and calcific aortic stenosis led to our

repurposing of drugs used to treat osteoporosis to test this hypothesis. Our results did not reject the null hypothesis.

Given the failure to meet the primary endpoint, it is important to consider the potential reasons for this. First, was the trial intervention successfully applied and did it achieve the desired pharmacological effect? Compliance was excellent in all study arms and there were no differences between the active arms and those receiving placebos. This finding confirms that the active interventions were well tolerated in this population of patients with aortic stenosis. Furthermore, we observed the expected halving of serum C-terminal telopeptide concentrations in those receiving denosumab or alendronic acid, confirming the pharmacodynamic effect of these drugs on bone turnover and resorption in our study population. We can therefore be confident that the trial interventions were successfully administered and achieved their anticipated pharmacological effects.

We should consider whether we have failed to detect an effect of the intervention because of insensitivity of the measurements of aortic stenosis progression or a lack of power. We set out to undertake a comprehensive assessment of aortic stenosis severity and progression using three complementary but distinctly independent methods: aortic valve calcium scoring, Doppler echocardiography and 18F-NaF PET-CT. Aortic valve calcium scoring and echocardiography are standard clinical tools used to assess disease severity (Baumgartner et al., 2017; Doris et al., 2020; Otto et al., 2021), and we were able to identify and to quantify disease progression across all three trial treatment arms using both of these methods. We observed an overall rate of haemodynamic progression that is consistent with published series and trials (Chan et al., 2010; Cowell et al., 2005; Otto et al., 1997; Rossebo et al., 2008). In

addition, we also demonstrate that baseline 18F-NaF PET, a measure of calcification activity, correlated with progression of both peak aortic jet velocity and aortic valve calcium score. This confirms our prior observational data demonstrating similar correlations (Jenkins et al., 2015). Thus, these techniques have assessed drug efficacy from three distinct but complementary approaches and found a concordant lack of effect in the two active trial interventions.

We acknowledge that our sample size was modest, with a preponderance of males. In addition, a proportion (13%) of patients developed a clinical indication for aortic valve replacement and did not complete the full 24-month study period. Importantly, many of these patients still contributed to the study endpoints, based on the available imaging data at their final visit. The proportion of patients who did not complete the full study period is consistent with the severity, profile and completion rates of previously reported randomized controlled trials of aortic stenosis therapies (Chan et al., 2010; Cowell et al., 2005; Rossebo et al., 2008). These factors were anticipated and accounted for in our sample size calculations and statistical analysis plan. Our trial population recapitulated the same rates of disease progression, including the anticipated increase in aortic valve calcium score which was our pre-specified primary endpoint. We found no signal towards benefit or harm in either active treatment arm, and the 95% confidence intervals encompassed our pre-specified effect size of 40%.

Would a larger study in a population with less severe aortic stenosis demonstrate a difference? The vast majority (85%) of our trial population had mild or moderate disease. The natural history of aortic stenosis dictates that many years will elapse before mild aortic

stenosis will become severe. As the trial was powered for an effect size of 40%, it is possible we failed to detect a smaller treatment effect that could delay surgery in the longer term. However, we have recently examined the contemporary use of aortic valve calcium scoring for assessing disease progression, and demonstrated that modest sample sizes, not dissimilar to our present study, are needed to detect the desired effect size sought here (Doris et al., 2020).

Given that the trial intervention achieved its intended pharmacological effect and that multiple measures of disease severity and progression did not detect a treatment effect, was the underlying hypothesis incorrect? The molecular mechanisms underlying our hypothesis have been demonstrated in pre-clinical models, but the direct *in vivo* exploration of human valvular interstitial cell osteoclastic and osteoblastic differentiation and turnover has not been established and would be very challenging to undertake. We have previously demonstrated that microcalcification activity correlates well with aortic stenosis progression as measured by both aortic valve macrocalcification on non-contrast CT and haemodynamic stenosis on Doppler echocardiography (Jenkins et al., 2015). Severe aortic valve calcification on non-contrast CT is also strongly associated with future aortic valve replacement (Pawade et al., 2018). We therefore continue to believe that valvular calcification remains a major pathogenetic determinant of aortic stenosis progression. However, there are multiple other pathways which lead to calcification in the valve, with many pro-inflammatory mediators that initiate and promulgate disease progression. We chose denosumab and alendronic acid as established treatments for osteoporosis, in an attempt to slow valvular calcification whilst maintaining bone health. The absence of a detectable beneficial effect on valvular calcification suggests that either the pathophysiology of calcification in aortic stenosis is

independent of these pathways, or that much higher doses may have been needed, compared to those used for the treatment of osteoporosis. However, given the marked effects on markers of bone turnover, we believe the latter explanation is unlikely.

The main strength of our study is its rigorous design and the use of multiple measures of disease severity and activity to assess drug efficacy. It is the first double blind randomized controlled trial to test the hypothesis in question and has provided a clear answer, with concordant results across each imaging modality. However, the study is limited by its single centre design and a population skewed in ethnicity that, although representative of Scotland, may not be more widely generalizable. The under-representation of females in this study is an issue that we and others have encountered in previous similar trials and is clearly suboptimal (Chan et al., 2010; Cowell et al., 2005; Rossebo et al., 2008). We did include a small number (n=11, 7%) of patients with bicuspid aortic valves. This maybe a potential confounder, as the calcific and non-calcific mechanisms underlying valve degeneration may differ from tricuspid aortic valves. We would also highlight that this trial was powered to investigate disease progression rather than clinical events. However, elective aortic valve replacement is largely based on symptom assessment and non-invasive measurements of aortic stenosis severity, and we have clearly demonstrated no treatment effect on the latter. Given the long time-course of aortic stenosis, it would not have been feasible to demonstrate a difference in clinical events during the relatively short 24-month study period. However, previous trials have demonstrated concordance between measures of disease severity and subsequent large-scale clinical endpoint trials in aortic stenosis (Chan et al., 2010; Cowell et al., 2005; Rossebo et al., 2008).

5.6 Conclusion

In conclusion, we have demonstrated that denosumab and alendronic acid have no effect on the progression of aortic valve calcification or stenosis severity over 24 months in patients with asymptomatic aortic stenosis. Alternative pathways and mechanisms need to be explored in order to identify a disease-modifying therapy for this growing population of patients with a potentially fatal condition.

Chapter 6 – 18F-GP1 positron emission tomography-computed tomography in bioprosthetic aortic valves

Adapted from:

Bing R*, Deutsch M*, Sellers S*, Alcaide Corral C, Andrews JPM, van Beek EJR, Bleziffer S, Burschert W, Clark T, Dey D, Friedrichs K, Gummert J, Koglin N, Leipsic J, Lindner O, MacAskill M, Milting H, Pessotto R, Preuss R, Raftis JB, Rudolph TK, Rudolph V, Slomka P, Stephens AW, Tavares A, Tzolos E, Weir N, White AC, Williams MC, Zabel R, Dweck MR*, Hugenberg V*, Newby DE*. 18F-GP1 positron emission tomography and bioprosthetic aortic valve thrombus. Under submission.

* Authors contributed equally

6.1 Abstract

Background

Bioprosthetic valve thrombosis may have implications for valve function and durability.

Objectives

Using a novel glycoprotein IIb/IIIa receptor radiotracer 18F-GP1, we investigated whether positron emission tomography-computed tomography (PET-CT) could detect thrombus formation on bioprosthetic aortic valves.

Methods

Ex vivo experiments were performed on human platelets and explanted bioprosthetic aortic valves. In a cross-sectional study, patients with either bioprosthetic or normal native aortic valves underwent echocardiography, CT angiography and 18F-GP1 PET-CT.

Results

Flow cytometric analysis, histology, immunohistochemistry and autoradiography demonstrated selective binding of 18F-GP1 to activated platelet glycoprotein IIb/IIIa receptors and thrombus adherent to prosthetic valves. Seventy-five participants (53 with bioprosthetic valves (median time from implantation 37 [12-80] months), 22 with normal native aortic valves) were recruited. Three participants had obstructive valve thrombosis, while a further three participants had asymptomatic hypoattenuated leaflet thickening (HALT) on CT angiography. All bioprosthetic valves, but none of the native aortic valves, demonstrated focal 18F-GP1 uptake on the valve leaflets: median maximum target-to-

background ratio 2.81 [interquartile range 2.29 to 3.48] versus 1.43 [1.28 to 1.53] ($p<0.001$). Higher 18F-GP1 uptake was independently associated with duration of valve implantation and HALT. All three participants with obstructive valve thrombosis were anticoagulated for three months, leading to resolution of their symptoms, improvement in mean valve gradients and a reduction in 18F-GP1 uptake.

Conclusions

Adherence of activated platelets is a common and sustained finding on bioprosthetic aortic valves. 18F-GP1 uptake is higher in the presence of thrombus, regresses with anticoagulation and has potential utility as an adjunctive clinical tool.

6.2 Introduction

Aortic valve replacement can improve symptoms and prognosis in severe aortic valve disease, but there are potential complications to be considered when seeking to optimise outcomes. Although the thrombogenicity of bioprosthetic valves is lower than mechanical prostheses, bioprosthetic valve thrombus is a recognised finding, with a variable prevalence of 12-40% reported in registries (Chakravarty et al., 2017; Makkar et al., 2015) and sub-studies of randomized controlled trials (De Backer et al., 2020; Makkar et al., 2020). Computed tomography (CT) and echocardiography are the current diagnostic imaging modalities of choice but rely on surrogates to detect the presence or haemodynamic effects of leaflet thrombus. Bioprosthetic valve thrombosis may also lead to valve obstruction, while observational data have raised the hypothesis that thrombus may be associated with premature structural valve deterioration (Cartlidge et al., 2019), and that anticoagulation after transcatheter aortic valve replacement (TAVI) may be associated with less valvular haemodynamic deterioration (Del Trigo et al., 2018; Del Trigo et al., 2016). Structural prosthetic valve degeneration is a major consideration (Genereux et al., 2021), especially given the increased risks of repeat valve replacement and the increasingly younger population in whom TAVI is being considered.

18F-GP1 is a novel elarofiban-derived radiotracer that binds to the glycoprotein (GP) IIb/IIIa receptor on activated platelets (Lohrke et al., 2017). Case studies have demonstrated that 18F-GP1 positron emission tomography (PET) can detect *in vivo* venous and arterial thrombi (Chae et al., 2019; Hugenberg et al., 2019; Kim et al., 2018; Lohrke et al., 2017). We

hypothesised that 18F-GP1 PET-CT could be used to detect bioprosthetic aortic valve thrombus.

6.3 Methods

18F-GP1 Radiosynthesis

Centre for Cardiovascular Science, University of Edinburgh, UK: Radiosynthesis of 18F-GP1 was carried out using a NEPTIS Perform synthesiser (Optimised Radiochemical Applications, Neuville, Belgium). The synthesis is a two-step process, involving the nucleophilic fluorination of the tosylate precursor (GP1 precursor) followed by the removal of the protecting groups. After neutralization and separation by semi-preparative High-Performance Liquid Chromatography (HPLC), 18F-GP1 was obtained in radiochemical yields of 19-42% (n=10), 50 min after start of synthesis. 18F-GP1 was then formulated in phosphate buffer before being terminally sterilised in an autoclave.

University Hospital Ruhr-University, Germany: Radiosynthesis of 18F-GP1 was performed starting from Boc-protected tosylate precursor (GP1 precursor). The labelling reaction with fluorine-18 was realized by nucleophilic fluorination of the tosylate precursor in 10 min at 120 °C using the dried K(K222)[18F]F complex in dry acetonitrile. Detachment of the protecting groups was accomplished with acidic acid at 105 °C for 5 min. After neutralization, separation by semi-preparative HPLC and cartridge purification and formulation 18F-GP1 was obtained in radiochemical yields of 27–43 % (decay corrected, n = 5) and radiochemical purities of >98% after 76 – 79 min from the end of radionuclide production. Determined specific activities were in the range of 740–9430 GBq/μmol at the end of the radiosynthesis.

***In Vitro* GP1 Validation**

Platelets were isolated from whole blood taken from 4 healthy volunteers. Forty mL of blood was slowly drawn without a tourniquet from the antecubital vena fossa and anticoagulated immediately with citrate (3.8%). Following initial centrifugation at 350 × g for 20 min, the platelet-rich plasma was removed and centrifuged at 300 × g for 10 min in the presence of 300 ng/ml prostacyclin (PGI2) (Enzo Life Sciences, Farmingdale, NY). Pelleted platelets were re-suspended carefully to their original volume in Hanks' Balanced Salt Solution (HBSS; PAA Laboratories, Australia) with Ca2+ and Mg2+ (for activated platelets) or without Ca2+ and Mg2+ (minimally activated platelets) and incubated at 20°C for 20 min to allow the inhibitory effects of PGI2 to subside before activation.

To assess 18F-GP1 binding in activated platelets versus minimally activated platelets, 10 μM adenosine diphosphate (ADP; Enzo Life Sciences, Farmingdale, NY) was added to 100 μL of washed platelets in triplicate. HBSS without Ca2+ and Mg2+ was used as the vehicle control in the minimally activated group. 18F-GP1 was added to both groups (100 kBq/mL) and left to incubate for 1 h at room temperature. Platelets were then harvested from the incubation medium using vacuum filtration through solid phase extraction columns (Isolute PPT+, Biotage, Sweden), followed by a wash step using HBSS without Ca2+ and Mg2+. After incubation, 1 μM PGI2 was added to prevent further activation, and the radioactivity in the columns, incubation medium and wash was measured immediately by gamma counter (Wizard2, Perkin Elmer, UK) and the % radioactivity bound to the platelets calculated. A blank control was included which contained only 18F-GP1 and buffer.

In a parallel experiment, platelet surface expression of glycoprotein (GP) IIb/IIIa receptors was measured by flow cytometry in activated and minimally activated platelets both in the

absence and presence of 10 μM ADP using CD42a PerCP (BD Biosciences, San Jose, CA) and PAC-1 FITC (BD Biosciences, San Jose, CA) at a timepoint corresponding with the end of the 18F-GP1 experiment. Platelets were gated based on characteristic forward and side scatter and positivity for CD42a. 10,000 CD42a positive events were acquired in the forward scatter side scatter gate, from which those expressing activated GP IIb/IIIa were measured with the Attune NxT acoustic focusing cytometer (Thermo Fisher Scientific, Waltham, MA).

Ex vivo GP1 Validation

Ex vivo experiments were conducted on eight explanted transcatheter aortic valve bioprostheses that were obtained from patients at time of cardiac transplant or surgical replacement (Supplemental Table 1) from a subset of valves described previously (Sellers et al., 2019). Immunohistochemistry was completed for CD41 with a rabbit monoclonal [EPR4330] antibody to CD41 (Abcam, lot #GR3259786) at a dilution of 1:500. Staining was performed via automated staining with a Leica Bond Rx system using Bond Epitope Retrieval Solution 1 (pH=6, Catalog No: AR9961) and Bond Polymer Refine Red Detection (Catalog No: DS9390). The omission of the primary antibody served as negative controls. High-resolution images were generated using an Aperio Slide Scanner and ImageScope software (Leica Biosystems, Germany).

Formalin-fixed, wax processed slides for autoradiography were rehydrated and equilibrated in phosphate buffered saline (PBS) for 30 min prior to the incubation. The slides were incubated with 20 nM 18F-GP1 for 1 hour at room temperature with and without a blocking agent (either 10 μM non-radioactive GP1 or 10 μM tirofiban) before two washes in PBS and one in deionised water. The dried slides were exposed to a high-resolution autoradiography

plate (BAS-IP-SR 2040, Cytiva, USA) which was imaged on an autoradiography imager (Amersham Typhoon IP Biomolecular Imager, Cytiva, USA). Finally, 18F-GP1 micro-PET-CT was performed on one explanted thrombosed mechanical aortic valve.
One non-implanted transcatheter heart valve leaflet (Sapien 3 [Edwards Lifesciences, Irvine, US], embedded in paraffin) was examined as a control valve.

Study Design and Populations

The clinical study comprised a prospective case-control study (n=75, NCT04073875 and NCT03943966, UK) and a proof-of-concept case study (n=2; Germany), conducted in accordance with the Declaration of Helsinki, which were combined for analysis. All participants provided written informed consent.

For the case-control study, patients over 50 years of age who had undergone surgical or transcatheter aortic valve replacement at least one month previously and were not on anticoagulation were recruited from the Edinburgh Heart Centre. Exclusion criteria included inability to provide informed consent, pregnancy or breastfeeding, contraindications to iodinated contrast, use of anticoagulant therapies, estimated glomerular filtration rate <30 mL/min/1.73 m2, metastatic malignancy and an inability to tolerate the supine position. Patients underwent 2-dimensional transthoracic echocardiography and 18-GP1 cardiac PET-CT. The primary endpoint was 18F-GP1 bioprosthetic aortic valve uptake. If there was evidence of valve thrombosis, repeat imaging at 3 months could be performed. The study was approved by the South East Scotland Regional Ethics Committee (18/SS/0163). Patients with a normal native aortic valve and recent myocardial infarction who underwent 18F-GP1

cardiac PET-CT with prospective electrocardiogram gating as part of a concurrent study (NCT03943966) formed a control cohort.

For the proof-of-concept case study, patients with a surgical or transcatheter bioprosthetic valve replacement and symptomatic valve thrombosis ((i) symptomatic, severe haemodynamic prosthesis dysfunction (mean gradient ≥ 40 mmHg or ≥ 20 mmHg change from baseline [before discharge or within 30 days of valve replacement]), (ii) no clinical or biochemical signs of acute infective endocarditis, (iii) leaflet thickening or suspected thrombus formation on echocardiography, and (iv) confirmed hypoattenuated leaflet thickening (HALT) on contrast-enhanced 4-dimensional CT) underwent 18F-GP1 cardiac PET-CT under compassionate use regulations in accordance with the ordinance on Medicinal Products Act (Arzneimittelgesetz – AMG), section 13 (2b), for Compassionate Use of the Federal Institute for Drugs and Medical Devices and the European Medicines Agency Guideline on Compassionate Use of Medicinal Products. The compassionate use was approved by the local Institutional Review Board (2020/639).

Cardiac Imaging Acquisition

Transthoracic echocardiography for the case-control study was performed by a dedicated British Society of Echocardiography-accredited sonographer as previously described. Transthoracic or transoesophageal echocardiography for the case series was performed on a clinical basis. For all patients, combined 18F-GP1 cardiac PET-CT and contrast-enhanced cardiac CT were performed with retrospective electrocardiogram gating. For the case-control study, combined 18F-GP1 cardiac PET-CT was performed on a 128-multidetector row scanner (Biograph mCT, Siemens, Erlangen, Germany) in a dedicated research imaging

centre (Edinburgh Imaging facility, Queen's Medical Research Institute, University of Edinburgh) with electrocardiogram gating. Positron emission tomography list mode acquisition was performed 60 min after intravenous injection of 247 (interquartile range [IQR] 241 – 248) MBq 18F-GP1 with a single bed position centred on the aortic valve, preceded by an attenuation correction CT scan. Contrast-enhanced retrospectively gated cardiac CT was performed after 30 min of PET acquisition (80 mL Iomeron 400 mg/ml, Bracco, Milan, Italy) using automated dose modulation (CARE Dose4D; Siemens, Erlangen, Germany) and tube voltage selection (CARE kV; Siemens, Erlangen, Germany) with a slice thickness of 0.75 mm during expiratory breath-hold. PET images were reconstructed using an ordered subset expectation maximisation algorithm with time-of-flight capability enabled, undergoing 4 iterations of 21 subsets and split into 4 equal gates, each representing 25% of the cardiac cycle. Reconstructions were scaled to a 256 x 256-pixel matrix and used a zoom factor of 2. Gaussian smoothing was applied with a 3-mm full-width at half-maximum kernel.

For the case series, 4-dimensional contrast-enhanced cardiac CT was first performed on a multidetector row scanner (Aquilion One GENESIS, Canon Medical Systems, Neuss, Germany; 80 mL Accupaque 300 mg/mL, Medikamio, Germany) with electrocardiogram gating, a tube voltage of 100 kV and 0.5 mm slice thickness reconstructions. Following this, 18F-GP1 PET was performed (Biograph mCT, Siemens, Erlangen, Germany) 60 to 90 min after injection of 177 – 234 MBq of 18F-GP1. Serial whole-body acquisition covering vertex to thighs was conducted. Low-dose CT (120 kV, 35 mAs, CARE Dose, Siemens Healthcare GmbH, Erlangen, Germany) for attenuation correction was acquired. PET data were acquired in 3-dimensional mode (matrix, 200 × 200) using FlowMotion (Siemens Healthcare GmbH, Erlangen, Germany) and emission data corrected for randoms, scatter and decay.

Reconstruction was performed with ordered-subset expectation maximization using two iterations and 21 subsets and Gaussian filtration to a transaxial resolution of 5 mm in full width at half maximum.

Image Analysis

Cardiac CT images were assessed using Osirix v.12.0.1 (Pixmeo SARL, Geneva, Switzerland) and Vitrea v6.9.68.1 (Vitrea Advanced, Vital Images, Minnetonka, Minnesota, USA) in a systematic fashion in diastole and systole (Jilaihawi et al., 2017). Images were re-oriented into an en face view of the aortic valve (Pawade et al., 2016) and the presence or absence of HALT was established in diastole. If HALT was present, the percentage of leaflet involvement was semi-qualitatively assessed along a curvilinear orientation of the affected leaflet on a long axis view (Blanke et al., 2019) and maximal leaflet opening examined in systole to determine if there was reduced leaflet motion. The percentage of reduced leaflet motion was quantified as the distance from the frame to the affected leaflet tip at maximal excursion divided by the valve radius at that level (Jilaihawi et al., 2017).

18F-GP1 PET-CT images were assessed using FusionQuant v1.20.05.14 (Cedars-Sinai, Los Angeles, California, USA) using a standardized method (Massera et al., 2020; Pawade et al., 2016). After fusing diastolic PET images with the contrast-enhanced CT, an en face view was established and the PET window level adjusted to allow visual determination of the point of maximal specific valvular uptake. A 3-dimensional polyhedron, 6 mm in height and contoured to the valve frame, was centred on this point and formed the volume of interest. 18F-GP1 blood pool uptake was measured in the right atrium with a cylinder 8 mm in radius by 9 mm in height. Where present, pacing leads in the right atrium were excluded. In the

control cohort, the valvular region of interest was centred on the valve leaflets in the z-axis, ensuring the lower border included the leaflet bases.

The aortic valve maximum target-to-background ratio (TBRmax), a measure of the point of most intense 18F-GP1 uptake within the volume of interest, was calculated as the valvular maximum standardized uptake value (SUVmax) divided by the blood pool mean standardized uptake value (SUVmean) accounting for weight. TBRmean, a measure of the average 18F-GP1 uptake in the volume of interest, was calculated as the valvular SUVmean divided by the blood pool SUVmean.

Statistical analysis

Categorical variables are presented as number (percent). Continuous variables were assessed with quantile-quantile plots and presented as mean ± standard deviation or median [interquartile range]. Between group comparisons were undertaken with the Wilcoxon rank sum test. Associations with 18F-GP1 uptake were examined with Spearman's rank correlation efficient and linear regression models. A multivariable model was constructed with log2-transformed TBRmax as the independent variable and age, sex, time after aortic valve replacement, presence of HALT, valve type (transcatheter vs standard sutured surgical prosthesis) and log2-transformed mean gradient as dependent variables, selected on the basis of clinically relevant and plausible mechanisms that may relate to valvular platelet activity and thrombus. Model residuals were checked against fitted values and distributions confirmed with quantile-quantile plots. Two-sided p-values <0.05 were considered statistically significant. Analysis was performed using R version 4.0.3 (R Foundation for Statistical Computing, Vienna, Austria).

6.4 Results

GP1 Validation

Activated platelets demonstrated markedly increased 18F-GP1 binding compared to minimally activated platelets (Figure 6.1). Autoradiography demonstrated selective 18F-GP1 uptake in regions of platelet aggregation and thrombus on explanted transcatheter valves that were confirmed on histology and immunohistochemistry (targeting CD41, a subunit of the GPIIb/IIIa receptor) as well as blocking experiments with tirofiban, another GPIIb/IIIa receptor antagonist (Figure 6.2A). There was no specific uptake in regions of valvular calcium or fibrosis or on the non-implanted control valve leaflets, with no associated CD41 expression (Figure 6.3A-F). The explanted thrombosed mechanical aortic valve demonstrated intense 18F-GP1 uptake on micro-PET-CT that correlated with the hypoattenuated lesions on *in vivo* CT angiography as well as the *ex vivo* micro-CT (Figure 6.2B).

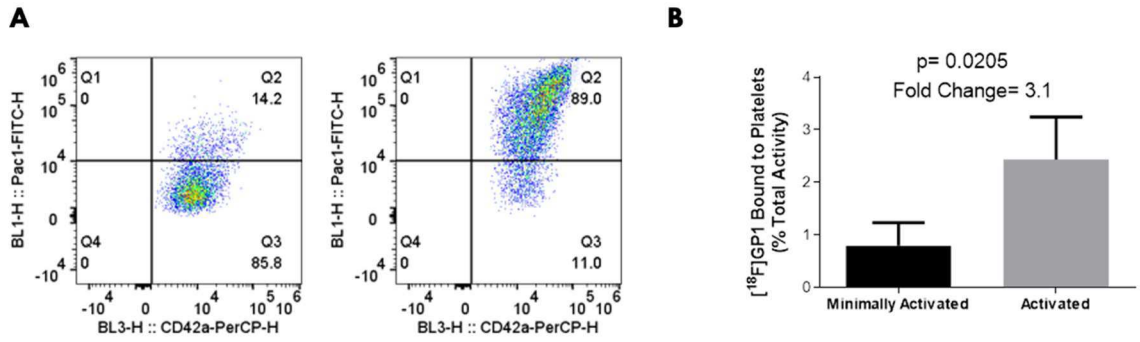

Figure 6.1 *In vitro* 18F-GP1 activity

In vitro selectivity of 18F-GP1 for activated versus minimally activated platelets. A) Fluorescence activated cell sorting analysis of unstimulated (minimally activated, left) and adenosine diphosphate-stimulated (activated, right) platelets demonstrating activation as indicated by the increased CD42a/Pac1+/+ population. B) Quantification of 18F-GP1 binding to minimally activated and activated platelets. Results shown as the mean±SEM, n=4, paired t-test.

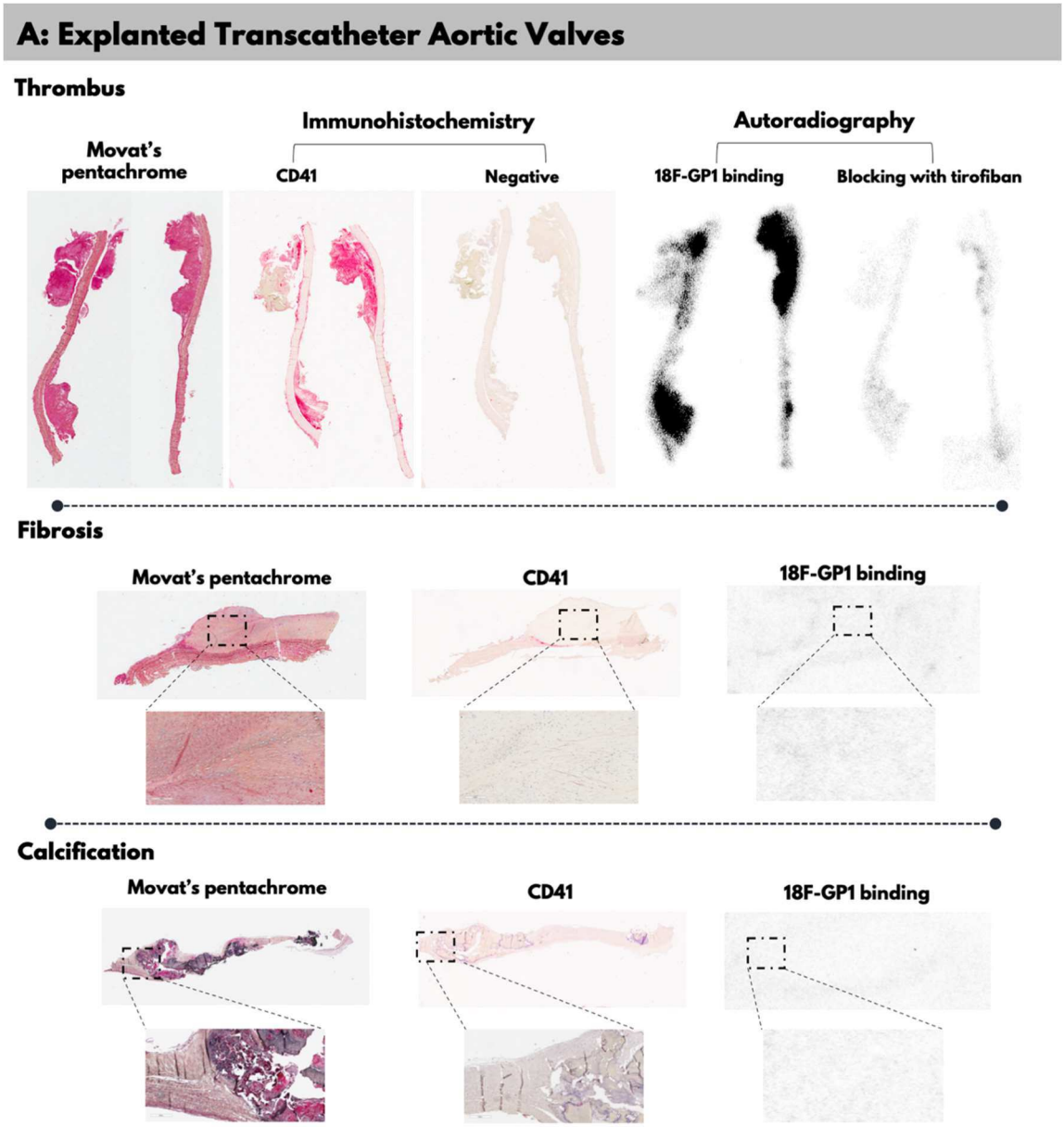
A: Explanted Transcatheter Aortic Valves
Thrombus
Immunohistochemistry
Autoradiography
Movat's pentachrome
CD41
Negative
18F-GP1 binding
Blocking with tirofiban
Fibrosis
Movat's pentachrome
CD41
18F-GP1 binding
Calcification
Movat's pentachrome
CD41
18F-GP1 binding
B: Thrombosed Mechanical Aortic Valve
In vivo CT
Ex vivo micro-CT
Ex vivo 18F-GP1 micro-PET-CT

Figure 6.2 *Ex vivo* 18F-GP1 validation on prosthetic aortic valves - 1

A) Sections of explanted transcatheter heart valve leaflets examined with histology (left; Movat's pentachrome), immunohistochemistry (middle; CD41 staining) and 18F-GP1 autoradiography (right). The top row demonstrates leaflet thrombus with 18F-GP1 binding to discrete regions of thrombus which can be blocked with tirofiban – a glycoprotein IIb/IIIa receptor antagonist (Valve ID 3). The second (Valve ID 1) and third (Valve ID 6) rows demonstrates fibrotic and calcific leaflet degeneration with no CD41 activity or 18F-GP1 uptake.

B) Patient with mechanical aortic valve thrombosis demonstrated *in vivo* by hypoattenuated lesions on pre-operative computed tomography angiography. On excision, the mechanical valve was imaged by *ex vivo* micro-CT and 18F-GP1 micro-PET, confirming the detection of valve thrombosis.

Abbreviations: CT, computed tomography; PET, positron emission tomography.

Valve IDs correspond to details in table appended to Figure 3.

3A

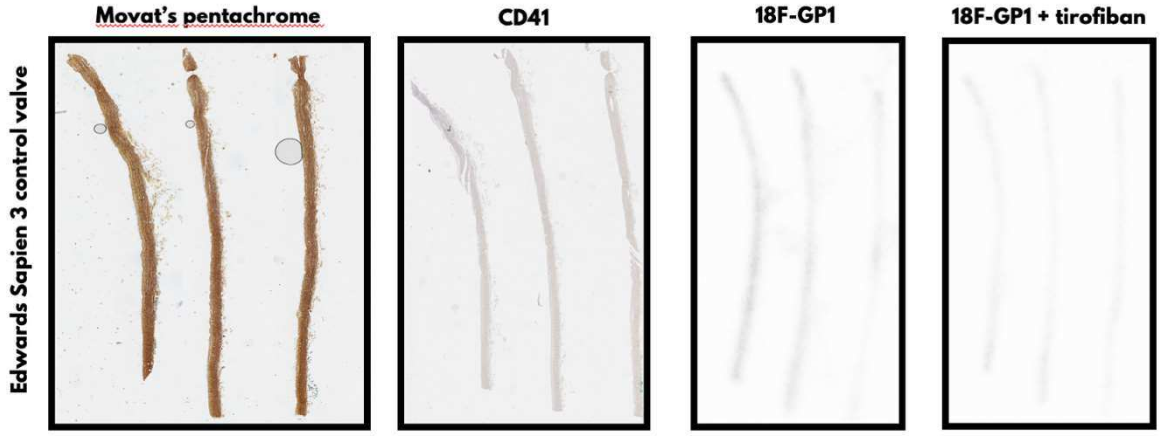
Movat's pentachrome
CD41
18F-GP1
18F-GP1 + tirofiban
Edwards Sapien 3 control valve

3B

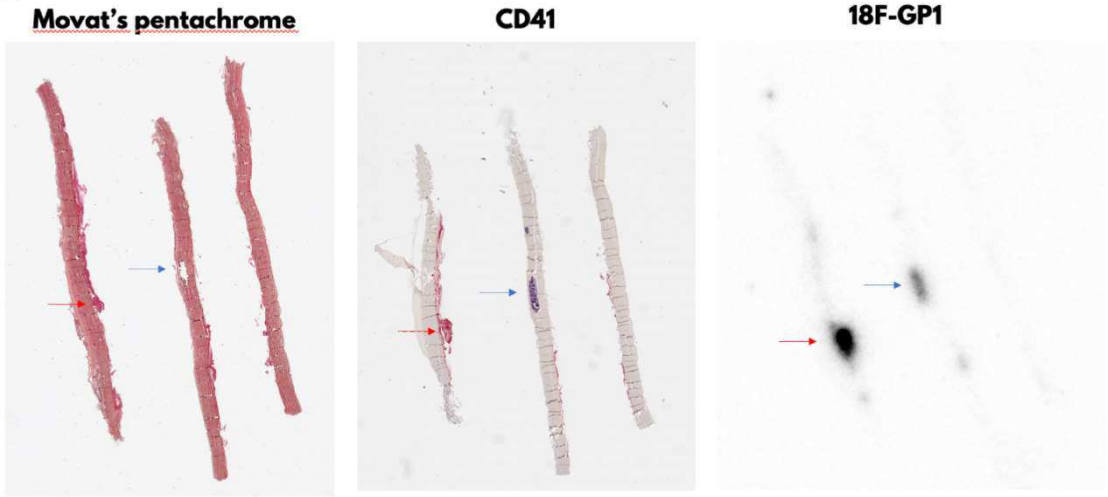
Movat's pentachrome
CD41
18F-GP1

3C

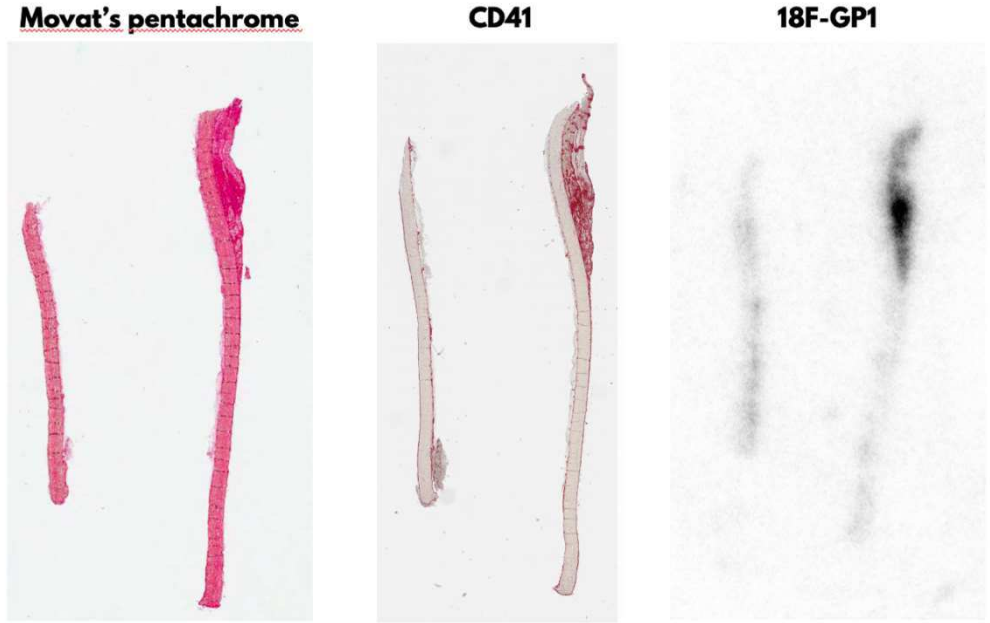
Movat's pentachrome
CD41
18F-GP1

3D

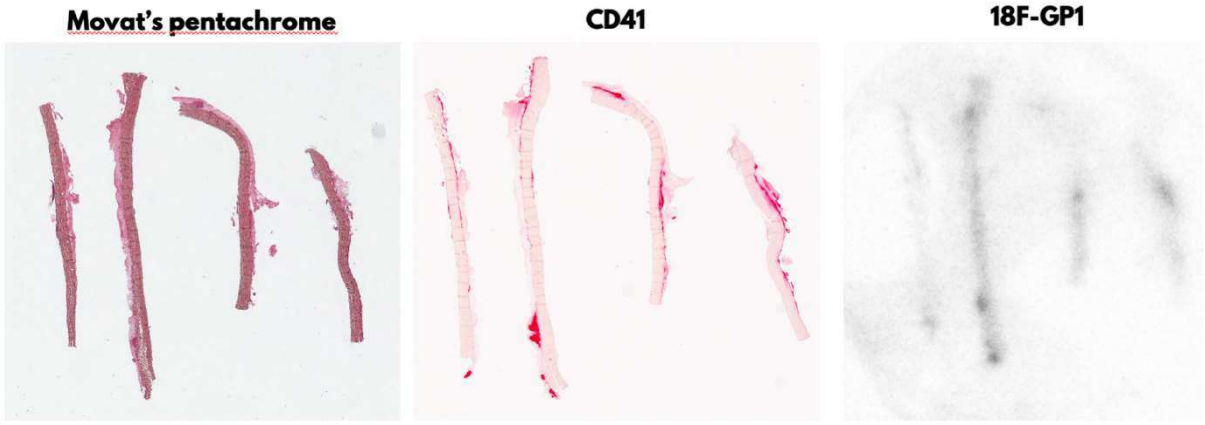
Movat's pentachrome
CD41
18F-GP1

3E

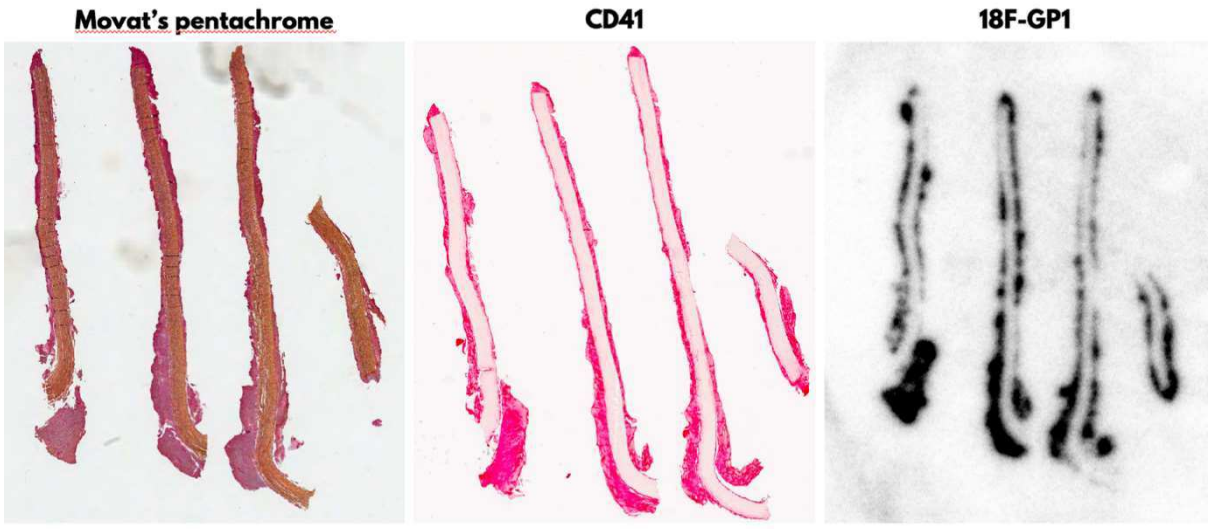
Movat's pentachrome
CD41
18F-GP1

3F

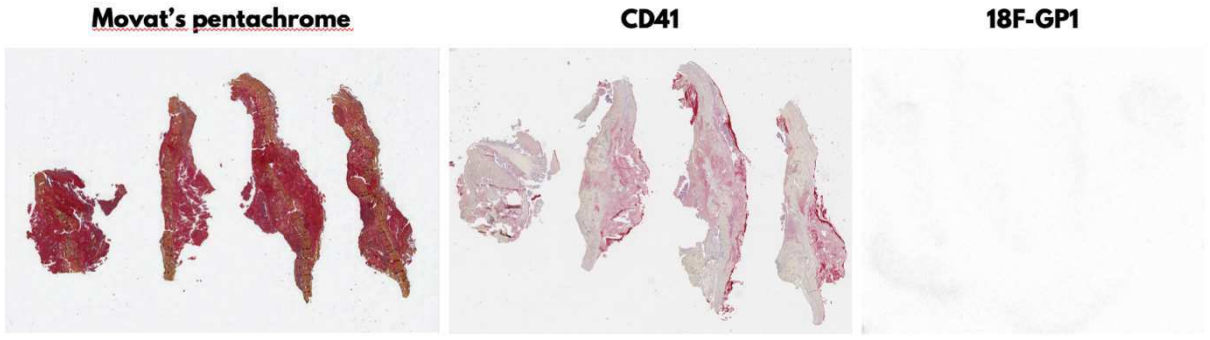
Movat's pentachrome
CD41
18F-GP1

Figure 6.3 *Ex vivo* 18F-GP1 validation on prosthetic aortic valves - 2

A) *Ex vivo* validation of 18F-GP1 in a non-implanted Edwards Sapien 3 control valve, with no evidence of thrombus on histology or immunohistochemistry and no specific 18F-GP1 uptake.

B-F) *Ex vivo* validation of 18F-GP1 uptake in leaflet sections of transcatheter aortic valves with corresponding histology and CD41 immunohistochemistry.

B: Valve ID 2 – thrombus (red arrow) and calcified nodule (blue arrow). On autoradiography there is specific 18F-GP1 uptake in the former, while the uptake in the latter is non-specific, confirmed on blocking experiments.

C: Valve ID 4 – thrombus

D: Valve ID 5 – thrombus

E: Valve ID 7 – thrombus

F: Valve ID 8 – heavily calcified valve with extensive fibrin deposition and inflammatory infiltrate with possible associated infection.

Valve IDs correspond to details in table below.

Valve ID	Valve Type	Implant Duration (days)	Mode of Explant
1	23-mm Sapien XT	1611	Post-mortem
2	26-mm Cribier-Edwards	2496	Post-mortem
3	26-mm Sapien XT	4	Post-mortem
4	25-mm Portico	2	Post-mortem
5	23-mm Sapien XT	28	Post-mortem
6	23-mm Cribier-Edwards	2583	Post-mortem
7	29-mm Sapien 3	0	Surgical
8	23-mm Sapien XT	1598	Post-mortem

Study Population

Eighty-three participants were recruited between October 2019 and March 2021, of whom eight either withdrew or were unable to attend due to government public health restrictions, leaving 75 in the analysis: 53 patients with aortic valve bioprostheses and 22 control subjects who underwent 18F-GP1 PET-CT (Table 6.1). The mean age in the bioprosthetic valve cohort was 73±7 years and one quarter were female. The median time from aortic valve replacement to PET-CT was 37 [12 to 80] months, with aortic stenosis being the primary indication for aortic valve replacement. The prostheses were predominantly bovine pericardial valves, except for the porcine Carpentier-Edwards supra-annular valve (Edwards Lifesciences) and Evolut R valve (Medtronic, Minneapolis, US). Eight valves were transcatheter heart valves (Sapien S3 and Evolut R). Most patients with aortic valve bioprostheses were maintained on anti-platelet monotherapy.

Most of the cohort were asymptomatic of valvular heart disease. One patient had suspected clinical valve thrombosis based on an unexpected deterioration in valve haemodynamic measurements and a recent increase in exertional dyspnoea (25-mm Carpentier-Edwards supra-annular valve, 6.3 years after surgical valve replacement, mean gradient 60 mmHg, on maintenance aspirin therapy). Two further patients had

Table 6.1 Baseline characteristics

	Native aortic valves (n=22)	**Bioprosthetic aortic valves (n=53)**
Age (years)	60 (55 to 66)	73 (68 to 77)
Female sex	5 (23%)	13 (25%)
Height (m)	1.68 (1.64 to 1.78)	1.73 (1.64 to 1.78)

Weight (kg)	82 (73 to 85)	83 (73 to 95)
Past medical history		
Hypertension	8 (36%)	38 (72%)
Hypercholesterolaemia	5 (23%)	39 (72%)
Diabetes mellitus	2 (9%)	6 (11%)
Current or ex-smoker	15 (68%)	29 (55%)
Prior coronary artery disease	4 (18%)	26 (49%)
Prior myocardial infarction	4 (18%)	8 (15%)
Stroke/TIA	1 (5%)	8 (15%)
Chronic kidney disease	0 (0%)	3 (6%)
COPD	0 (0%)	4 (8%)
Peripheral vascular disease	0 (0%)	8 (15%)
NYHA class		
1	-	41 (77%)
2	-	9 (18%)
3	-	3 (2%)
4	-	0 (0%)
Prior procedures		
Aortic valve replacement	0 (0%)	1 (2%)
Coronary artery bypass grafting	1 (4.5%)	7 (13%)
Aortic root replacement	0 (0%)	1 (2%)
Percutaneous coronary intervention	4 (18%)	12 (23%)
Permanent pacemaker	0 (0%)	4 (8%)
Antiplatelet agents		
Aspirin	20 (91%)	41 (77%)
Clopidogrel	20 (91%)	7 (13%)
Index aortic valve replacement		
Bicuspid valve	-	12 (23%)
Root replacement	-	0 (0%)
Ascending aorta repair	-	3 (6%)
Coronary artery bypass grafting	-	15 (28%)

Valve model		
Edwards CE SAV	-	5 (10%)
Edwards Inspiris Resilia	-	5 (10%)
Edwards Perimount Magna	-	4 (8%)
Edwards Perimount Magna-Ease	-	16 (32%)
Edwards Perimount	-	10 (20%)
Sorin Perceval	-	5 (10%)
Edwards Sapien S3 (THV)	-	4 (8%)
Medtronic Evolut R (THV)	-	3 (6%)
Baseline echocardiography*		
Normal left ventricular systolic function	3 (21%)	44 (85%)
Peak aortic valve velocity (m/s)	1.21 (1.13 to 1.37)	2.46 (2.2 to 3.0)
Mean aortic valve gradient (mmHg)	3 (2 to 4)	12 (9 to 17)
Indexed EOA (cm^2/m^2)	-	0.77 (0.59 to 0.89)

n (%); median (interquartile range)

*Native aortic valve measurements from clinical echocardiograms performed in 14/22 patients.

Abbreviations: TIA, transient ischaemic attack; COPD, chronic obstructive pulmonary disease; NYHA, New York Heart Association; CE SAV, Carpentier-Edwards supra-annular valve; THV, transcatheter heart valve; EOA, effective orifice area.

confirmed clinical valve thrombosis (21-mm Perimount Magna [Edwards Lifesciences], 14 months after surgical valve replacement, mean gradient 45 mmHg, on rivaroxaban 20 mg daily for atrial fibrillation; 26-mm Sapien 3, 24 months after TAVI, mean gradient 57 mmHg, no antithrombotic therapy). Two other patients had long-standing patient-prosthesis mismatch (21-mm Perimount Magna, mean gradient 37 mmHg, indexed effective orifice area 0.55 cm2/m2; 19-mm Perimount Magna-Ease [Edwards Lifesciences], mean gradient 39

mmHg, indexed effective orifice area 0.38 cm2/m2) without a recent change in symptoms or valve haemodynamic measurements.

Echocardiography and Computed Tomography

No abnormality of valve leaflet motion was seen on echocardiography in patients recruited into the case-control study, including the patient with suspected valve thrombosis (Table 6.1). In the two patients with clinically confirmed valve thrombosis, echocardiography demonstrated leaflet thickening with restricted motion.

All three patients with suspected or confirmed valve thrombosis had extensive HALT involving >50% of all leaflets with associated reduced leaflet motion. Three other asymptomatic patients were found to have HALT of a single leaflet: two with 50-75% leaflet involvement and <50% reduced leaflet motion, one with <25% leaflet involvement and normal leaflet motion. Neither patient with known patient-prosthesis mismatch had HALT. Finally, one asymptomatic patient with a recent TAVI (29-mm Evolut R) was found to have discrete hypoattenuating lesions external to the valve frame within the right and non-coronary sinuses, consistent with thrombus. The valve leaflets had no HALT.

Valvular 18F-GP1 Uptake

No native aortic valves in control subjects (n=22) had any visually identifiable discrete 18F-GP1 uptake (Figure 6.4A). In contrast, visually positive discrete 18F-GP1 uptake was identifiable on the aortic valve leaflets of all patients with a bioprosthetic valve (Figure 6.4B-D). In patients with bioprostheses, the valvular TBRmax (2.81 [2.29 to 3.48] vs 1.43 [1.28 to 1.53], p <0.001) and TBRmean (1.59 [1.41 to 1.87] vs 0.95 [0.91 to 0.98], p<0.001) were

higher than in patients with native aortic valves (Figure 6.5A-B). The valve frames and stents were relatively free of uptake.

In the three patients with asymptomatic HALT and no valve obstruction, 18F-GP1 uptake was manifest across all leaflets (Figure 6.6A-C). The three patients with obstructive valve thrombosis had intense valvular 18F-GP1 uptake (TBRmax 4.47 to 7.40; Figure 6.7). The patient with sinus hypoattenuation had 18F-GP1 activity that co-localised to the discrete lesions (TBRmax 2.12), while the normal valve leaflets also had focal uptake that was similar to the rest of the cohort (TBRmax 1.79). The TBRmax in the two patients with known patient-prosthesis mismatch were slightly higher than the cohort median (2.95 and 3.08).

18F-GP1 TBRmax and TBRmean correlated inversely with valve age, rather than any echocardiographic measures of valve function (Table 6.2; Figure 6.5C-D). Linear regression models demonstrated univariable associations between valve 18F-GP1 TBRmax and a shorter time from aortic valve implantation and the presence of HALT. There was no association with type of valve (surgical versus transcatheter). On multivariable analysis, HALT and a more recent valve implant remained independently associated with a higher valve TBRmax (Table 6.3). The same model constructed with TBRmean as the dependent variable showed similar independent associations (adjusted R2 0.32, $p<0.001$).

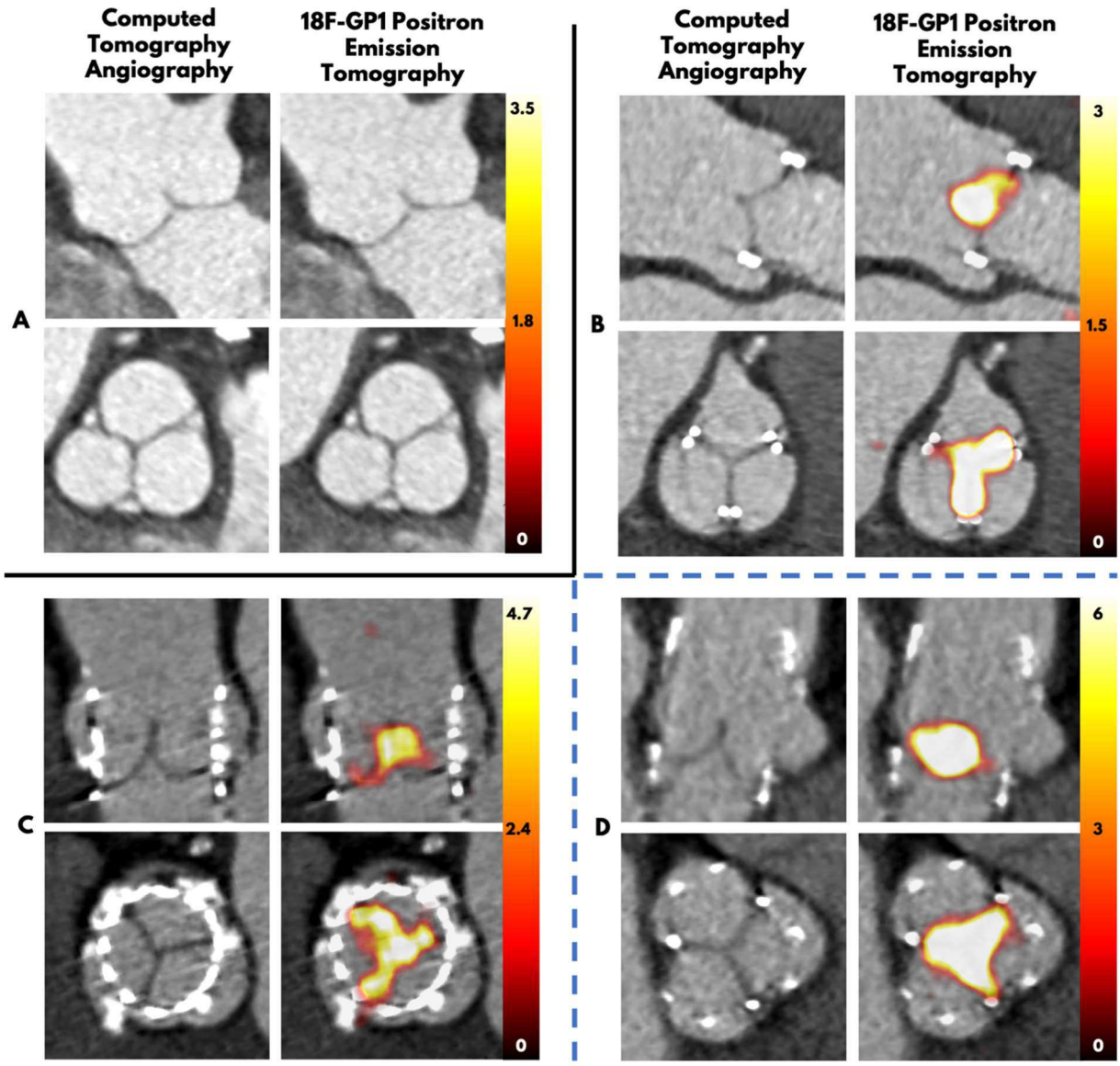

Figure 6.4 *In vivo* assessment of aortic valve leaflets

A) A control patient with a normal aortic valve and no 18F-GP1 uptake.

B-D) Three examples of bioprosthetic aortic valves (23-mm Magna Ease, 29-mm Sapien 3 and Perceval S) with normal function. There is no evidence of leaflet thrombus on CT, but focal 18F-GP1 which is most intense along the leaflet edges.

Scale bars represent standardised uptake values. Images were windowed until no blood pool activity seen but regional uptake could be recognised.

Abbreviations: CT, computed tomography.

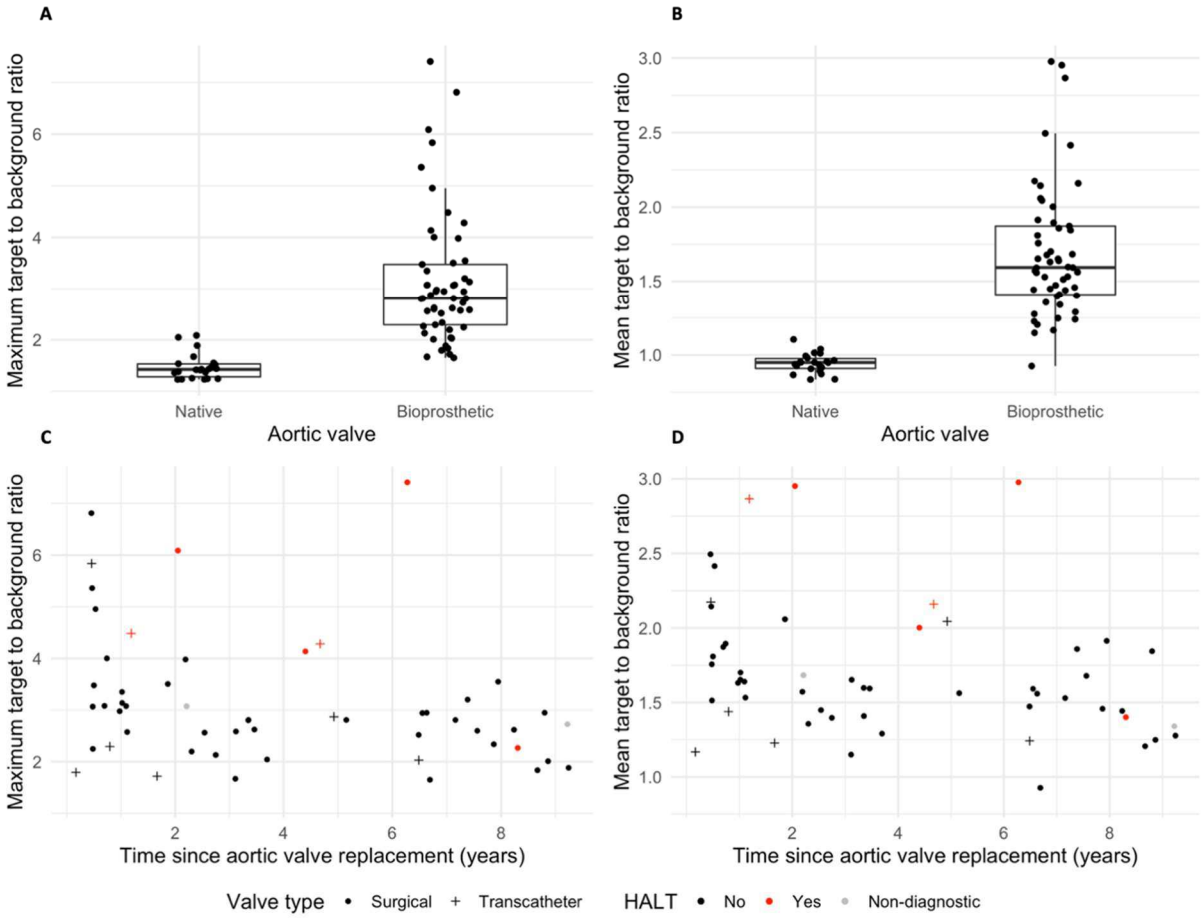

Figure 6.5 18F-GP1 uptake in native and bioprosthetic aortic valves

A) TBRmax in native compared to bioprosthetic aortic valves.

Wilcoxon rank sum test p<0.001.

B) TBRmean in native compared to bioprosthetic aortic valves.

Wilcoxon rank sum test p<0.001.

C) TBRmax by duration of bioprosthetic valve implantation (Spearman's ρ = -0.36, p=0.007) and valve type.

D) TBRmean by duration of bioprosthetic valve implantation (Spearman's ρ = -0.36, p=0.009) and valve type.

Abbreviations: TBR, target-to-background ratio.

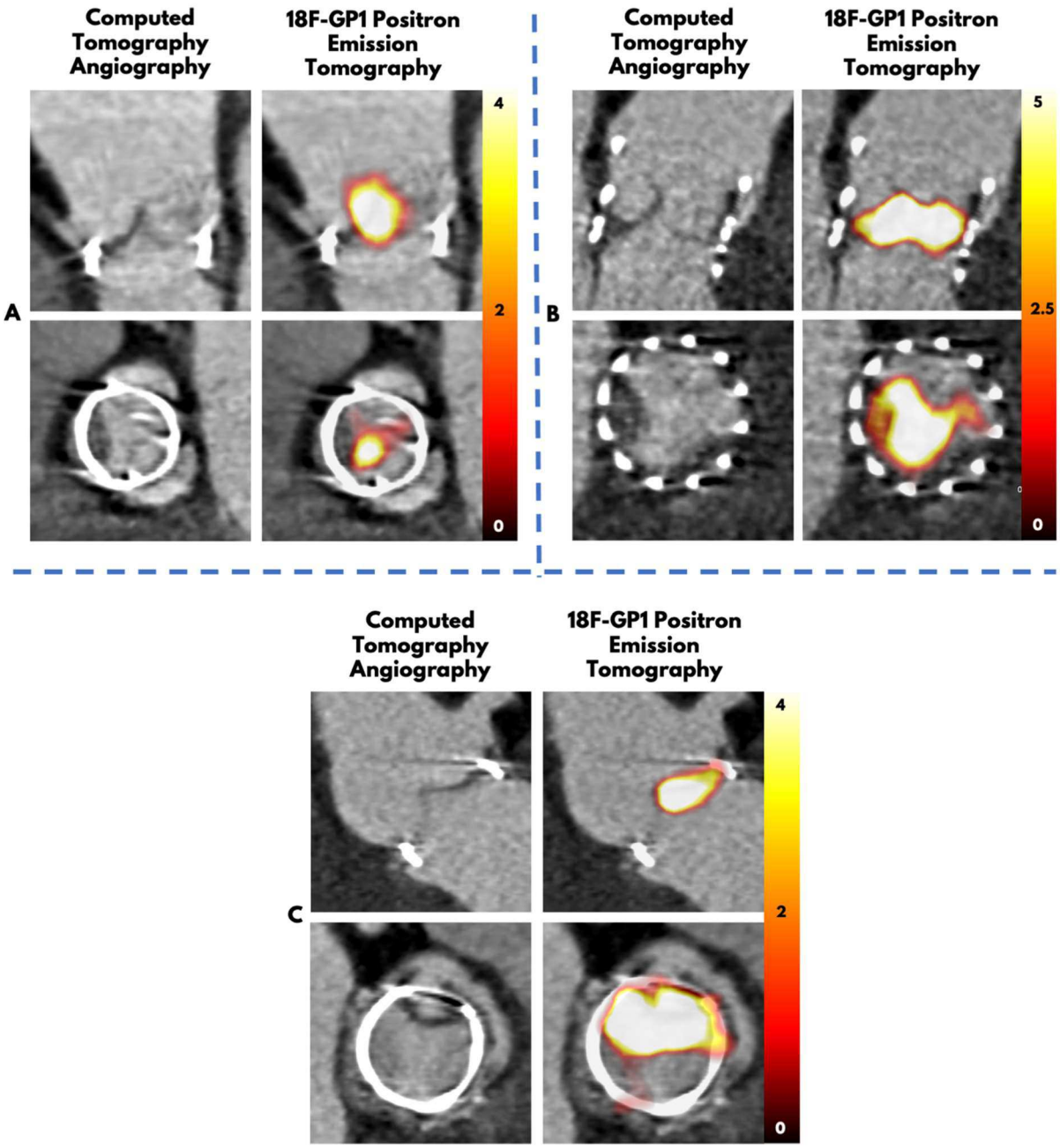

Figure 6.6 Subclinical valve thrombosis

A) 19-mm Edwards Perimount Magna, 8.3 years after surgical aortic valve replacement. Mean gradient 17 mmHg, indexed effective orifice area 0.84 cm^2/m^2, TBRmax 2.27, TBRmean 1.40, <50% reduced leaflet motion.

B) 26-mm Edwards Sapien S3, 4.7 years after transcatheter aortic valve replacement. Mean gradient 16 mmHg, indexed effective orifice area 0.53 cm^2/m^2, TBRmax 4.28, TBRmean 2.16, <50% reduced leaflet motion.

C) 25-mm Edwards Perimount Magna Ease, 4.4 years after surgical aortic valve replacement. Mean gradient 14 mmHg, indexed effective orifice area 0.79 cm^2/m^2, TBRmax 4.14, TBRmean 2.00, normal leaflet motion.

Scale bars represent standardised uptake values. Images were windowed until no blood pool activity seen but regional uptake could be recognised.

Abbreviations: TBR, target-to-background ratio.

Baseline
Follow-up
Computed Tomography Angiography
18F-GP1 Positron Emission Tomography
A
B
C
D
E
F
0
5
10
2.5
4
8

Figure 6.7 Obstructive valve thrombosis

A) 25-mm Carpentier-Edwards supra-annular valve, 6.3 years after surgical AVR, mean gradient 60 mmHg, patient on aspirin. There is extensive HALT, particularly on the aortic aspect of the right coronary cusp, consistent with thrombus. There is intense 18F-GP1 uptake (TBRmax 7.40) which is most avid in the region of heaviest thrombus burden.

B) 21-mm Perimount Magna valve, 14 months after surgical AVR, mean gradient 45 mmHg, patient on rivaroxaban 20mg d for atrial fibrillation. All three leaflets have extensive HALT involving most of the leaflet body, with associated intense 18F-GP1 uptake (TBRmax 6.12).

C) 26-mm Sapien 3 valve, 24 months after TAVI, mean gradient 57 mmHg, no antithrombotic therapy. There is typical HALT extending from the leaflet bases of all three leaflets and associated 18F-GP1 uptake (TBRmax 4.47).

D) Patient (A), 3 months after commencing therapeutic anticoagulation with apixaban. The mean gradient has fallen to 8 mmHg. The thrombus has largely resolved, with residual pannus around the valve frame. 18F-GP1 uptake has reduced (TBRmax 4.44) but is still present in the leaflets. There is no activity in regions of pannus.

E) Patient (B), 3 months after changing from rivaroxaban to phenoprocoumon. The mean gradient has fallen to 15 mmHg. There is complete resolution of the thrombus and no 18F-GP1 uptake (TBRmax 1.52).

F) Patient (C), 3 months after commencing phenoprocoumon. The mean gradient has fallen to 13 mmHg. There is complete resolution of thrombus but residual 18F-GP1 uptake (TBRmax 3.17).

Table 6.2 Correlations between echocardiography, 18F-GP1 and duration of valve implantation

	TBRmax		**TBRmean**	
	ρ	**p value**	ρ	**p value**
Peak aortic valve velocity	0.05	0.70	0.14	0.30
Mean gradient	0.08	0.59	0.15	0.28
Indexed EOA*	-0.21	0.15	-0.27	0.06
Months after AVR	-0.36	0.007	-0.36	0.009

ρ and p values for Spearman's rank correlation coefficient.
* Aortic valve area not available in two patients due to poor image quality
Abbreviations: TBR, target-to-background ratio; EOA, effective orifice area; AVR, aortic valve replacement.

Response to Anticoagulant Therapy

Of the three patients with obstructive valve thrombosis, one was treated with apixaban 5 mg twice daily (previously on aspirin) while the other two were treated with the vitamin K antagonist, phenoprocoumon. All three had follow-up 18F-GP1 PET-CT imaging at three months which showed improvements in mean valve gradients (60 to 8 mmHg, 45 to 15 mmHg and 57 to 13 mmHg); there was associated resolution of symptoms. In all three cases, there was resolution of HALT, although one patient had persisting hypoattenuation around the base of the valve frame, consistent with pannus. 18F-GP1 uptake fell, with residual uptake in two patients and complete resolution of all uptake in the remaining patient (Figure 6.7).

Table 6.3 Linear regression models for aortic valve maximum 18F-GP1 target-to-background ratio

	Univariable		Multivariable		
	Coefficient (95% CI)	**p value**	**Coefficient (95% CI)**	**p value**	**Adjusted R2**
Age (per decade)	0.03 (-0.19 to 0.25)	0.81	0.07 (-0.15 to 0.29)	0.55	0.28 p=0.002
Male sex	003 (-0.33 to 0.39)	0.86	0.20 (-0.13 to 0.53)	0.23	
Time after AVR (per month)	-0.005 (-0.009 to -0.001)	0.02	-0.006 (-0.01 to -0.002)	0.002	
Mean gradient (log2[mmHg])	0.13 (-0.04 to 0.31)	0.13	-0.002 (-0.18 to 0.18)	0.98	
Transcatheter valve	-0.04 (-0.45 to 0.36)	0.83	-0.38 (-0.79 to 0.04)	0.07	
HALT	0.69 (0.27 to 1.10)	0.002	0.82 (0.34 to 1.29)	0.001	
Abbreviations: CI, confidence interval; AVR, aortic valve replacement; HALT, hypoattenuated leaflet thickening					

Extra-valvular 18F-GP1 Uptake

Three patients who received ascending aorta interposition grafts (gelatin-sealed polyester or polytetrafluoroethylene) at the time of aortic valve replacement demonstrated focal 18F-GP1 uptake at the graft sites. Two operations were within 12 months of the PET-CT, while one was more than 3 years prior to imaging (Figure 6.8A). This contrasted with one patient who had previously undergone valve-sparing root and ascending aorta replacement (gelatin-sealed polyester) 8 years previously, in whom there was no aortic uptake.

Twelve patients had undergone percutaneous coronary intervention in the past (median time from stenting to PET-CT 5.2 [2.5 to 14.8] years). There was no focal uptake in any of the

coronary stents. However, one intervention, which occurred more than 5 years prior to PET-CT, was complicated by disarticulation of the distal portion of a guide wire which was jailed behind a stent in the right coronary artery. There was intense 18F-GP1 uptake at the site of this retained wire (Figure 6.8B).

Four patients had undergone permanent pacemaker implantation, the most distant of which occurred 7 years prior to PET-CT. All pacemaker leads demonstrated regions of focal 18F-GP1 uptake in the superior vena cava and right atrium (Figure 6.8C). Finally, one patient underwent percutaneous paravalvular leak closure in the 12 months prior to PET-CT, with focal uptake at the site of the vascular plug which appeared distinct from the adjacent bioprosthetic valve leaflets.

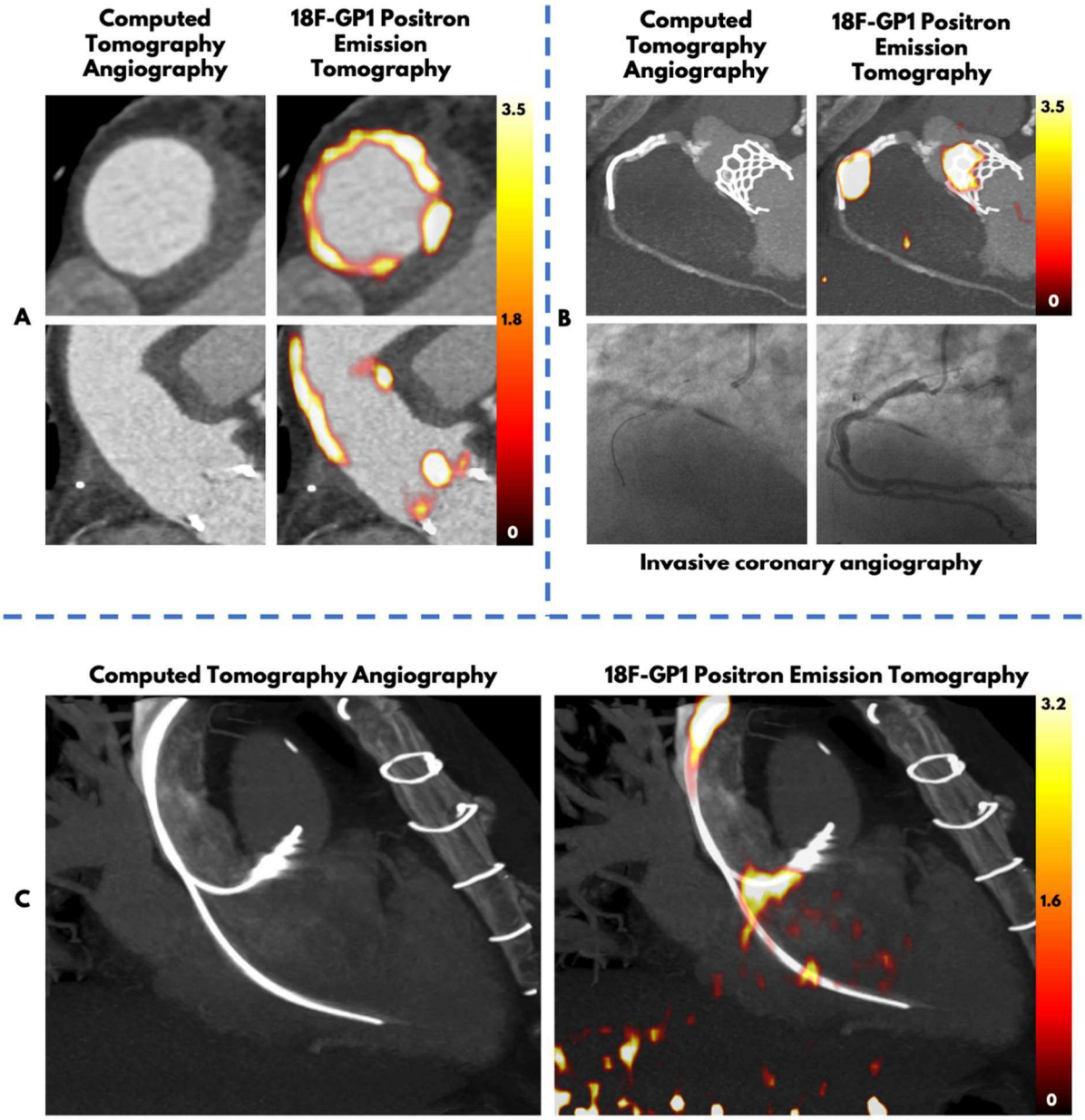

Figure 6.8 Incidental cardiac 18F-GP1 uptake in patients with prosthetic material

A) An aortic interposition graft. Note the circumferential 18F-GP1 uptake around the graft and also the uptake in the valve.

B) A retained length of coronary guidewire jailed behind a stent from a procedure 5 years previously. Note the 18F-GP1 uptake in the region of the free portion of the wire and also the uptake in the valve.

C) A dual-chamber permanent pacemaker with focal 18F-GP1 uptake along leads in the superior vena cava, right atrium and right ventricle.

Scale bars represent standardised uptake values. Images were windowed until no blood pool activity seen but regional uptake could be recognised.

6.5 Discussion

This is the first study to investigate the use of 18F-GP1 PET-CT to detect bioprosthetic aortic valve thrombus. We observed no 18F-GP1 uptake on native aortic valves but found it to be universally present on the leaflets of bioprosthetic aortic valves in patients not on anticoagulation. 18F-GP1 uptake was higher in the early period after aortic valve replacement but persisted for many years after implantation, was associated with HALT, was markedly elevated in the presence of clinical valve thrombosis and regressed following therapeutic anticoagulation.

Clinical experience with the 18F-GP1 radiotracer has previously been limited to small case series. We wished to apply this tracer to aortic valve prostheses because of the growing concern regarding the clinical implications of prosthetic valve thrombus. We first wished to validate the tracer's selectivity for activated platelets. In its resting state, the affinity of GPIIb/IIIa for fibrinogen is low. Elarofiban was uniquely developed as a mimic of the type II beta-turn structure on the fibrinogen gamma-chain which is principally present on activated platelets (Damiano et al., 2001; Hoekstra et al., 1995). Other GPIIb/IIIa receptor inhibitors have cross-reactivity with other domains and can bind to both the inactive and active forms of GPIIb/IIIa (Lohrke et al., 2017; Topol et al., 1999). We have demonstrated that 18F-GP1 binding is markedly increased in activated platelets, and that it binds selectively and specifically to areas of thrombus formation on explanted prosthetic aortic valves.

The finding that *in vivo* 18F-GP1 uptake was present in all patients with aortic valve bioprostheses was perhaps surprising. We believe this likely reflects several factors. First,

molecular 18F-GP1 imaging is highly sensitive and detects even small areas of platelet aggregation beyond the resolution of CT. Second, prosthetic material strongly attracts the adherence of platelets, evidenced by 18F-GP1 uptake on prosthetic materials in other parts of the heart and circulation. Third, the high shear environment across the aortic valve favours platelet adherence to denuded areas of the arterial lumen. Fourth, reduced valve leaflet pliability and motion may result in blood stasis and thrombus formation at the base of the leaflets. However, there are issues of cause and effect, with thrombus itself causing restricted mobility, potentially causing amplification of the thrombogenic process.

Increased 18F-GP1 uptake was independently associated with the presence of HALT. However, HALT is a descriptive CT appearance. More generally, hypoattenuation in the valve leaflets or frame can represent different pathologies, such as fibrosis, and is not specific for thrombus. The distribution and pattern of hypoattenuating lesions is important to consider. Fibrosis is a known factor contributing to bioprosthetic valve leaflet thickening and may occur relatively (after 60 days). The extent to which fibrosis can contribute to HALT on clinical CT, outside of the classic circumferential pattern seen with overt pannus formation, is unknown. However, we did not observe uptake of 18F-GP1 in areas of fibrosis of explanted valves, suggesting that 18F-GP1 may differentiate leaflet thickening due to thrombus from that due to fibrosis. Notably, we demonstrated a clear dynamic change in uptake in the three patients with clinical valve thrombosis who were treated with anticoagulation. 18F-GP1 has the potential to distinguish thrombus from other processes which may lead to HALT, although the underlying pathology must also be considered. For instance, vegetations due to infective endocarditis are well recognised to be partially comprised of fibrin and platelet-rich

thrombus. Indeed, denuded valve endothelium with platelet aggregation can be an early nidus for bacterial colonisation. In this scenario, 18F-GP1 imaging is unlikely to be useful.

Thrombus formation on bioprosthetic aortic valves is a growing topic of interest due to the increasing use of bioprosthetic valves, especially for TAVI. Cases of clinical outflow obstruction can be resolved with oral anticoagulation. The clinical relevance of asymptomatic subclinical valve thrombosis is far less certain and is a diagnosis principally made on CT imaging. Consequently, this has mostly been studied in the context of trials or imaging registries, since most asymptomatic patients do not have a clinical indication for dedicated CT imaging after aortic valve replacement. Across these existing data, the prevalence of HALT-defined leaflet thrombus on CT is highly variable and may resolve both spontaneously and with anticoagulation (Blanke et al., 2020; Chakravarty et al., 2017; Hansson et al., 2016; Makkar et al., 2020; Makkar et al., 2015; Sondergaard et al., 2017; Yanagisawa et al., 2016). Furthermore, the presence of HALT or reduced leaflet motion is not necessarily associated with worse valve haemodynamic performance in the short term (Blanke et al., 2020; Chakravarty et al., 2019; Makkar et al., 2020). Although some reports describe an association between subclinical or clinical valve thrombosis and cerebrovascular events (Chakravarty et al., 2017; Makkar et al., 2015; Rheude et al., 2021), these are confounded by selection bias and there are no data showing an association between subclinical leaflet thrombosis and repeat valve intervention or death. Randomized controlled trial data in patients with TAVI have shown that routine preventative anti-thrombotic therapies have little overall clinical benefit. In the Global study comparing a rivAroxaban-based antithrombotic strategy to an antipLatelet-based strategy after transcatheter aortIc vaLve rEplacement to Optimize clinical outcomes (GALILEO), treatment with rivaroxaban 10 mg daily (plus aspirin for 3 months)

compared to aspirin (plus clopidogrel for 3 months) increased the risk of death or thromboembolism despite a reduction in the prevalence of leaflet thickening and abnormal motion (Dangas et al., 2020; De Backer et al., 2020). It would be interesting to see if the risk-to-benefit balance would be in favour of anticoagulation in more selected patient populations with a high burden of activated platelet adherence.

A potentially more relevant consideration is valve durability. Maximising valve longevity is increasingly important due to the escalating use of bioprostheses, especially with TAVI in younger patients. We recently demonstrated that increased 18F-sodium fluoride valvular uptake – a marker of active microcalcification – is associated with more rapid valvular haemodynamic deterioration, and that tracer uptake co-localized with regions of thrombus on histology as well as HALT on CT (Cartlidge et al., 2019). Detailed histopathology of explanted aortic transcatheter heart valves has revealed that adherent leaflet thrombus is a consistent finding with a time-dependent transition to other associated pathologies such as fibrosis and calcification (Sellers et al., 2019). Other small histological series describe a lower prevalence of thrombus, which may be due to selection bias or differing definitions (Yahagi et al., 2018). Our present findings confirm that ongoing platelet activation and adherence to bioprosthetic leaflets is a constant feature in keeping with these *ex vivo* data.

It is important to consider the clinical utility of our findings. Given the evidence outlined above, we envisage that enhanced detection of subclinical leaflet thrombosis may have a role in understanding and optimising valve durability, but not routinely for the prevention of stroke or clinical valve thrombosis. Given some of the limitations of echocardiography and CT, there are situations where the mechanisms underlying bioprosthetic valve dysfunction

are unclear. 18F-GP1 PET-CT may help elucidate different pathologies and provide greater clinical diagnostic certainty. It may also have a role in monitoring the response to therapeutic interventions in patients with thrombotic bioprosthetic valve dysfunction. Finally, given its apparent sensitivity and ability to demonstrate a range of thrombotic lesions, 18F-GP1 may have broader applications in other cardiovascular diseases.

We should acknowledge some limitations of our work. These data are the first observational description of cardiac 18F-GP1 use and the sample size is modest. We must be circumspect in the interpretation of our findings which are limited by the small number of patients with TAVI, a heterogenous population with varied valve models, a wide range of implantation durations, potential confounding and substantial unexplained variance in the models constructed to examine associations with 18F-GP1 uptake. As the sensitivity of the technique was unexpected – that is, the finding of avid and consistent uptake in even normal functioning bioprostheses – we are unable to describe thresholds for "normal" uptake. Although we hypothesise that 18F-GP1 may be able to differentiate leaflet thrombus from other pathologies, we did not have any patients with structural valve degeneration. These patients are likely to have a degree of uptake (as we demonstrated in normal prostheses), so the specificity of 18F-GP1 uptake remains uncertain. Finally, we do not have longitudinal follow-up so cannot draw conclusions regarding associations with clinical events.

6.6 Conclusion

18F-GP1 PET-CT is a novel tool that may be useful for the *in vivo* detection of platelet activation at the molecular level. We have demonstrated that platelet activation and adherence appear to be a universal finding on prosthetic aortic valve leaflets in the absence of anticoagulation. However, quantitative 18F-GP1 PET-CT holds promise as a technique to detect bioprosthetic valve thrombosis and monitor the impact of therapeutic interventions. This might be valuable where there is diagnostic uncertainty and for further understanding factors that predispose to leaflet thrombosis. Finally, its sensitivity warrants further investigation in other cardiovascular pathologies where the detection of thrombus may aid diagnosis or guide patient management.

Chapter 7 – Summary and the future

Adapted from:

Bing R, Dweck M. Management of asymptomatic severe aortic stenosis: check or all in? Heart. 2020 Nov 4:heartjnl-2020-317160. doi: 10.1136/heartjnl-2020-317160.

Bing R, Everett R, Tuck C et al. Rationale and design of the randomized, controlled Early Valve Replacement Guided by Biomarkers of Left Ventricular Decompensation in Asymptomatic Patients with Severe Aortic Stenosis (EVOLVED) trial. Am Heart J. 2019 Mar 15;212:91-100. doi: 10.1016.

7.1. Axial imaging in cardiology is here to stay

Although transthoracic echocardiography remains the first-line imaging test for aortic stenosis, and rightly so, the utility of an anatomical imaging modality that can stratify disease severity is evident, as shown by the widespread uptake of non-contrast computed tomography calcium scoring (CT-AVC). This technique has several major limitations, as previously discussed, yet despite these limitations CT-AVC is a good discriminator of disease severity and an excellent prognostic tool. Therefore, we hypothesised that the use of contemporary contrast-enhanced cardiac CT, which overcomes these limitations, would correlate at least as well with echocardiography, with the added ability to characterise non-calcific valve tissue. Testing this hypothesis in cohort of patients with a spectrum of aortic stenosis severity, we found that contrast-enhanced CT quantification of calcific leaflet volume as well as fibro-calcific (calcific plus non-calcific) leaflet volume correlated well with peak aortic jet velocity and CT-AVC. Notably, fibro-calcific volume correlated better with peak aortic jet velocity than CT-AVC in women, who also had a higher fibro-calcific ratio than men, although one of the chief limitations of this analysis was the small number of women. Our study demonstrates the feasibility of using contrast-enhanced CT for the assessment of aortic stenosis, which may be of logistic value in clinical workflow integration as well as diagnostic value in patients where fibrosis is a significant contributor to valve obstruction. With iterations in software and image analysis, followed by multi-centre validation, we anticipate that this may become a useful clinical tool that can be easily and widely utilised, as well as a potential imaging endpoint in clinical trials.

Our research into the application of Autoplaque, which is in progress and unpublished, has undergone several iterations. Although the software interface is rapid and intuitive, the predominant challenge was determining Hounsfield Unit thresholds for non-calcific tissue (e.g. normal leaflet tissue or fibrosis), blood pool and calcific tissue. Several variations including the use of blood pool standard deviations and formulae were tested in a small cohort of control patients and patients with aortic stenosis, but there was substantial variation in accuracy between patients due to blood pool opacification. This was evident both visually (as Autoplaque provides a 3-dimensional image with each of the tissue groups highlighted) as well as when correlating with echocardiography. This method has been published by our collaborators (Grodecki et al., 2020), but relies too much upon manual calibration of thresholds, while the published analysis was conducted in a TAVI population, limiting its applicability in non-severe aortic stenosis, which is exactly the population of patients that may require a diagnostic tie-breaker. An automated method of thresholding has now been devised and integrated into the software, using Gaussian mixture models to set thresholds for n number of tissue populations (e.g. n=3 populations in typical aortic stenosis, consisting of non-calcific tissue, blood pool and calcific tissue). Inter- and intraobserver reproducibility is excellent, and correlation with peak aortic jet velocity and CT-AVC – conducted in the same cohort as our published proof-of-concept data (Chapter 3) – is also very similar to our prior data. Essentially, most of the information with regards to stenosis severity is offered by calcific volume, which correlates strongly with CT-AVC and echocardiography, while the addition of non-calcific volume – giving the total fibrocalcific volume – improves correlation with echocardiographic parameters in women.

We plan to take this forward with international collaborators as follows. First, expand the derivation pool to a multicentre cohort with core lab analysis to determine a threshold for severe aortic stenosis, using concordant echocardiography as the gold standard. Second, validate these thresholds for severe disease in a multicentre cohort with local lab image analysis. Third, validate these threshold against clinical outcomes – AVR or death – in a population restricted to asymptomatic patients. One of the main challenges will be gathering a sufficient number of scans, since we require cohorts with a range of aortic stenosis severities that have undergone contrast-enhanced ECG-gated cardiac CT, contemporaneous echocardiography and ideally non-contrast CT-AVC. Nevertheless, there is substantial interest from multiple groups, and we are hoping to include over 1000 patients. Although this perhaps lacks the novelty and buzz-factor of other research projects, it is the closest to realising a validated, clinical useful role that could be rolled out to centres as quickly as it takes to download an 86 MB file and do a little training.

7.2 Subtle changes in left ventricular contractility - the devil is in the detail

It is no great surprise to find that having left ventricular impairment is worse than having normal left ventricular function. The more pertinent question is: how much left ventricular impairment is clinically relevant? An ejection fraction <50% in asymptomatic patients is supported by major society guidelines as a trigger for aortic valve replacement (AVR), but ejection fraction is a crude functional surrogate for myocardial health in aortic stenosis that is preserved until late in the disease process. We hypothesised that first-phase ejection fraction (EF1) – the ejection fraction from the onset of systole to the time of peak aortic velocity - would be a more sensitive prognostic marker than overall ejection fraction, and found this to be the case, with EF1 being independently associated with future AVR. Interestingly, we also found that global afterload, extracellular myocardial volume expansion and the presence of myocardial infarction were independently associated with EF1. Another salient finding was the optimal EF1 threshold of 24% for the discrimination of future AVR or death, which was very close to the previously described threshold of 25% derived from an external cohort of patients with aortic stenosis. Overall, our findings are plausible and highlight the potential for multimodality assessments to inform prognosis, even in patients with preserved overall left ventricular ejection fraction.

We have subsequently repeated this analysis, but with CMR-derived EF1 and phase contrast flow to determine the time of peak aortic velocity (Gu, Bing, et al., 2021). Of course, the overall findings with regards to EF1 are largely unchanged, but CMR-derived EF1 was

notably more reproducible than echocardiography-derived EF1, which is in keeping with the differences between these two modalities. EF1 has also been retrospectively applied in COVID-19, where a depressed EF1 correlated with an increased risk of mortality (Gu, Cirillo, et al., 2021). Ultimately, the concept is clear: there are early and subtle changes in left ventricular contractility that precede a fall in overall ejection fraction and the onset of symptoms, and methods of quantifying this change, such as EF1, global longitudinal strain or time to peak aortic velocity, can add prognostic information to current standard assessments. Apart from their "predictive" value, features that will most recommend these parameters for clinical application will be ease and rapidity of use, compatibility with widely available software and reproducibility. However, whether any of these adverse prognostic features can be used to modify outcomes through earlier AVR remains to be seen (Chapter 7.5).

7.3 Medical therapy for aortic stenosis – a Celtic unicorn

Another one bites the dust. As disappointing as SALTIRE, SEAS and ASTRONOMER were – conclusively demonstrating that statin therapy had no effect on aortic stenosis progression – valuable lessons were learned regarding the design and conduct of randomised controlled trials of drug therapies in aortic stenosis, particularly with regards to study endpoints. Enter SALTIRE2 – conclusively demonstrating that denosumab and alendronic acid had no effect on aortic stenosis progression. Although the trial has limitations as discussed, it utilised contemporary measures of stenosis severity and calcification in a double-blind randomised controlled trial design, and the failure to meet the primary endpoint is most likely due to a true lack of effect, rather than a weakness in trial methodology or power. We would submit that the trial findings are robust and obviate the need for any further investigation of these agents for the treatment of aortic stenosis. There are not so many ongoing randomised trials testing disease-modifying therapies. Some of these include Early Aortic Valve Lipoprotein(a) Lowering Trial (niacin; NCT02109614; last clinicaltrials.gov update 2016), Evaluating the Effectiveness of Atorvastatin on the Progression of Aortic Dilatation and Valvular Degeneration in Patients With Bicuspid Aortic Valve (atorvastatin; NCT02679261; recruitment complete), PCSK9 Inhibitors in the Progression of Aortic Stenosis (NCT03051360, last clinicaltrials.gov update 2017) and Bicuspid Aortic Valve Stenosis and the Effect of vItamin K2 on Calcium metabolism on 18F-NaF PET/MRI (NCT02917525, last clinicaltrials.gov update 2018). The field is a little fallow.

Our findings also provide yet another example of the importance of randomised controlled trials when investigating treatments that are associated with outcomes of interest in observational data. Confounding often obscures the true nature of these associations, and, short of a dramatic effect size that is rarely seen in modern cardiology, randomisation is usually required. As I have stated elsewhere, when commenting on an interesting study of dipeptidyl peptidase-4 inhibitors in aortic stenosis (Lee et al., 2020) that is a prelude to a double-blind randomised controlled trial (NCT04055883), "Truth will out – but in the case of disease-modifying medical therapy for aortic stenosis, where effect sizes may be small and mechanisms complex, only after an adequately powered and well-conducted randomised controlled trial." (Bing & Dweck, 2020).

7.4 18F-GP1 and pluripotentiality

There was more than a brief stir of excitement with the first *ex vivo* and *in vivo* 18F-GP1 images. The ability to non-invasively detect small volumes of thrombus beyond the resolution of current imaging modalities could have wide-ranging clinical applications. In bioprosthetic valves, our *ex vivo* data supported the specificity of GP1 for regions of thrombus and platelet activation, confirmed on histology and immunohistochemistry. We were surprised, however, by the *in vivo* sensitivity of 18F-GP1 positron emission tomography (PET). The uniformly apparent and avid uptake in all normal bioprostheses in our cohort is consistent with platelet activation on the prosthetic leaflets (not valve frames), but we had not anticipated this level of 18F-GP1 signal. We were able to demonstrate that increased 18F-GP1 activity was associated with hypoattenuated leaflet thickening (HALT), was very high in clinical valve thrombosis, and regressed with therapeutic anticoagulation and resolution of obstructive thrombus. The totality of our findings, including the *in vitro* experiments and extra-valvular and extra-cardiac 18F-GP1 identified in this study as well as other ongoing cohorts (Figure 7.1; NCT03943966; Bing R, Andrew J, Williams M, et al. 2021 Am J Respir Crit Care Med, under submission), confirm the selectivity of 18F-GP1 for regions of platelet activation or thrombus. However, the unexpectedly consistent uptake in normal prosthetic valves raises the question about clinical relevance, particularly in the context of the existing observational, registry and randomised controlled trials examining the associations between HALT and adverse events as well as the utility of therapeutic anticoagulation. We envisage that a large cohort with longitudinal follow-up of sufficient duration to examine structural valve degeneration would offer insights into “normal” 18F-GP1 thresholds that may help risk stratification, as well as potential differences between valve types – particularly transcatheter

versus surgical prostheses. These are intriguing questions, but our pilot study is unable to address them.

Of at least equal interest is the application of 18F-GP1 hybrid PET imaging in other cardiovascular conditions – particularly where the identification of thrombus might alter clinical management (Figure 7.2; Tzolos E, Bing R, Newby D, Dweck M. 2021 Lancet, in press). Ongoing and future studies will investigate the use of 18F-GP1 to detect left ventricular thrombus after anterior myocardial infarction, as well as intracardiac thrombus after cryptogenic stroke.

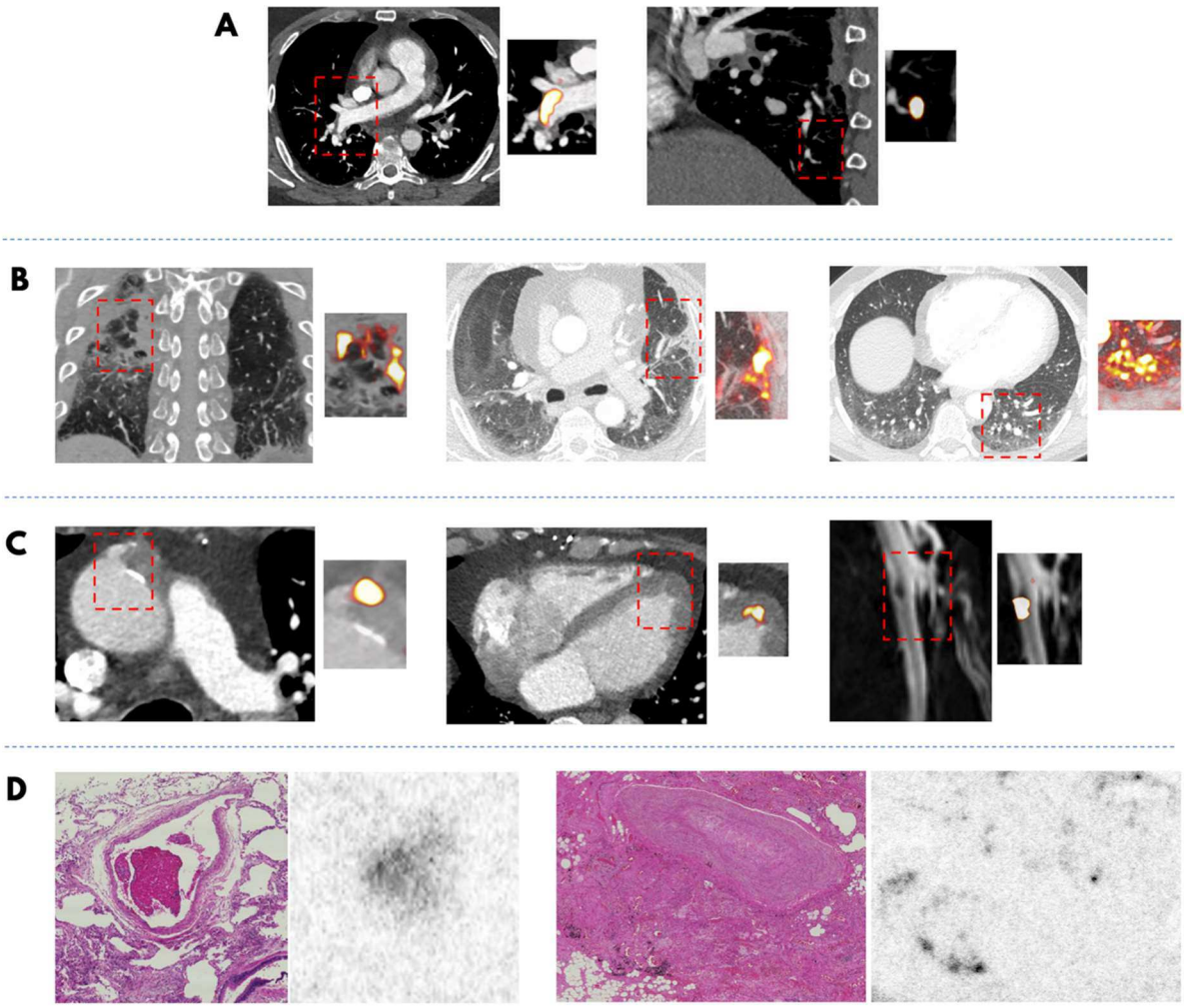

Figure 7.1 18F-GP1 in recovered COVID-19 patients with pulmonary embolism

A. *Left*: Segmental pulmonary embolus with associated 18F-GP1 uptake. *Right:* Focal 18F-GP1 uptake without computed tomography pulmonary angiogram evidence of subsegmental thrombus.

B. Three examples of parenchymal 18F-GP1 uptake associated with consolidation (*left)*, healing peripheral infarction (*middle)* and nodular uptake in ground-glass changes with an associated dilated pulmonary artery but no evidence of pulmonary embolism at this site on computed tomography pulmonary angiogram (*right)*.

C. Incidental systemic intravascular thrombosis and associated 18F-GP1 uptake at the site of an occluded saphenous vein coronary artery bypass graft (*left*), apical left ventricular thrombus (*middle*), left common femoral vein deep vein thrombosis (*right*).

D. Haematoxylin and eosin-stained sections of post-mortem pulmonary tissue with corresponding 18F-GP1 autoradiography in two patients who died of COVID-19. Diffuse alveolar damage and microvascular thrombosis was seen on histopathology. 18F-GP1 co-localises to intravascular thrombus (*left, centre-left)* but not to more organised thrombus of older duration (*centre-right, right)*. There is also 18F-GP1 signal in smoking-related anthracotic pigment.

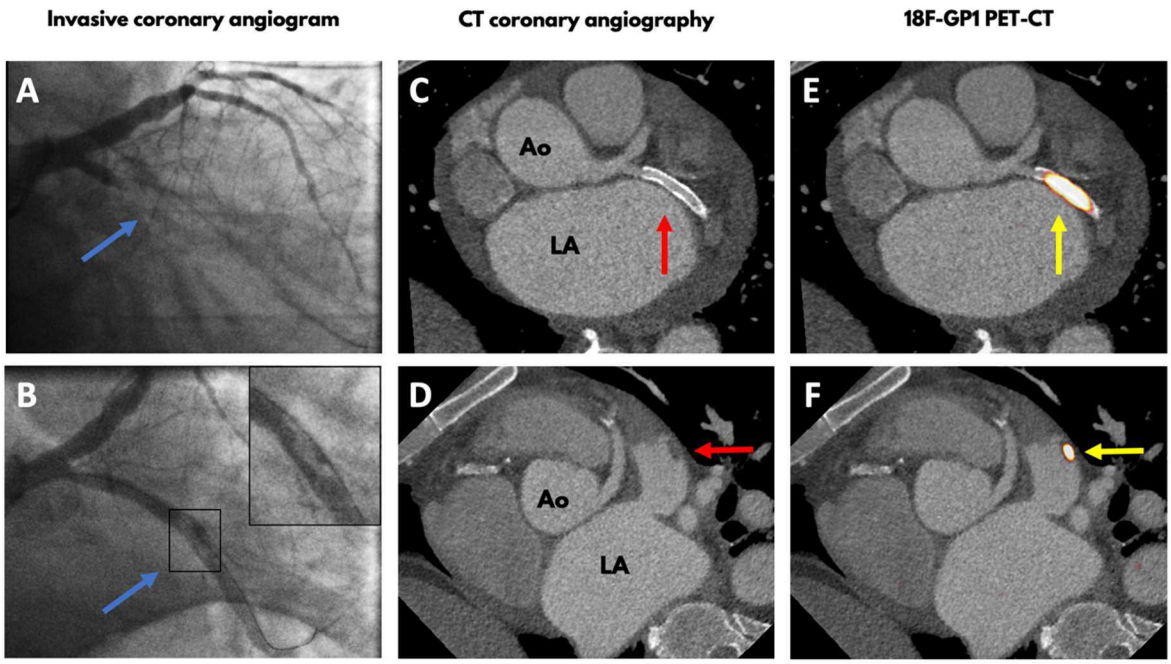

Figure 7.2 18F-GP1 in myocardial infarction due to coronary thromboembolism

A. Invasive coronary angiography showing an occluded left circumflex artery at the time of primary percutaneous coronary intervention for ST elevation myocardial infarction (blue arrow).

B. Persistent filling defect following recanalisation of the left circumflex artery, consistent with a large thrombus burden (blue arrow; inset).

C. Computed tomography angiography 5 days later showing a patent left circumflex artery stent with no visualised thrombus (red arrow).

D. However, a discrete filling defect in the left atrial appendage is seen, possibly consistent with thrombus (red arrow).

E. Hybrid positron emission tomography-computed tomography showing 18F-GP1 uptake co-localising to the patent left circumflex artery stent (yellow arrow).

F. There is also 18F-GP1 uptake co-localising to the left atrial appendage lesion, consistent with thrombus.

Abbreviations: Ao, aorta; LA, left atrium.

7.5 Precise timing in precision medicine – the EVOLVED trial and its compatriots

There is a window of opportunity for each patient where the benefits and risks of AVR are most in favour of the former. This window may be narrow or wide and is not fixed to a certain timepoint in the disease process. One can consider valve intervention as a package that consists not only of "what", "why" and "how", but also "when". In the absence of any effective medical therapies for aortic stenosis, the primary purpose of increasingly nuanced risk stratification and clinical surveillance is to deliver the most balanced package possible. Risk stratification, whether that be through plasma biomarkers, exercise treadmill testing, echocardiographic stages of cardiac damage or EF1 does not equate to modifiable risk. Since there are relatively straightforward guidelines for the first three components of this therapeutic package, the main modifiable variable that remains largely unexplored is "when". To paraphrase our prior question: if myocardial disease in aortic stenosis accrues subclinically, may be irreversible and is prognostically relevant in a "dose-dependent" fashion, can we refine the timing of valve intervention in asymptomatic patients with severe aortic stenosis?

Given the safety and efficacy of modern surgical and transcatheter aortic valve interventions when applied within the current treatment paradigm, any proposed alteration in strategy in asymptomatic patients must be supported by robust randomised data showing prognostic benefit. Several caveats immediately come to mind. First, one of the major perceived benefits

offered by conventionally timed intervention – amelioration of symptoms – is obviously not seen. In fact, patients undergoing AVR will feel worse for a period after surgery, before (ideally) returning to their asymptomatic baseline. Although it may be posited that early intervention is preventing the onset of symptoms, there is no guarantee that a given patient will come to require, or undergo, AVR in the future for traditional indications. This is the nature of prevention. Second, the risks of intervention, both peri-procedural and long-term, must be considered carefully. The former is particularly pertinent in patients with more co-morbidities who are at higher risk of acute complications – a population in whom the prognostic benefits may also be less certain. The modality of intervention also requires consideration, both from a health economic perspective and the procedure itself, as transcatheter valves remain (for now) several times more expensive than surgical valves, while a clear inverse association exists between case volume (both operator and institutional) and 30-day mortality (Vemulapalli et al., 2019; Wassef et al., 2018). Long-term complications are more pertinent in younger patients, with three principal concerns – valve durability, permanent pacing and paravalvular regurgitation. Valve durability is a consideration for both surgical and transcatheter bioprostheses, although the former is more of a known quantity that the latter, given the decades of experience accrued with iterations of surgical valves. Early valve intervention may feasibly bring forward valve implantation by several years. Although valve-in-valve TAVI is now commonplace and is probably preferable to re-do sternotomy, anatomy permitting (Al-Abcha et al., 2021), one must consider that even two bioprostheses may not provide sufficient longevity in an otherwise healthy 60-year-old patient. Permanent pacing is also a consideration for both surgical and transcatheter prostheses, although more so for certain self-expanding versions of the latter, while paravalvular regurgitation has clear associations with increased mortality (Kodali et al.,

2015) and remains one of the main disadvantages of TAVI. Again, although it can be rationalised that these risks will accrue for a given patient at some point in their future, given the natural history of aortic stenosis, there is no guarantee of this for an individual patient. The risks are also not necessarily equivalent, particularly in asymptomatic patients who may be deemed suitable for surgical AVR at present, but may be TAVI candidates should their intervention be performed down the track.

On the other hand, observational data comparing conservative management with initial AVR have suggested benefit with the latter (Kang et al., 2010; Taniguchi et al., 2015). As we all appreciate, these observations are confounded and are insufficient to change practice. More pertinently, the first randomised trial of early intervention in asymptomatic severe aortic stenosis was recently published. The landmark Randomized Comparison of Early Surgery versus Conventional Treatment in Very Severe Aortic Stenosis (RECOVERY) trial (n=145) demonstrated a reduction in all-cause mortality with early surgical intervention at a median follow-up of >6 years (7 vs 21%, hazard ratio 0.33, 95% confidence interval 0.12-0.90) (Kang et al., 2020). The marked treatment effect in this trial is impressive and the use of all-cause mortality as the primary endpoint laudable, however it is crucial to appreciate some key aspects of the study, particularly with regards to the small study size and select population, that are nicely summarised in the accompanying editorial (Lancellotti & Vannan, 2020). Most notably, this was a relatively young Korean cohort with very severe aortic stenosis, 61% of whom had bicuspid valves, and surgical outcomes were excellent (no operative deaths). The generalisability of this study is therefore somewhat limited.

The stage is thus set for further randomised trials of early intervention in asymptomatic severe aortic stenosis, of which there are five currently recruiting (Table 7.1), to support or refute these initial findings. The patient populations are either "all-comers" or have undergone risk stratification with CMR. The former offers simplicity and pragmatism, while the latter is more nuanced and identifies a higher-risk population but adds complexity. As part of our ongoing research programme here, Edinburgh are leading the Early Valve Replacement Guided by Biomarkers of Left Ventricular Decompensation in Asymptomatic Patients with Severe Aortic Stenosis (EVOLVED) trial (Figure 7.3) (Bing, Everett, et al., 2019) and are also enrolling patients into the Early Valve Replacement in Severe Asymptomatic Aortic Stenosis Study (EASY-AS). These trials are complementary, with EVOLVED providing mechanistic insights based on CMR tissue characterisation, and the trial teams having developed a seamless co-enrolment algorithm which is running smoothly across multiple sites.

Success of these randomised trials will require rigorous patient recruitment and enthusiastic participation of clinicians and institutions. We may each have preferences for how this patient group is best treated, but the truth is that these preferences are largely shaped by observational data and our own experiences and biases. This is an era of incremental gain in cardiology, and modest treatment effects in complex diseases that affect a heterogenous

population cannot be conclusively supported by these methods alone. Randomised trials are the answer.

Figure 7.3 EVOLVED trial flow chart

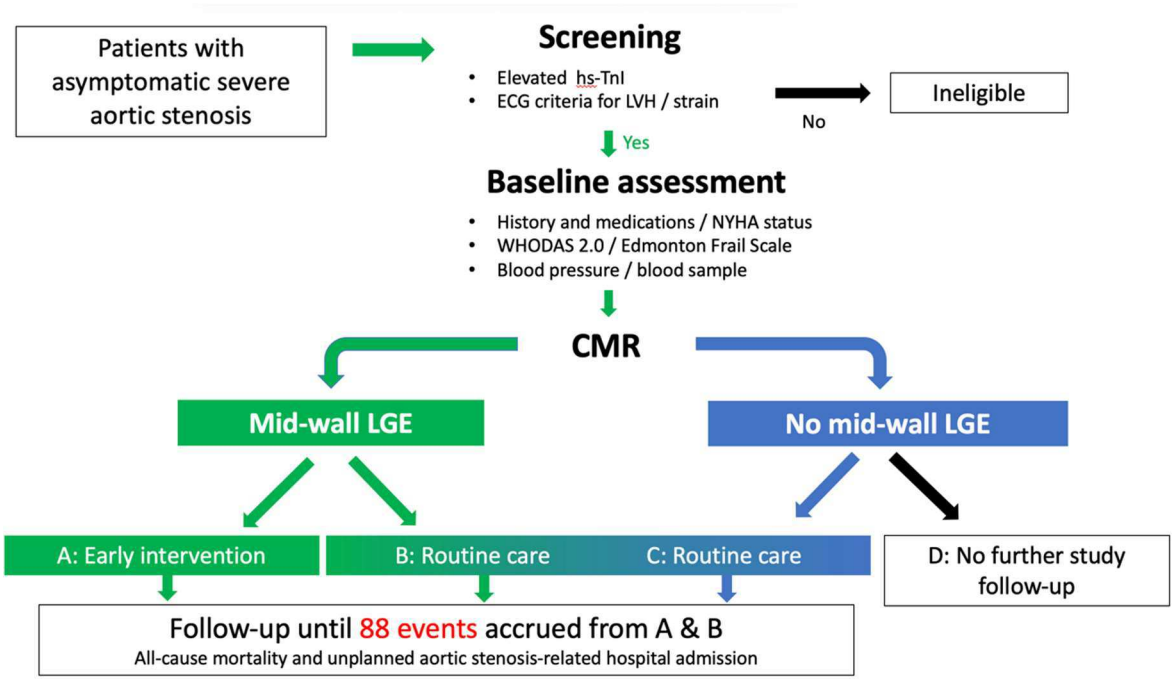

The sample size has been calculated based on an event rate of 25.0% in the routine care arm and 13.4% in the early intervention arm over the first 2 years; 88 observed primary outcome events will give 90% power at 5% significance level.

Abbreviations: hsTnI = high sensitivity troponin I, ECG = electrocardiogram, LVH = left ventricular hypertrophy, NYHA = New York Heart Association, WHODAS = World Health Organization Disability Assessment Schedule, CMR = cardiac magnetic resonance, LGE = late gadolinium enhancement.

Table 7.1 Ongoing randomised controlled trials of early intervention in asymptomatic severe aortic stenosis

Trial	Start year and region	N	Definition of severity	Other key criteria	Intervention	Primary outcome
Aortic valve replacement versus conservative treatment in	2015 Europe	~ 312 (event-driven)	Vmax ≥4.0m/s or	≥18 years STS score <8%	SAVR	Composite: all-cause death, acute myocardial infarction, cerebrovascular insult

asymptomatic severe aortic stenosis (AVATAR)(Banovic et al., 2016) NCT02436655			MG ≥40mmHg and AVA ≤1.0 cm^2 or AVAi ≤0.6 cm^2/m^2	LVEF >50%		and unplanned hospitalisation for heart failure requiring intravenous treatment.
Evaluation of transcatheter aortic valve replacement compared to surveillance for patients with asymptomatic severe aortic stenosis (EARLY-TAVI) NCT03042104	2017 United States	1109	Severe aortic stenosis	≥65 years Favourable iliofemoral anatomy Tricuspid aortic valve	Transfemoral TAVI	Composite: all-cause death, stroke and unplanned cardiovascular hospitalisation
Early valve replacement guided by biomarkers of left ventricular decompensation in asymptomatic patients with severe aortic stenosis (EVOLVED)(Bing, Everett, et al., 2019) NCT 03094143	2017 United Kingdom	~ 400 (event-driven)	Vmax ≥4.0m/s or Vmax ≥3.5m/s and AVAi <0.6cm^2/m^2	>18 years Presence of mid-wall late gadolinium enhancement on cardiac magnetic resonance LVEF >50%	TAVI/SAVR	Composite: all-cause mortality and unplanned aortic stenosis-related hospitalisation
Early surgery for patients with asymptomatic aortic stenosis (ESTIMATE) NCT02627391	2016 France	360	Vmax >4.0m/s and/or MG >40mmHg	18-80 years EuroSCORE II ≤5% LVEF >50% No symptoms/fall in BP during exercise test	SAVR	Composite: overall mortality and cardiac morbidity, including cardiac event requiring hospitalisation
Early valve replacement in severe asymptomatic aortic stenosis study (EASY-AS) NCT04204915	2019 United Kingdom Australia New Zealand	2844	Vmax ≥4.0m/s or MG ≥40mmHg and AVA ≤1.0 cm^2 or AVAi ≤0.6 cm^2/m^2	>18 years LVEF >50%	TAVI/SAVR	Composite: cardiovascular death and hospitalisation for heart failure
Abbreviations: Vmax, peak aortic valve velocity; MG, mean gradient; AVA, aortic valve area; AVAi, indexed aortic valve area; STS, Society of Thoracic Surgery, LVEF, left ventricular ejection fraction; SAVR, surgical aortic valve replacement; TAVI, transcatheter aortic valve replacement.						

7.6 Conclusion

We are privileged to be physicians in an era where the search for new investigations or interventions that may improve patient outcomes – in first-world cardiology, an important

proviso - usually requires large-scale, costly trials that are powered to detect modest absolute risk reductions. This speaks to the major gains accrued in preceding years. In our enthusiasm for investigating new and exciting tests, techniques and therapies, we must remain cognisant of the ultimate goal – to improve quality of life, duration of life or both, in a safe and cost-effective manner. From this base, the body of work presented and discussed here a) covers the development of novel, incremental developments in the assessment of aortic stenosis which, after refinement and prospective validation, could be easily integrated into routine clinical practice, b) robustly tests and disproves a potential avenue of medical therapy for aortic stenosis, and c) provides pilot data for a new and unique cardiovascular molecular imaging technique, which is nascent and far from clinical application but has wide-ranging potential. I am pleased to submit these data for my doctoral thesis.

Publications during PhD

Kwiecinski J, Tzolos E, Cartlidge TRG, Fletcher A, Doris MK, **Bing R**, Tarkin JM, Seidman MA, Gulsin GS, Cruden NL, Barton AK, Uren NG, Williams MC, Van Beek EJR, Leipsic J, Dey D, Makkar RR, Slomka PJ, Rudd JHF, Newby DE, Sellers SL, Berman DS, Dweck MR. Native Aortic Valve Disease Progression and Bioprosthetic Valve Degeneration in Patients with Transcatheter Aortic Valve Implantation. Circulation. 2021 Aug 29. doi: 10.1161/CIRCULATIONAHA.121.056891.

Shah ASV, Lee KK, Pérez JAR, Campbell D, Astengo F, Logue J, Gallacher PJ, Katikireddi SV, **Bing R**, Alam SR, Anand A, Sudlow C, Fischbacher CM, Lewsey J, Perel P, Newby DE, Mills NL, McAllister DA. Clinical burden, risk factor impact and outcomes following myocardial infarction and stroke: A 25-year individual patient level linkage study. Lancet Reg Health Eur. 2021 Aug;7:100141. doi: 10.1016/j.lanepe.2021.100141.

Bing R, Andrews JP, Williams MC, van Beek EJR, Lucatelli C, MacNaught G, Clark T, Koglin N, Stephens AW, MacAskill MG, Tavares AA, Dhaliwal K, Dorward DA, Lucas C, Dweck MR, Newby DE. In vivo Thrombosis Imaging in Patients Recovering from COVID-19 and Pulmonary Embolism. Am J Respir Crit Care Med. 2021 Aug 10. doi: 10.1164/rccm.202011-4182IM.

Tzolos E, **Bing R,** Newby DE, Dweck MR. Categorising myocardial infarction with advanced cardiovascular imaging. Lancet. 2021 Aug 7;398(10299):e9. doi: 10.1016/S0140-6736(21)01329-5.

Kwak S, Everett RJ, Treibel TA, Yang S, Hwang D, Ko T, Williams MC, **Bing R**, Singh T, Joshi S, Lee H, Lee W, Kim YJ, Chin CWL, Fukui M, Al Musa T, Rigolli M, Singh A, Tastet L, Dobson LE, Wiesemann S, Ferreira VM, Captur G, Lee S, Schulz-Menger J, Schelbert EB, Clavel MA, Park SJ, Rheude T, Hadamitzky M, Gerber BL, Newby DE, Myerson SG, Pibarot P, Cavalcante JL, McCann GP, Greenwood JP, Moon JC, Dweck MR, Lee SP. Markers of Myocardial Damage Predict Mortality in Patients With Aortic Stenosis. J Am Coll Cardiol. 2021 Aug 10;78(6):545-558. doi: 10.1016/j.jacc.2021.05.047.

Gu H, **Bing R**, Chin C, Fang L, White AC, Everett R, Spath N, Park E, Chambers JB, Newby DE, Chiribiri A, Dweck MR, Chowienczyk P. First-phase ejection fraction by cardiovascular magnetic resonance predicts outcomes in aortic stenosis. J Cardiovasc Magn Reson. 2021 Jun 10;23(1):73. doi: 10.1186/s12968-021-00756-x.

Gu H, **Bing R**, Chin C, Fang L, White A, Everett R, Spath N, Park E, Chambers J, Newby D, Chiribiri A, Dweck M, Chowienczyk P. First-phase ejection fraction by CMR predicts outcomes in aortic stenosis. J Cardiovasc Magn Reson. 2021. In press.

Sengupta PP, Shrestha S, Kagiyama N, Hamirani Y, Kulkarni H, Yanamala N, **Bing R**, Chin CWL, Pawade TA, Messika-Zeitoun D, Tastet L, Shen M, Newby DE, Clavel MA, Pibarot P, Dweck MR; Artificial Intelligence for Aortic Stenosis at Risk International Consortium. A

Machine-Learning Framework to Identify Distinct Phenotypes of Aortic Stenosis Severity. JACC Cardiovasc Imaging. 2021 May 11:S1936-878X(21)00286-2. doi: 10.1016/j.jcmg.2021.03.020.

Singh T, **Bing R**. Antiplatelet therapy after percutaneous coronary intervention: is less more (more or less)? Heart. 2021 May 13. doi: 10.1136/heartjnl-2021-319126.

Pawade TA*, Doris MK*, **Bing R***, White AC, Forsyth L, Evans E, Graham C, Williams MC, van Beek EJR, Fletcher A, Adamson PD, Andrews JPM, Cartlidge TRG, Jenkins WSA, Syed M, Fujisawa T, Lucatelli C, Fraser W, Ralston SH, Boon N, Prendergast B, Newby DR, Dweck MRD. Effect of Denosumab or Alendronic Acid on the Progression of Aortic Stenosis: A Double-Blind Randomized Controlled Trial. Circulation. 2021 Apr 29. doi: 10.1161/CIRCULATIONAHA.121.053708.

Cartlidge TR*, **Bing R***, Kwiecinski J, Guzzetti E, Pawade TA, Doris MK, Adamson PD, Massera D, Lembo M, Peeters FECM, Couture C, Berman DS, Dey D, Slomka P, Pibarot P, Newby DE, Clavel MA, Dweck MR. Contrast-enhanced computed tomography assessment of aortic stenosis. Heart. 2021 Jan 29:heartjnl-2020-318556. doi: 10.1136/heartjnl-2020-318556.

Fletcher AJ, Lembo M, Kwiecinski J, Syed MBJ, Nash J, Tzolos E, **Bing R**, Cadet S, MacNaught G, van Beek EJR, Moss AJ, Doris MK, Walker NL, Dey D, Adamson PD, Newby DE, Slomka PJ, Dweck MR. Quantifying microcalcification activity in the thoracic aorta. J Nucl Cardiol. 2021 Jan 20. doi: 10.1007/s12350-020-02458-w.

Williams MC, Massera D, Moss AJ, **Bing R**, Bularga A, Adamson PD, Hunter A, Alam S, Shah ASV, Pawade T, Roditi G, van Beek EJR, Nicol ED, Newby DE, Dweck MR. Prevalence and clinical implications of valvular calcification on coronary computed tomography angiography.
Eur Heart J Cardiovasc Imaging. 2020 Dec 11:jeaa263. doi: 10.1093/ehjci/jeaa263.

Doris MK, Meah MN, Moss AJ, Andrews JPM, **Bing R**, Gillen R, Weir N, Syed M, Daghem M, Shah A, Williams MC, van Beek EJR, Forsyth L, Dey D, Slomka PJ, Dweck MR, Newby DE, Adamson PD. Coronary 18F-Fluoride Uptake and Progression of Coronary Artery Calcification.
Circ Cardiovasc Imaging. 2020 Dec;13(12):e011438. doi: 10.1161/CIRCIMAGING.120.011438. Epub 2020 Dec 10.

Bing R, Dweck M. Management of asymptomatic severe aortic stenosis: check or all in?
Heart. 2020 Nov 4:heartjnl-2020-317160. doi: 10.1136/heartjnl-2020-317160.

Lee KK, **Bing R**, Kiang J, Bashir S, Spath N, Stelzle D, Mortimer K, Bularga A, Doudesis D, Joshi SS, Strachan F, Gumy S, Adair-Rohani H, Attia EF, Chung MH, Miller MR, Newby DE, Mills NL, McAllister DA, Shah ASV. Adverse health effects associated with household air pollution: a systematic review, meta-analysis, and burden estimation study. Lancet Glob Health. 2020 Nov;8(11):e1427-e1434. doi: 10.1016/S2214-109X(20)30343-0.

Bing R, Adamson PD. Cardiac catheterisation laboratory in a global pandemic: ceding centre stage. Heart. 2020 Oct 14:heartjnl-2020-318263. doi: 10.1136/heartjnl-2020-318263.

Doris MK, Jenkins W, Robson P, Pawade T, Andrews JP, **Bing R**, Cartlidge T, Shah A, Pickering A, Williams MC, Fayad ZA, White A, van Beek EJ, Newby DE, Dweck MR. Computed tomography aortic valve calcium scoring for the assessment of aortic stenosis progression. Heart. 2020 Oct 5:heartjnl-2020-317125.

Bing R, Dweck MR. The quest for an aortic stenosis cure. Heart. 2020 Sep 11:heartjnl-2020-317421.

Bularga A, **Bing R**, Shah AS, Adamson PD, Behan M, Newby DE, Flapan A, Uren N, Cruden N. Clinical outcomes following balloon aortic valvuloplasty. Open Heart. 2020 Sep;7(2):e001330. doi: 10.1136/openhrt-2020-001330.

Dweck MR, Bularga A, Hahn RT, **Bing R**, Lee KK, Chapman AR, White A, Salvo GD, Sade LE, Pearce K, Newby DE, Popescu BA, Donal E, Cosyns B, Edvardsen T, Mills NL, Haugaa K. Global evaluation of echocardiography in patients with COVID-19. Eur Heart J Cardiovasc Imaging. 2020 Jun 18:jeaa178. doi: 10.1093/ehjci/jeaa178.

Singh T, **Bing R**, Dweck M, van Beek E, Mills N, Williams M, Villines T, Newby D, Adamson P. Exercise Electrocardiography and Computed Tomography Coronary Angiography for Patients With Suspected Stable Angina Pectoris: A Post Hoc Analysis of the Randomized SCOT-HEART Trial2020 Jun 3;5(8):1-10. doi: 10.1001/jamacardio.2020.1567.

Bing R, Hamra M, Newby D. Cold feet, warm heart. Heart. 2020 Jul;106(13):959-1032. doi: 10.1136/heartjnl-2020-316815.

Shah ASV, McAllister DA, Gallacher P, Astengo F, Perez JAR, Hall J, Lee KK, **Bing R**, Anand A, Nathwani D, Mills NL, Newby DE, Marwick C, Cruden NLM. Incidence, Microbiology and Outcomes in Patient Hospitalized with Infective Endocarditis. Circulation. 2020;10.1161/CIRCULATIONAHA.119.044913.

Bing R*, Gu H*, Chin C, Fang L, White A, Everett R, Spath N, Park E, Jenkins W, Shah A, Mills N, Flapan A, Chamber J, Newby D, Chowienczyk P*, Dweck M*. Determinants and prognostic value of echocardiographic first-phase ejection fraction in aortic stenosis. Heart. 2020. 10.1136/heartjnl-2020-316684.

Bing R, Mitchell A, Newby D. Chest pain – when in doubt….Heart. 2020 May;106(9):690-706. doi: 10.1136/heartjnl-2019-316458.

Bing R, Behan M, Pessotto R, Cruden N, Northridge D. Percutaneous repair of ventricular ruptures. JACC Case Reports. 2020. doi: 10.1016/j.jaccas.2019.11.088.

Calin A, Mateescu A, Popescu A, **Bing R**, Dweck M, Popescu B. Role of advanced left ventricular imaging in adults with aortic stenosis. Heart. 2020. doi: 10.1136/heartjnl-2019-315211.

Meah M, **Bing R**, Newby D. Primacy of coronary CT angiography as the gatekeeper for the cardiac catheterization laboratory. Am Heart J. 2020. doi: 10.1016/j.ahj.2020.01.017.

Bing R, Singh T, Dweck M, Mills N, Williams M, Adamson P, Newby D. Validation of European Society of Cardiology pre-test probabilities for obstructive coronary artery disease in suspected stable angina. Eur Heart J Qual Care Clin Outcomes. 2020. doi: 10.1093/ehjqcco/qcaa006.

Bing R, Loganath K, Adamson P, Newby D, Moss A. Non-invasive imaging of high-risk coronary plaque: the role of computed tomography and positron emission tomography. Br J Radiol. 2019 Dec 18:20190740. doi: 10.1259/bjr.20190740.

Bing R, Dweck M. Myocardial fibrosis – why image, how to image and clinical implications. Heart. 2019. doi: 10.1136/heartjnl-2019-315560.

Bing R, Dweck M. Aortic valve and coronary 18F-sodium fluoride activity – a common cause? J Nucl Cardiol. 2019. doi: 10.1007/s12350-019-01901-x.

Adamson PD, Williams MC, Dweck MR, Mills NL, Boon NA, Daghem M, **Bing R**, Moss AJ, Mangion K, Flather M, Forbes J, Hunter A, Norrie J, Shah ASV, Timmis AD, van Beek EJR, Ahmadi AA, Leipsic J, Narula J, Newby DE, Roditi G, McAllister D, Berry C. Mechanisms of Improved Five-year Outcomes After Coronary CT Angiography in Patients with Stable Chest Pain. J Am Coll Cardiol. 2019;74(16):2058-70.

Moss A, Dweck M, Doris M, Andrews J, **Bing R**, Forsythe R, Cartlidge T, Pawade T, Daghem M, Raftis J, Williams M, van Beek E, Forsythe R, Lewis S, Lee R, Shah A, Mills N, Newby D, Adamson P. Ticagrelor to reduce myocardial injury in patients with high-risk coronary artery plaque. J Am Coll Cardiol Img. 2019;10.1016/j.jcmg.2019.05.023.

Daghem M, **Bing R**, Dweck M, Fayad Z. Non-Invasive Imaging to Assess Atherosclerotic Plaque Composition and Disease Activity. J Am Coll Cardiol Img. 2019;10.1016/j.jcmg.2019.03.033.

Moss AJ, Doris MK, Andrews JPM, **Bing R**, Daghem M, van Beek EJR, Forsyth L, Shah ASV, Williams MC, Sellers S, Leipsic J, Dweck MR, Parker RA, Newby DE, Adamson PD. Molecular coronary plaque imaging using 18F-Fluoride. Circ Cardiovasc Imaging. 2019 Aug;12(8):e008574.

Lee KK, Stelzle D, **Bing R**, Anwar M, Strachan F, Bashir S, Newby DE, Shah JS, Chung MH, Bloomfield GS, Longenecker CT, Bagchi S, Kottilil S, Blach S, Razavi H, Mills PR, Mills NL, McAllister DA, Shah ASV. Global burden of atherosclerotic cardiovascular disease in hepatitis C virus infection: a systematic review, meta-analysis, and modelling study.
Lancet Gastroenterol Hepatol. 2019. doi: 10.1016/S2468-1253(19)30227-4.

Bing R, Driessen RS, Knaapen P, Dweck MR. The clinical utility of hybrid imaging for the identification of vulnerable plaque and vulnerable patients. J Cardiovasc Comput Tomogr. 2019;10.1016.

Bing R, Henderson J, Hunter A, Williams M, Moss A, Shah A, McAllister D, Dweck M, Newby D, Mills N, Adamson P. Clinical determinants of plasma cardiac biomarkers in patients with stable chest pain. Heart. 2019. doi: 10.1136/heartjnl-2019-314892.

Fukui M, **Bing R**, Dweck MD, Cavalcante J. Assessment of aortic stenosis by cardiac magnetic resonance imaging. Quantification of flow, characterization of myocardial injury, transcatheter aortic valve replacement planning and more. Magn Reson Imaging Clin N Am. 2019 Aug;27(3):427-437. doi: 10.1016/j.mric.2019.04.004.

Bing R, Dweck MD. Myocardial fibrosis in classical low-flow low-gradient severe aortic stenosis - the missing piece of the puzzle? Circ Cardiovasc Imaging. 2019 May;12(5):e009187. doi: 10.1161/CIRCIMAGING.119.009187.

Bing R, Everett R, Tuck C et al. Rationale and design of the randomized, controlled Early Valve Replacement Guided by Biomarkers of Left Ventricular Decompensation in Asymptomatic Patients with Severe Aortic Stenosis (EVOLVED) trial. Am Heart J. 2019 Mar 15;212:91-100. doi: 10.1016.

Bing R, Cavalcante JL, Everett RJ, Clavel MA, Newby DE, Dweck MD. Imaging and impact of myocardial fibrosis in aortic stenosis. J Am Coll Cardiol Img. Feb 2019, 12 (2) 283-296; doi: 0.1016/j.jcmg.2018.11.026.

Dweck M, **Bing R**. Diffuse myocardial fibrosis in aortic stenosis – time to act? J Am Coll Cardiol Img. 2019 Jan;12(1):120-122. doi: 10.1016/j.jcmg.2018.06.026.

Bing R, Cruden N. Risk assessment for non-cardiac surgery after coronary stenting – keeping it simple. Eur Heart J Qual Care Clin Outcomes. 2019 Jan 1;5(1):1-3. doi: 10.1093/ehjqcco/qcy043.

References

Achenbach, S., Delgado, V., Hausleiter, J., Schoenhagen, P., Min, J. K., & Leipsic, J. A. (2012, Nov-Dec). SCCT expert consensus document on computed tomography imaging before transcatheter aortic valve implantation (TAVI)/transcatheter aortic valve replacement (TAVR). *J Cardiovasc Comput Tomogr, 6*(6), 366-380. https://doi.org/10.1016/j.jcct.2012.11.002

Agatston, A. S., Janowitz, W. R., Hildner, F. J., Zusmer, N. R., Viamonte, M., Jr., & Detrano, R. (1990, Mar 15). Quantification of coronary artery calcium using ultrafast computed tomography. *J Am Coll Cardiol, 15*(4), 827-832. https://doi.org/10.1016/0735-1097(90)90282-t

Aksoy, O., Cam, A., Goel, S. S., Houghtaling, P. L., Williams, S., Ruiz-Rodriguez, E., Menon, V., Kapadia, S. R., Tuzcu, E. M., Blackstone, E. H., & Griffin, B. P. (2012, Apr 17). Do bisphosphonates slow the progression of aortic stenosis? *J Am Coll Cardiol, 59*(16), 1452-1459. https://doi.org/10.1016/j.jacc.2012.01.024

Al-Abcha, A., Saleh, Y., Boumegouas, M., Prasad, R., Herzallah, K., Baloch, Z. Q., Abdelkarim, O., Rayamajhi, S., & Abela, G. S. (2021, May 1). Meta-Analysis of Valve-in-Valve Transcatheter Aortic Valve Implantation Versus Redo-surgical Aortic

Valve Replacement in Failed Bioprosthetic Aortic Valve. *Am J Cardiol, 146*, 74-81. https://doi.org/10.1016/j.amjcard.2021.01.028

Azevedo, C. F., Nigri, M., Higuchi, M. L., Pomerantzeff, P. M., Spina, G. S., Sampaio, R. O., Tarasoutchi, F., Grinberg, M., & Rochitte, C. E. (2010, Jul 20). Prognostic significance of myocardial fibrosis quantification by histopathology and magnetic resonance imaging in patients with severe aortic valve disease. *J Am Coll Cardiol, 56*(4), 278-287. https://doi.org/10.1016/j.jacc.2009.12.074

Banovic, M., Iung, B., Bartunek, J., Asanin, M., Beleslin, B., Biocina, B., Casselman, F., da Costa, M., Deja, M., Gasparovic, H., Kala, P., Labrousse, L., Loncar, Z., Marinkovic, J., Nedeljkovic, I., Nedeljkovic, M., Nemec, P., Nikolic, S. D., Pencina, M., Penicka, M., Ristic, A., Sharif, F., Van Camp, G., Vanderheyden, M., Wojakowski, W., & Putnik, S. (2016, Apr). Rationale and design of the Aortic Valve replAcemenT versus conservative treatment in Asymptomatic seveRe aortic stenosis (AVATAR trial): A randomized multicenter controlled event-driven trial. *Am Heart J, 174*, 147-153. https://doi.org/10.1016/j.ahj.2016.02.001

Barone-Rochette, G., Pierard, S., De Meester de Ravenstein, C., Seldrum, S., Melchior, J., Maes, F., Pouleur, A. C., Vancraeynest, D., Pasquet, A., Vanoverschelde, J. L., & Gerber, B. L. (2014, Jul 15). Prognostic significance of LGE by CMR in aortic

stenosis patients undergoing valve replacement. *J Am Coll Cardiol, 64*(2), 144-154. https://doi.org/10.1016/j.jacc.2014.02.612

Baumgartner, H., Falk, V., Bax, J. J., De Bonis, M., Hamm, C., Holm, P. J., Iung, B., Lancellotti, P., Lansac, E., Rodriguez Munoz, D., Rosenhek, R., Sjogren, J., Tornos Mas, P., Vahanian, A., Walther, T., Wendler, O., Windecker, S., Zamorano, J. L., & Group, E. S. C. S. D. (2017, Sep 21). 2017 ESC/EACTS Guidelines for the management of valvular heart disease. *Eur Heart J, 38*(36), 2739-2791. https://doi.org/10.1093/eurheartj/ehx391

Baumgartner, H., Hung, J., Bermejo, J., Chambers, J. B., Evangelista, A., Griffin, B. P., Iung, B., Otto, C. M., Pellikka, P. A., Quinones, M., American Society of, E., & European Association of, E. (2009, Jan). Echocardiographic assessment of valve stenosis: EAE/ASE recommendations for clinical practice. *J Am Soc Echocardiogr, 22*(1), 1-23; quiz 101-102. https://doi.org/10.1016/j.echo.2008.11.029

Bermejo, J., Antoranz, J. C., Burwash, I. G., Alvarez, J. L., Moreno, M., García-Fernández, M. A., & Otto, C. M. (2002, Jul). In-vivo analysis of the instantaneous transvalvular pressure difference-flow relationship in aortic valve stenosis: implications of unsteady fluid-dynamics for the clinical assessment of disease severity. *J Heart Valve Dis, 11*(4), 557-566.

Bing, R., Cavalcante, J. L., Everett, R. J., Clavel, M. A., Newby, D. E., & Dweck, M. R. (2019, Feb). Imaging and Impact of Myocardial Fibrosis in Aortic Stenosis. *JACC Cardiovasc Imaging, 12*(2), 283-296. https://doi.org/10.1016/j.jcmg.2018.11.026

Bing, R., & Dweck, M. R. (2020, Dec). The quest for an aortic stenosis cure. *Heart, 106*(23), 1790-1791. https://doi.org/10.1136/heartjnl-2020-317421

Bing, R., Everett, R. J., Tuck, C., Semple, S., Lewis, S., Harkess, R., Mills, N. L., Treibel, T. A., Prasad, S., Greenwood, J. P., McCann, G. P., Newby, D. E., & Dweck, M. R. (2019, Jun). Rationale and design of the randomized, controlled Early Valve Replacement Guided by Biomarkers of Left Ventricular Decompensation in Asymptomatic Patients with Severe Aortic Stenosis (EVOLVED) trial. *Am Heart J, 212*, 91-100. https://doi.org/10.1016/j.ahj.2019.02.018

Blackman, D. J., Saraf, S., MacCarthy, P. A., Myat, A., Anderson, S. G., Malkin, C. J., Cunnington, M. S., Somers, K., Brennan, P., Manoharan, G., Parker, J., Aldalati, O., Brecker, S. J., Dowling, C., Hoole, S. P., Dorman, S., Mullen, M., Kennon, S., Jerrum, M., Chandrala, P., Roberts, D. H., Tay, J., Doshi, S. N., Ludman, P. F., Fairbairn, T. A., Crowe, J., Levy, R. D., Banning, A. P., Ruparelia, N., Spence, M. S., & Hildick-Smith, D. (2019, Feb 12). Long-Term Durability of Transcatheter Aortic

Valve Prostheses. *J Am Coll Cardiol, 73*(5), 537-545. https://doi.org/10.1016/j.jacc.2018.10.078

Blanke, P., Leipsic, J. A., Popma, J. J., Yakubov, S. J., Deeb, G. M., Gada, H., Mumtaz, M., Ramlawi, B., Kleiman, N. S., Sorajja, P., Askew, J., Meduri, C. U., Kauten, J., Melnitchouk, S., Inglessis, I., Huang, J., Boulware, M., Reardon, M. J., & Evolut Low Risk, L. T. I. S. I. (2020, May 19). Bioprosthetic Aortic Valve Leaflet Thickening in the Evolut Low Risk Sub-Study. *J Am Coll Cardiol, 75*(19), 2430-2442. https://doi.org/10.1016/j.jacc.2020.03.022

Blanke, P., Weir-McCall, J. R., Achenbach, S., Delgado, V., Hausleiter, J., Jilaihawi, H., Marwan, M., Norgaard, B. L., Piazza, N., Schoenhagen, P., & Leipsic, J. A. (2019, Jan). Computed Tomography Imaging in the Context of Transcatheter Aortic Valve Implantation (TAVI)/Transcatheter Aortic Valve Replacement (TAVR): An Expert Consensus Document of the Society of Cardiovascular Computed Tomography. *JACC Cardiovasc Imaging, 12*(1), 1-24. https://doi.org/10.1016/j.jcmg.2018.12.003

Bloomfield, P., Wheatley, D. J., Prescott, R. J., & Miller, H. C. (1991, Feb 28). Twelve-year comparison of a Bjork-Shiley mechanical heart valve with porcine bioprostheses. *N Engl J Med, 324*(9), 573-579. https://doi.org/10.1056/NEJM199102283240901

Braunwald, E. (1990, Apr). On the natural history of severe aortic stenosis. *J Am Coll Cardiol, 15*(5), 1018-1020. https://doi.org/10.1016/0735-1097(90)90235-h

Brener, S. J., Duffy, C. I., Thomas, J. D., & Stewart, W. J. (1995, Feb). Progression of aortic stenosis in 394 patients: relation to changes in myocardial and mitral valve dysfunction. *J Am Coll Cardiol, 25*(2), 305-310. https://doi.org/10.1016/0735-1097(94)00406-g

Briand, M., Dumesnil, J. G., Kadem, L., Tongue, A. G., Rieu, R., Garcia, D., & Pibarot, P. (2005, Jul 19). Reduced systemic arterial compliance impacts significantly on left ventricular afterload and function in aortic stenosis: implications for diagnosis and treatment. *J Am Coll Cardiol, 46*(2), 291-298. https://doi.org/10.1016/j.jacc.2004.10.081

Bucay, N., Sarosi, I., Dunstan, C. R., Morony, S., Tarpley, J., Capparelli, C., Scully, S., Tan, H. L., Xu, W., Lacey, D. L., Boyle, W. J., & Simonet, W. S. (1998, May 1). osteoprotegerin-deficient mice develop early onset osteoporosis and arterial calcification. *Genes Dev, 12*(9), 1260-1268. https://doi.org/10.1101/gad.12.9.1260

Bunting, K. V., Steeds, R. P., Slater, L. T., Rogers, J. K., Gkoutos, G. V., & Kotecha, D. (2019, Dec). A Practical Guide to Assess the Reproducibility of Echocardiographic

Measurements. *J Am Soc Echocardiogr, 32*(12), 1505-1515. https://doi.org/10.1016/j.echo.2019.08.015

Carroll, J. D., Mack, M. J., Vemulapalli, S., Herrmann, H. C., Gleason, T. G., Hanzel, G., Deeb, G. M., Thourani, V. H., Cohen, D. J., Desai, N., Kirtane, A. J., Fitzgerald, S., Michaels, J., Krohn, C., Masoudi, F. A., Brindis, R. G., & Bavaria, J. E. (2020, Nov 24). STS-ACC TVT Registry of Transcatheter Aortic Valve Replacement. *J Am Coll Cardiol, 76*(21), 2492-2516. https://doi.org/10.1016/j.jacc.2020.09.595

Cartlidge, T. R. G., Doris, M. K., Sellers, S. L., Pawade, T. A., White, A. C., Pessotto, R., Kwiecinski, J., Fletcher, A., Alcaide, C., Lucatelli, C., Densem, C., Rudd, J. H. F., van Beek, E. J. R., Tavares, A., Virmani, R., Berman, D., Leipsic, J. A., Newby, D. E., & Dweck, M. R. (2019, Mar 19). Detection and Prediction of Bioprosthetic Aortic Valve Degeneration. *J Am Coll Cardiol, 73*(10), 1107-1119. https://doi.org/10.1016/j.jacc.2018.12.056

Chae, S. Y., Kwon, T. W., Jin, S., Kwon, S. U., Sung, C., Oh, S. J., Lee, S. J., Oh, J. S., Han, Y., Cho, Y. P., Lee, N., Kim, J. Y., Koglin, N., Berndt, M., Stephens, A. W., & Moon, D. H. (2019, Jan 7). A phase 1, first-in-human study of (18)F-GP1 positron emission tomography for imaging acute arterial thrombosis. *EJNMMI Res, 9*(1), 3. https://doi.org/10.1186/s13550-018-0471-8

Chakravarty, T., Patel, A., Kapadia, S., Raschpichler, M., Smalling, R. W., Szeto, W. Y., Abramowitz, Y., Cheng, W., Douglas, P. S., Hahn, R. T., Herrmann, H. C., Kereiakes, D., Svensson, L., Yoon, S. H., Babaliaros, V. C., Kodali, S., Thourani, V. H., Alu, M. C., Liu, Y., McAndrew, T., Mack, M., Leon, M. B., & Makkar, R. R. (2019, Sep 3). Anticoagulation After Surgical or Transcatheter Bioprosthetic Aortic Valve Replacement. *J Am Coll Cardiol, 74*(9), 1190-1200. https://doi.org/10.1016/j.jacc.2019.06.058

Chakravarty, T., Sondergaard, L., Friedman, J., De Backer, O., Berman, D., Kofoed, K. F., Jilaihawi, H., Shiota, T., Abramowitz, Y., Jorgensen, T. H., Rami, T., Israr, S., Fontana, G., de Knegt, M., Fuchs, A., Lyden, P., Trento, A., Bhatt, D. L., Leon, M. B., Makkar, R. R., Resolve, & Investigators, S. (2017, Jun 17). Subclinical leaflet thrombosis in surgical and transcatheter bioprosthetic aortic valves: an observational study. *Lancet, 389*(10087), 2383-2392. https://doi.org/10.1016/S0140-6736(17)30757-2

Chambers, J. (2006, Mar). The left ventricle in aortic stenosis: evidence for the use of ACE inhibitors. *Heart, 92*(3), 420-423. https://doi.org/10.1136/hrt.2005.074112

Chan, K. L., Teo, K., Dumesnil, J. G., Ni, A., Tam, J., & Investigators, A. (2010, Jan 19). Effect of Lipid lowering with rosuvastatin on progression of aortic stenosis: results of the aortic stenosis progression observation: measuring effects of rosuvastatin (ASTRONOMER) trial. *Circulation, 121*(2), 306-314. https://doi.org/10.1161/CIRCULATIONAHA.109.900027

Chen, C. L., Chen, N. C., Wu, F. Z., & Wu, M. T. (2020, Aug). Impact of denosumab on cardiovascular calcification in patients with secondary hyperparathyroidism undergoing dialysis: a pilot study. *Osteoporosis international : a journal established as result of cooperation between the European Foundation for Osteoporosis and the National Osteoporosis Foundation of the USA, 31*(8), 1507-1516. https://doi.org/10.1007/s00198-020-05391-3

Chin, C. W., Semple, S., Malley, T., White, A. C., Mirsadraee, S., Weale, P. J., Prasad, S., Newby, D. E., & Dweck, M. R. (2014, May). Optimization and comparison of myocardial T1 techniques at 3T in patients with aortic stenosis. *Eur Heart J Cardiovasc Imaging, 15*(5), 556-565. https://doi.org/10.1093/ehjci/jet245

Chin, C. W. L., Everett, R. J., Kwiecinski, J., Vesey, A. T., Yeung, E., Esson, G., Jenkins, W., Koo, M., Mirsadraee, S., White, A. C., Japp, A. G., Prasad, S. K., Semple, S., Newby, D. E., & Dweck, M. R. (2017, Nov). Myocardial Fibrosis and Cardiac

Decompensation in Aortic Stenosis. *JACC Cardiovasc Imaging, 10*(11), 1320-1333. https://doi.org/10.1016/j.jcmg.2016.10.007

Clavel, M. A., Magne, J., & Pibarot, P. (2016, Sep 7). Low-gradient aortic stenosis. *Eur Heart J, 37*(34), 2645-2657. https://doi.org/10.1093/eurheartj/ehw096

Clavel, M. A., Messika-Zeitoun, D., Pibarot, P., Aggarwal, S. R., Malouf, J., Araoz, P. A., Michelena, H. I., Cueff, C., Larose, E., Capoulade, R., Vahanian, A., & Enriquez-Sarano, M. (2013, Dec 17). The complex nature of discordant severe calcified aortic valve disease grading: new insights from combined Doppler echocardiographic and computed tomographic study. *J Am Coll Cardiol, 62*(24), 2329-2338. https://doi.org/10.1016/j.jacc.2013.08.1621

Clavel, M. A., Pibarot, P., Messika-Zeitoun, D., Capoulade, R., Malouf, J., Aggarval, S., Araoz, P. A., Michelena, H. I., Cueff, C., Larose, E., Miller, J. D., Vahanian, A., & Enriquez-Sarano, M. (2014, Sep 23). Impact of aortic valve calcification, as measured by MDCT, on survival in patients with aortic stenosis: results of an international registry study. *J Am Coll Cardiol, 64*(12), 1202-1213. https://doi.org/10.1016/j.jacc.2014.05.066

Cote, N., Mahmut, A., Fournier, D., Boulanger, M. C., Couture, C., Despres, J. P., Trahan, S., Bosse, Y., Page, S., Pibarot, P., & Mathieu, P. (2014). Angiotensin receptor blockers are associated with reduced fibrosis and interleukin-6 expression in calcific aortic valve disease. *Pathobiology, 81*(1), 15-24. https://doi.org/10.1159/000350896

Cowell, S. J., Newby, D. E., Prescott, R. J., Bloomfield, P., Reid, J., Northridge, D. B., Boon, N. A., Scottish Aortic, S., & Lipid Lowering Trial, I. o. R. I. (2005, Jun 9). A randomized trial of intensive lipid-lowering therapy in calcific aortic stenosis. *N Engl J Med, 352*(23), 2389-2397. https://doi.org/10.1056/NEJMoa043876

Damiano, B. P., Mitchell, J. A., Giardino, E., Corcoran, T., Haertlein, B. J., de Garavilla, L., Kauffman, J. A., Hoekstra, W. J., Maryanoff, B. E., & Andrade-Gordon, P. (2001, Oct 15). Antiplatelet and antithrombotic activity of RWJ-53308, a novel orally active glycoprotein IIb/IIIa antagonist. *Thromb Res, 104*(2), 113-126. https://doi.org/10.1016/s0049-3848(01)00353-x

Dangas, G. D., Tijssen, J. G. P., Wohrle, J., Sondergaard, L., Gilard, M., Mollmann, H., Makkar, R. R., Herrmann, H. C., Giustino, G., Baldus, S., De Backer, O., Guimaraes, A. H. C., Gullestad, L., Kini, A., von Lewinski, D., Mack, M., Moreno, R., Schafer, U., Seeger, J., Tchetche, D., Thomitzek, K., Valgimigli, M., Vranckx, P., Welsh, R. C., Wildgoose, P., Volkl, A. A., Zazula, A., van Amsterdam, R. G. M., Mehran, R., Windecker, S., & Investigators, G. (2020, Jan 9). A Controlled Trial of Rivaroxaban

after Transcatheter Aortic-Valve Replacement. *N Engl J Med, 382*(2), 120-129. https://doi.org/10.1056/NEJMoa1911425

Davies, S. W., Gershlick, A. H., & Balcon, R. (1991, Jan). Progression of valvar aortic stenosis: a long-term retrospective study. *Eur Heart J, 12*(1), 10-14. https://doi.org/10.1093/oxfordjournals.eurheartj.a059815

Dayanand, P., Sandhyavenu, H., Dayanand, S., Martinez, J., & Rangaswami, J. (2018). Role of Bisphosphonates in Vascular calcification and Bone Metabolism: A Clinical Summary. *Curr Cardiol Rev, 14*(3), 192-199. https://doi.org/10.2174/1573403X14666180619103258

De Backer, O., Dangas, G. D., Jilaihawi, H., Leipsic, J. A., Terkelsen, C. J., Makkar, R., Kini, A. S., Veien, K. T., Abdel-Wahab, M., Kim, W. K., Balan, P., Van Mieghem, N., Mathiassen, O. N., Jeger, R. V., Arnold, M., Mehran, R., Guimaraes, A. H. C., Norgaard, B. L., Kofoed, K. F., Blanke, P., Windecker, S., Sondergaard, L., & Investigators, G.-D. (2020, Jan 9). Reduced Leaflet Motion after Transcatheter Aortic-Valve Replacement. *N Engl J Med, 382*(2), 130-139. https://doi.org/10.1056/NEJMoa1911426

Del Trigo, M., Munoz-Garcia, A. J., Latib, A., Auffret, V., Wijeysundera, H. C., Nombela-Franco, L., Gutierrez, E., Cheema, A. N., Serra, V., Amat-Santos, I. J., Kefer, J., Benitez, L. M., Leclercq, F., Mangieri, A., Le Breton, H., Jimenez-Quevedo, P., Garcia Del Blanco, B., Dager, A., Abdul-Jawad Altisent, O., Puri, R., Pibarot, P., & Rodes-Cabau, J. (2018, May). Impact of anticoagulation therapy on valve haemodynamic deterioration following transcatheter aortic valve replacement. *Heart, 104*(10), 814-820. https://doi.org/10.1136/heartjnl-2017-312514

Del Trigo, M., Munoz-Garcia, A. J., Wijeysundera, H. C., Nombela-Franco, L., Cheema, A. N., Gutierrez, E., Serra, V., Kefer, J., Amat-Santos, I. J., Benitez, L. M., Mewa, J., Jimenez-Quevedo, P., Alnasser, S., Garcia Del Blanco, B., Dager, A., Abdul-Jawad Altisent, O., Puri, R., Campelo-Parada, F., Dahou, A., Paradis, J. M., Dumont, E., Pibarot, P., & Rodes-Cabau, J. (2016, Feb 16). Incidence, Timing, and Predictors of Valve Hemodynamic Deterioration After Transcatheter Aortic Valve Replacement: Multicenter Registry. *J Am Coll Cardiol, 67*(6), 644-655. https://doi.org/10.1016/j.jacc.2015.10.097

DePace, N. L., Ren, J. F., Iskandrian, A. S., Kotler, M. N., Hakki, A. H., & Segal, B. L. (1983, Apr). Correlation of echocardiographic wall stress and left ventricular pressure and function in aortic stenosis. *Circulation, 67*(4), 854-859. https://doi.org/10.1161/01.cir.67.4.854

Doris, M. K., Jenkins, W., Robson, P., Pawade, T., Andrews, J. P., Bing, R., Cartlidge, T., Shah, A., Pickering, A., Williams, M. C., Fayad, Z. A., White, A., van Beek, E. J., Newby, D. E., & Dweck, M. R. (2020, Dec). Computed tomography aortic valve calcium scoring for the assessment of aortic stenosis progression. *Heart, 106*(24), 1906-1913. https://doi.org/10.1136/heartjnl-2020-317125

Du Bois, D., & Du Bois, E. F. (1989, Sep-Oct). A formula to estimate the approximate surface area if height and weight be known. 1916. *Nutrition, 5*(5), 303-311; discussion 312-303. https://www.ncbi.nlm.nih.gov/pubmed/2520314

Durko, A. P., Osnabrugge, R. L., Van Mieghem, N. M., Milojevic, M., Mylotte, D., Nkomo, V. T., & Pieter Kappetein, A. (2018, Jul 21). Annual number of candidates for transcatheter aortic valve implantation per country: current estimates and future projections. *Eur Heart J, 39*(28), 2635-2642. https://doi.org/10.1093/eurheartj/ehy107

Dweck, M. R., Boon, N. A., & Newby, D. E. (2012, Nov 6). Calcific aortic stenosis: a disease of the valve and the myocardium. *J Am Coll Cardiol, 60*(19), 1854-1863. https://doi.org/10.1016/j.jacc.2012.02.093

Dweck, M. R., Jenkins, W. S., Vesey, A. T., Pringle, M. A., Chin, C. W., Malley, T. S., Cowie, W. J., Tsampasian, V., Richardson, H., Fletcher, A., Wallace, W. A., Pessotto,

R., van Beek, E. J., Boon, N. A., Rudd, J. H., & Newby, D. E. (2014, Mar). 18F-sodium fluoride uptake is a marker of active calcification and disease progression in patients with aortic stenosis. *Circ Cardiovasc Imaging, 7*(2), 371-378. https://doi.org/10.1161/CIRCIMAGING.113.001508

Dweck, M. R., Jones, C., Joshi, N. V., Fletcher, A. M., Richardson, H., White, A., Marsden, M., Pessotto, R., Clark, J. C., Wallace, W. A., Salter, D. M., McKillop, G., van Beek, E. J., Boon, N. A., Rudd, J. H., & Newby, D. E. (2012, Jan 3). Assessment of valvular calcification and inflammation by positron emission tomography in patients with aortic stenosis. *Circulation, 125*(1), 76-86. https://doi.org/10.1161/CIRCULATIONAHA.111.051052

Dweck, M. R., Joshi, S., Murigu, T., Alpendurada, F., Jabbour, A., Melina, G., Banya, W., Gulati, A., Roussin, I., Raza, S., Prasad, N. A., Wage, R., Quarto, C., Angeloni, E., Refice, S., Sheppard, M., Cook, S. A., Kilner, P. J., Pennell, D. J., Newby, D. E., Mohiaddin, R. H., Pepper, J., & Prasad, S. K. (2011, Sep 13). Midwall fibrosis is an independent predictor of mortality in patients with aortic stenosis. *J Am Coll Cardiol, 58*(12), 1271-1279. https://doi.org/10.1016/j.jacc.2011.03.064

Dweck, M. R., Williams, M. C., Moss, A. J., Newby, D. E., & Fayad, Z. A. (2016, Nov 15). Computed Tomography and Cardiac Magnetic Resonance in Ischemic Heart Disease. *J Am Coll Cardiol, 68*(20), 2201-2216. https://doi.org/10.1016/j.jacc.2016.08.047

Elmariah, S., Delaney, J. A., O'Brien, K. D., Budoff, M. J., Vogel-Claussen, J., Fuster, V., Kronmal, R. A., & Halperin, J. L. (2010, Nov 16). Bisphosphonate Use and Prevalence of Valvular and Vascular Calcification in Women MESA (The Multi-Ethnic Study of Atherosclerosis). *J Am Coll Cardiol, 56*(21), 1752-1759. https://doi.org/10.1016/j.jacc.2010.05.050

Etchells, E., Bell, C., & Robb, K. (1997, Feb 19). Does this patient have an abnormal systolic murmur? *JAMA, 277*(7), 564-571.

Eveborn, G. W., Schirmer, H., Heggelund, G., Lunde, P., & Rasmussen, K. (2013, Mar). The evolving epidemiology of valvular aortic stenosis. the Tromso study. *Heart, 99*(6), 396-400. https://doi.org/10.1136/heartjnl-2012-302265

Everett, R. J., Tastet, L., Clavel, M. A., Chin, C. W. L., Capoulade, R., Vassiliou, V. S., Kwiecinski, J., Gomez, M., van Beek, E. J. R., White, A. C., Prasad, S. K., Larose, E., Tuck, C., Semple, S., Newby, D. E., Pibarot, P., & Dweck, M. R. (2018, Jun). Progression of Hypertrophy and Myocardial Fibrosis in Aortic Stenosis: A Multicenter Cardiac Magnetic Resonance Study. *Circ Cardiovasc Imaging, 11*(6), e007451. https://doi.org/10.1161/CIRCIMAGING.117.007451

Everett, R. J., Treibel, T. A., Fukui, M., Lee, H., Rigolli, M., Singh, A., Bijsterveld, P., Tastet, L., Musa, T. A., Dobson, L., Chin, C., Captur, G., Om, S. Y., Wiesemann, S., Ferreira, V. M., Piechnik, S. K., Schulz-Menger, J., Schelbert, E. B., Clavel, M. A., Newby, D. E., Myerson, S. G., Pibarot, P., Lee, S., Cavalcante, J. L., Lee, S. P., McCann, G. P., Greenwood, J. P., Moon, J. C., & Dweck, M. R. (2020, Jan 28). Extracellular Myocardial Volume in Patients With Aortic Stenosis. *J Am Coll Cardiol, 75*(3), 304-316. https://doi.org/10.1016/j.jacc.2019.11.032

Farhat, G. N., Cauley, J. A., Matthews, K. A., Newman, A. B., Johnston, J., Mackey, R., Edmundowicz, D., & Sutton-Tyrrell, K. (2006, Dec). Volumetric BMD and vascular calcification in middle-aged women: the Study of Women's Health Across the Nation. *J Bone Miner Res, 21*(12), 1839-1846. https://doi.org/10.1359/jbmr.060903

Fontana, M., White, S. K., Banypersad, S. M., Sado, D. M., Maestrini, V., Flett, A. S., Piechnik, S. K., Neubauer, S., Roberts, N., & Moon, J. C. (2012, Dec 28). Comparison of T1 mapping techniques for ECV quantification. Histological validation and reproducibility of ShMOLLI versus multibreath-hold T1 quantification equilibrium contrast CMR. *J Cardiovasc Magn Reson, 14*, 88. https://doi.org/10.1186/1532-429X-14-88

Genereux, P., Piazza, N., Alu, M. C., Nazif, T., Hahn, R. T., Pibarot, P., Bax, J. J., Leipsic, J. A., Blanke, P., Blackstone, E. H., Finn, M. T., Kapadia, S., Linke, A., Mack, M. J.,

Makkar, R., Mehran, R., Popma, J. J., Reardon, M., Rodes-Cabau, J., Van Mieghem, N. M., Webb, J. G., Cohen, D. J., & Leon, M. B. (2021, Apr 19). Valve Academic Research Consortium 3: updated endpoint definitions for aortic valve clinical research. *Eur Heart J*. https://doi.org/10.1093/eurheartj/ehaa799

Goody, P. R., Hosen, M. R., Christmann, D., Niepmann, S. T., Zietzer, A., Adam, M., Bonner, F., Zimmer, S., Nickenig, G., & Jansen, F. (2020, Apr). Aortic Valve Stenosis: From Basic Mechanisms to Novel Therapeutic Targets. *Arterioscler Thromb Vasc Biol, 40*(4), 885-900. https://doi.org/10.1161/ATVBAHA.119.313067

Griffith, M. J., Carey, C. M., Byrne, J. C., Coltart, D. J., Jenkins, B. S., & Webb-Peploe, M. M. (1991, Mar). Echocardiographic left ventricular wall thickness: a poor predictor of the severity of aortic valve stenosis. *Clin Cardiol, 14*(3), 227-231. https://doi.org/10.1002/clc.4960140310

Gu, H., Bing, R., Chin, C., Fang, L., White, A. C., Everett, R., Spath, N., Park, E., Chambers, J. B., Newby, D. E., Chiribiri, A., Dweck, M. R., & Chowienczyk, P. (2021, Jun 10). First-phase ejection fraction by cardiovascular magnetic resonance predicts outcomes in aortic stenosis. *J Cardiovasc Magn Reson, 23*(1), 73. https://doi.org/10.1186/s12968-021-00756-x

Gu, H., Cirillo, C., Nabeebaccus, A. A., Sun, Z., Fang, L., Xie, Y., Demir, O., Desai, N., He, L., Lü, Q., Nakou, E., O'Gallagher, K., Tountas, C., Marvaki, A., Monaghan, M., Perera, D., Pericao, A., Ryan, M., Sinclair, H., Stylianidis, V., Victor, K., Wang, B., Wang, J., Wang, R., Wu, C., Yang, Y., Yuan, H., Zhang, D., Zhang, Y., Faconti, L., Papachristidis, A., Zhang, L., Carr-White, G., Shah, A. M., Xie, M., & Chowienczyk, P. (2021, Jun). First-Phase Ejection Fraction, a Measure of Preclinical Heart Failure, Is Strongly Associated With Increased Mortality in Patients With COVID-19. *Hypertension, 77*(6), 2014-2022. https://doi.org/10.1161/hypertensionaha.121.17099

Gu, H., Li, Y., Fok, H., Simpson, J., Kentish, J. C., Shah, A. M., & Chowienczyk, P. J. (2017, Apr). Reduced First-Phase Ejection Fraction and Sustained Myocardial Wall Stress in Hypertensive Patients With Diastolic Dysfunction: A Manifestation of Impaired Shortening Deactivation That Links Systolic to Diastolic Dysfunction and Preserves Systolic Ejection Fraction. *Hypertension, 69*(4), 633-640. https://doi.org/10.1161/HYPERTENSIONAHA.116.08545

Gu, H., Saeed, S., Boguslavskyi, A., Carr-White, G., Chambers, J. B., & Chowienczyk, P. (2019, Jan). First-Phase Ejection Fraction Is a Powerful Predictor of Adverse Events in Asymptomatic Patients With Aortic Stenosis and Preserved Total Ejection Fraction. *JACC Cardiovasc Imaging, 12*(1), 52-63. https://doi.org/10.1016/j.jcmg.2018.08.037

Gurvitch, R., Webb, J. G., Yuan, R., Johnson, M., Hague, C., Willson, A. B., Toggweiler, S., Wood, D. A., Ye, J., Moss, R., Thompson, C. R., Achenbach, S., Min, J. K., Labounty, T. M., Cury, R., & Leipsic, J. (2011, Nov). Aortic annulus diameter determination by multidetector computed tomography: reproducibility, applicability, and implications for transcatheter aortic valve implantation. *JACC Cardiovasc Interv, 4*(11), 1235-1245. https://doi.org/10.1016/j.jcin.2011.07.014

Hak, A. E., Pols, H. A., van Hemert, A. M., Hofman, A., & Witteman, J. C. (2000, Aug). Progression of aortic calcification is associated with metacarpal bone loss during menopause: a population-based longitudinal study. *Arterioscler Thromb Vasc Biol, 20*(8), 1926-1931. https://doi.org/10.1161/01.atv.20.8.1926

Hansson, N. C., Grove, E. L., Andersen, H. R., Leipsic, J., Mathiassen, O. N., Jensen, J. M., Jensen, K. T., Blanke, P., Leetmaa, T., Tang, M., Krusell, L. R., Klaaborg, K. E., Christiansen, E. H., Terp, K., Terkelsen, C. J., Poulsen, S. H., Webb, J., Botker, H. E., & Norgaard, B. L. (2016, Nov 8). Transcatheter Aortic Valve Thrombosis: Incidence, Predisposing Factors, and Clinical Implications. *J Am Coll Cardiol, 68*(19), 2059-2069. https://doi.org/10.1016/j.jacc.2016.08.010

Harkness, A., Ring, L., Augustine, D. X., Oxborough, D., Robinson, S., & Sharma, V. (2020, 01 Mar. 2020). Normal reference intervals for cardiac dimensions and function for use in echocardiographic practice: a guideline from the British Society of

Echocardiography. *Echo Research and Practice, 7*(1), G1-G18. https://doi.org/10.1530/erp-19-0050

Hein, S., Arnon, E., Kostin, S., Schonburg, M., Elsasser, A., Polyakova, V., Bauer, E. P., Klovekorn, W. P., & Schaper, J. (2003, Feb 25). Progression from compensated hypertrophy to failure in the pressure-overloaded human heart: structural deterioration and compensatory mechanisms. *Circulation, 107*(7), 984-991. https://doi.org/10.1161/01.cir.0000051865.66123.b7

Hekimian, G., Boutten, A., Flamant, M., Duval, X., Dehoux, M., Benessiano, J., Huart, V., Dupre, T., Berjeb, N., Tubach, F., Iung, B., Vahanian, A., & Messika-Zeitoun, D. (2013, Jul). Progression of aortic valve stenosis is associated with bone remodelling and secondary hyperparathyroidism in elderly patients--the COFRASA study. *Eur Heart J, 34*(25), 1915-1922. https://doi.org/10.1093/eurheartj/ehs450

Herrmann, S., Stork, S., Niemann, M., Lange, V., Strotmann, J. M., Frantz, S., Beer, M., Gattenlohner, S., Voelker, W., Ertl, G., & Weidemann, F. (2011, Jul 19). Low-gradient aortic valve stenosis myocardial fibrosis and its influence on function and outcome. *J Am Coll Cardiol, 58*(4), 402-412. https://doi.org/10.1016/j.jacc.2011.02.059

Heymans, S., Schroen, B., Vermeersch, P., Milting, H., Gao, F., Kassner, A., Gillijns, H., Herijgers, P., Flameng, W., Carmeliet, P., Van de Werf, F., Pinto, Y. M., & Janssens, S. (2005, Aug 23). Increased cardiac expression of tissue inhibitor of metalloproteinase-1 and tissue inhibitor of metalloproteinase-2 is related to cardiac fibrosis and dysfunction in the chronic pressure-overloaded human heart. *Circulation, 112*(8), 1136-1144. https://doi.org/10.1161/CIRCULATIONAHA.104.516963

Hinton, R. B., Jr., Lincoln, J., Deutsch, G. H., Osinska, H., Manning, P. B., Benson, D. W., & Yutzey, K. E. (2006, Jun 9). Extracellular matrix remodeling and organization in developing and diseased aortic valves. *Circ Res, 98*(11), 1431-1438. https://doi.org/10.1161/01.RES.0000224114.65109.4e

Hoekstra, W. J., Beavers, M. P., Andrade-Gordon, P., Evangelisto, M. F., Keane, P. M., Press, J. B., Tomko, K. A., Fan, F., Kloczewiak, M., Mayo, K. H., & et al. (1995, May 12). Design and evaluation of nonpeptide fibrinogen gamma-chain based GPIIb/IIIa antagonists. *J Med Chem, 38*(10), 1582-1592. https://doi.org/10.1021/jm00010a002

Hugenberg, V., Burchert, W., Preuss, R., Koglin, N., Berndt, M., Stephens, A., Feldmann, C., Kassner, A., & Milting, H. (2019, Oct). Detection of Thrombi inside LVADs using F-18-GP1 PET/CT - Preliminary Results [Meeting Abstract]. *Eur J Nucl Med Mol Imaging, 46*(SUPPL 1), S98-S99. <Go to ISI>://WOS:000492444400157

Iung, B., Baron, G., Butchart, E. G., Delahaye, F., Gohlke-Barwolf, C., Levang, O. W., Tornos, P., Vanoverschelde, J. L., Vermeer, F., Boersma, E., Ravaud, P., & Vahanian, A. (2003, Jul). A prospective survey of patients with valvular heart disease in Europe: The Euro Heart Survey on Valvular Heart Disease. *Eur Heart J, 24*(13), 1231-1243. https://doi.org/10.1016/s0195-668x(03)00201-x

Jenkins, W. S., Vesey, A. T., Shah, A. S., Pawade, T. A., Chin, C. W., White, A. C., Fletcher, A., Cartlidge, T. R., Mitchell, A. J., Pringle, M. A., Brown, O. S., Pessotto, R., McKillop, G., Van Beek, E. J., Boon, N. A., Rudd, J. H., Newby, D. E., & Dweck, M. R. (2015, Sep 8). Valvular (18)F-Fluoride and (18)F-Fluorodeoxyglucose Uptake Predict Disease Progression and Clinical Outcome in Patients With Aortic Stenosis. *J Am Coll Cardiol, 66*(10), 1200-1201. https://doi.org/10.1016/j.jacc.2015.06.1325

Jilaihawi, H., Asch, F. M., Manasse, E., Ruiz, C. E., Jelnin, V., Kashif, M., Kawamori, H., Maeno, Y., Kazuno, Y., Takahashi, N., Olson, R., Alkhatib, J., Berman, D., Friedman, J., Gellada, N., Chakravarty, T., & Makkar, R. R. (2017, Apr). Systematic CT Methodology for the Evaluation of Subclinical Leaflet Thrombosis. *JACC Cardiovasc Imaging, 10*(4), 461-470. https://doi.org/10.1016/j.jcmg.2017.02.005

Kandalam, V., Basu, R., Moore, L., Fan, D., Wang, X., Jaworski, D. M., Oudit, G. Y., & Kassiri, Z. (2011, Nov 8). Lack of tissue inhibitor of metalloproteinases 2 leads to exacerbated left ventricular dysfunction and adverse extracellular matrix remodeling in response to biomechanical stress. *Circulation, 124*(19), 2094-2105. https://doi.org/10.1161/CIRCULATIONAHA.111.030338

Kang, D. H., Park, S. J., Lee, S. A., Lee, S., Kim, D. H., Kim, H. K., Yun, S. C., Hong, G. R., Song, J. M., Chung, C. H., Song, J. K., Lee, J. W., & Park, S. W. (2020, Jan 9). Early Surgery or Conservative Care for Asymptomatic Aortic Stenosis. *N Engl J Med, 382*(2), 111-119. https://doi.org/10.1056/NEJMoa1912846

Kang, D. H., Park, S. J., Rim, J. H., Yun, S. C., Kim, D. H., Song, J. M., Choo, S. J., Park, S. W., Song, J. K., Lee, J. W., & Park, P. W. (2010, Apr 6). Early surgery versus conventional treatment in asymptomatic very severe aortic stenosis. *Circulation, 121*(13), 1502-1509. https://doi.org/10.1161/CIRCULATIONAHA.109.909903

Katz, R., Wong, N. D., Kronmal, R., Takasu, J., Shavelle, D. M., Probstfield, J. L., Bertoni, A. G., Budoff, M. J., & O'Brien, K. D. (2006, May 2). Features of the metabolic syndrome and diabetes mellitus as predictors of aortic valve calcification in the Multi-Ethnic Study of Atherosclerosis. *Circulation, 113*(17), 2113-2119. https://doi.org/10.1161/CIRCULATIONAHA.105.598086

Kim, C., Lee, J. S., Han, Y., Chae, S. Y., Jin, S., Sung, C., Son, H. J., Oh, S. J., Lee, S. J., Oh, J. S., Cho, Y. P., Kwon, T. W., Lee, D. H., Jang, S., Kim, B., Koglin, N., Berndt, M., Stephens, A. W., & Moon, D. H. (2018, Jun 29). Glycoprotein IIb/IIIa receptor imaging with (18)F-GP1 positron emission tomography for acute venous thromboembolism: an open-label, non-randomized, first-in-human phase 1 study. *J Nucl Med, 60*(2), 244-249. https://doi.org/10.2967/jnumed.118.212084

Kodali, S., Pibarot, P., Douglas, P. S., Williams, M., Xu, K., Thourani, V., Rihal, C. S., Zajarias, A., Doshi, D., Davidson, M., Tuzcu, E. M., Stewart, W., Weissman, N. J., Svensson, L., Greason, K., Maniar, H., Mack, M., Anwaruddin, S., Leon, M. B., & Hahn, R. T. (2015, Feb 14). Paravalvular regurgitation after transcatheter aortic valve replacement with the Edwards sapien valve in the PARTNER trial: characterizing patients and impact on outcomes. *Eur Heart J, 36*(7), 449-456. https://doi.org/10.1093/eurheartj/ehu384

Krayenbuehl, H. P., Hess, O. M., Monrad, E. S., Schneider, J., Mall, G., & Turina, M. (1989, Apr). Left ventricular myocardial structure in aortic valve disease before, intermediate, and late after aortic valve replacement. *Circulation, 79*(4), 744-755. https://doi.org/10.1161/01.cir.79.4.744

Krayenbuehl, H. P., Hess, O. M., Ritter, M., Monrad, E. S., & Hoppeler, H. (1988, Apr). Left ventricular systolic function in aortic stenosis. *Eur Heart J, 9 Suppl E*, 19-23. https://doi.org/10.1093/eurheartj/9.suppl_e.19

Lancellotti, P., Magne, J., Dulgheru, R., Clavel, M. A., Donal, E., Vannan, M. A., Chambers, J., Rosenhek, R., Habib, G., Lloyd, G., Nistri, S., Garbi, M., Marchetta, S., Fattouch, K., Coisne, A., Montaigne, D., Modine, T., Davin, L., Gach, O., Radermecker, M., Liu, S., Gillam, L., Rossi, A., Galli, E., Ilardi, F., Tastet, L., Capoulade, R., Zilberszac, R., Vollema, E. M., Delgado, V., Cosyns, B., Lafitte, S., Bernard, A., Pierard, L. A., Bax, J. J., Pibarot, P., & Oury, C. (2018, Nov 1). Outcomes of Patients With Asymptomatic Aortic Stenosis Followed Up in Heart Valve Clinics. *JAMA Cardiol, 3*(11), 1060-1068. https://doi.org/10.1001/jamacardio.2018.3152

Lancellotti, P., & Vannan, M. A. (2020, Jan 9). Timing of Intervention in Aortic Stenosis. *N Engl J Med, 382*(2), 191-193. https://doi.org/10.1056/NEJMe1914382

Lee, S., Lee, S.-A., Choi, B., Kim, Y.-J., Oh, S. J., Choi, H.-M., Kim, E. K., Kim, D.-H., Cho, G.-Y., Song, J.-M., Park, S. W., Kang, D.-H., & Song, J.-K. (2020). Dipeptidyl peptidase-4 inhibition to prevent progression of calcific aortic stenosis. *Heart, 106*(23), 1824. https://doi.org/10.1136/heartjnl-2020-317024

Leon, M. B., Mack, M. J., Hahn, R. T., Thourani, V. H., Makkar, R., Kodali, S. K., Alu, M. C., Madhavan, M. V., Chau, K. H., Russo, M., Kapadia, S. R., Malaisrie, S. C., Cohen, D. J., Blanke, P., Leipsic, J. A., Williams, M. R., McCabe, J. M., Brown, D. L., Babaliaros, V., Goldman, S., Herrmann, H. C., Szeto, W. Y., Genereux, P., Pershad, A., Lu, M., Webb, J. G., Smith, C. R., & Pibarot, P. (2021, 2021/03/09). Outcomes 2 Years After Transcatheter Aortic Valve Replacement in Patients at Low Surgical Risk. *Journal of the American College of Cardiology, 77*(9), 1149-1161. https://doi.org/10.1016/j.jacc.2020.12.052

Lindman, B. R., Otto, C. M., Douglas, P. S., Hahn, R. T., Elmariah, S., Weissman, N. J., Stewart, W. J., Ayele, G. M., Zhang, F., Zajarias, A., Maniar, H. S., Jilaihawi, H., Blackstone, E., Chinnakondepalli, K. M., Tuzcu, E. M., Leon, M. B., & Pibarot, P. (2017, Jul). Blood Pressure and Arterial Load After Transcatheter Aortic Valve Replacement for Aortic Stenosis. *Circ Cardiovasc Imaging, 10*(7). https://doi.org/10.1161/CIRCIMAGING.116.006308

Lohrke, J., Siebeneicher, H., Berger, M., Reinhardt, M., Berndt, M., Mueller, A., Zerna, M., Koglin, N., Oden, F., Bauser, M., Friebe, M., Dinkelborg, L. M., Huetter, J., & Stephens, A. W. (2017, Jul). (18)F-GP1, a Novel PET Tracer Designed for High-Sensitivity, Low-Background Detection of Thrombi. *J Nucl Med, 58*(7), 1094-1099. https://doi.org/10.2967/jnumed.116.188896

lung, B., & Vahanian, A. (2011, 2011/03//

//). Epidemiology of valvular heart disease in the adult [Clinical report]. *Nature Reviews Cardiology, 8*, 162+. http://link.galegroup.com.ezproxy.is.ed.ac.uk/apps/doc/A250658146/AONE?u=ed_itw&sid=AONE&xid=db472fc2

Makkar, R. R., Blanke, P., Leipsic, J., Thourani, V., Chakravarty, T., Brown, D., Trento, A., Guyton, R., Babaliaros, V., Williams, M., Jilaihawi, H., Kodali, S., George, I., Lu, M., McCabe, J. M., Friedman, J., Smalling, R., Wong, S. C., Yazdani, S., Bhatt, D. L., Bax, J., Kapadia, S., Herrmann, H. C., Mack, M., & Leon, M. B. (2020, Jun 23). Subclinical Leaflet Thrombosis in Transcatheter and Surgical Bioprosthetic Valves: PARTNER 3 Cardiac Computed Tomography Substudy. *J Am Coll Cardiol, 75*(24), 3003-3015. https://doi.org/10.1016/j.jacc.2020.04.043

Makkar, R. R., Fontana, G., Jilaihawi, H., Chakravarty, T., Kofoed, K. F., De Backer, O., Asch, F. M., Ruiz, C. E., Olsen, N. T., Trento, A., Friedman, J., Berman, D., Cheng, W., Kashif, M., Jelnin, V., Kliger, C. A., Guo, H., Pichard, A. D., Weissman, N. J., Kapadia, S., Manasse, E., Bhatt, D. L., Leon, M. B., & Sondergaard, L. (2015, Nov 19). Possible Subclinical Leaflet Thrombosis in Bioprosthetic Aortic Valves. *N Engl J Med, 373*(21), 2015-2024. https://doi.org/10.1056/NEJMoa1509233

Marquis-Gravel, G., Redfors, B., Leon, M. B., & Genereux, P. (2016, Nov 29). Medical Treatment of Aortic Stenosis. *Circulation, 134*(22), 1766-1784. https://doi.org/10.1161/CIRCULATIONAHA.116.023997

Massera, D., Doris, M. K., Cadet, S., Kwiecinski, J., Pawade, T. A., Peeters, F., Dey, D., Newby, D. E., Dweck, M. R., & Slomka, P. J. (2020, Jun). Analytical quantification of aortic valve 18F-sodium fluoride PET uptake. *J Nucl Cardiol, 27*(3), 962-972. https://doi.org/10.1007/s12350-018-01542-6

Messroghli, D. R., Greiser, A., Frohlich, M., Dietz, R., & Schulz-Menger, J. (2007, Oct). Optimization and validation of a fully-integrated pulse sequence for modified look-locker inversion-recovery (MOLLI) T1 mapping of the heart. *J Magn Reson Imaging, 26*(4), 1081-1086. https://doi.org/10.1002/jmri.21119

Messroghli, D. R., Moon, J. C., Ferreira, V. M., Grosse-Wortmann, L., He, T., Kellman, P., Mascherbauer, J., Nezafat, R., Salerno, M., Schelbert, E. B., Taylor, A. J., Thompson, R., Ugander, M., van Heeswijk, R. B., & Friedrich, M. G. (2017, Oct 9). Clinical recommendations for cardiovascular magnetic resonance mapping of T1, T2, T2* and extracellular volume: A consensus statement by the Society for Cardiovascular Magnetic Resonance (SCMR) endorsed by the European Association for Cardiovascular Imaging (EACVI). *J Cardiovasc Magn Reson, 19*(1), 75. https://doi.org/10.1186/s12968-017-0389-8

Minners, J., Allgeier, M., Gohlke-Baerwolf, C., Kienzle, R. P., Neumann, F. J., & Jander, N. (2010, Sep). Inconsistent grading of aortic valve stenosis by current guidelines: haemodynamic studies in patients with apparently normal left ventricular function. *Heart, 96*(18), 1463-1468. https://doi.org/10.1136/hrt.2009.181982

Morony, S., Tintut, Y., Zhang, Z., Cattley, R. C., Van, G., Dwyer, D., Stolina, M., Kostenuik, P. J., & Demer, L. L. (2008, Jan 22). Osteoprotegerin inhibits vascular calcification without affecting atherosclerosis in ldlr(-/-) mice. *Circulation, 117*(3), 411-420. https://doi.org/10.1161/CIRCULATIONAHA.107.707380

Moss, A. J., Doris, M. K., Andrews, J. P. M., Bing, R., Daghem, M., van Beek, E. J. R., Forsyth, L., Shah, A. S. V., Williams, M. C., Sellers, S., Leipsic, J., Dweck, M. R., Parker, R. A., Newby, D. E., & Adamson, P. D. (2019, Aug). Molecular Coronary Plaque Imaging Using (18)F-Fluoride. *Circ Cardiovasc Imaging, 12*(8), e008574. https://doi.org/10.1161/CIRCIMAGING.118.008574

Moura, L. M., Ramos, S. F., Pinto, F. J., Barros, I. M., & Rocha-Gonçalves, F. (2011, Jan). Analysis of variability and reproducibility of echocardiography measurements in valvular aortic valve stenosis. *Rev Port Cardiol, 30*(1), 25-33.

Munt, B., Legget, M. E., Kraft, C. D., Miyake-Hull, C. Y., Fujioka, M., & Otto, C. M. (1999, Feb). Physical examination in valvular aortic stenosis: correlation with stenosis severity and prediction of clinical outcome. *Am Heart J, 137*(2), 298-306. https://doi.org/10.1053/hj.1999.v137.95496

Musa, T. A., Treibel, T. A., Vassiliou, V. S., Captur, G., Singh, A., Chin, C., Dobson, L. E., Pica, S., Loudon, M., Malley, T., Rigolli, M., Foley, J. R. J., Bijsterveld, P., Law, G. R., Dweck, M. R., Myerson, S. G., McCann, G. P., Prasad, S. K., Moon, J. C., & Greenwood, J. P. (2018, Oct 30). Myocardial Scar and Mortality in Severe Aortic Stenosis. *Circulation, 138*(18), 1935-1947. https://doi.org/10.1161/CIRCULATIONAHA.117.032839

Nazarzadeh, M., Pinho-Gomes, A. C., Smith Byrne, K., Canoy, D., Raimondi, F., Ayala Solares, J. R., Otto, C. M., & Rahimi, K. (2019, Aug 1). Systolic Blood Pressure and Risk of Valvular Heart Disease: A Mendelian Randomization Study. *JAMA Cardiol, 4*(8), 788-795. https://doi.org/10.1001/jamacardio.2019.2202

Nishimura, R. A., Otto, C. M., Bonow, R. O., Carabello, B. A., Erwin, J. P., 3rd, Fleisher, L. A., Jneid, H., Mack, M. J., McLeod, C. J., O'Gara, P. T., Rigolin, V. H., Sundt, T. M., 3rd, & Thompson, A. (2017, Jul 11). 2017 AHA/ACC Focused Update of the 2014 AHA/ACC Guideline for the Management of Patients With Valvular Heart Disease: A Report of the American College of Cardiology/American Heart Association Task

Force on Clinical Practice Guidelines. *J Am Coll Cardiol, 70*(2), 252-289. https://doi.org/10.1016/j.jacc.2017.03.011

Nkomo, V. T., Gardin, J. M., Skelton, T. N., Gottdiener, J. S., Scott, C. G., & Enriquez-Sarano, M. (2006, Sep 16). Burden of valvular heart diseases: a population-based study. *Lancet, 368*(9540), 1005-1011. https://doi.org/10.1016/S0140-6736(06)69208-8

Obokata, M., Nagata, Y., Wu, V. C., Kado, Y., Kurabayashi, M., Otsuji, Y., & Takeuchi, M. (2016, May). Direct comparison of cardiac magnetic resonance feature tracking and 2D/3D echocardiography speckle tracking for evaluation of global left ventricular strain. *Eur Heart J Cardiovasc Imaging, 17*(5), 525-532. https://doi.org/10.1093/ehjci/jev227

Osnabrugge, R. L., Mylotte, D., Head, S. J., Van Mieghem, N. M., Nkomo, V. T., LeReun, C. M., Bogers, A. J., Piazza, N., & Kappetein, A. P. (2013, Sep 10). Aortic stenosis in the elderly: disease prevalence and number of candidates for transcatheter aortic valve replacement: a meta-analysis and modeling study. *J Am Coll Cardiol, 62*(11), 1002-1012. https://doi.org/10.1016/j.jacc.2013.05.015

Otto, C. M., Burwash, I. G., Legget, M. E., Munt, B. I., Fujioka, M., Healy, N. L., Kraft, C. D., Miyake-Hull, C. Y., & Schwaegler, R. G. (1997, May 6). Prospective study of asymptomatic valvular aortic stenosis. Clinical, echocardiographic, and exercise predictors of outcome. *Circulation, 95*(9), 2262-2270. https://doi.org/10.1161/01.cir.95.9.2262

Otto, C. M., Kuusisto, J., Reichenbach, D. D., Gown, A. M., & O'Brien, K. D. (1994, Aug). Characterization of the early lesion of 'degenerative' valvular aortic stenosis. Histological and immunohistochemical studies. *Circulation, 90*(2), 844-853. https://doi.org/10.1161/01.cir.90.2.844

Otto, C. M., Nishimura, R. A., Bonow, R. O., Carabello, B. A., Erwin, J. P., 3rd, Gentile, F., Jneid, H., Krieger, E. V., Mack, M., McLeod, C., O'Gara, P. T., Rigolin, V. H., Sundt, T. M., 3rd, Thompson, A., & Toly, C. (2021, Feb 2). 2020 ACC/AHA Guideline for the Management of Patients With Valvular Heart Disease: A Report of the American College of Cardiology/American Heart Association Joint Committee on Clinical Practice Guidelines. *Circulation, 143*(5), e72-e227. https://doi.org/10.1161/CIR.0000000000000923

Otto, C. M., Pearlman, A. S., & Gardner, C. L. (1989, Mar 1). Hemodynamic progression of aortic stenosis in adults assessed by Doppler echocardiography. *J Am Coll Cardiol, 13*(3), 545-550. https://doi.org/10.1016/0735-1097(89)90590-1

Otto, C. M., & Prendergast, B. (2014, Aug 21). Aortic-valve stenosis--from patients at risk to severe valve obstruction. *N Engl J Med, 371*(8), 744-756. https://doi.org/10.1056/NEJMra1313875

Oxenham, H., Bloomfield, P., Wheatley, D. J., Lee, R. J., Cunningham, J., Prescott, R. J., & Miller, H. C. (2003, Jul). Twenty year comparison of a Bjork-Shiley mechanical heart valve with porcine bioprostheses. *Heart, 89*(7), 715-721. https://doi.org/10.1136/heart.89.7.715

Palta, S., Pai, A. M., Gill, K. S., & Pai, R. G. (2000, May 30). New insights into the progression of aortic stenosis: implications for secondary prevention. *Circulation, 101*(21), 2497-2502. https://doi.org/10.1161/01.cir.101.21.2497

Pawade, T., Clavel, M. A., Tribouilloy, C., Dreyfus, J., Mathieu, T., Tastet, L., Renard, C., Gun, M., Jenkins, W. S. A., Macron, L., Sechrist, J. W., Lacomis, J. M., Nguyen, V., Galian Gay, L., Cuellar Calabria, H., Ntalas, I., Cartlidge, T. R. G., Prendergast, B., Rajani, R., Evangelista, A., Cavalcante, J. L., Newby, D. E., Pibarot, P., Messika Zeitoun, D., & Dweck, M. R. (2018, Mar). Computed Tomography Aortic Valve Calcium Scoring in Patients With Aortic Stenosis. *Circ Cardiovasc Imaging, 11*(3), e007146. https://doi.org/10.1161/CIRCIMAGING.117.007146

Pawade, T., Sheth, T., Guzzetti, E., Dweck, M. R., & Clavel, M. A. (2019, Sep). Why and How to Measure Aortic Valve Calcification in Patients With Aortic Stenosis. *JACC Cardiovasc Imaging, 12*(9), 1835-1848. https://doi.org/10.1016/j.jcmg.2019.01.045

Pawade, T. A., Cartlidge, T. R., Jenkins, W. S., Adamson, P. D., Robson, P., Lucatelli, C., Van Beek, E. J., Prendergast, B., Denison, A. R., Forsyth, L., Rudd, J. H., Fayad, Z. A., Fletcher, A., Tuck, S., Newby, D. E., & Dweck, M. R. (2016, Oct). Optimization and Reproducibility of Aortic Valve 18F-Fluoride Positron Emission Tomography in Patients With Aortic Stenosis. *Circ Cardiovasc Imaging, 9*(10), e005131. https://doi.org/10.1161/circimaging.116.005131

Pawade, T. A., Newby, D. E., & Dweck, M. R. (2015, Aug 4). Calcification in Aortic Stenosis: The Skeleton Key. *J Am Coll Cardiol, 66*(5), 561-577. https://doi.org/10.1016/j.jacc.2015.05.066

Pellikka, P. A., Nishimura, R. A., Bailey, K. R., & Tajik, A. J. (1990, Apr). The natural history of adults with asymptomatic, hemodynamically significant aortic stenosis. *J Am Coll Cardiol, 15*(5), 1012-1017. https://doi.org/10.1016/0735-1097(90)90234-g

Pellikka, P. A., Sarano, M. E., Nishimura, R. A., Malouf, J. F., Bailey, K. R., Scott, C. G., Barnes, M. E., & Tajik, A. J. (2005, Jun 21). Outcome of 622 adults with asymptomatic, hemodynamically significant aortic stenosis during prolonged follow-up. *Circulation, 111*(24), 3290-3295. https://doi.org/10.1161/CIRCULATIONAHA.104.495903

Pibarot, P., Ternacle, J., Jaber, W. A., Salaun, E., Dahou, A., Asch, F. M., Weissman, N. J., Rodriguez, L., Xu, K., Annabi, M. S., Guzzetti, E., Beaudoin, J., Bernier, M., Leipsic, J., Blanke, P., Clavel, M. A., Rogers, E., Alu, M. C., Douglas, P. S., Makkar, R., Miller, D. C., Kapadia, S. R., Mack, M. J., Webb, J. G., Kodali, S. K., Smith, C. R., Herrmann, H. C., Thourani, V. H., Leon, M. B., Hahn, R. T., & Investigators, P. (2020, Oct 20). Structural Deterioration of Transcatheter Versus Surgical Aortic Valve Bioprostheses in the PARTNER-2 Trial. *J Am Coll Cardiol, 76*(16), 1830-1843. https://doi.org/10.1016/j.jacc.2020.08.049

Popma, J. J., Deeb, G. M., Yakubov, S. J., Mumtaz, M., Gada, H., O'Hair, D., Bajwa, T., Heiser, J. C., Merhi, W., Kleiman, N. S., Askew, J., Sorajja, P., Rovin, J., Chetcuti, S. J., Adams, D. H., Teirstein, P. S., Zorn, G. L., 3rd, Forrest, J. K., Tchetche, D., Resar, J., Walton, A., Piazza, N., Ramlawi, B., Robinson, N., Petrossian, G., Gleason, T. G., Oh, J. K., Boulware, M. J., Qiao, H., Mugglin, A. S., Reardon, M. J., & Evolut Low Risk Trial, I. (2019, May 2). Transcatheter Aortic-Valve Replacement with a Self-Expanding Valve in Low-Risk Patients. *N Engl J Med, 380*(18), 1706-1715. https://doi.org/10.1056/NEJMoa1816885

Price, P. A., Faus, S. A., & Williamson, M. K. (2001, May). Bisphosphonates alendronate and ibandronate inhibit artery calcification at doses comparable to those that inhibit bone resorption. *Arterioscler Thromb Vasc Biol, 21*(5), 817-824. https://doi.org/10.1161/01.atv.21.5.817

Puntmann, V. O., Peker, E., Chandrashekhar, Y., & Nagel, E. (2016, Jul 8). T1 Mapping in Characterizing Myocardial Disease: A Comprehensive Review. *Circ Res, 119*(2), 277-299. https://doi.org/10.1161/CIRCRESAHA.116.307974

Rahimi, K., Mohseni, H., Kiran, A., Tran, J., Nazarzadeh, M., Rahimian, F., Woodward, M., Dwyer, T., MacMahon, S., & Otto, C. M. (2018, Oct 14). Elevated blood pressure and risk of aortic valve disease: a cohort analysis of 5.4 million UK adults. *Eur Heart J, 39*(39), 3596-3603. https://doi.org/10.1093/eurheartj/ehy486

Rajamannan, N. M., Evans, F. J., Aikawa, E., Grande-Allen, K. J., Demer, L. L., Heistad, D. D., Simmons, C. A., Masters, K. S., Mathieu, P., O'Brien, K. D., Schoen, F. J., Towler, D. A., Yoganathan, A. P., & Otto, C. M. (2011, Oct 18). Calcific aortic valve disease: not simply a degenerative process: A review and agenda for research from the National Heart and Lung and Blood Institute Aortic Stenosis Working Group.

Executive summary: Calcific aortic valve disease-2011 update. *Circulation, 124*(16), 1783-1791. https://doi.org/10.1161/CIRCULATIONAHA.110.006767

Rajamannan, N. M., Subramaniam, M., Rickard, D., Stock, S. R., Donovan, J., Springett, M., Orszulak, T., Fullerton, D. A., Tajik, A. J., Bonow, R. O., & Spelsberg, T. (2003, May 6). Human aortic valve calcification is associated with an osteoblast phenotype. *Circulation, 107*(17), 2181-2184. https://doi.org/10.1161/01.CIR.0000070591.21548.69

Rheude, T., Pellegrini, C., Stortecky, S., Marwan, M., Xhepa, E., Ammon, F., Pilgrim, T., Mayr, N. P., Husser, O., Achenbach, S., Windecker, S., Cassese, S., & Joner, M. (2021, Jan 1). Meta-Analysis of Bioprosthetic Valve Thrombosis After Transcatheter Aortic Valve Implantation. *Am J Cardiol, 138*, 92-99. https://doi.org/10.1016/j.amjcard.2020.10.018

Rosenhek, R., Binder, T., Porenta, G., Lang, I., Christ, G., Schemper, M., Maurer, G., & Baumgartner, H. (2000, Aug 31). Predictors of outcome in severe, asymptomatic aortic stenosis. *N Engl J Med, 343*(9), 611-617. https://doi.org/10.1056/NEJM200008313430903

Rosenhek, R., Klaar, U., Schemper, M., Scholten, C., Heger, M., Gabriel, H., Binder, T., Maurer, G., & Baumgartner, H. (2004, Feb). Mild and moderate aortic stenosis. Natural history and risk stratification by echocardiography. *Eur Heart J, 25*(3), 199-205. https://doi.org/10.1016/j.ehj.2003.12.002

Rosenhek, R., Zilberszac, R., Schemper, M., Czerny, M., Mundigler, G., Graf, S., Bergler-Klein, J., Grimm, M., Gabriel, H., & Maurer, G. (2010, Jan 5). Natural history of very severe aortic stenosis. *Circulation, 121*(1), 151-156. https://doi.org/10.1161/CIRCULATIONAHA.109.894170

Ross, J., Jr. (1976, Aug). The concept of afterload mismatch and its implications in the clinical assessment of cardiac contractility. *Jpn Circ J, 40*(8), 865-875. https://doi.org/10.1253/jcj.40.865

Ross, J., Jr. (1985, Apr). Afterload mismatch in aortic and mitral valve disease: implications for surgical therapy. *J Am Coll Cardiol, 5*(4), 811-826. https://doi.org/10.1016/s0735-1097(85)80418-6

Ross, J., Jr., & Braunwald, E. (1968, Jul). Aortic stenosis. *Circulation, 38*(1 Suppl), 61-67. https://doi.org/10.1161/01.cir.38.1s5.v-61

Rossebo, A. B., Pedersen, T. R., Boman, K., Brudi, P., Chambers, J. B., Egstrup, K., Gerdts, E., Gohlke-Barwolf, C., Holme, I., Kesaniemi, Y. A., Malbecq, W., Nienaber, C. A., Ray, S., Skjaerpe, T., Wachtell, K., Willenheimer, R., & Investigators, S. (2008, Sep 25). Intensive lipid lowering with simvastatin and ezetimibe in aortic stenosis. *N Engl J Med, 359*(13), 1343-1356. https://doi.org/10.1056/NEJMoa0804602

Sacchi, S., Dhutia, N. M., Shun-Shin, M. J., Zolgharni, M., Sutaria, N., Francis, D. P., & Cole, G. D. (2018, Dec 1). Doppler assessment of aortic stenosis: a 25-operator study demonstrating why reading the peak velocity is superior to velocity time integral. *Eur Heart J Cardiovasc Imaging, 19*(12), 1380-1389. https://doi.org/10.1093/ehjci/jex218

Sansoni, P., Passeri, G., Fagnoni, F., Mohagheghpour, N., Snelli, G., Brianti, V., & Engleman, E. G. (1995, Nov). Inhibition of antigen-presenting cell function by alendronate in vitro. *J Bone Miner Res, 10*(11), 1719-1725. https://doi.org/10.1002/jbmr.5650101115

Sellers, S. L., Turner, C. T., Sathananthan, J., Cartlidge, T. R. G., Sin, F., Bouchareb, R., Mooney, J., Norgaard, B. L., Bax, J. J., Bernatchez, P. N., Dweck, M. R., Granville, D. J., Newby, D. E., Lauck, S., Webb, J. G., Payne, G. W., Pibarot, P., Blanke, P., Seidman, M. A., & Leipsic, J. A. (2019, Jan). Transcatheter Aortic Heart Valves: Histological Analysis Providing Insight to Leaflet Thickening and Structural Valve

Degeneration. *JACC Cardiovasc Imaging, 12*(1), 135-145. https://doi.org/10.1016/j.jcmg.2018.06.028

Shen, M., Tastet, L., Capoulade, R., Larose, E., Bedard, E., Arsenault, M., Chetaille, P., Dumesnil, J. G., Mathieu, P., Clavel, M. A., & Pibarot, P. (2017, Jan 1). Effect of age and aortic valve anatomy on calcification and haemodynamic severity of aortic stenosis. *Heart, 103*(1), 32-39. https://doi.org/10.1136/heartjnl-2016-309665

Simard, L., Cote, N., Dagenais, F., Mathieu, P., Couture, C., Trahan, S., Bosse, Y., Mohammadi, S., Page, S., Joubert, P., & Clavel, M. A. (2017, Feb 17). Sex-Related Discordance Between Aortic Valve Calcification and Hemodynamic Severity of Aortic Stenosis: Is Valvular Fibrosis the Explanation? *Circ Res, 120*(4), 681-691. https://doi.org/10.1161/CIRCRESAHA.116.309306

Singh, A., Horsfield, M. A., Bekele, S., Khan, J. N., Greiser, A., & McCann, G. P. (2015, Jul). Myocardial T1 and extracellular volume fraction measurement in asymptomatic patients with aortic stenosis: reproducibility and comparison with age-matched controls. *Eur Heart J Cardiovasc Imaging, 16*(7), 763-770. https://doi.org/10.1093/ehjci/jev007

Skolnick, A. H., Osranek, M., Formica, P., & Kronzon, I. (2009, Jul 1). Osteoporosis treatment and progression of aortic stenosis. *Am J Cardiol, 104*(1), 122-124. https://doi.org/10.1016/j.amjcard.2009.02.051

Smith, L. A., Cowell, S. J., White, A. C., Boon, N. A., Newby, D. E., & Northridge, D. B. (2004, Mar). Contrast agent increases Doppler velocities and improves reproducibility of aortic valve area measurements in patients with aortic stenosis. *J Am Soc Echocardiogr, 17*(3), 247-252. https://doi.org/10.1016/j.echo.2003.11.001

Sondergaard, L., De Backer, O., Kofoed, K. F., Jilaihawi, H., Fuchs, A., Chakravarty, T., Kashif, M., Kazuno, Y., Kawamori, H., Maeno, Y., Bieliauskas, G., Guo, H., Stone, G. W., & Makkar, R. (2017, Jul 21). Natural history of subclinical leaflet thrombosis affecting motion in bioprosthetic aortic valves. *Eur Heart J, 38*(28), 2201-2207. https://doi.org/10.1093/eurheartj/ehx369

Sondergaard, L., Ihlemann, N., Capodanno, D., Jorgensen, T. H., Nissen, H., Kjeldsen, B. J., Chang, Y., Steinbruchel, D. A., Olsen, P. S., Petronio, A. S., & Thyregod, H. G. H. (2019, Feb 12). Durability of Transcatheter and Surgical Bioprosthetic Aortic Valves in Patients at Lower Surgical Risk. *J Am Coll Cardiol, 73*(5), 546-553. https://doi.org/10.1016/j.jacc.2018.10.083

Spath, N. B., Gomez, M., Everett, R. J., Semple, S., Chin, C. W. L., White, A. C., Japp, A. G., Newby, D. E., & Dweck, M. R. (2019, Oct). Global Longitudinal Strain Analysis Using Cardiac MRI in Aortic Stenosis: Comparison with Left Ventricular Remodeling, Myocardial Fibrosis, and 2-year Clinical Outcomes. *Radiol Cardiothorac Imaging, 1*(4), e190027. https://doi.org/10.1148/ryct.2019190027

Stewart, B. F., Siscovick, D., Lind, B. K., Gardin, J. M., Gottdiener, J. S., Smith, V. E., Kitzman, D. W., & Otto, C. M. (1997, Mar 1). Clinical factors associated with calcific aortic valve disease. Cardiovascular Health Study. *J Am Coll Cardiol, 29*(3), 630-634. https://doi.org/10.1016/s0735-1097(96)00563-3

Strange, G., Stewart, S., Celermajer, D., Prior, D., Scalia, G. M., Marwick, T., Ilton, M., Joseph, M., Codde, J., Playford, D., & National Echocardiography Database of Australia contributing, s. (2019, Oct 15). Poor Long-Term Survival in Patients With Moderate Aortic Stenosis. *J Am Coll Cardiol, 74*(15), 1851-1863. https://doi.org/10.1016/j.jacc.2019.08.004

Stritzke, J., Linsel-Nitschke, P., Markus, M. R., Mayer, B., Lieb, W., Luchner, A., Doring, A., Koenig, W., Keil, U., Hense, H. W., Schunkert, H., & Investigators, M. K. (2009, Aug). Association between degenerative aortic valve disease and long-term exposure to cardiovascular risk factors: results of the longitudinal population-based

KORA/MONICA survey. *Eur Heart J, 30*(16), 2044-2053. https://doi.org/10.1093/eurheartj/ehp287

Taniguchi, T., Morimoto, T., Shiomi, H., Ando, K., Kanamori, N., Murata, K., Kitai, T., Kawase, Y., Izumi, C., Miyake, M., Mitsuoka, H., Kato, M., Hirano, Y., Matsuda, S., Nagao, K., Inada, T., Murakami, T., Takeuchi, Y., Yamane, K., Toyofuku, M., Ishii, M., Minamino-Muta, E., Kato, T., Inoko, M., Ikeda, T., Komasa, A., Ishii, K., Hotta, K., Higashitani, N., Kato, Y., Inuzuka, Y., Maeda, C., Jinnai, T., Morikami, Y., Sakata, R., Kimura, T., & Investigators, C. A. R. (2015, Dec 29). Initial Surgical Versus Conservative Strategies in Patients With Asymptomatic Severe Aortic Stenosis. *J Am Coll Cardiol, 66*(25), 2827-2838. https://doi.org/10.1016/j.jacc.2015.10.001

Tastet, L., Tribouilloy, C., Marechaux, S., Vollema, E. M., Delgado, V., Salaun, E., Shen, M., Capoulade, R., Clavel, M. A., Arsenault, M., Bedard, E., Bernier, M., Beaudoin, J., Narula, J., Lancellotti, P., Bax, J. J., Genereux, P., & Pibarot, P. (2019, Jul 30). Staging Cardiac Damage in Patients With Asymptomatic Aortic Valve Stenosis. *J Am Coll Cardiol, 74*(4), 550-563. https://doi.org/10.1016/j.jacc.2019.04.065

Topol, E. J., Byzova, T. V., & Plow, E. F. (1999, Jan 16). Platelet GPIIb-IIIa blockers. *Lancet, 353*(9148), 227-231. https://doi.org/10.1016/S0140-6736(98)11086-3

Treibel, T. A., Kozor, R., Schofield, R., Benedetti, G., Fontana, M., Bhuva, A. N., Sheikh, A., Lopez, B., Gonzalez, A., Manisty, C., Lloyd, G., Kellman, P., Diez, J., & Moon, J. C. (2018, Feb 27). Reverse Myocardial Remodeling Following Valve Replacement in Patients With Aortic Stenosis. *J Am Coll Cardiol, 71*(8), 860-871. https://doi.org/10.1016/j.jacc.2017.12.035

Treibel, T. A., Lopez, B., Gonzalez, A., Menacho, K., Schofield, R. S., Ravassa, S., Fontana, M., White, S. K., DiSalvo, C., Roberts, N., Ashworth, M. T., Diez, J., & Moon, J. C. (2018, Feb 21). Reappraising myocardial fibrosis in severe aortic stenosis: an invasive and non-invasive study in 133 patients. *Eur Heart J, 39*(8), 699-709. https://doi.org/10.1093/eurheartj/ehx353

Vemulapalli, S., Carroll, J. D., Mack, M. J., Li, Z., Dai, D., Kosinski, A. S., Kumbhani, D. J., Ruiz, C. E., Thourani, V. H., Hanzel, G., Gleason, T. G., Herrmann, H. C., Brindis, R. G., & Bavaria, J. E. (2019, Jun 27). Procedural Volume and Outcomes for Transcatheter Aortic-Valve Replacement. *N Engl J Med, 380*(26), 2541-2550. https://doi.org/10.1056/NEJMsa1901109

Vollema, E. M., Amanullah, M. R., Ng, A. C. T., van der Bijl, P., Prevedello, F., Sin, Y. K., Prihadi, E. A., Marsan, N. A., Ding, Z. P., Genereux, P., Pibarot, P., Leon, M. B.,

Narula, J., Ewe, S. H., Delgado, V., & Bax, J. J. (2019, Jul 30). Staging Cardiac Damage in Patients With Symptomatic Aortic Valve Stenosis. *J Am Coll Cardiol, 74*(4), 538-549. https://doi.org/10.1016/j.jacc.2019.05.048

Warren, B. A., & Yong, J. L. (1997, Nov). Calcification of the aortic valve: its progression and grading. *Pathology, 29*(4), 360-368. https://doi.org/10.1080/00313029700169315

Wassef, A. W. A., Rodes-Cabau, J., Liu, Y., Webb, J. G., Barbanti, M., Munoz-Garcia, A. J., Tamburino, C., Dager, A. E., Serra, V., Amat-Santos, I. J., Alonso Briales, J. H., San Roman, A., Urena, M., Himbert, D., Nombela-Franco, L., Abizaid, A., de Brito, F. S., Jr., Ribeiro, H. B., Ruel, M., Lima, V. C., Nietlispach, F., & Cheema, A. N. (2018, Sep 10). The Learning Curve and Annual Procedure Volume Standards for Optimum Outcomes of Transcatheter Aortic Valve Replacement: Findings From an International Registry. *JACC Cardiovasc Interv, 11*(17), 1669-1679. https://doi.org/10.1016/j.jcin.2018.06.044

Weber, K. T., & Brilla, C. G. (1991, Jun). Pathological hypertrophy and cardiac interstitium. Fibrosis and renin-angiotensin-aldosterone system. *Circulation, 83*(6), 1849-1865. https://doi.org/10.1161/01.cir.83.6.1849

Weidemann, F., Herrmann, S., Stork, S., Niemann, M., Frantz, S., Lange, V., Beer, M., Gattenlohner, S., Voelker, W., Ertl, G., & Strotmann, J. M. (2009, Aug 18). Impact of myocardial fibrosis in patients with symptomatic severe aortic stenosis. *Circulation, 120*(7), 577-584. https://doi.org/10.1161/CIRCULATIONAHA.108.847772

Williams, M. C., Massera, D., Moss, A. J., Bing, R., Bularga, A., Adamson, P. D., Hunter, A., Alam, S., Shah, A. S. V., Pawade, T., Roditi, G., van Beek, E. J. R., Nicol, E. D., Newby, D. E., & Dweck, M. R. (2020, Dec 11). Prevalence and clinical implications of valvular calcification on coronary computed tomography angiography. *Eur Heart J Cardiovasc Imaging*. https://doi.org/10.1093/ehjci/jeaa263

Yahagi, K., Torii, S., Ladich, E., Kutys, R., Romero, M. E., Mori, H., Kolodgie, F. D., Popma, J. J., Virmani, R., & Finn, A. V. (2018, Apr 1). Pathology of self-expanding transcatheter aortic valves: Findings from the CoreValve US pivotal trials [https://doi.org/10.1002/ccd.27314]. *Catheter Cardiovasc Interv, 91*(5), 947-955. https://doi.org/10.1002/ccd.27314

Yanagisawa, R., Hayashida, K., Yamada, Y., Tanaka, M., Yashima, F., Inohara, T., Arai, T., Kawakami, T., Maekawa, Y., Tsuruta, H., Itabashi, Y., Murata, M., Sano, M., Okamoto, K., Yoshitake, A., Shimizu, H., Jinzaki, M., & Fukuda, K. (2016, Dec 8). Incidence, Predictors, and Mid-Term Outcomes of Possible Leaflet Thrombosis After TAVR. *JACC Cardiovasc Imaging*. https://doi.org/10.1016/j.jcmg.2016.11.005

Yang, W., Wang, B. H., Wang, I., Huang, L., Savira, F., Kompa, A., Jucker, B. M., Willette, R. N., Kelly, D., Krum, H., Li, Z., & Fu, Q. (2017, Dec 14). Inhibition of Apoptosis Signal-Regulating Kinase 1 Attenuates Myocyte Hypertrophy and Fibroblast Collagen Synthesis. *Heart Lung Circ, 10.1016/j.hlc.2017.12.001*. https://doi.org/10.1016/j.hlc.2017.12.001

Yetkin, E., & Waltenberger, J. (2009, Jun 12). Molecular and cellular mechanisms of aortic stenosis. *Int J Cardiol, 135*(1), 4-13. https://doi.org/10.1016/j.ijcard.2009.03.108

Yotti, R., Bermejo, J., Gutierrez-Ibanes, E., Perez del Villar, C., Mombiela, T., Elizaga, J., Benito, Y., Gonzalez-Mansilla, A., Barrio, A., Rodriguez-Perez, D., Martinez-Legazpi, P., & Fernandez-Aviles, F. (2015, Feb 10). Systemic vascular load in calcific degenerative aortic valve stenosis: insight from percutaneous valve replacement. *J Am Coll Cardiol, 65*(5), 423-433. https://doi.org/10.1016/j.jacc.2014.10.067

Yutzey, K. E., Demer, L. L., Body, S. C., Huggins, G. S., Towler, D. A., Giachelli, C. M., Hofmann-Bowman, M. A., Mortlock, D. P., Rogers, M. B., Sadeghi, M. M., & Aikawa, E. (2014, Nov). Calcific aortic valve disease: a consensus summary from the Alliance of Investigators on Calcific Aortic Valve Disease. *Arterioscler Thromb Vasc Biol, 34*(11), 2387-2393. https://doi.org/10.1161/ATVBAHA.114.302523

Zilberszac, R., Gabriel, H., Schemper, M., Laufer, G., Maurer, G., & Rosenhek, R. (2017, Jan). Asymptomatic Severe Aortic Stenosis in the Elderly. *JACC Cardiovasc Imaging, 10*(1), 43-50. https://doi.org/10.1016/j.jcmg.2016.05.015